

STRATIGRAPHY AND PETROLEUM GEOLOGY OF THE
BLUE MONDAY SANDSTONE, CENTRAL WEST VIRGINIA

By

Megan E. Ganak

May 2011

Chair: Donald W. Neal

Major Department: Geological Sciences.

The Upper Mississippian Blue Monday sandstone is a primarily gas producing unit found in several central West Virginia gas fields. The purpose of this study was to characterize the stratigraphy and petroleum geology as well as establishing the depositional setting.

Stratigraphically, with the underlying Lillydale Shale (Pencil Cave), it occupies a position between the Greenbrier Limestone (Big Lime) below and the Reynolds Limestone Member of the Bluefield Formation (Little Lime) above. In the study area it was deposited as a sheet sand from anastomosing fluvial channels flowing into the Bluefield Sea with a delta/barrier system to the south. This was deposited during the regressive sequence between the transgressive Pencil Cave and Little Lime.

The Blue Monday sandstone has been a prolific producer in the past and remains a secondary target for exploration. Production data for wells completed only in the Blue Monday are sparse as Blue Monday sandstone production is typically commingled with production from other zones. Well log porosity in the Blue Monday sandstone ranges from one to twenty percent. Well logs exemplify the fact that the sand has lenses of more and less porous material, indicating flow unit differentiation. Production might be enhanced by hydraulic or chemical fracturing. The highest well log porosities were not always found in the channels which may be due to diagenetic factors such as cementation or the presence of shale interbeds.

STRATIGRAPHY AND PETROLEUM GEOLOGY OF THE
BLUE MONDAY SANDSTONE, CENTRAL WEST VIRGINIA

A Thesis

Presented To

the Faculty of the Department of Geological Sciences

East Carolina University

In Partial Fulfillment

of the Requirements for the Degree

Master of Science in Geology

by

Megan E. Ganak

May 2011

© COPYRIGHT

by

Megan E. Ganak

2011

All Rights Reserved

STRATIGRAPHY AND PETROLEUM GEOLOGY OF THE
BLUE MONDAY SANDSTONE, CENTRAL WEST VIRGINIA

by

Megan E. Ganak

APPROVED BY:

DIRECTOR OF THESIS: _____
Donald W. Neal

COMMITTEE MEMBER: _____
Stephen B. Harper

COMMITTEE MEMBER: _____
Richard K. Spruill

COMMITTEE MEMBER: _____
K. Lee Avary

CHAIRMAN OF THE DEPARTMENT
OF GEOLOGICAL SCIENCES: _____
Stephen J. Culver

DEAN OF THE GRADUATE SCHOOL: _____
Paul Gemperline

STATEMENT OF PERMISSION TO USE BY AUTHOR

In submitting this thesis as partial fulfillment of the requirements for a master's degree at East Caroline University, I agree that the J.Y. Joyner Library at East Carolina University shall make it available to borrowers under rules of the Library.

I have indicated my intention to copyright this thesis by including a copyright notice page. Copying is permitted only for scholarly purposes, consistent with "fair use" as defined by the U.S. Copyright Law. Brief quotations from this thesis are allowed without special permission, provided that accurate acknowledgement of the source is made. Requests for permission for extended quotation from or reproduction of this thesis in whole or in part may be granted only by the copyright holder.

Megan E. Ganak
2011

This work is dedicated to Corbyn Whalen (1987-2010) who said,

‘School is the most important thing right now. Go for it.’

This happened because you believe in me, despite having left me.

Acknowledgements:

I would like to first and foremost thank my advisor, Don Neal. Without your vast knowledge on this topic, this thesis wouldn't have been possible. Thank you for your understanding and patience during my times of procrastination and writers block.

A big thank you to my committee members: K. Lee Avary, Richard Spruill and Stephen Harper for being there when I needed you.

To my adults, Ted and Nanci Weil, without you generously opening your home to me while winding this up, I would have been homeless! So thank you for the roof, the amazing meals and care you've shown me.

For friends: Angela Lilly, Jamie Skeen: you've always been there for me (no matter how long it had been since we've spoken). I am deeply appreciative. For friends Cynthia Crane, Nathan Gwyn, and Nidhi Patel: without your constant encouragement and sometimes daily lunches, this wouldn't have been possible. Thank you.

Finally, a special thank you to my parents, George and Jackie Ganak, and sister Elizabeth Ganak for always being there when I needed an ear to hear my complaining. Without your strength, love and encouragement, this wouldn't have been possible.

TABLE OF CONTENTS

DEDICATION	vi
ACKNOWLEDGEMENTS	vii
LIST OF TABLES	x
LIST OF FIGURES	xi
1 INTRODUCTION	1
PURPOSE.....	1
LOCATION.....	2
PREVIOUS WORK.....	5
METHODS.....	8
2 RESULTS	12
THICKNESS VARIATION.....	12
CROSS SECTIONS.....	20
STRUCTURE.....	29
LOG SIGNATURES.....	31
LITHOLOGY.....	35
PRODUCTION.....	37

	POROSITY.....	41
3	DISCUSSION.....	52
	STRATIGRAPHY.....	52
	DEPOSITIONAL ENVIRONMENT.....	54
	PETROLEUM GEOLOGY.....	57
4	CONCLUSIONS.....	61
5	REFERENCES CITED.....	62
	APPENDIX I- WELL CUTTINGS DESCRIPTION	65
	APPENDIX II- CROSS-SECTIONS	70
	APPENDIX III- WELL LOG CROSS-SECTIONS.....	76
	APPENDIX IV- DATA COMPILATION.....	144

LIST OF TABLES

1. Percentages of porosity derived from well logs and type34
2. Type of production and number of wells across primary counties.....37

LIST OF FIGURES

1.	Stratigraphic column of the Upper Mississippian section.....	2
2.	West Virginia Location map.....	3
3.	Paleogeographic location of study area.....	4
4.	Flowers' Isopach Map (1956)	6
5.	Neal's Blue Monday sandstone interval (1997).....	8
6.	Map: Location of wells.....	9
7.	Type log for the section.....	11
8.	Isopach map of the clastic section between limestones.....	13
9.	Blue Monday sandstone isopach map.....	15
10.	Little Lime isopach map.....	16
11.	Pencil Cave shale isopach map.....	17
12.	Wells with no Pencil Cave in the column.....	18
13.	Big Lime isopach map.....	19
14.	Location map of the cross-sections.....	20
15.	Southern Braxton County cross-section and location map.....	22
16.	Western Braxton County cross-section and location map.....	23

17.	Clay County cross-section and location map.....	24
18.	Kanawha-Roane counties cross-section and location map.....	25
19.	Western Nicholas County cross-section and location map.....	27
20.	Central Nicholas County cross-section and location map.....	28
21.	Greenbrier Limestone structure contour map.....	29
22.	West Virginia basement structural geology.....	30
23.	Examples of the log signatures associated with the Blue Monday sandstone.....	32
24.	Log signature map overlying the Blue Monday isopach map.....	33
25.	Location map of the Webster Springs Sandstone outcrop.....	35
26.	Picture of the Webster Springs Sandstone outcrop.....	36
27.	Picture of the Webster Springs Sandstone outcrop.....	36
28.	Field names and locations across the study area.....	38
29.	Nicholas County decline curve.....	40
30.	Clay County decline curve.....	40
31.	Braxton County decline curve.....	41
32.	Example well log showing the section and porosity.....	42
33.	Well log porosity map.....	43

34.	Upshur County well log porosity cross-section and location map.....	45
35.	West-central Nicholas County well log porosity cross-section.....	46
36.	Western Nicholas County well log porosity cross-section.....	46
37.	Eastern Nicholas County well log porosity cross-section.....	47
38.	Location map for Figures 34, 35, and 36.....	47
39.	Southern Braxton County well log porosity cross-section.....	49
40.	Central Braxton County well log porosity cross-section.....	49
41.	North Braxton and Gilmer counties well log porosity cross-section.....	50
42.	Location map for Figures 38, 39 and 40.....	51
43.	Sea level change.....	55
44.	First depositional model for the Blue Monday sandstone.....	58
45.	Second depositional model for the Blue Monday sandstone.....	59

1 INTRODUCTION

The Upper Mississippian Blue Monday sandstone of the Bluefield Formation, Mauch Chunk Group is Chesterian (Late Mississippian) in age (Fig. 1). It is the dominant sand in the lower Bluefield Group, and is widespread across the central West Virginia basin. The Bluefield is the transition between the underlying marine carbonates of the Greenbrier Group and the overlying terrigenous Hinton Formation (Corbitt, 1986) and therefore has a mix of carbonate and terrigenous materials. Gas, oil and liquid condensate have been produced from the Blue Monday.

PURPOSE

This investigation studied the Blue Monday sandstone which is often grouped together with surrounding strata due to their productive nature. Little has been published about it due to its insignificant size; therefore, this paper intends to

- 1) characterize the stratigraphy of the Blue Monday sandstone,
- 2) propose the depositional environment of the Blue Monday sandstone, and
- 3) characterize the petroleum geology associated with the Blue Monday sandstone.

Upper Mississippian			Name	Drillers Name
	Mauch Chunk Group	Bluefield Formation	Lower Maxon Sandstone	Good Hope
			Reynolds Limestone	Little Lime
			Bickett Shale	None Given
			Webster Springs Sandstone	Blue Monday sandstone
			Lillydale Shale	Pencil Cave shale
			Greenbrier Limestone	Big Lime

Figure 1: Stratigraphic column showing the Blue Monday sandstone and surrounding strata.

LOCATION

Braxton, Clay, Nicholas, and Webster counties in West Virginia were chosen for this study because this is where historical Blue Monday oil and gas production occurred. Wells were investigated in the surrounding counties of Calhoun, Fayette, Gilmer, Greenbrier, Kanawha,

Lewis, Randolph, Roane, and Upshur to ensure that the data established in the four counties were not anomalous (Fig. 2).

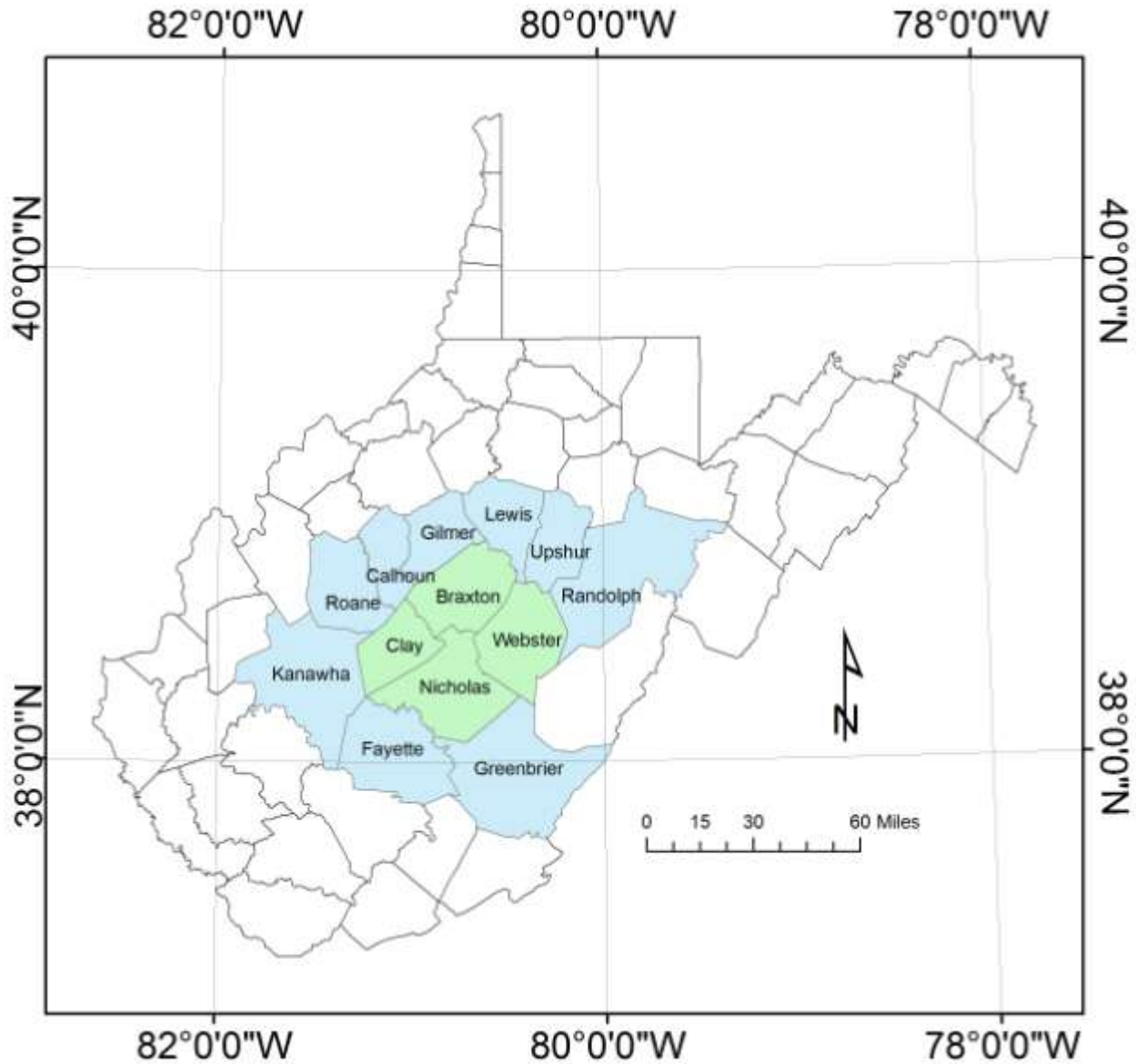


Figure 2: Location of study area in central West Virginia counties. Counties shaded green are the primary study area. Counties shaded blue had few wells used to reinforce the data from the green counties.

During the time of deposition this area was located near the paleoequator in the Appalachian Mountain foreland basin resulting from the incipient Appalachian Orogeny as shown by the box in Figure 3 (Humphreville, 1981). This area was covered by an epicontinental

seaway transgressing from the southwest which led to the deposition of the marine sediments. Terrestrial (fluvial) sediments were derived from the east and north (Flowers, 1956; Hoque 1968).

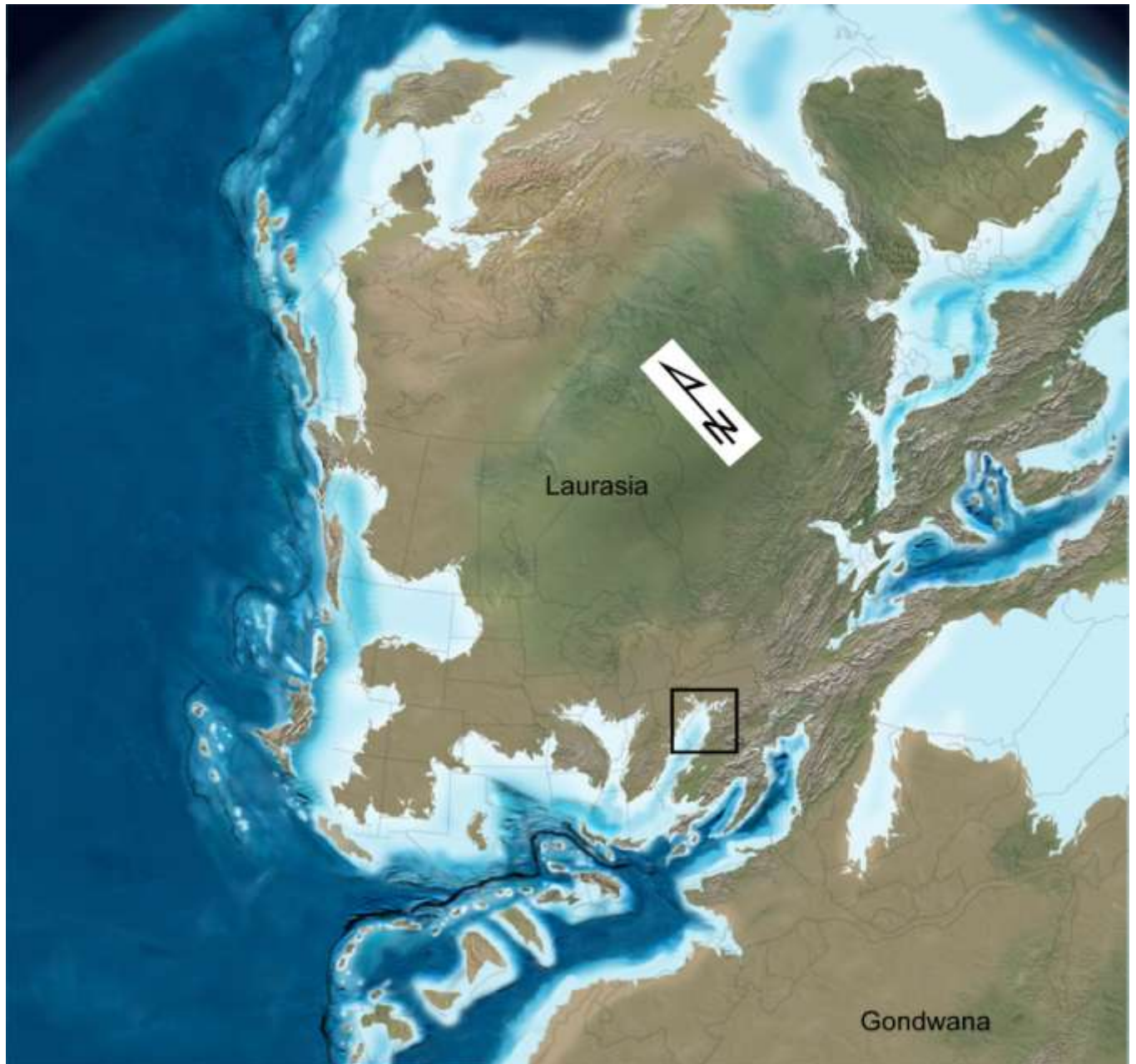


Figure 3: This is Blakey's (2011) recreation of the paleogeography of the late Mississippian. The study area is approximately shown by the black square.

PREVIOUS WORK

Reger (1920, 1921), Reger and Price (1926) and Hennen (1917) discussed the Mauch Chunk in their County Reports of West Virginia; however, any mention of Blue Monday is minor, giving its name and stratigraphic information. The Blue Monday sandstone is the oldest sandstone in the Bluefield Formation, which conformably overlies the Greenbrier Group (Cole, 2005). There are no accounts of early petroleum production.

Reger (1920) named the Webster Springs Sandstone and described it in the Webster County Report, and likened it to the subsurface drillers Blue Monday sandstone. According to Reger (1920) it is a massive or current-bedded, greenish-gray, micaceous, and medium-hard sandstone. He described a 50 to 75 feet thick section at “Lover’s Leap”, the base of which makes a series of cascades 10 to 15 feet high at Cherry Falls in the Elk River, southeast of Webster Springs. He suggested that this unit is the cliff-maker in Webster County and at Whitaker Falls at the Webster-Randolph County line, near the mouth of Deep Run. Also, at the mouth of Leatherwood Creek, there is a 100 foot thick cliff opposite the village of Bergoo (Reger, 1920).

Flowers (1956) studied the Middle Mississippian Greenbrier Limestone but also summarized the overlying strata. He described the Webster Springs Sandstone as a lenticular, fine to very fine grained sandstone with coarse siltstone beds. He postulated that the sand came from the east, though a source was not given. He suggested the Webster Springs or Blue Monday channel deposits were left by streams flowing southward but stated, “This latter possibility does not seem likely since marine shales or limestones occur everywhere beyond the limits of the sand body” (Flowers, 1956). His map (Fig. 4) shows his idea of the digitations extending to the north.

Carpenter (1976) discussed the Blue Monday in two quadrangles in Braxton and Gilmer counties, WV. He suggested that the Lillydale Shale (“Pencil Cave”) is the facies equivalent to the Blue Monday sandstone. He defined the Blue Monday as wedge-shaped, with finger-like digitations extending west. The sandstone is well sorted, white to light gray, very fine to fine-grained, and slightly to abundantly calcareous. He noted that the basal contact with the Greenbrier Limestone is sharp. An isopach map shows the sandstone to be thin (< 10 feet),

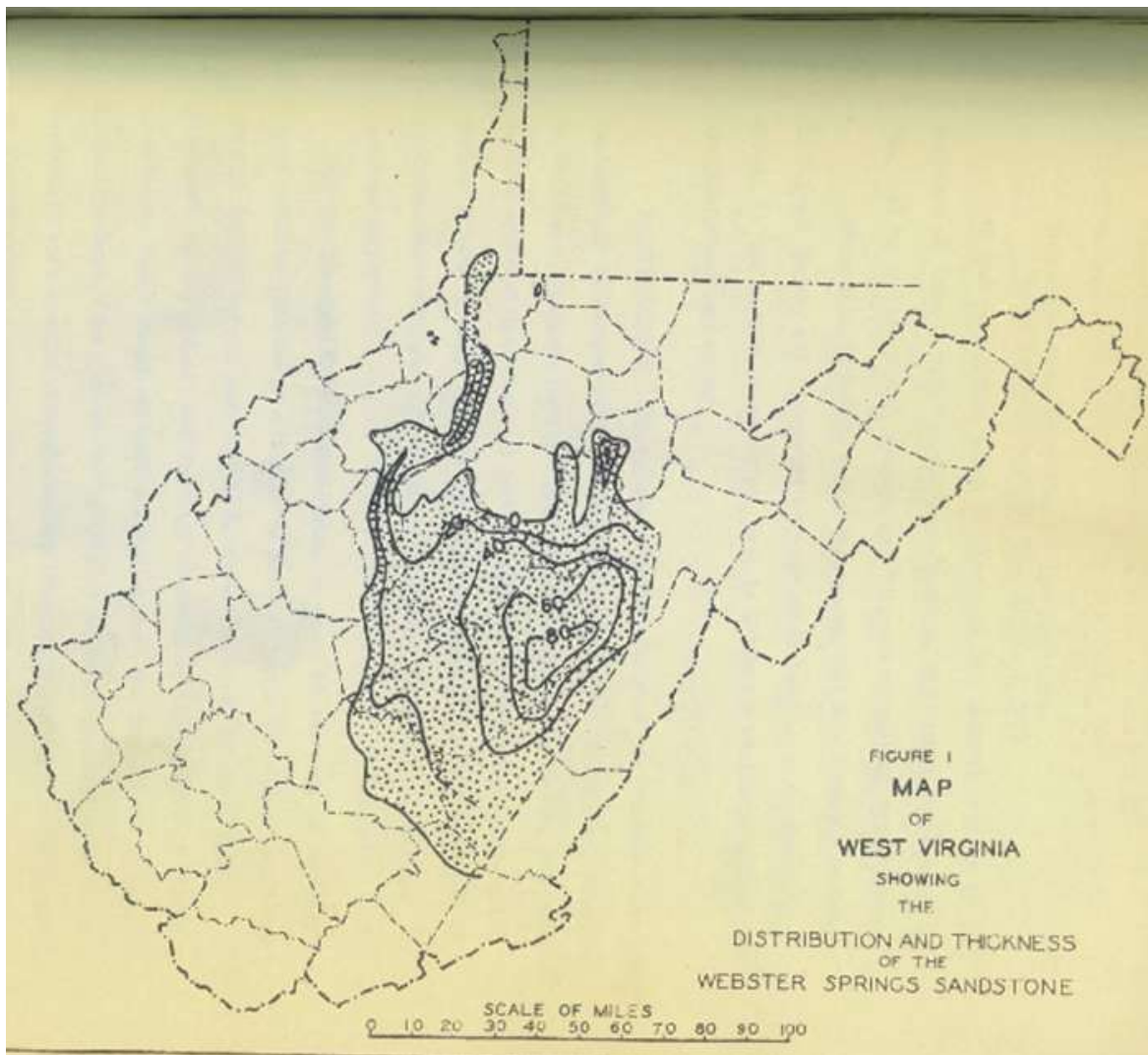


Figure 4: Isopach map created by Flowers (1956) to show the thickness (feet) of the Webster Springs Sandstone across West Virginia.

although there are thicker sections. He suggested tide-dominated submarine bars and/or tongues of an estuary as the depositional setting.

Barlow (1996) described gas production from the Mauch Chunk Group that consists of (in descending order) the Bluestone, Princeton, Hinton, and Bluefield formations. These formations include red, green and gray to black shale, sandstone, and limestone members. The Blue Monday is in the lower part of the Mauch Chunk. In central WV, it was a prolific producer. Nothing else is known except that it is equivalent to the Webster Springs Sandstone that has not been well documented (Barlow, 1996).

Neal (1997) discussed the Blue Monday sandstone (BMS) and its production history (Fig. 5). He defined the stratigraphic location between the Little Lime and Big Lime. Neal (1997) suggested the Blue Monday is a beach and shallow shelf sandstone located between continental deposits to the north and marine deposits to the south (Fig. 5). Thickness is less than 10 m (~30 feet) with linear accumulations of thick (>10 m) sandstone developed parallel to the inferred shoreline. He established the changes in color (and therefore depositional environment) of the Pencil Cave: green and red in the northern part of the state and gray to black in the southern part of the state. He suggested deposition of migrating beach ridges or tidal sand bars created these accumulations, but added that little is known about this stratum (Neal, 1997).

Wynn (2003) studied all of the Upper Mississippian sequence stratigraphy. He labeled the Webster Springs Sandstone and Reynolds Limestone as sequence C12, a lowstand-transgressive tract. This tract has a lowstand red bed system surrounded by sand and fed by the Taggard input system to the northeast. The Blue Monday sandstone was not discussed specifically; instead it was grouped with the rest of the Mauch Chunk Formation.

Blue Monday Interval

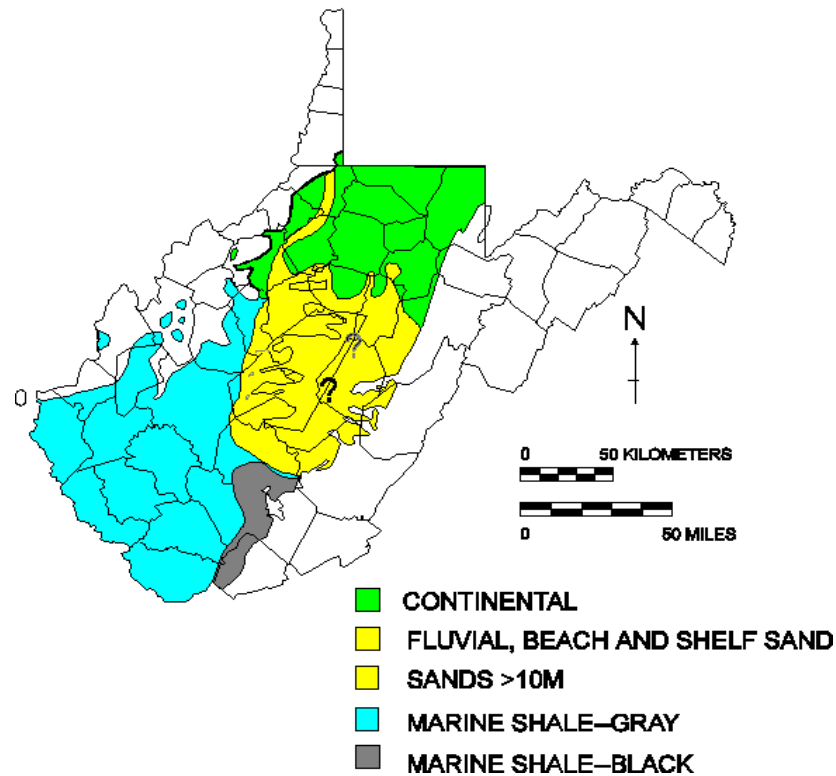


Figure 5: Neal's interpretation of the depositional setting of the Blue Monday (1997).

Cole (2005) studied the Reynolds Limestone in the outcrop belt in Garrett County, Maryland; Fayette County, Pennsylvania; and Grant, Monongalia, Pocahontas, and Randolph counties, West Virginia, but also discussed the Webster Springs Sandstone. He suggested that the Webster Springs represents a forced regressional event that is laterally discontinuous in his study of the over-lying Reynolds Limestone.

METHODS

Geophysical well logs were selected from the West Virginia Geological and Economic Survey (WVGES) online digital database. Many well logs were selected in order to give

uniform coverage across the study area (Fig. 6). Gamma ray logs were the primary type of log used in this study; they were chosen for their ability to measure natural radioactivity in formations (Asquith and Gibson, 1982) and were used to identify lithologies and correlate between wells. Other logs used were density-neutron logs to identify gas-bearing or liquid filled zones (Asquith and Gibson, 1982). Well logs used are shown in Appendix III.

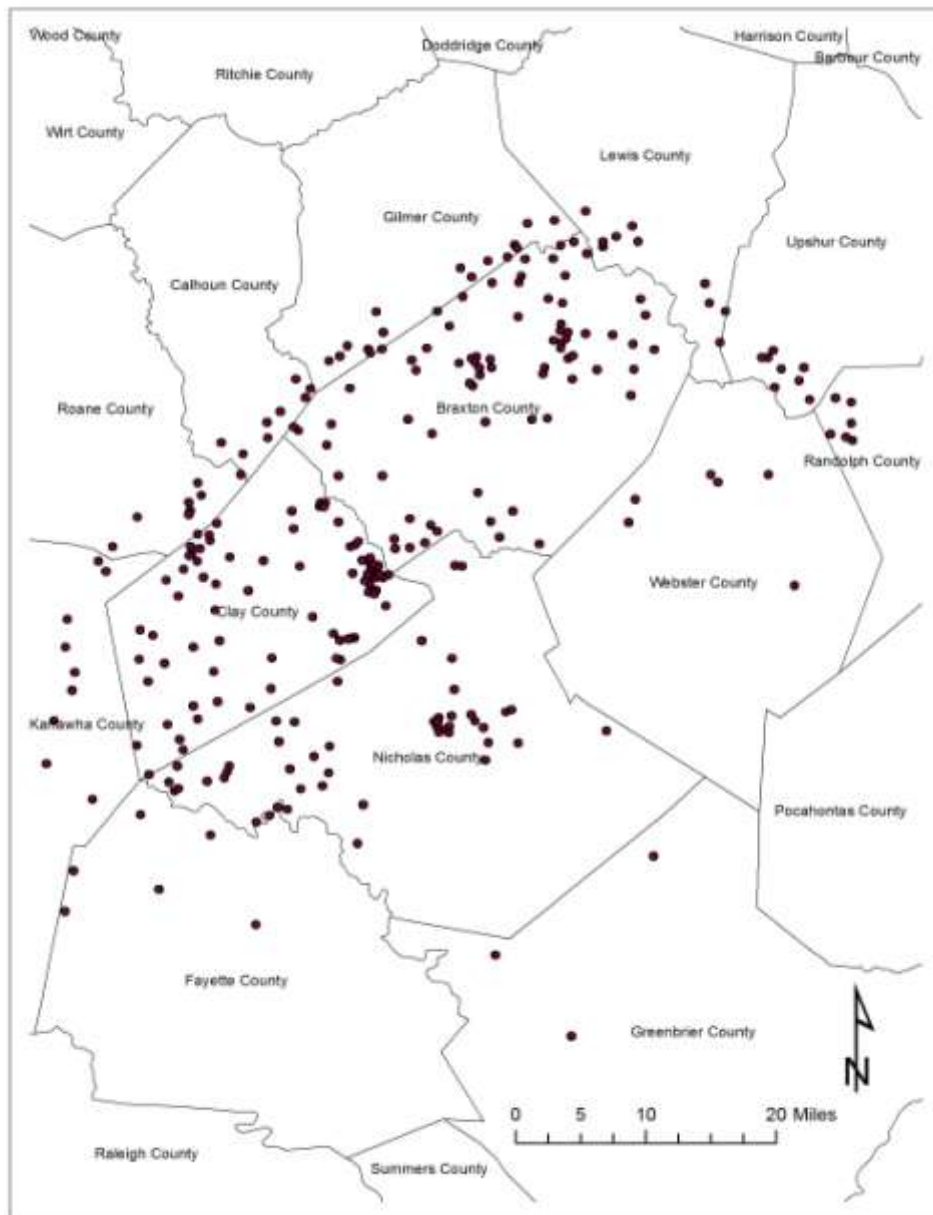


Figure 6: Location of wells used across the study area.

The stratigraphy of the section (Fig. 1) was obtained primarily using wireline well logs as well as previous investigations and data provided by the WVGES. A type log for this section is well #4701501796 (Fig. 7). The stratigraphy of this section is based on Reger's early classifications. The Big Lime is at the base of the study section. It has a variable gamma ray value of 20 to 60 API units. The Pencil Cave shale averages about 120 API units on the gamma ray log. The Blue Monday sandstone has the lowest radioactivity at 10 to 20 API units. The Little Lime is at the top of the section with a value of 50 to 65 API units.

API stands for the American Petroleum Institute and their units measure radioactivity in formations from the gamma ray tool. Carbonates and clean sandstones have low concentrations of radioactive material and give low API numbers (Asquith and Gibson, 1982). As shale content increases the API number also increases due to the radioactive material in shale. This radioactivity is due to the fact that the clay minerals often have a net negative charge and attract different cations.

Data from each well were gathered from WVGES. These included permit number, elevation of well head, total depth, and log types available. From these data and well logs, the thickness of each stratum, production data, type of show, completion method, which strata and if the well is producing were established. This collection of data is reported in Appendix IV. Production data were gathered from the West Virginia Department of Environmental Protection (WVDEP). Well cuttings from the Blue Monday sandstone interval were examined and described from four wells. Two of the wells were from Braxton County, numbers 4700700573 and 700700590 and two wells were from Clay County, numbers 4701500778 and 4701500835. These descriptions are in Appendix I.

Formal Name/ Drillers Name

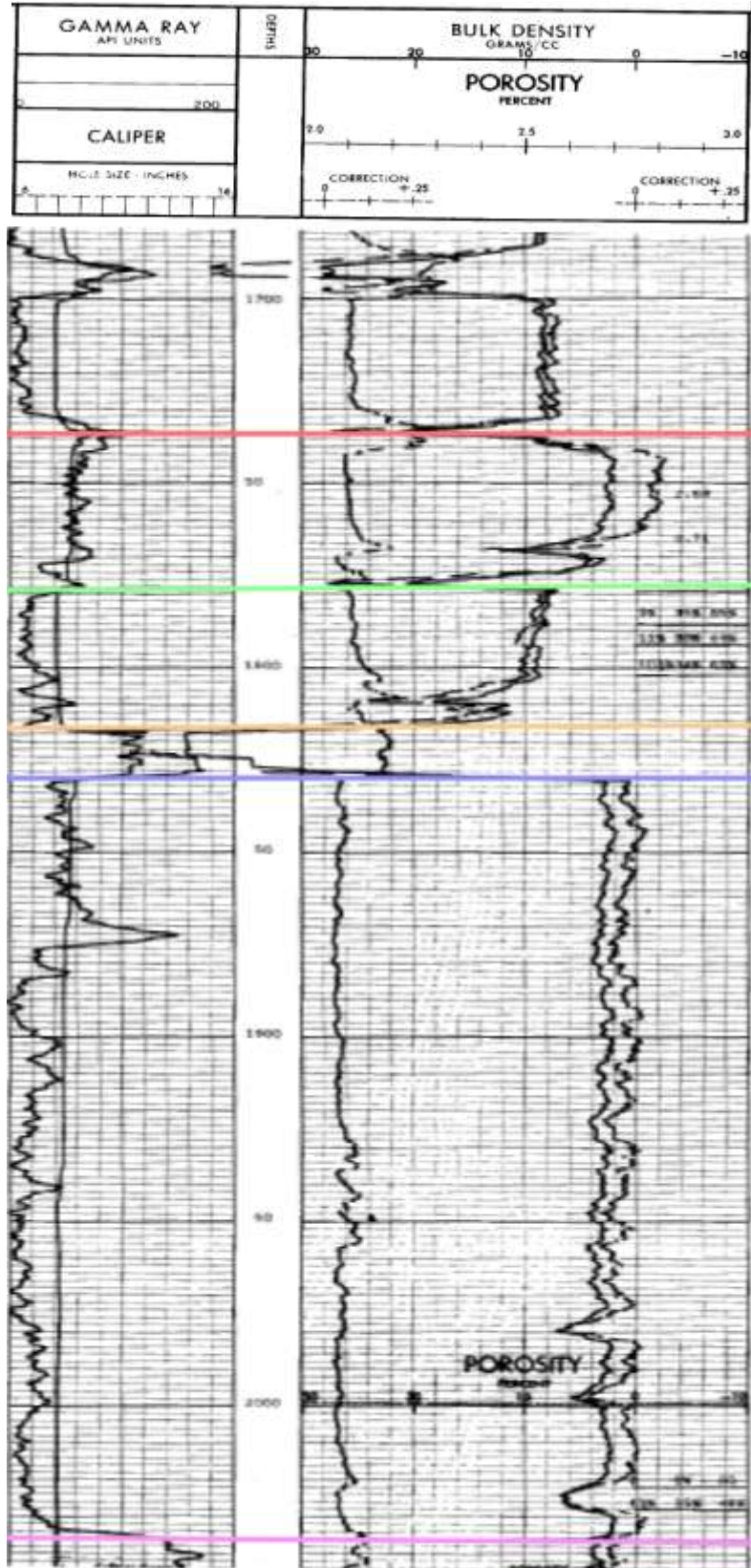
Reynolds Limestone/ Little Lime ~>

Webster Springs Sandstone/
Blue Monday sandstone ~>

Lillydale Shale/ Pencil Cave shale ~>

Greenbrier Limestone/ Big Lime ~>

Figure 7: Type log for the strata in question (shown above), well #4701501796. On the left side of the log, the jagged line shows the gamma ray and the straight line shows the caliper measurement. Depth is located down the middle in fifty foot increments. On the far right the bulk density porosity is shown. Scale for all measurements is shown at the top.



2 RESULTS

THICKNESS VARIATION

Within the study area the clastic interval between the top of the Greenbrier Limestone/ Big Lime and the base of the Reynolds Limestone/ Little Lime varies in thickness from 7 feet to 113 feet (Fig. 8). Each stratigraphic unit has an associated isopach map on which the small circles represent the wells used to construct that map. The warmer red colors represent thicker strata while the darker green colors represent thinner strata. The thicknesses are given in feet. These maps were created using ArcGIS 9.3.1, natural neighbor contouring method, with intervals shown in the scale.

The isopach map of the Blue Monday sandstone (Fig. 9) shows significant variation in thickness across the study area where thickness ranges from zero to 66 feet. Two north-south trending linear trends are located in central Braxton County and eastern Clay County with thicknesses up to about 45 feet. An area of thickening on the eastern edge of Webster County and extending into Upshur and Randolph counties appears to run parallel to the trends in Braxton and Clay counties but is truncated by the outcrop and the limit of the study area. The Blue Monday sandstone is a cliff former of about 80 feet thick in outcrop (Reger, 1920). These linear trends are truncated by an east-west trending area of thick Blue Monday sandstone located across Nicholas County. Geographic control on the location and extent of this thickening is limited in the eastern part of Nicholas County and Webster County due to a paucity of wells. The Blue Monday sandstone thins to the south and west where it can be recognized as a thin sandy interval usually less than 10 feet thick. There is also marked thinning between the linear trends in the northern half of the study area.

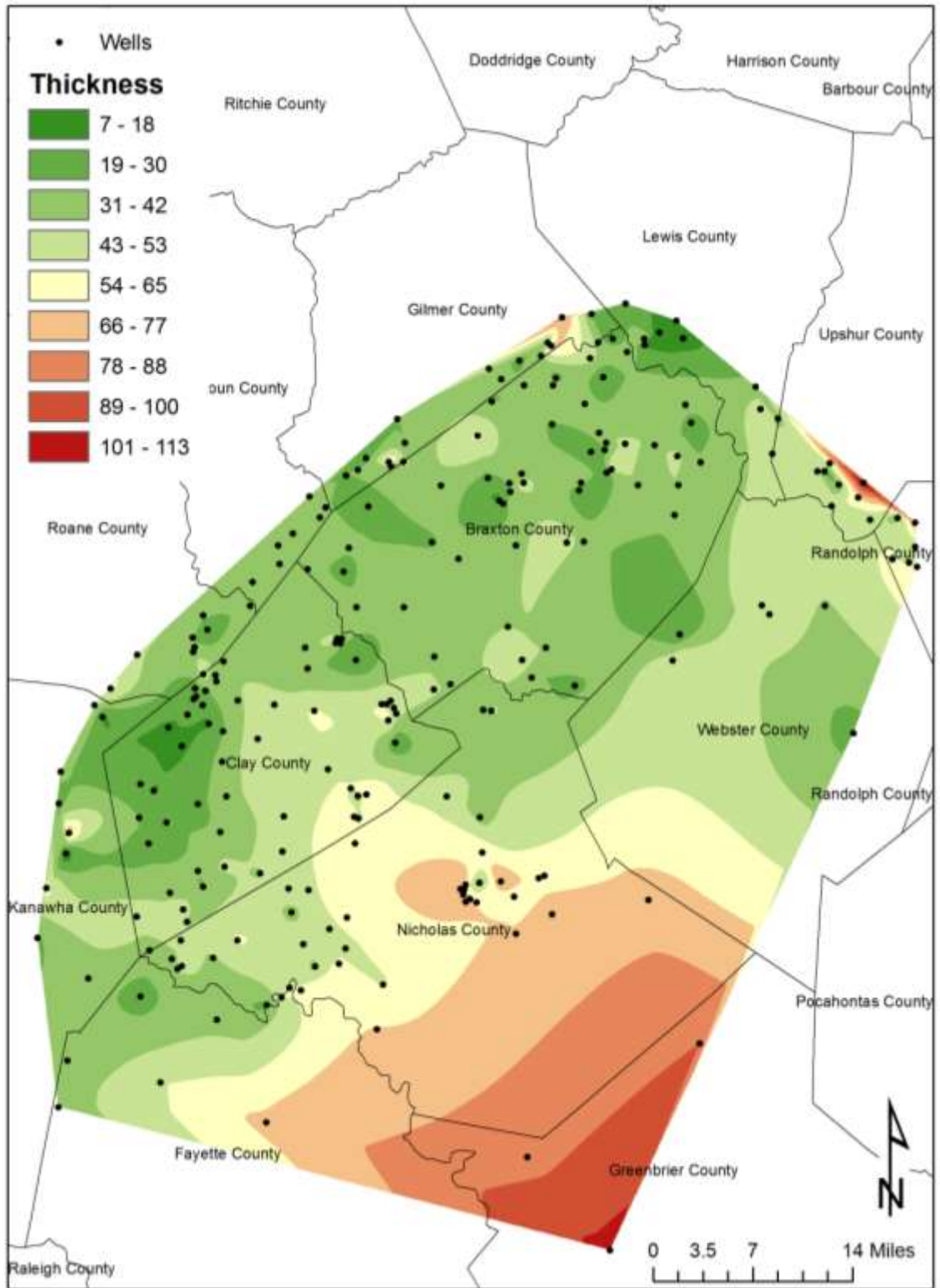


Figure 8: Isopach map showing the thickness of the clastic units from the base of the Little Lime to the top of the Big Lime.

Above the Blue Monday sandstone is the Little Lime (Reynolds Limestone). The Little Lime isopach map (Fig. 10) shows a thickness ranging from 10 to 40 feet across most of the study area with the exception of a thickening of strata (to 112 feet) in northern Nicholas and Webster counties and in northern Fayette County. These areas of thickening occur to the north and south of the trend of thickening in the underlying Blue Monday sandstone.

At the base of the Little Lime is a transitional shaly interval. In southern West Virginia this interval is designated the Bickett Shale (Reger and Price, 1926). In the study areas the shaly interval is usually less than 15 feet and is included with the Little Lime isopach.

Below the Blue Monday sandstone is the Pencil Cave (Lillydale Shale). The Pencil Cave shale isopach map (Fig. 11) shows uniform thinning of the unit from a thickness of about 90 feet in the south to a thickness of about 30 feet in the middle of Nicholas County. North of this line the Pencil Cave has an irregular variation in thickness. Within this area there are places where the Pencil Cave is not present (Fig. 12). These areas correspond to locations in Clay and Braxton counties where the overlying Blue Monday sandstone is thick (Fig. 9). There is no correspondence between thinning of the Pencil Cave and the thickening of the Blue Monday sandstone in Nicholas County.

The underlying Big Lime (Greenbrier Limestone) ranges from 92 feet to 613 feet across the study area (Fig. 13). The pattern of variation in thickness is very much like that of the Pencil Cave shale with a more uniform thickening in the south and a more variable thinning in the north and west. Axes of thinning in northern Nicholas, Clay and Braxton counties correspond generally with areas of thickening in the Blue Monday sandstone.

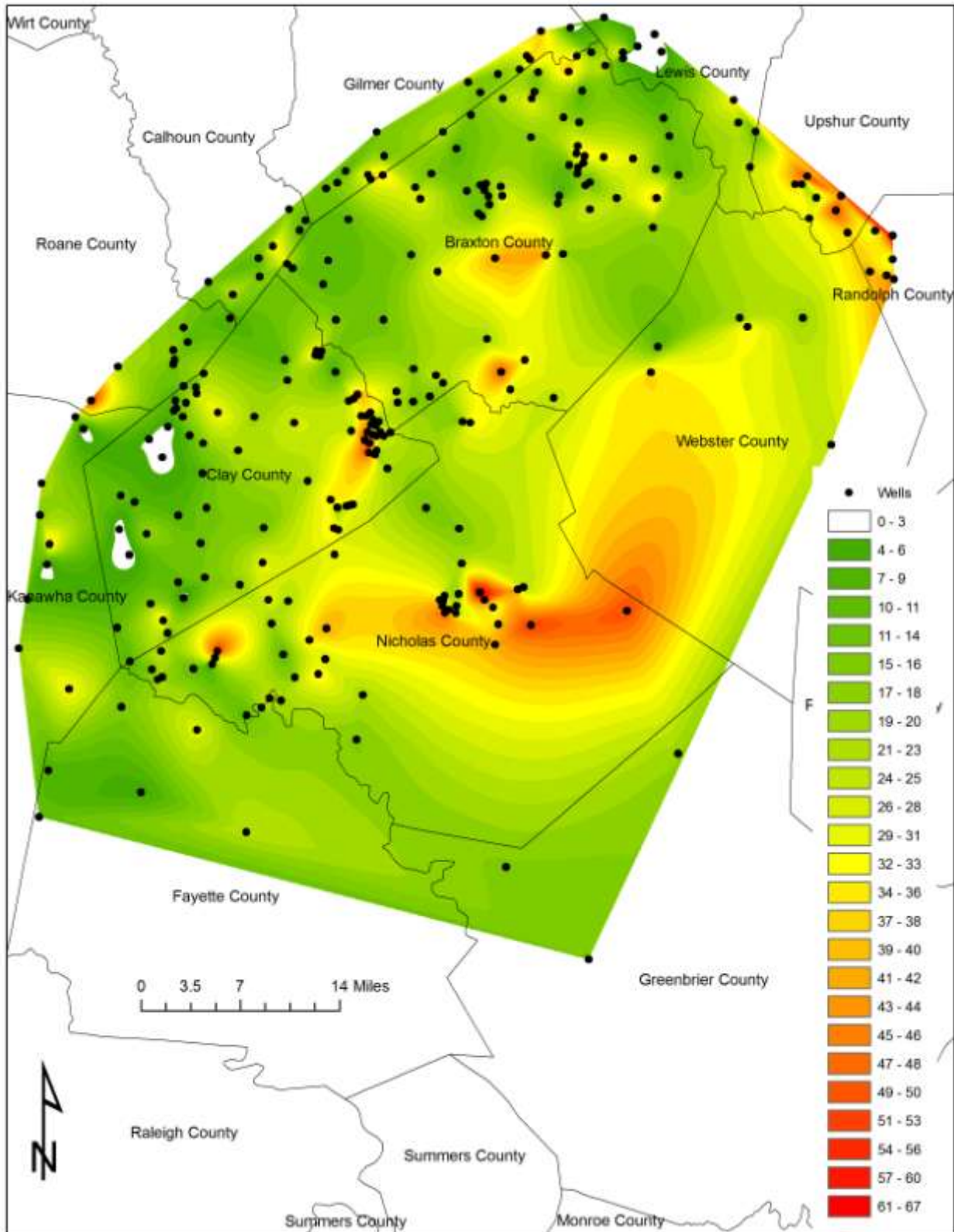


Figure 9: Blue Monday (Webster Springs) sandstone isopach map showing thickness of the stratum in feet.

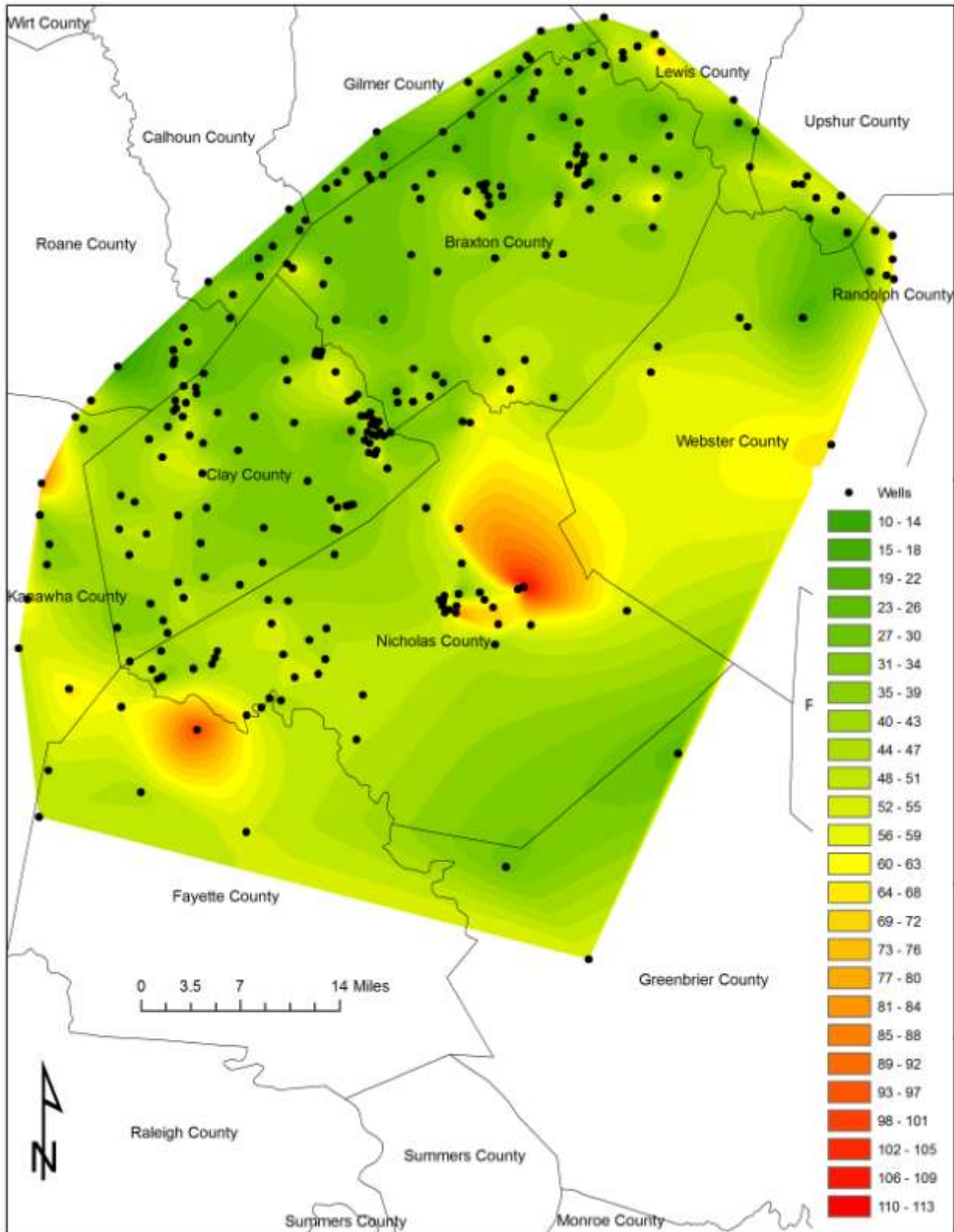


Figure 10: Little Lime (Reynolds Limestone) isopach map showing thickness of the unit in feet.

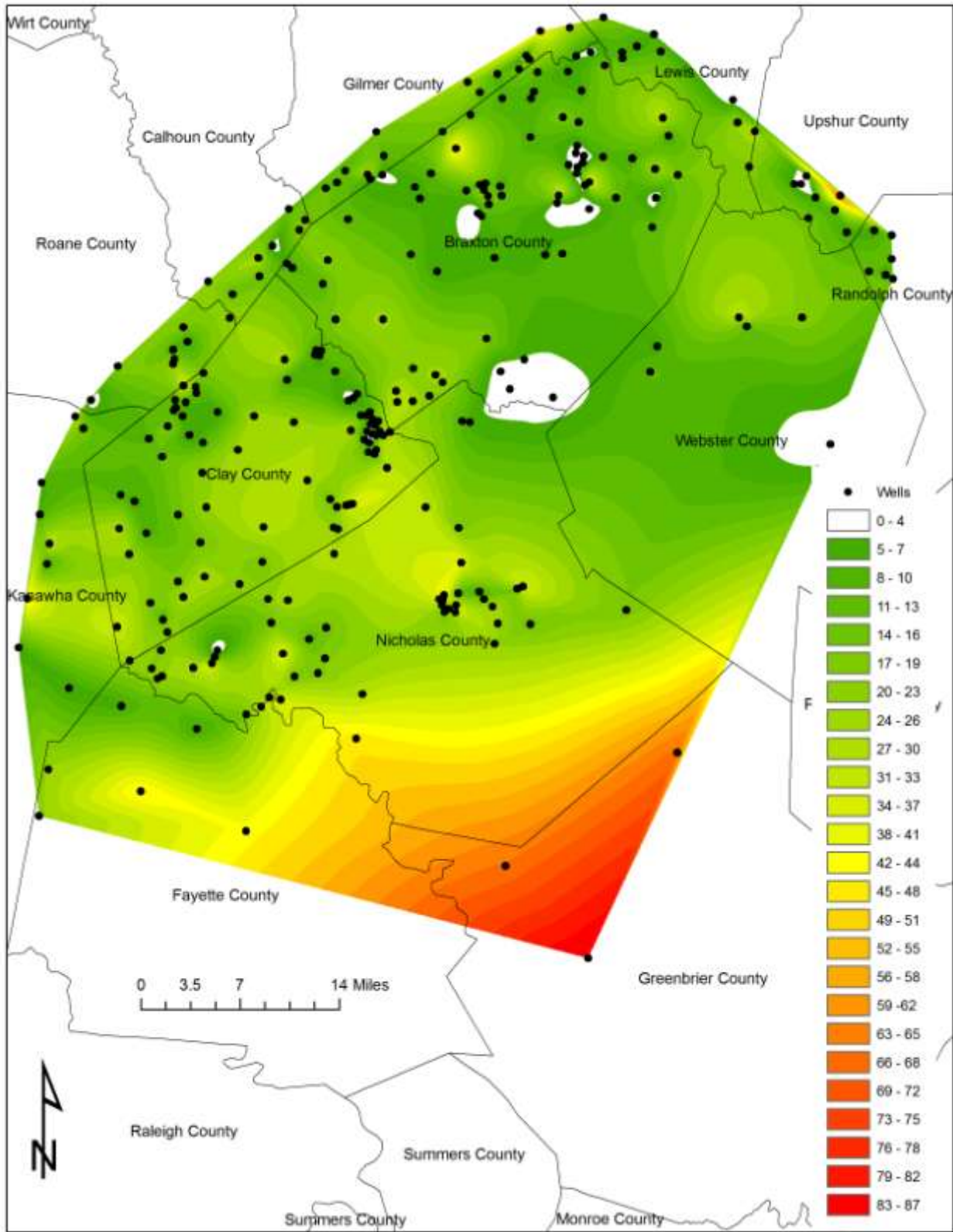


Figure 11: Isopach map of the Pencil Cave shale (Lillydale Shale) thickness of the stratum in feet.

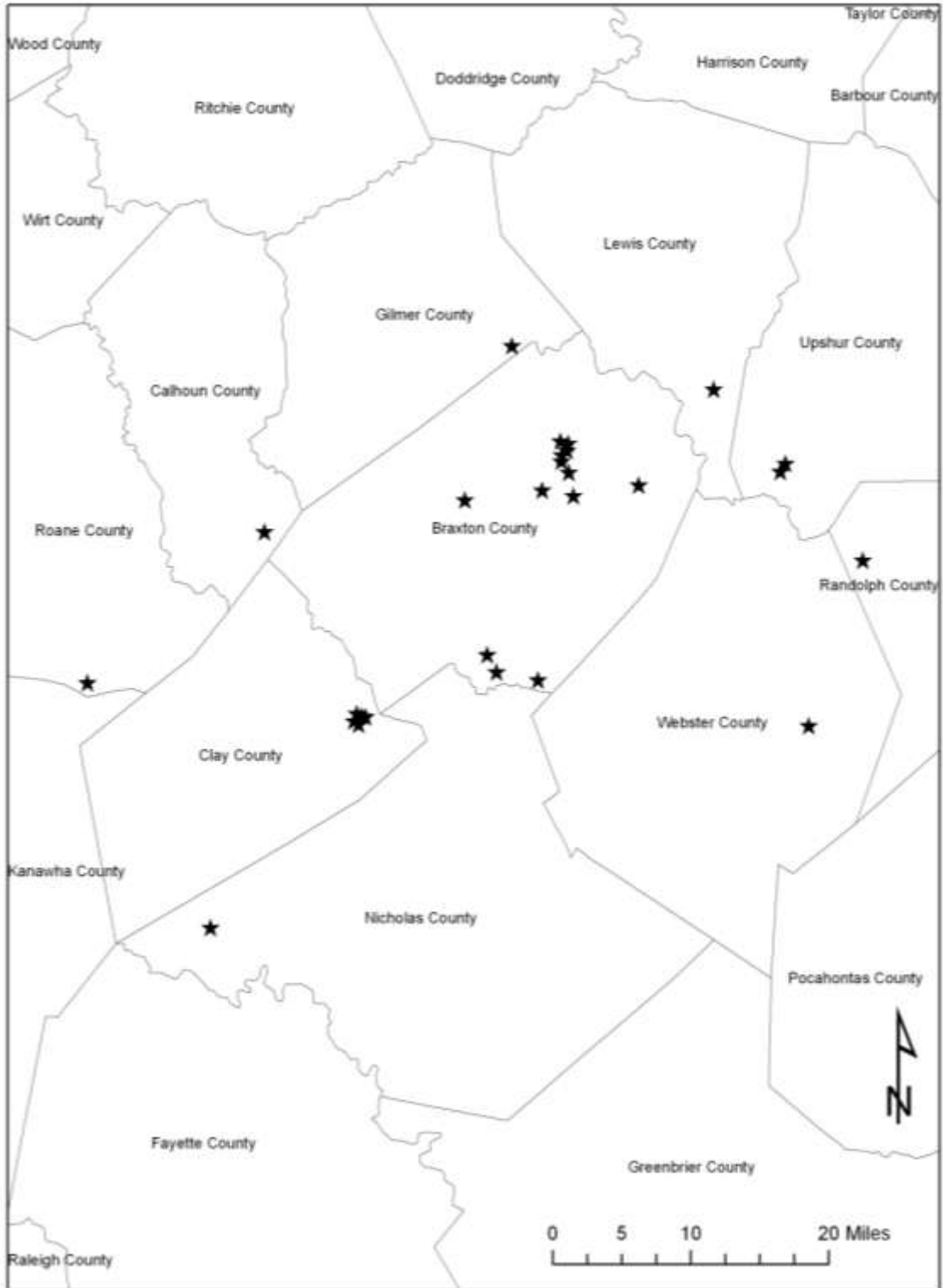


Figure 12: Map showing the locations of the wells with no Pencil Cave shale in the stratigraphic column.

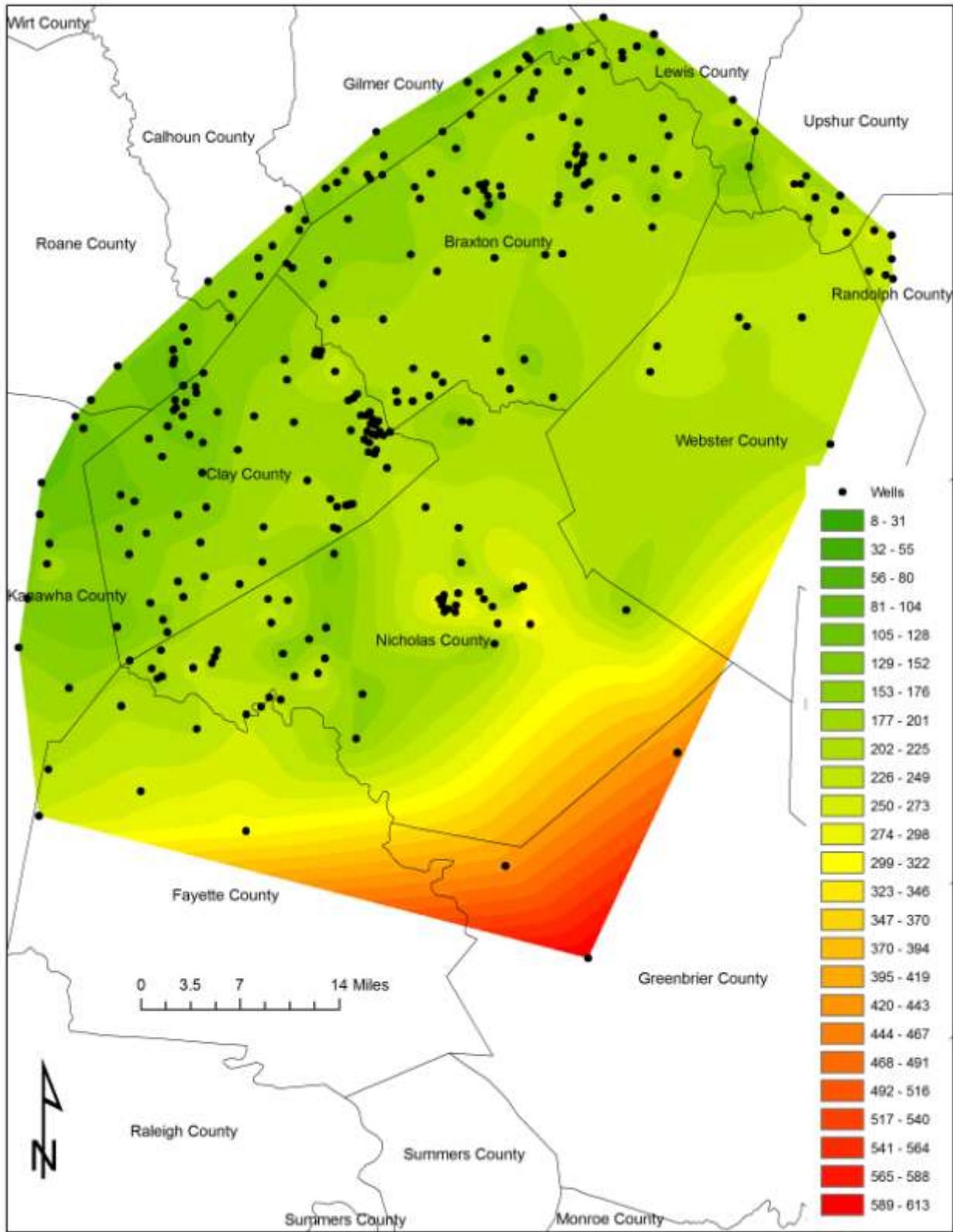


Figure 13: Map showing thickness of the Big Lime (Greenbrier Limestone) over the study area in feet.

CROSS SECTIONS

The following cross-sections show a red line marking the top of the Little Lime, the green marks the base, which also marks the top of the Blue Monday sandstone. The orange line at the base of the sand marks the top of the Pencil Cave, whose base is shown by a purple line. This purple line also marks the top of the Big Lime, whose base is shown by a pink line. The datum for the cross-sections is the Little Lime. The sandy strata of the Blue Monday are highlighted in yellow. Each well log is identified by the last three or four digits of the API number assigned to each well and the first letter of the county where it is located. The location map located under each cross-section shows the county names, locations of the wells, and full API numbers of the wells included in the cross-section. The locations of all of the cross-sections are shown in Figure 14.

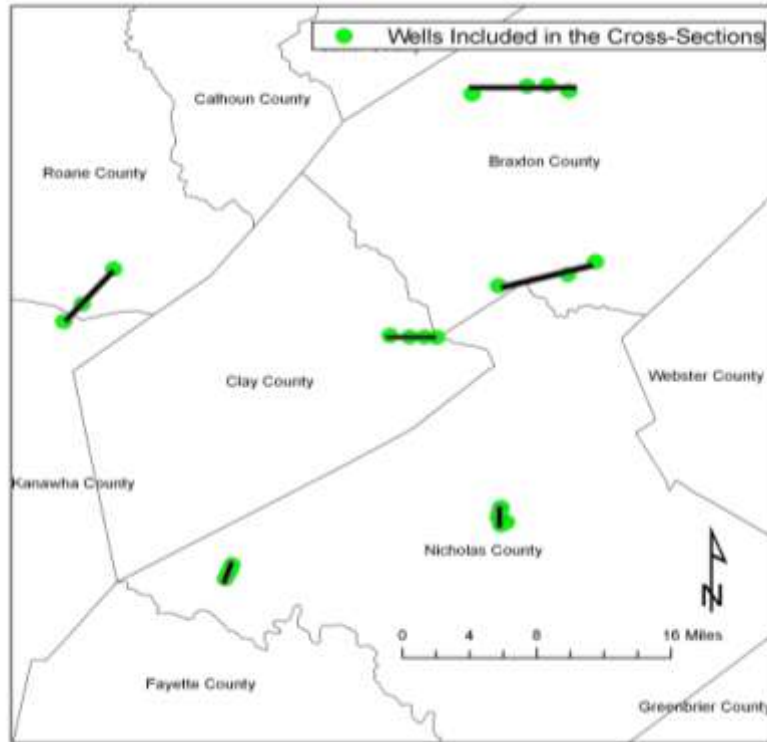


Figure 14: Location of wells included in cross-sections.

Figure 15 shows a cross-section in southern Braxton County. The Blue Monday sandstone is thick in well 1135B. At least three intervals are recognized separated by shaly layers. The Pencil Cave shale is thin in well 1135B and well 1409B. The Pencil Cave thickens in well 2105B where the deposition of sand occurred in pulses over time rather than during one large event.

Figure 16 shows a cross-section in north central Braxton County. It shows the Blue Monday sandstone progressing from a thick uniform sand in the west to pulses of deposition towards the east. These pulses of deposition (Kirkland, 1985) are separated by a small spike on the gamma ray. This and other spikes in other cross-sections indicate shale intervals due to higher amounts of radioactivity being read by the gamma ray tool. The spikes get progressively bigger towards the eastern end of the cross-section, further away from the uniformly thick sandstone. The Pencil Cave shale is thin towards the west and thickens considerably to the east.

Figure 17 is a cross-section in eastern Clay County. The Blue Monday sandstone thickens towards the center of the cross-section. The underlying Pencil Cave shale is thin where the Blue Monday sandstone is thick. The Blue Monday sandstone thins as the Pencil Cave shale thickens. The Blue Monday sandstone shows thinner intervals separated by shaly intervals away from the thick intervals.

Figure 18 is a cross-section in eastern Roane and Kanawha counties. The Blue Monday sandstone is a thick, low gamma ray sand in well 714Ro, with no Pencil Cave shale in the column due to scouring down to the underlying Big Lime. To the north and south, sand was deposited, with less scouring of the Pencil Cave shale. In well 4778K the Blue Monday sandstone coarsens upward.

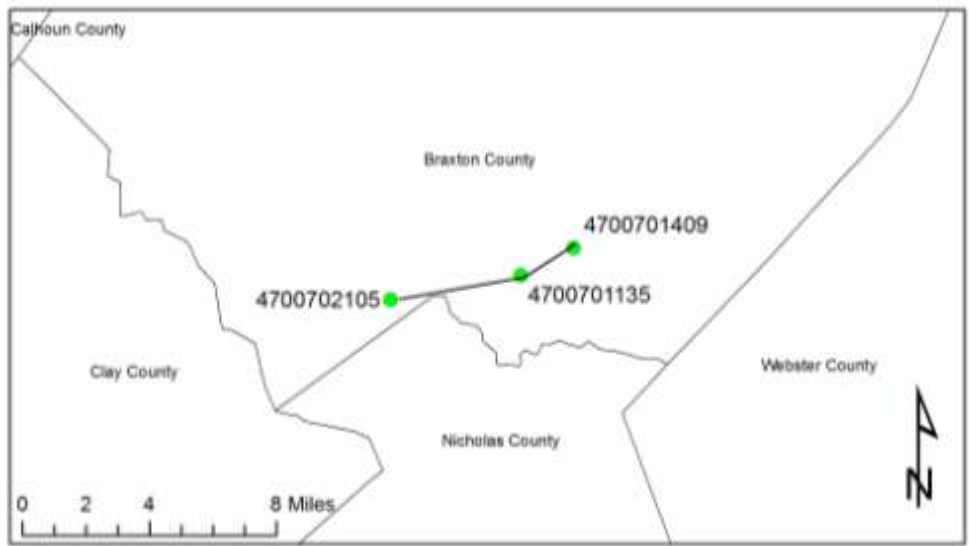
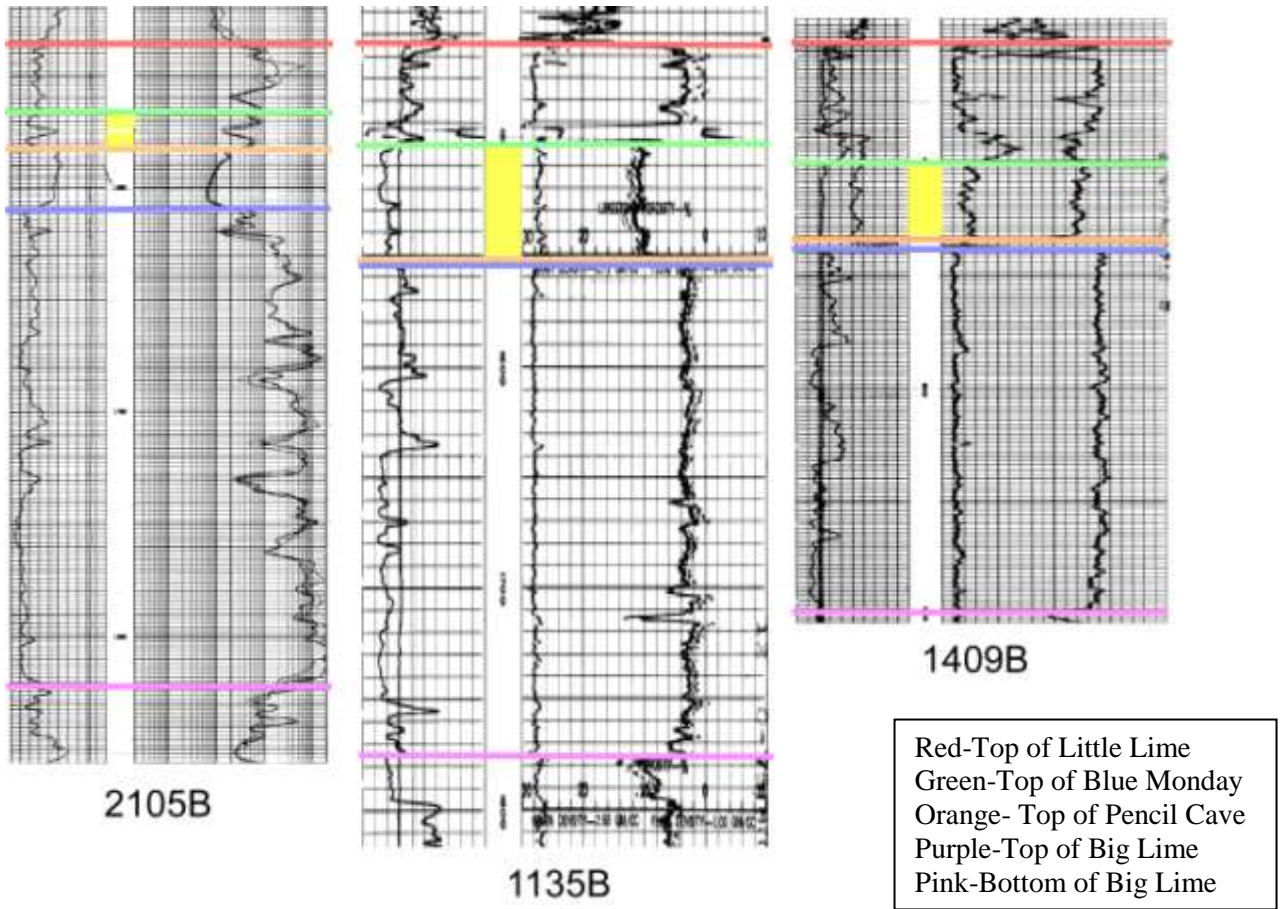
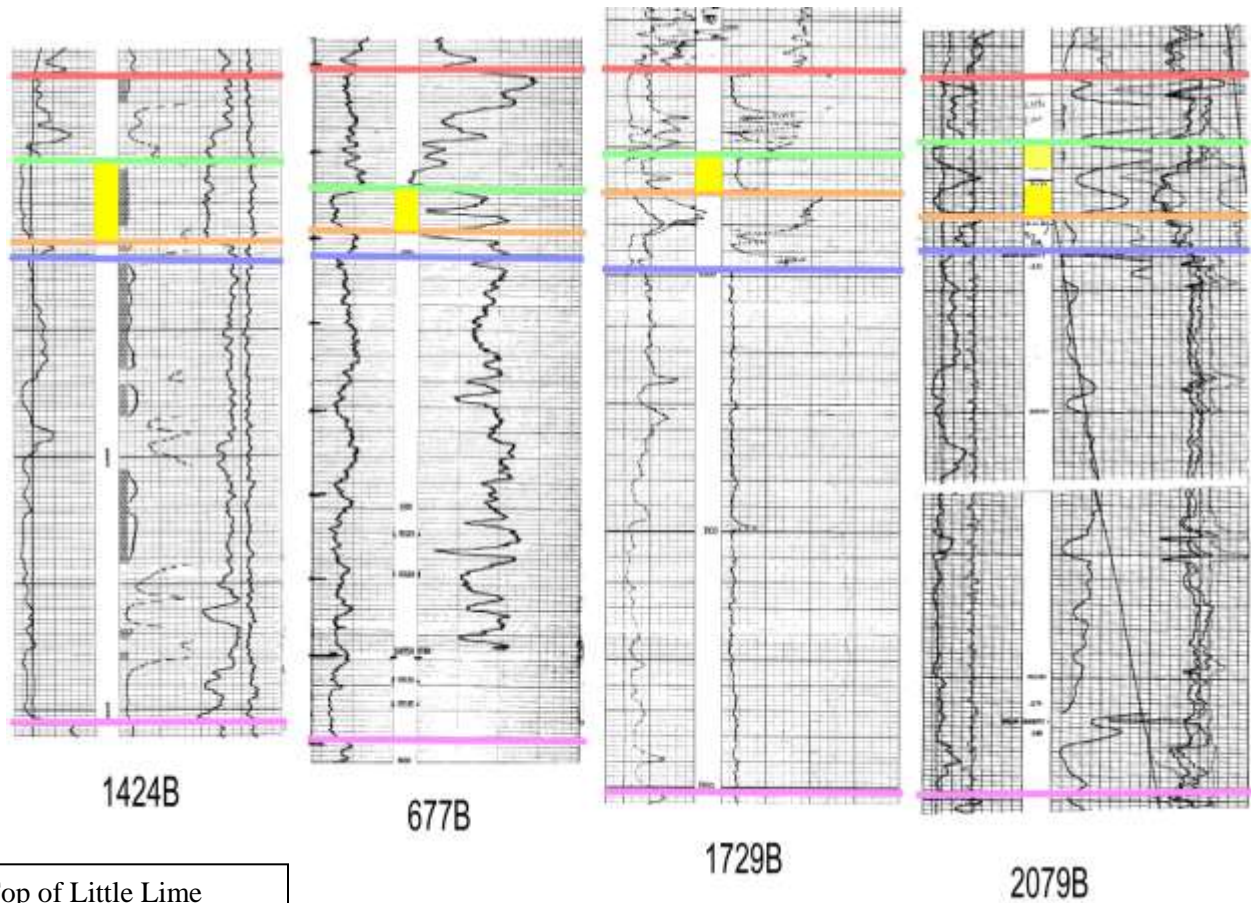


Figure 15: Southern Braxton County cross-section and associated location map.



Red-Top of Little Lime
 Green-Top of Blue Monday
 Orange- Top of Pencil Cave
 Purple-Top of Big Lime
 Pink-Bottom of Big Lime

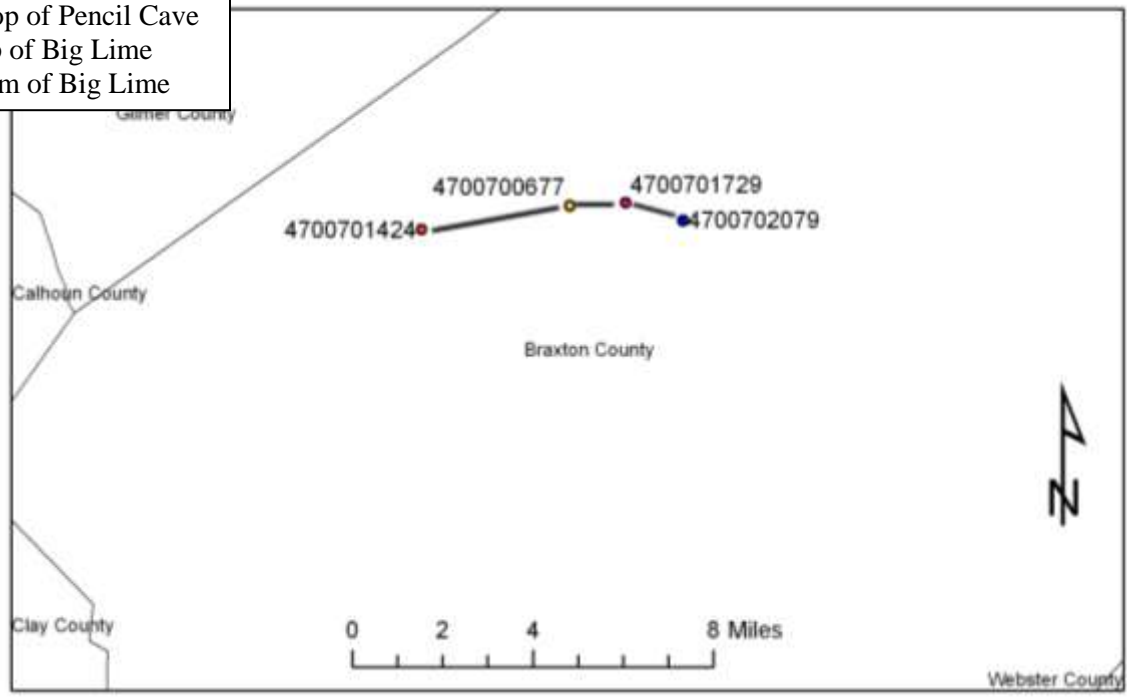
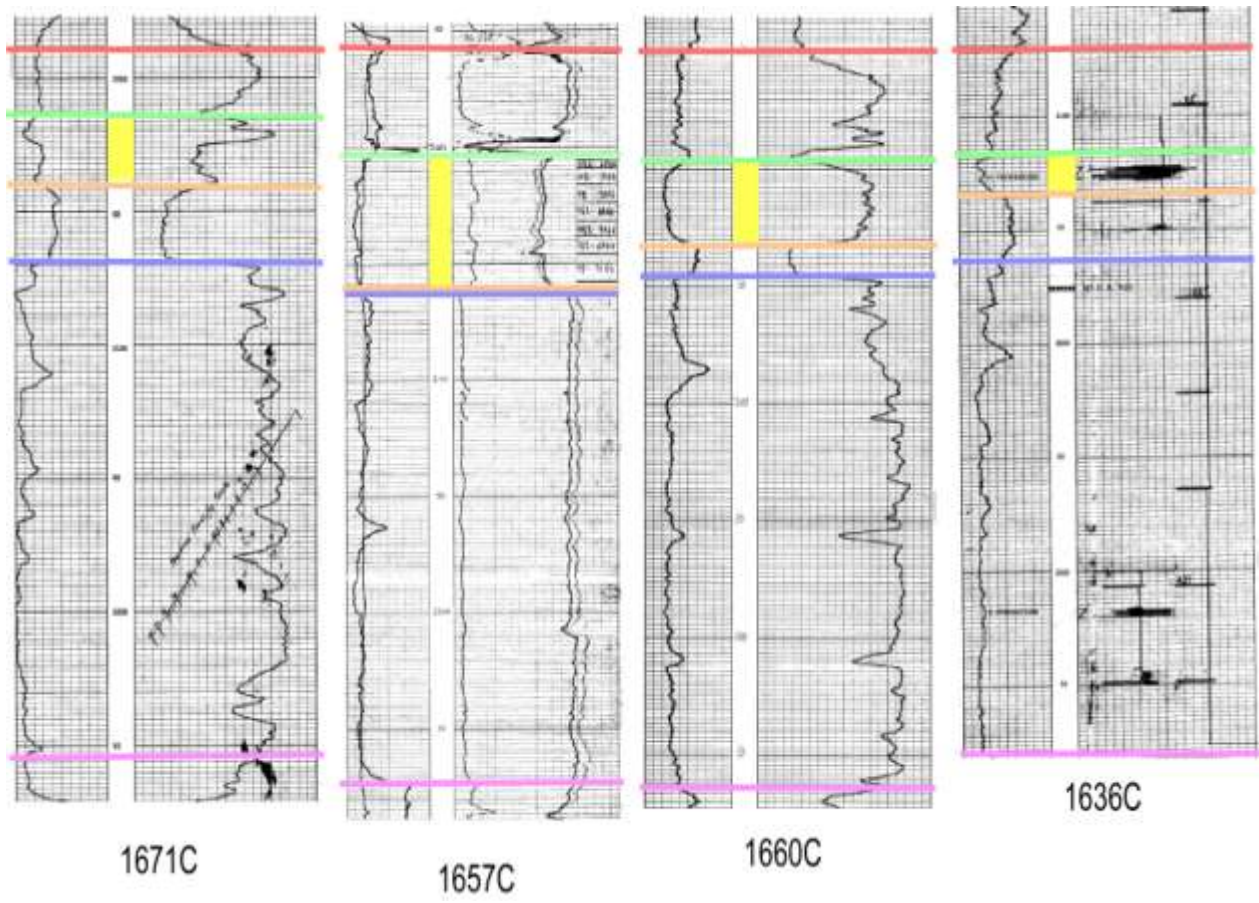


Figure 16: Northern Braxton County cross-section and associated location map.
 23



Red-Top of Little Lime
 Green-Top of Blue Monday
 Orange- Top of Pencil Cave
 Purple-Top of Big Lime
 Pink-Bottom of Big Lime

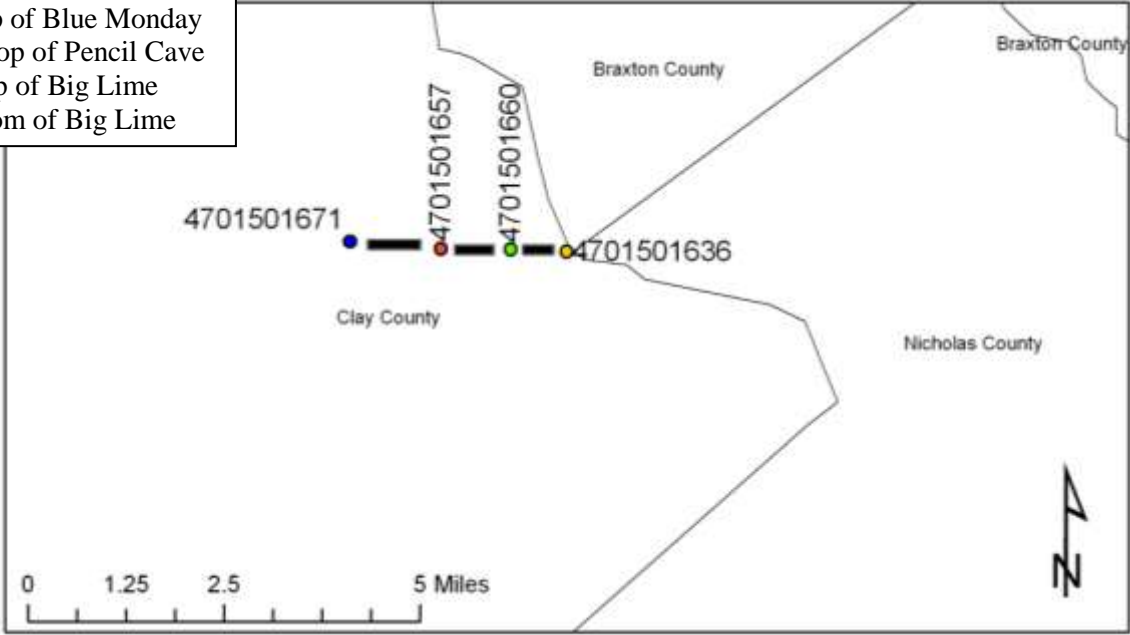


Figure 17: Eastern Clay County cross-section and associated location map.

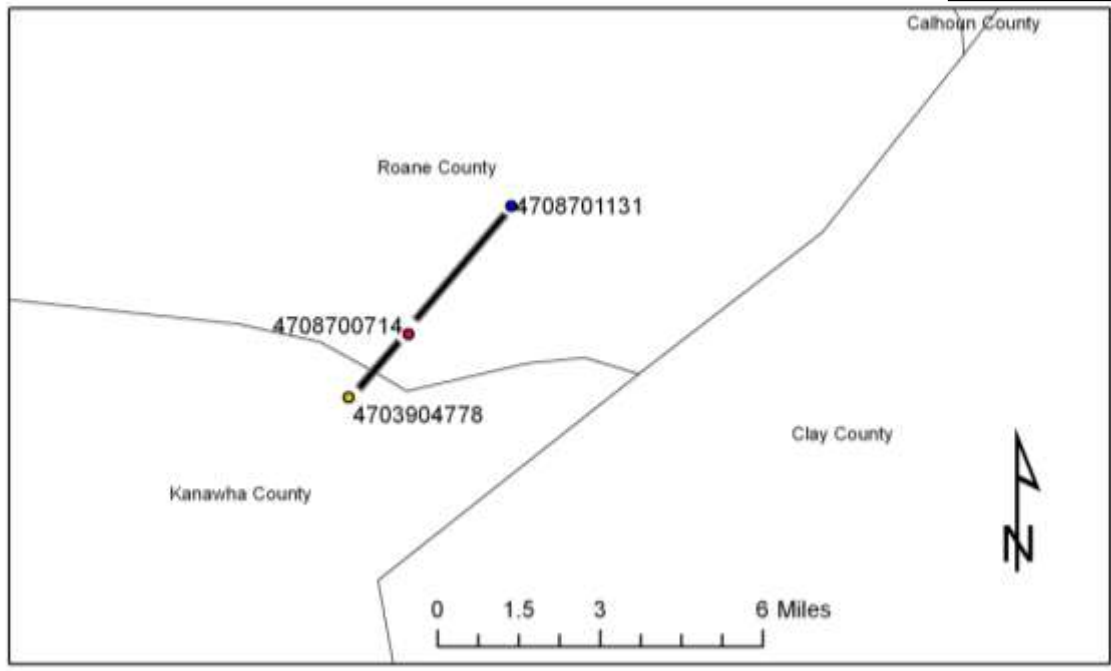
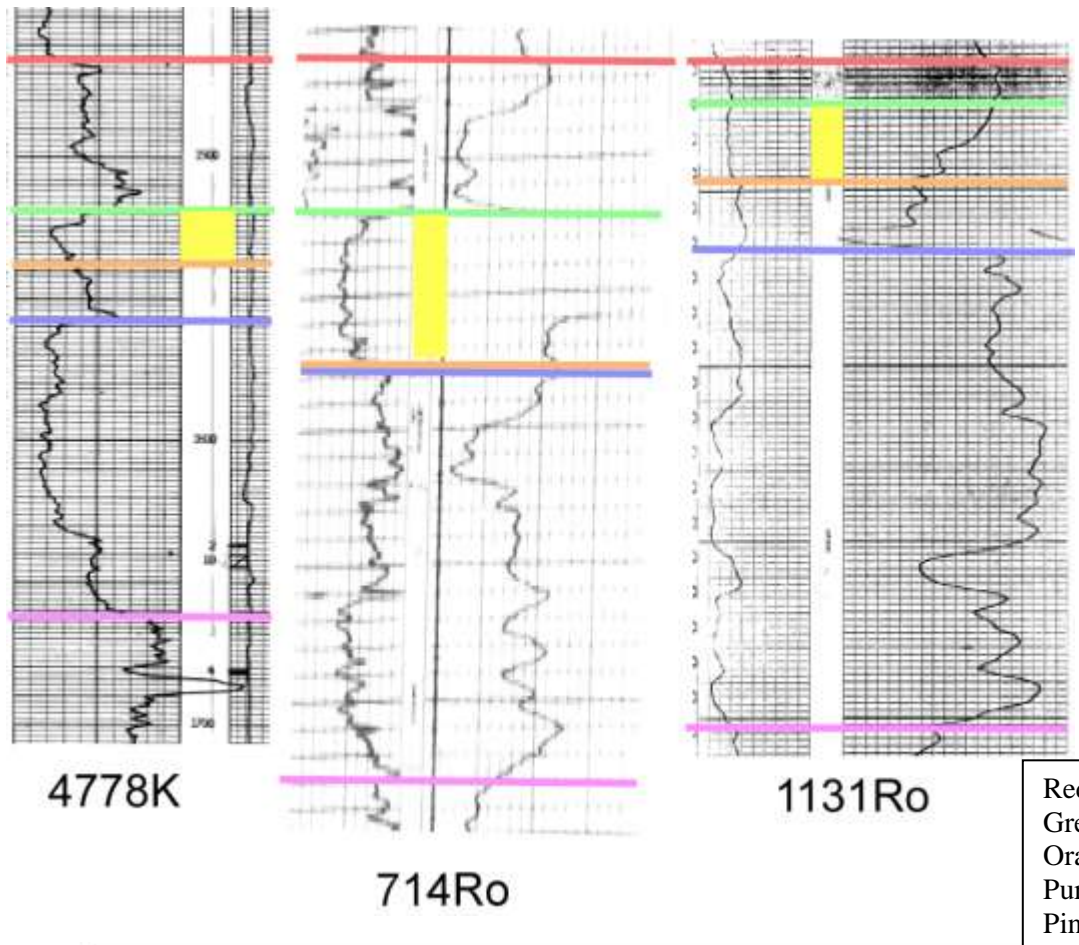


Figure 18: Kanawha and Roane counties cross-section and associated location map.

Figure 19 is a north-south cross-section in western Nicholas County. The Blue Monday sandstone thickens towards the north and thins abruptly to the south. The Pencil Cave is thin where the Blue Monday sandstone is thickest; the Pencil Cave gets progressively thicker to the south as the Blue Monday thins. Where the Blue Monday is thinnest, the Pencil Cave has caved into the well and created an atypical peak in porosity. Well 451N is uniformly low gamma ray sandstone whereas 523N shows a similar sandstone at the base with a more shaly sandstone signature above.

Figure 20 is a north-south cross-section from central Nicholas County. It shows the Blue Monday sandstone as a consistently thick sand across this area. The Pencil Cave shows some caving in the northernmost two wells.

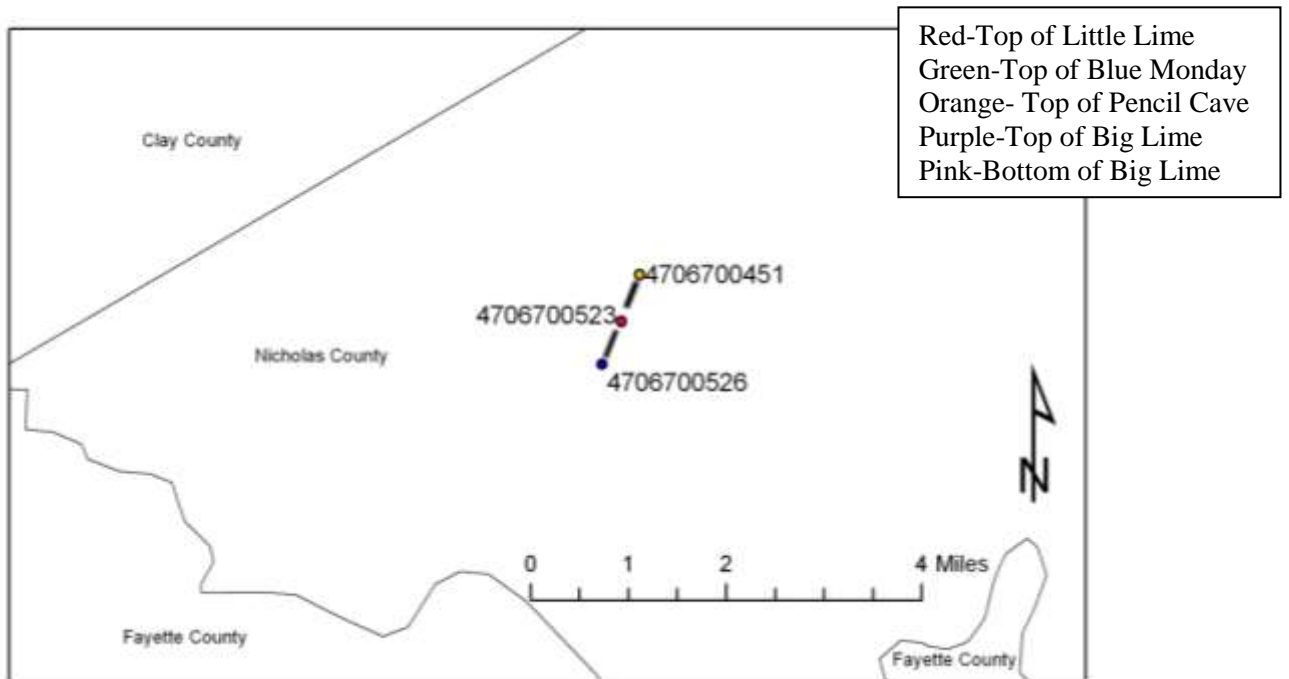
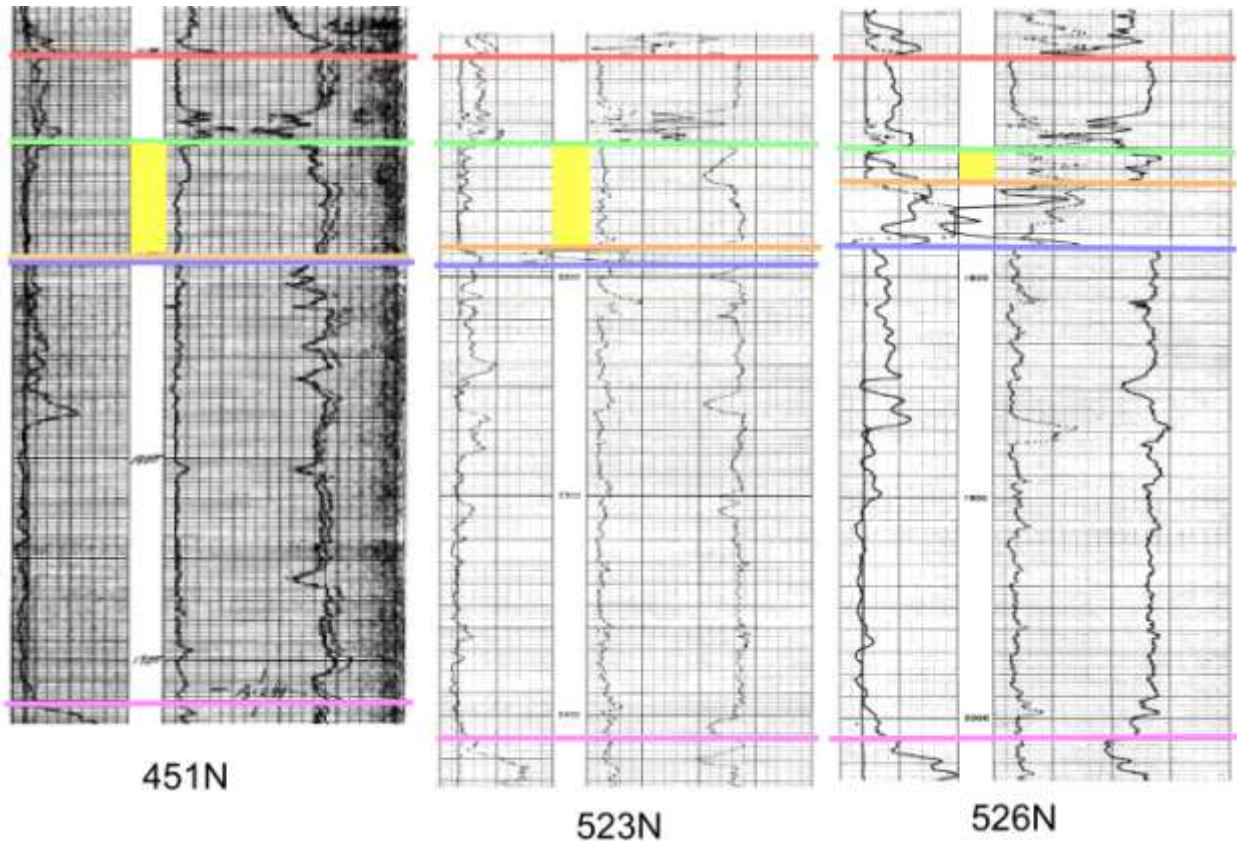
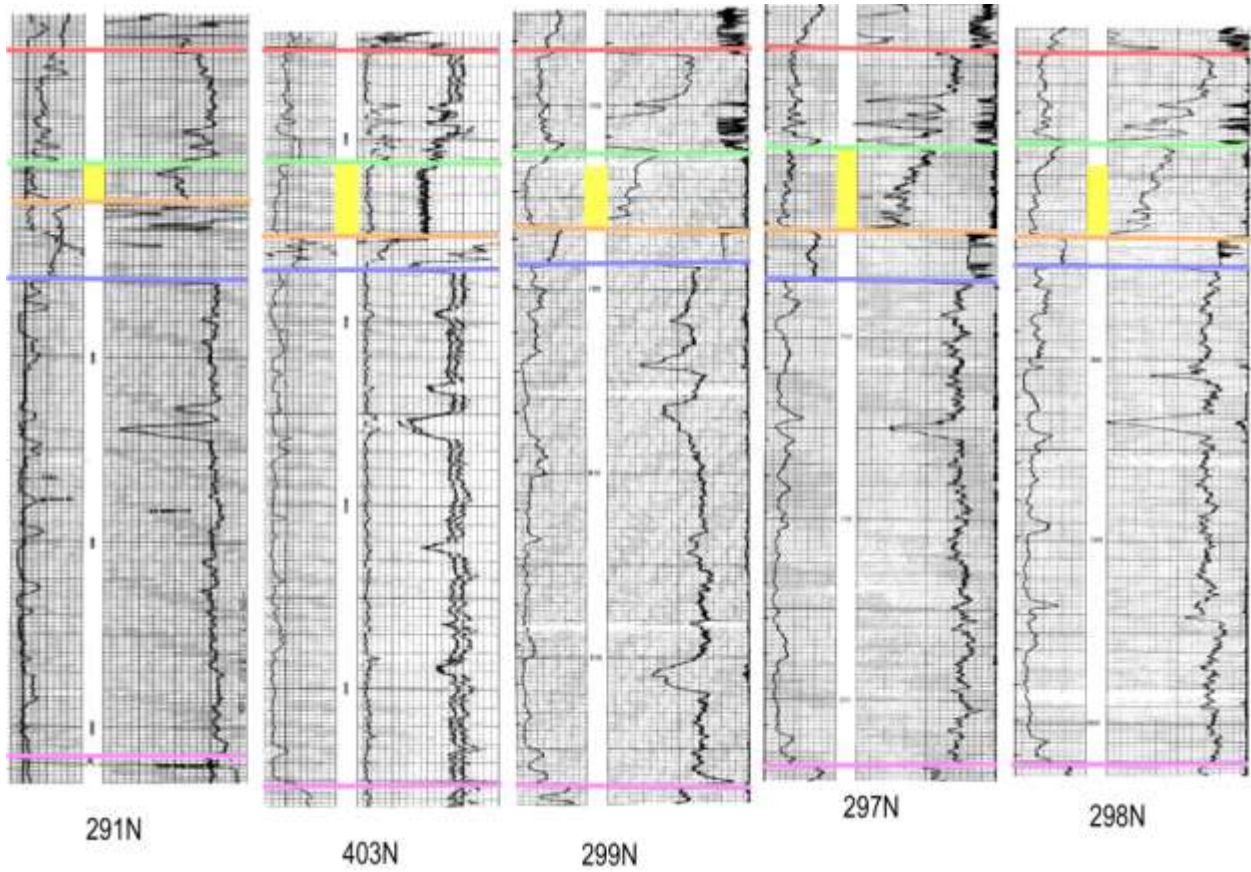


Figure 19: Western Nicholas County cross-section and associated location map.



Red-Top of Little Lime
 Green-Top of Blue Monday
 Orange- Top of Pencil Cave
 Purple-Top of Big Lime
 Pink-Bottom of Big Lime

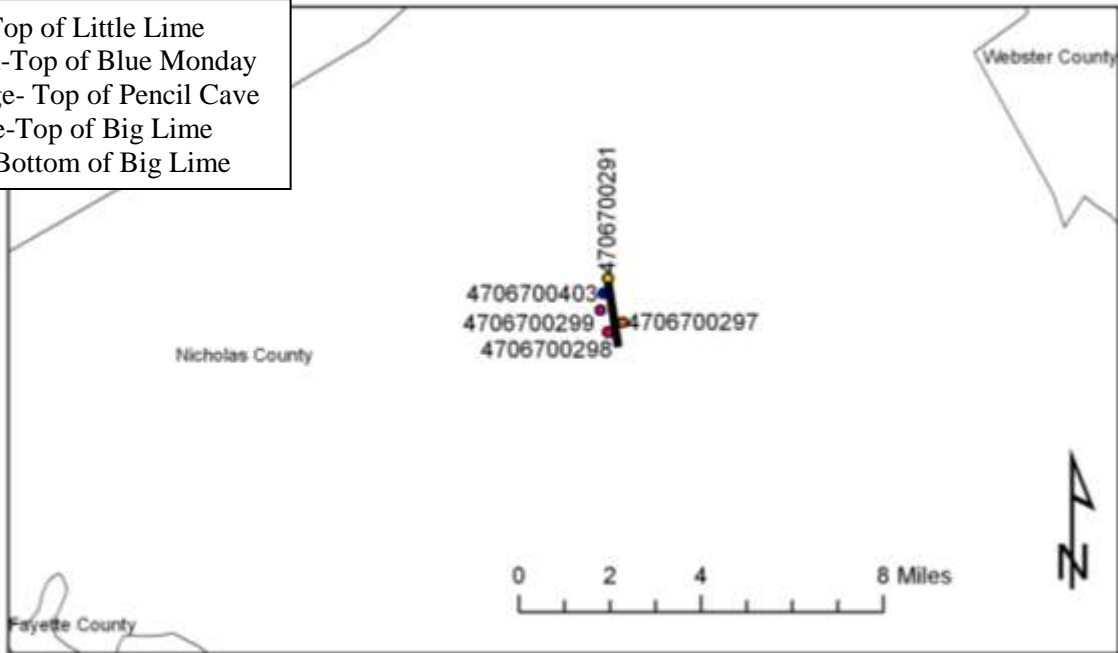


Figure 20: Central Nicholas County cross-section and associated location map.

The basement structure map (Fig. 22) shows the Rome Trough to the west of the study area which is shown by the box. The Blue Monday sandstone is not found west of the study area because of the Pennsylvanian sands coming from the north and eroding away underlying sediments, as well as the cross-strike basement faults reactivating and controlling depositional areas.

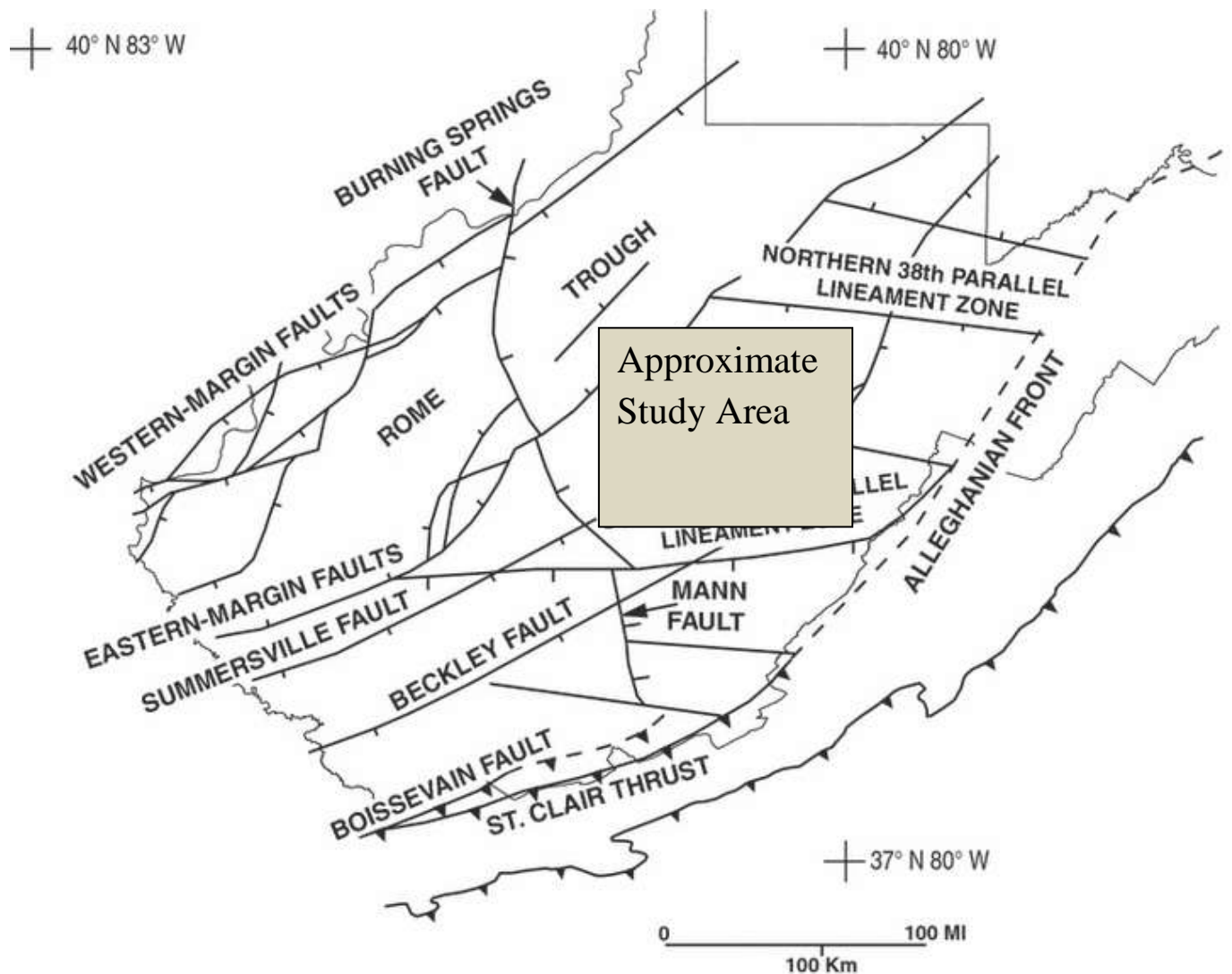


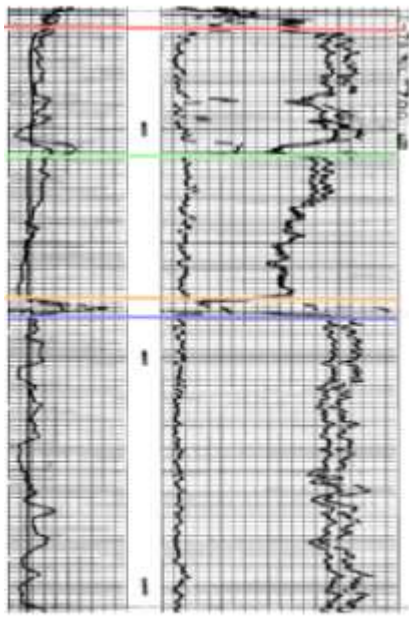
Figure 22: Map showing the basement structural geology of West Virginia (Wynn, 2003) and approximate study area.

LOG SIGNATURES

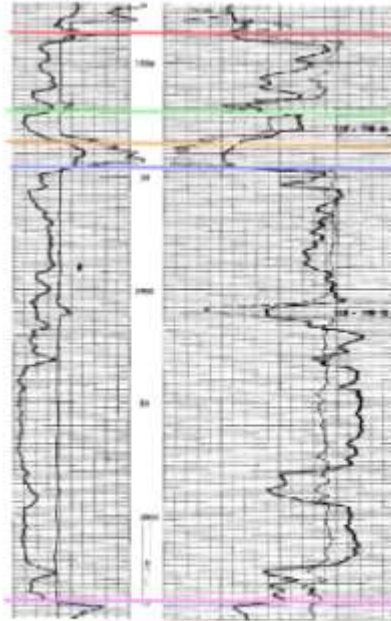
The Blue Monday sandstone has four distinct depositional types as identified by the shape of the curves on well logs shown in Figure 23 and as listed in Table 2. Type C, is a bed or cylinder shape with sharp upper and lower boundaries and little change within (Serra, 1989). This shape is indicative of deposition in fluvial channels (SEPM, 2009). Type E, the most common type, is indicative of an egg shape where the gamma ray signature decreases in value then increases (Serra, 1989). This cycle pattern commonly represents deposition in a first regressing then transgressing shoreface delta (SEPM, 2009). Type B is indicative of a bell shape where the gamma ray signature shows a gradual increase in value corresponding to an increase in clay minerals or dirtying up section thereby becoming finer grained (Serra, 1989). This indicates a decrease in environmental energy up section and possible shoreline retreat (SEPM, 2009). The last, Type F is a funnel shape where the gamma ray signature gradually decreases in value up section and is indicative of a coarsening upward sequence (Serra, 1989). This decrease in gamma ray indicates an increase in environmental energy up section and possible change from clastic to carbonate deposition (SEPM, 2009). The various placements of these types indicate different depositional settings and are shown in Figure 24.

A cylinder log signature occurs most often in the deeper channels of the Blue Monday sandstone. An egg shaped regressing and transgressing environment occurs primarily over the thinner deposits of Blue Monday. The funnel shaped, up-section increase in energy, occurs not in main channels, but just outside of them. The final bell shaped decrease in energy occurs in the thinnest to thickest deposits of Blue Monday. The funnel and bell shapes often occur near each other indicating the rapid changes in environmental energy over a short time period.

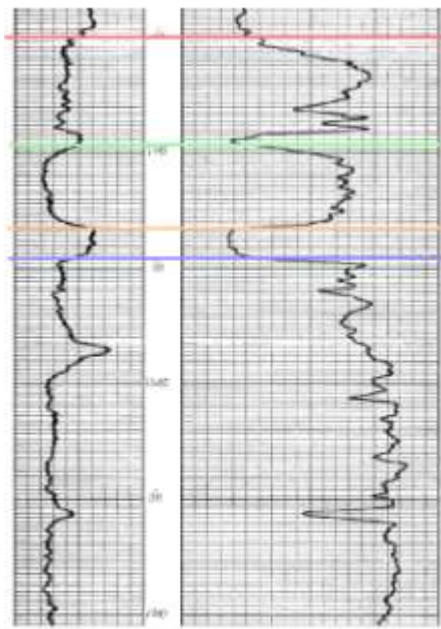
Gamma Ray	Porosity
-----------	----------



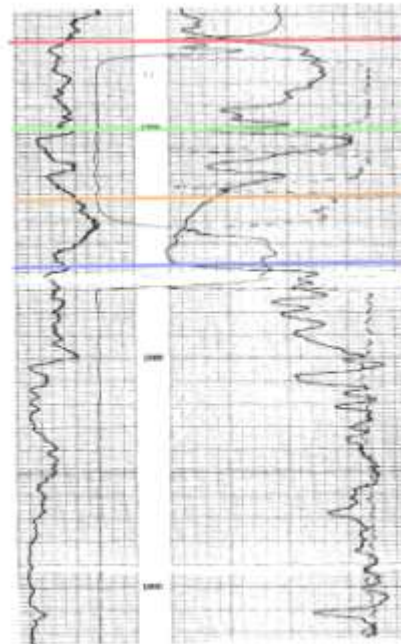
476N
Fining Upwards (B)



2287G
Coarsening Upwards (F)



1660C
Bed (C)



295N
Cycle (E)

Figure 23: Well logs demonstrating the different types of depositional patterns present in the Blue Monday sandstone, shown between the green and orange lines. The gamma ray tool is in the left track and the porosity in the right track.

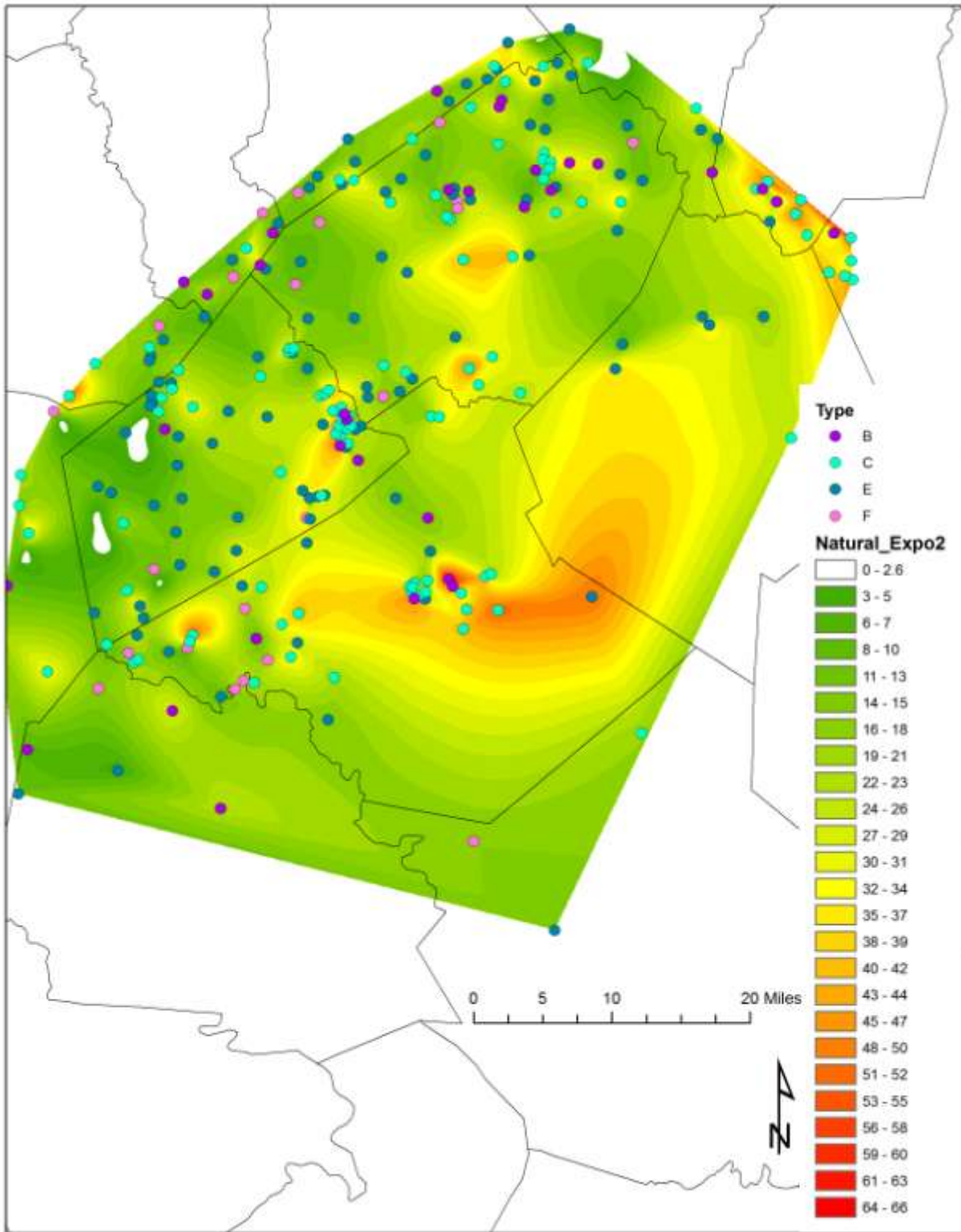


Figure 24: Map showing the log signature associated with each well, over the Blue Monday sandstone isopach map.

Table 1: Percentages of porosity in the BMS derived from well logs and how the BMS looks on the well log. Types: B: Bell shaped indicating a fining upward sequence, C: Cylinder shaped indicating a bed, F: Funnel shaped indicating a coarsening upward sequence, E: Egg shaped indicating a cycle (Data: WVGES 2010, (Schlumberger Limited, 1972).

County Name	Permit Number	Well log Porosity %	Type	County Name	Permit Number	Well log Porosity %	Type
Clay	1678	13	B	Clay	909	17	C
Clay	1684	15	B	Clay	1465	14	C
Braxton	1238	12	B	Clay	1657	14	C
Braxton	1643	6	B	Clay	1794	10	C
Braxton	1992	13	B	Clay	1795	16	C
				Clay	1796	20	C
Clay	966	20	E	Clay	2357	18	C
Clay	1315	16	E	Clay	2365	12	C
Clay	1558	6	E	Clay	2389	14	C
Clay	2381	20	E	Clay	2390	7	C
Clay	2392	10	E	Braxton	1135	13	C
Braxton	1996	6	E	Braxton	1946	6	C
Braxton	2079	14	E	Braxton	2062	16	C
Nicholas	389	13	E	Braxton	2087	17	C
				Braxton	2107	14	C
Clay	2309	18	F	Braxton	2111	6	C
Braxton	2068	10	F	Nicholas	372	13	C
Braxton	2077	8	F	Nicholas	815	20	C
Braxton	2081	9	F	Nicholas	451	5	C
Nicholas	398	16	F				
Nicholas	789	11	F				
Nicholas	791	9	F				

LITHOLOGY

In outcrop (Fig. 25) the Webster Spring Sandstone (Fig. 1) is a massive, medium-hard, unfossiliferous, white to greenish-gray sandstone that was first described by Reger (1920) in Webster Springs, Webster County, West Virginia (Figs 26, 27). The Blue Monday sandstone was studied in four sets of well cuttings (Appendix I). The samples are well sorted, white to light gray, very fine to fine-grained quartz sandstones. Some samples include medium coarse grain to very coarse grained sand. Cementation is predominantly calcite although some iron oxide staining is prevalent in the lower half of the section in the northern part of the study area.



Figure 25: Location map of the Webster Springs Sandstone outcrop in Webster Springs, WV (Figs. 26, 27).



Figure 26: Picture of the Webster Springs Sandstone in outcrop in Webster Springs, WV. Visible unit is about 7 feet thick.



Figure 27: Picture of the Webster Springs Sandstone in outcrop in Webster Springs, WV.

PRODUCTION

Gas production has occurred in 101 fields in 26 counties in West Virginia, according to the WVGES (Barlow, 1996). The 13 fields producing from the Blue Monday are shown in Figure 28. A source rock for the gas within the Mauch Chunk has yet to be identified, though there is sufficient organic carbon for gas production within the studied section (Trask, 1937; Cox 1946), while the trapping mechanism is stratigraphic (Barlow, 1996). The gas and oil could have moved either up or down the section based on structures, such as faults and fractures, as well as where flow units stop and start. More gas has been produced from the Mauch Chunk than oil. Table 2 shows the number of producing wells in the four counties that have produced specifically oil, gas, or oil and gas.

Table 2: Total number of wells that produce from the Blue Monday sandstone unit, and if they produce oil, gas or oil and gas in the four counties along with the number of producing wells (WVGES 2010).

Counties:	Braxton	Clay	Nicholas	Webster
Total Number of Producing wells:	144	224	47	4
Oil	11	4	0	0
Gas	127	213	47	4
Oil and Gas	6	7	0	0

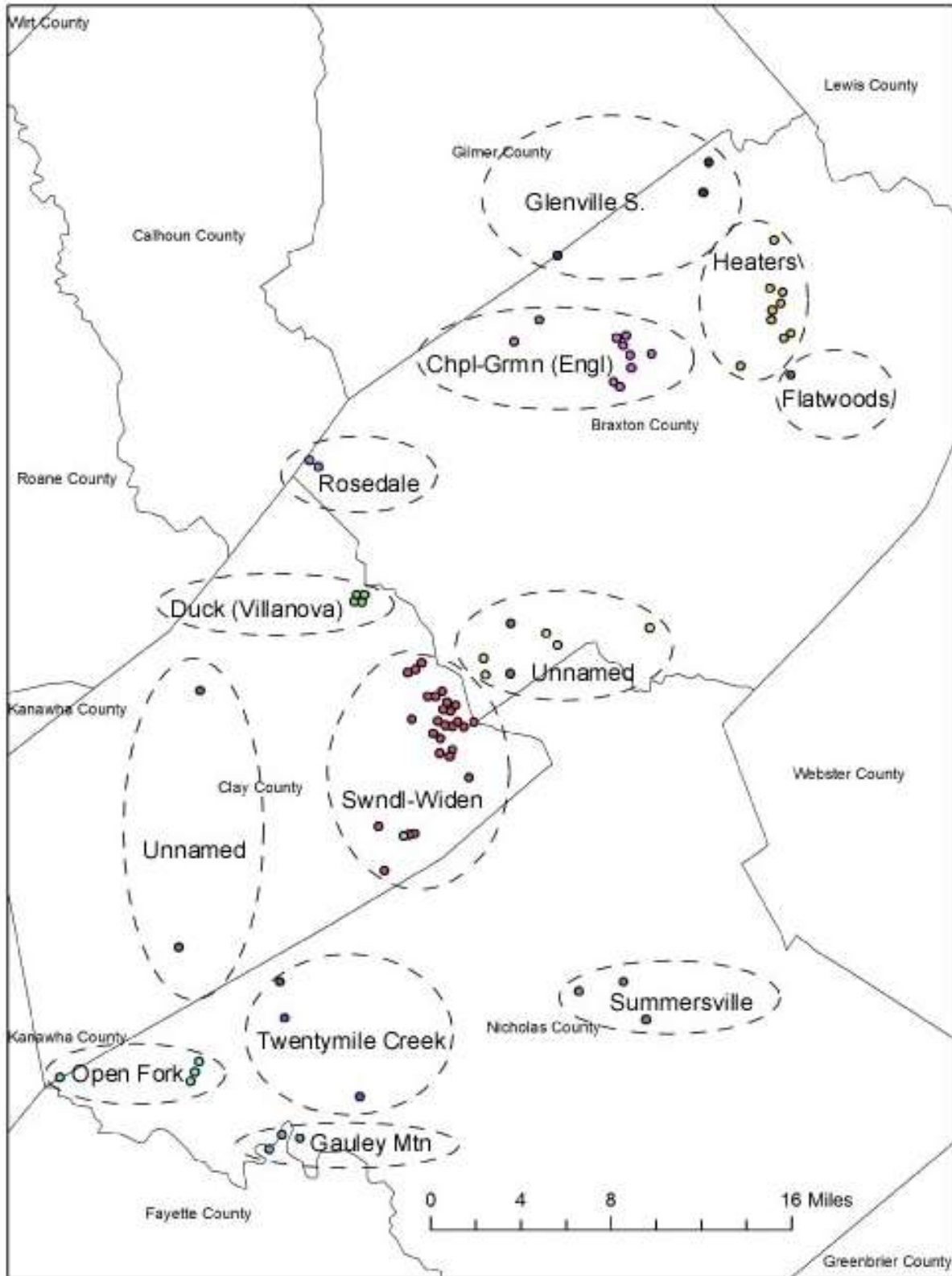


Figure 28: Fields with wells producing from the Blue Monday sandstone.

The production for the wells in this study show typical production decline curves (Fig. 29, 30, 31) (WVGES, 2010). Gaps in production data may be the result of wells being shut in or production not being reported. After these gaps, a spike in production may be the result of a well being shut in and then placed back into production, the well being worked over or drilled deeper. Most of the wells in the study area are completed in other zones besides the Blue Monday sandstone, so the data represent contributions from other reservoirs.

Oil production from this unit is not as prolific as gas production. This is shown by the percentage of wells producing oil compared to gas in Table 2. Wells that produce both oil and gas often have inconsistent oil and gas production data. The oil production data may be a reflecting of the way produced oil is transported to market. It is most often collected in a tank battery and trucked to a refinery. Depending on the volume of oil produced, oil may only be picked up every few months so production is reported at the time the oil is transferred from tank to truck rather than on a steady month-to-month basis. Also wells completed before 1979 have incomplete production histories.

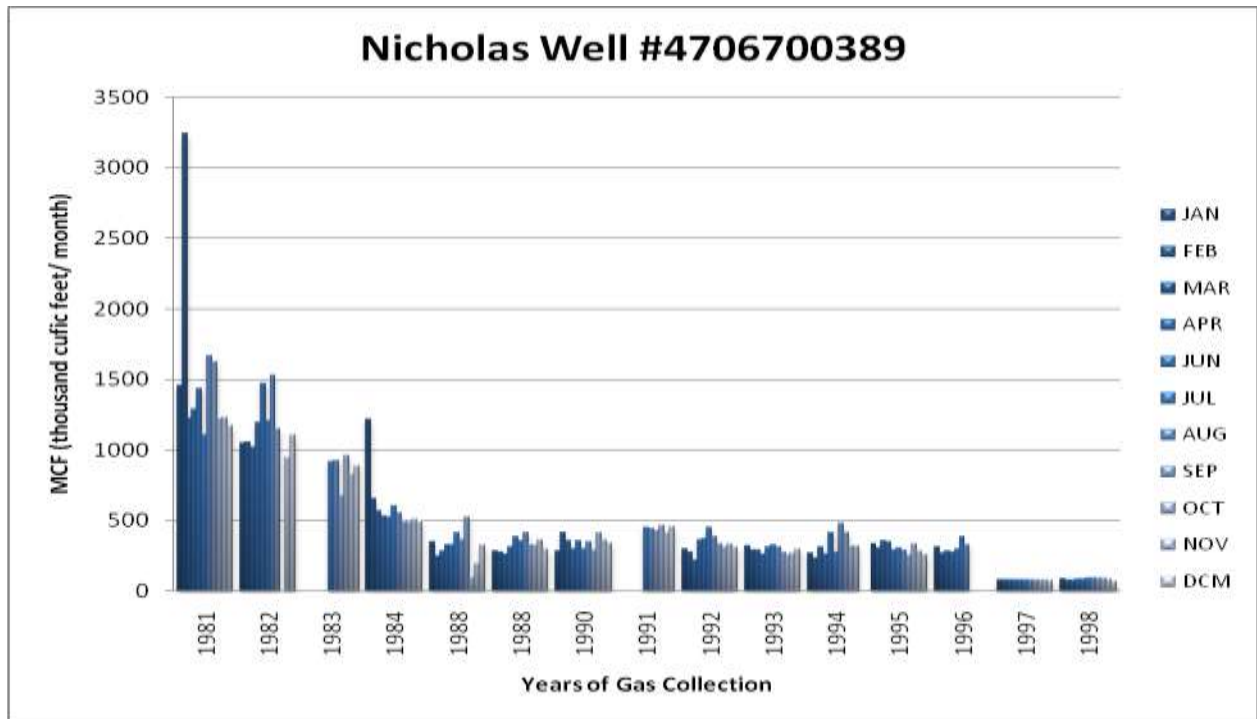


Figure 29: Production decline curve on well number 389 in Nicholas County. This well only produces from the Blue Monday sandstone and represents how the unit produces over time.

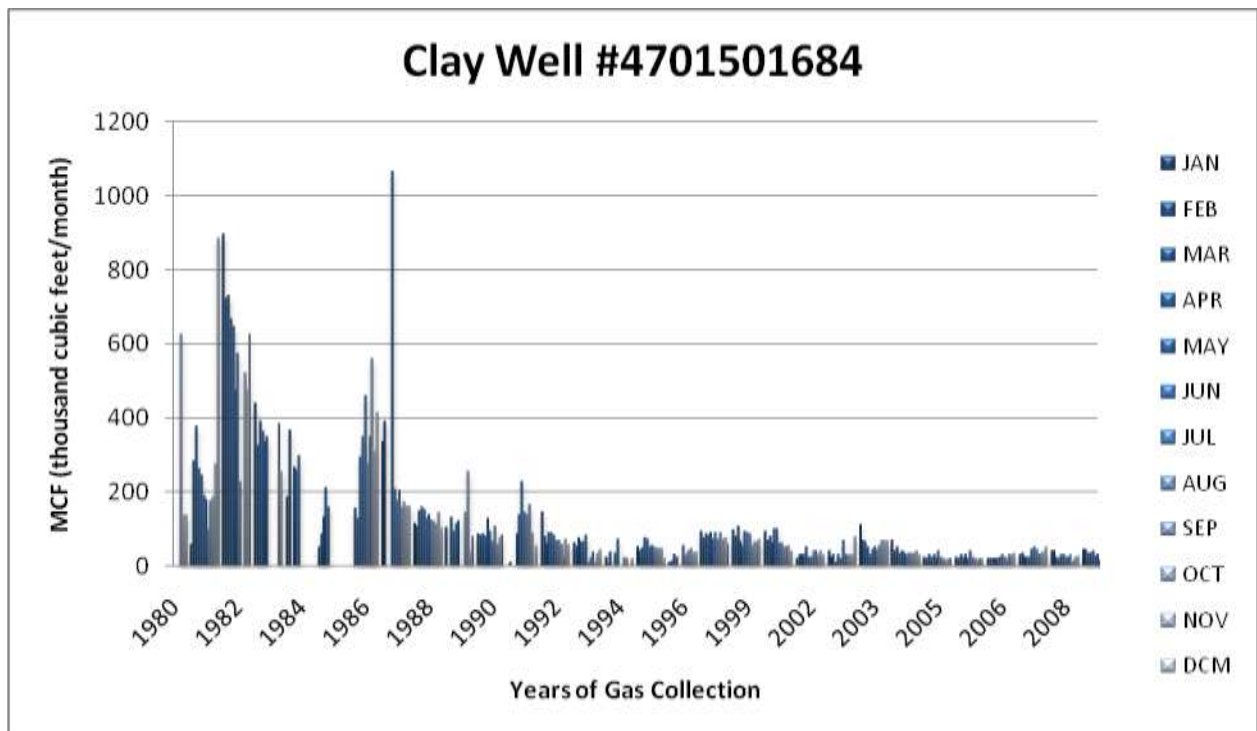


Figure 30: Production decline curve on well number 1684 in Clay County. This well only produces from the Blue Monday sandstone, and shows the general decline trend.

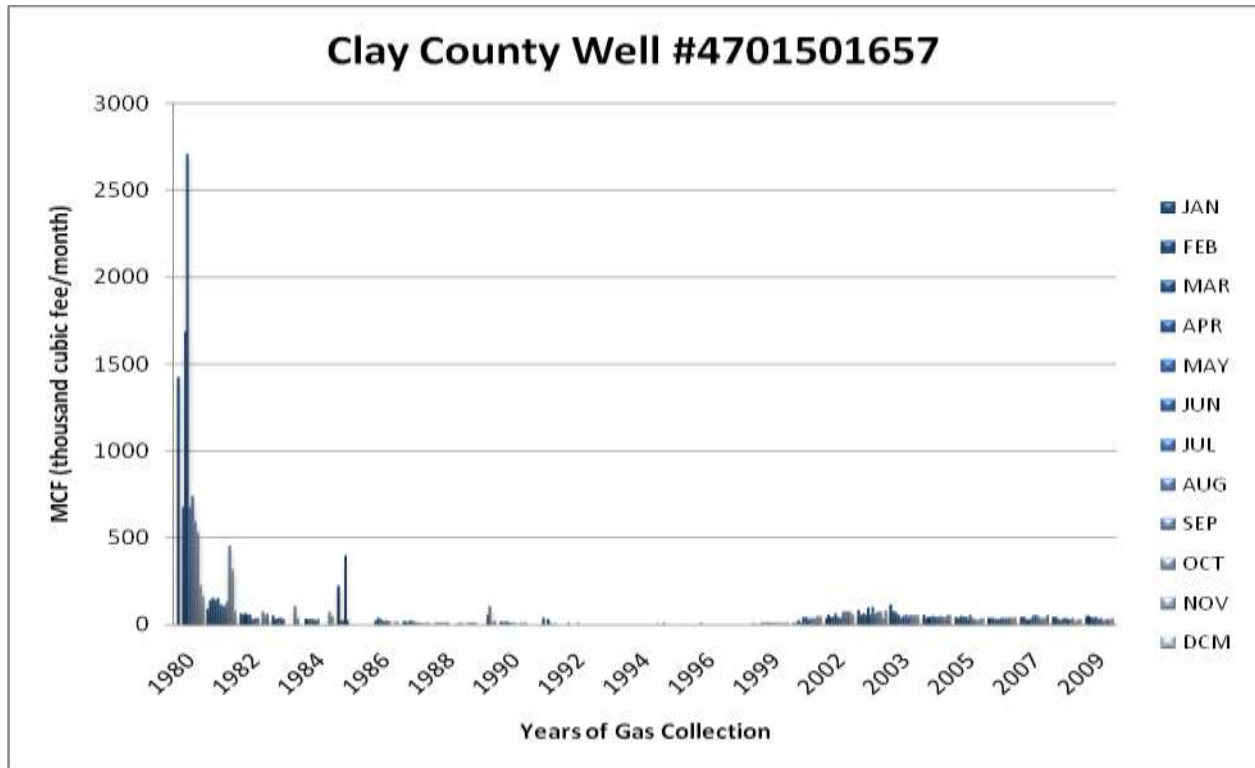


Figure 31: Production decline curve for Clay County well number 1657. This well only produces from the Blue Monday sandstone, but does not show a typical decline curve. This may be due to change in ownership of the well or post-depositional changes such as calcification.

POROSITY

Well log porosity was measured from wells with gamma ray and porosity logs where available (Figure 32). Porosity data are summarized in Table 2. Porosity ranges from 0 to 20 percent and is shown on Figure 33, along with the Blue Monday isopach data. To enhance porosity, two different completion methods were used gather more hydrocarbons from the units. These methods include: fracture and acid and fracture. Data for each well completion method are shown in Appendix IV.

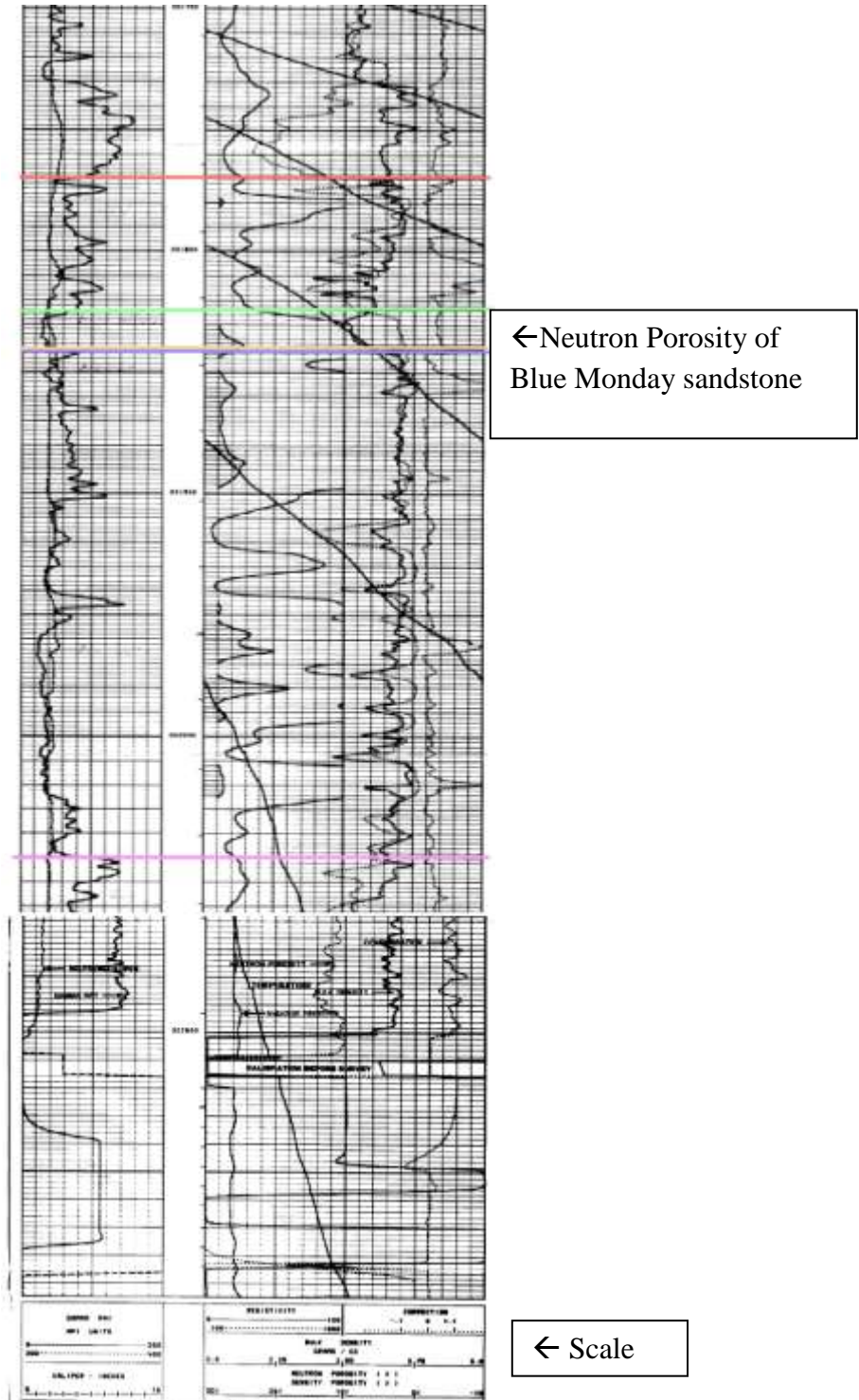


Figure 32: Example log: porosities were read directly from the neutron porosity and bulk density curves.

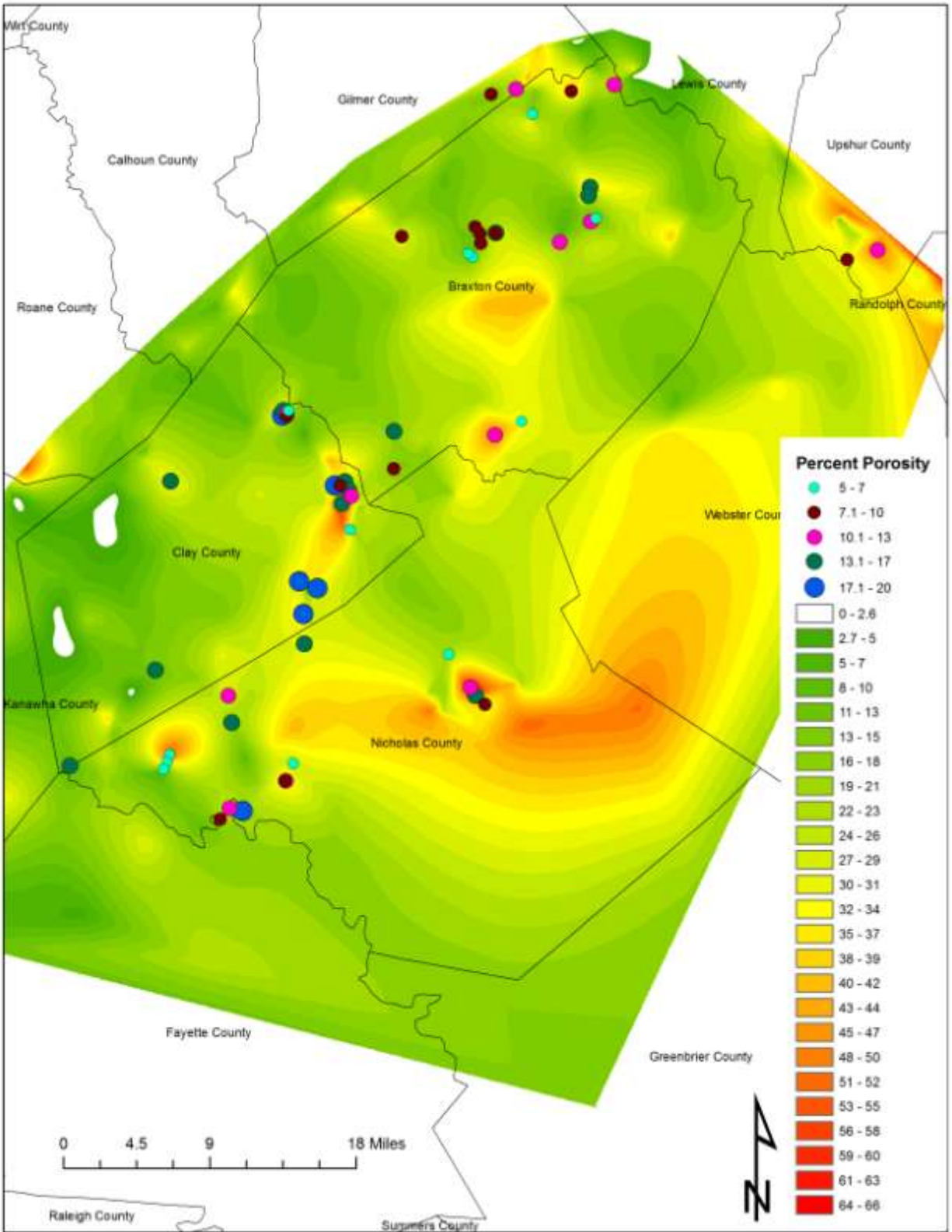
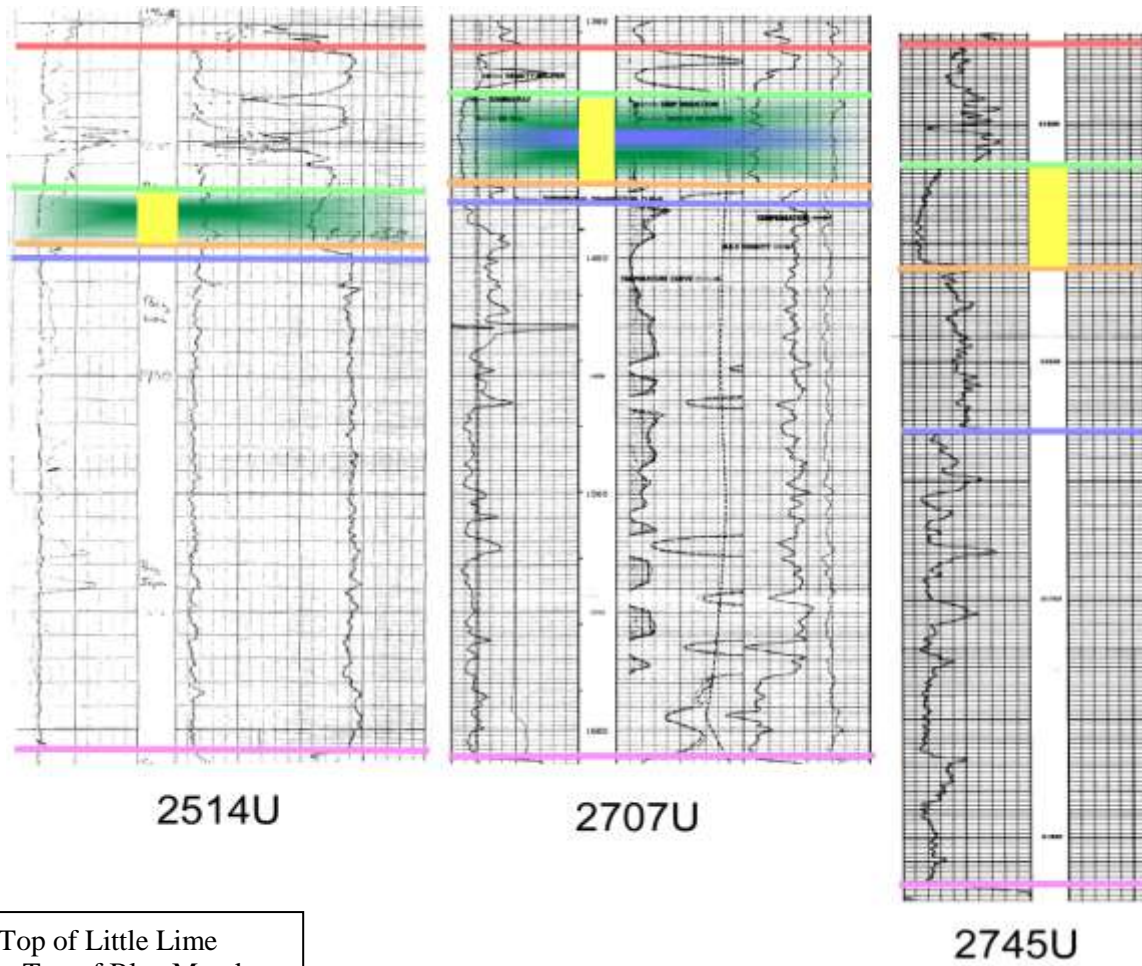


Figure 33: Well log porosity for Blue Monday in producing wells. Blue Monday isopach are also shown.

The following cross-sections transect areas of Blue Monday thickening that are shown on the Blue Monday sandstone isopach map (Fig. 9 and 33). A red line marks the top of the Little Lime, the green marks the base, which also marks the top of the Blue Monday sandstone. The orange line at the base of the sand marks the top of the Pencil Cave, whose base is shown by a purple line. This purple line also marks the top of the Big Lime, whose base is shown by a pink line. The datum for the cross-sections is the Little Lime. The sandy strata of the Blue Monday are highlighted in yellow. Each well log is identified by the last three or four digits of the API number assigned to each well and the first letter of the county where it is located. The location map for each cross-section shows the location of the wells and full API numbers of the wells included in the cross-section. The additional highlighting on the logs is indicative of the well log porosity of the Blue Monday sandstone. Pink highlights show a part of the Blue Monday sandstone which has up to 5% well log porosity, green highlights show 5-10% well log porosity, and purple highlights indicate 10+% of well log porosity.

Figure 34 shows a cross-section in southwestern Upshur County. The southernmost well 514U shows consistent well log porosity throughout the section of about 9%. The central well 2707U shows a spike of porosity to 11% in the center of consistent 9% porosity surrounding it. The northernmost well of the section does not have available porosity data.

Figure 35 shows a west-central cross-section in Nicholas County. The most northern well shows the Blue Monday sandstone broken into two depositional intervals. The lower interval of sand has a well log porosity of between zero and 10%. The upper interval's well log porosity is between 10 and 20%. There is a lens of shale between the two sandstone bodies.



Red-Top of Little Lime
 Green-Top of Blue Monday
 Orange- Top of Pencil Cave
 Purple-Top of Big Lime
 Pink-Bottom of Big Lime

Porosities
 Pink- 0-5%
 Green- 5-10%
 Purple- 10+%

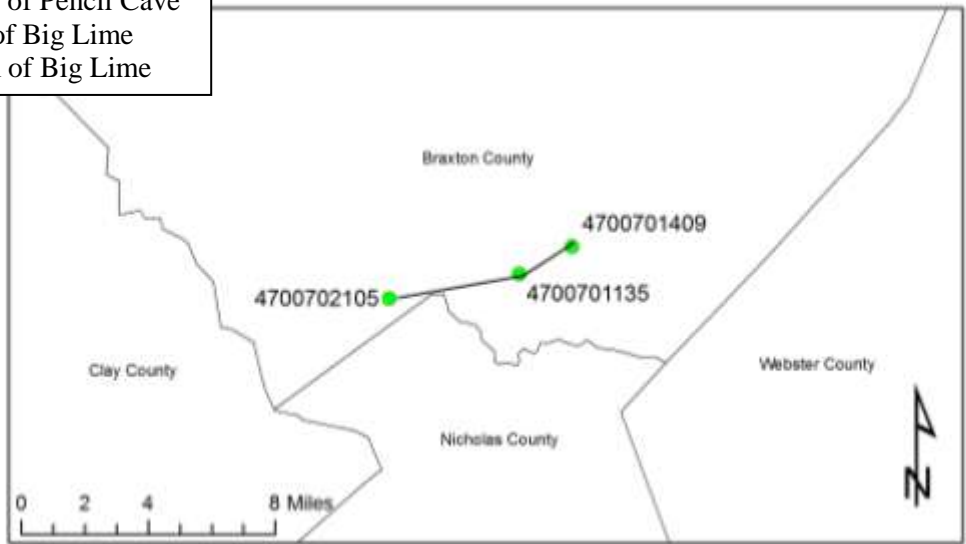


Figure 34: Southern Upshur County porosity cross-section and associated location map.

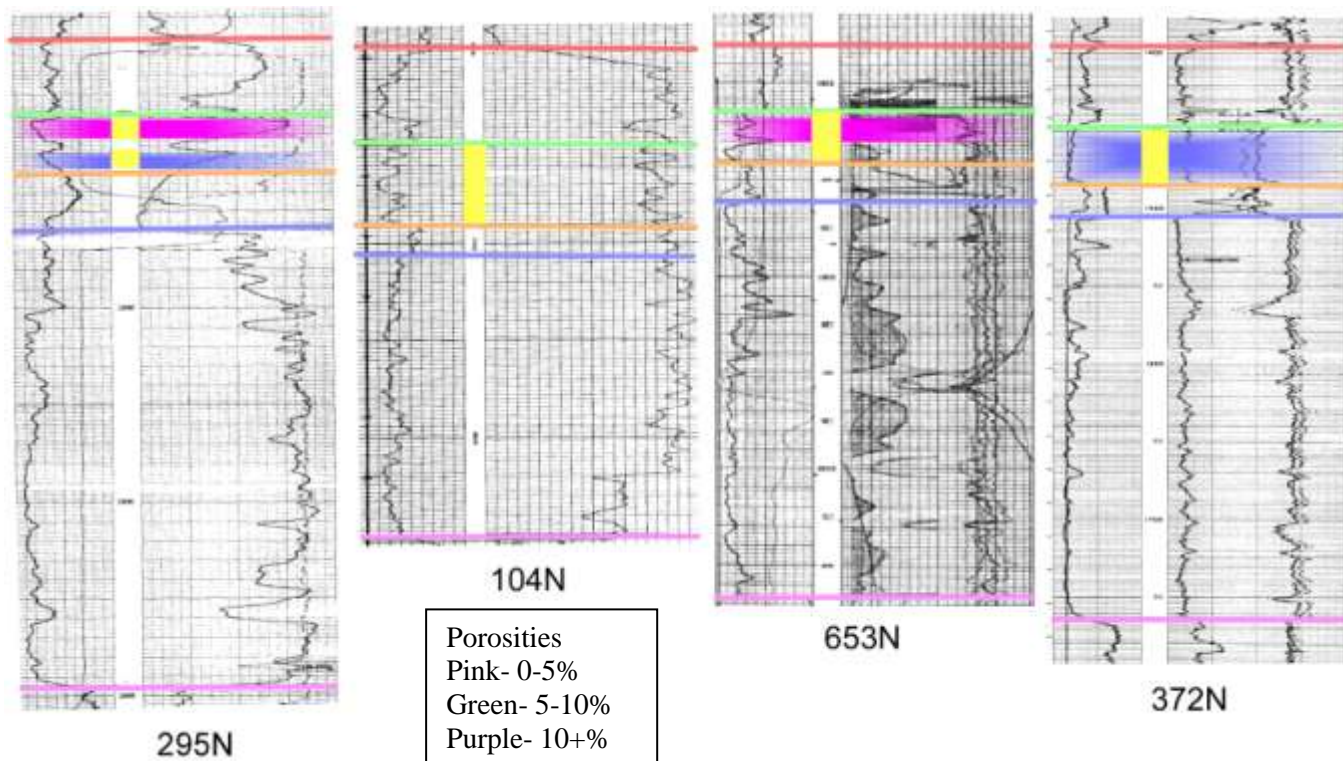


Figure 35: Central Nicholas County porosity cross-section. See Figure 38 for location of cross-section.

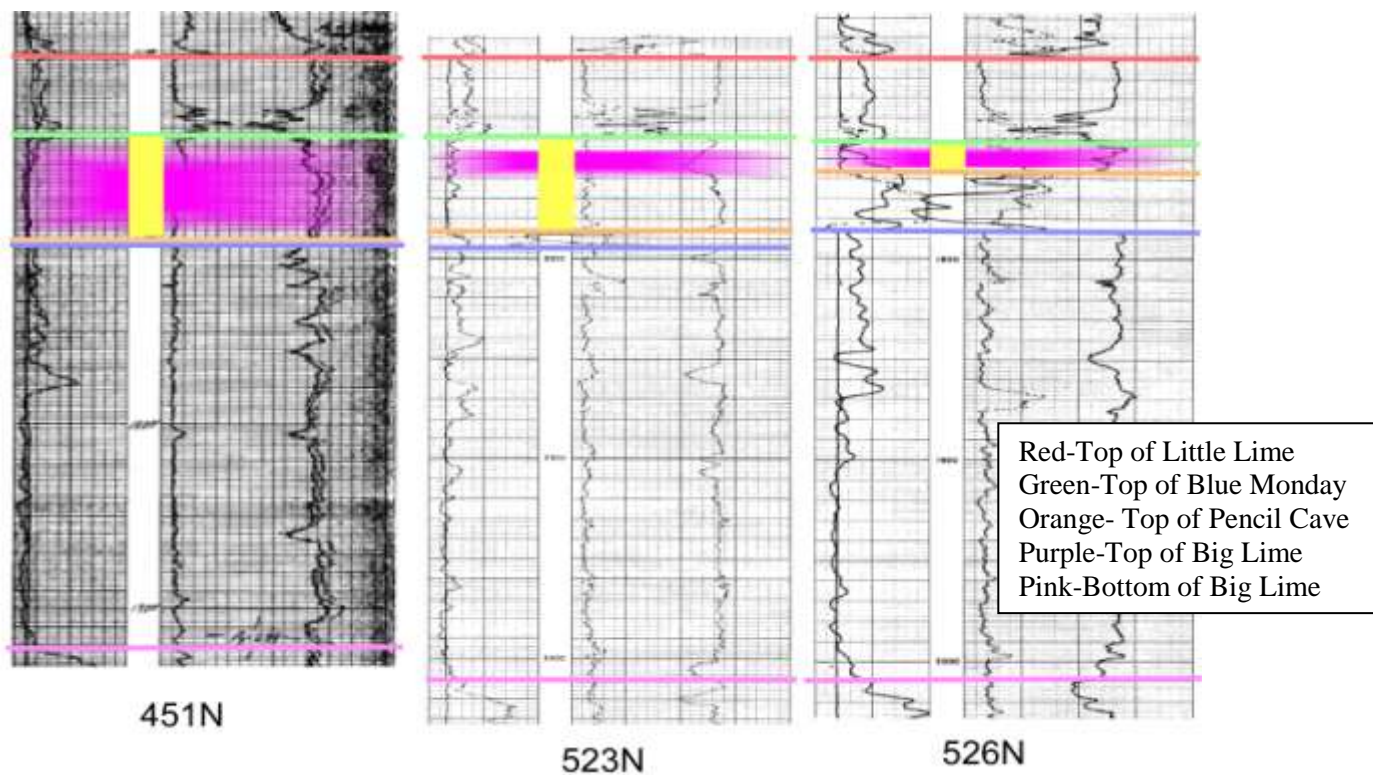


Figure 36: Western Nicholas County porosity cross-section. See Figure 38 for location of cross-section.

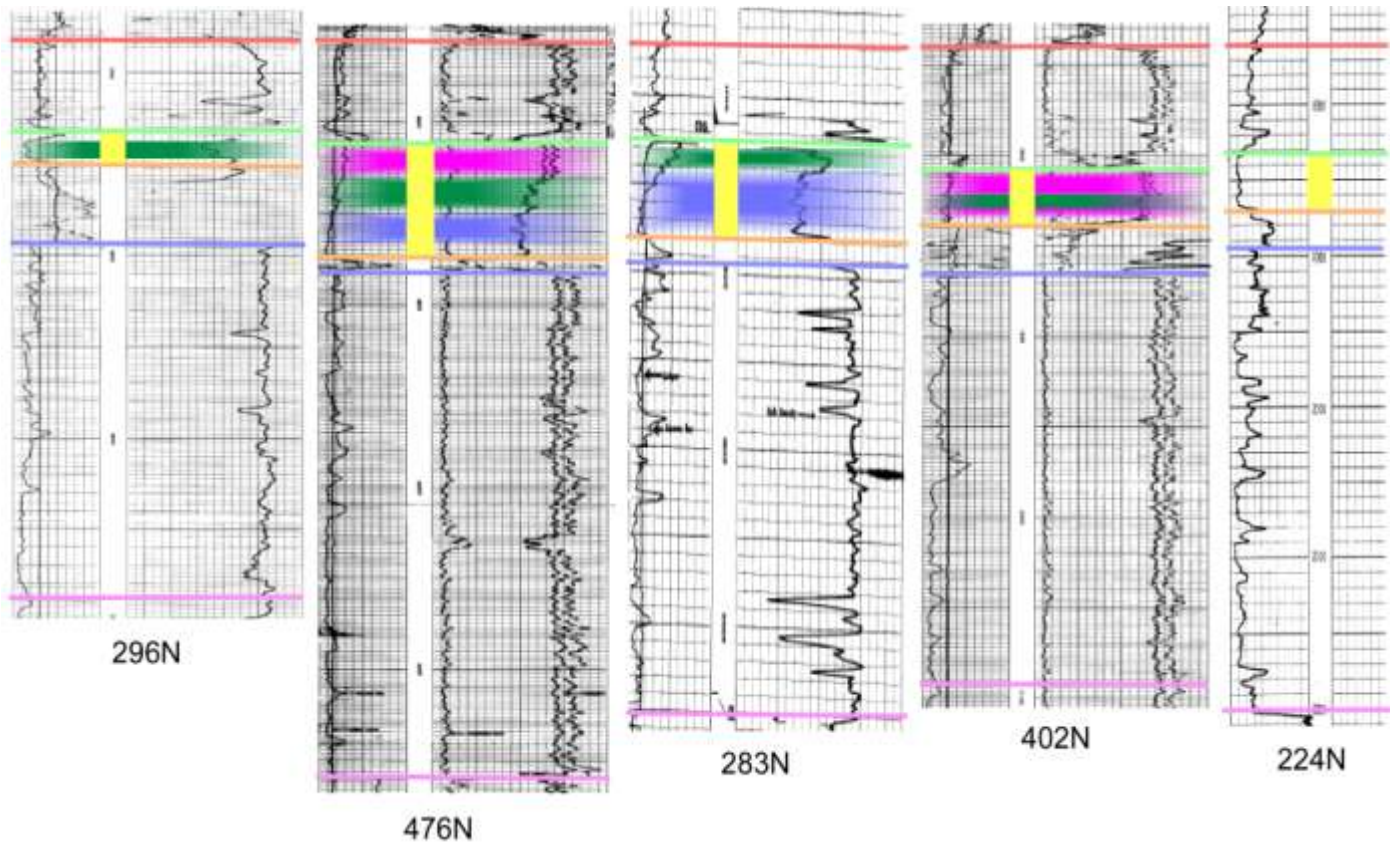


Figure 37: Eastern Nicholas County porosity cross-section. See Figure 38 for location of cross-section.

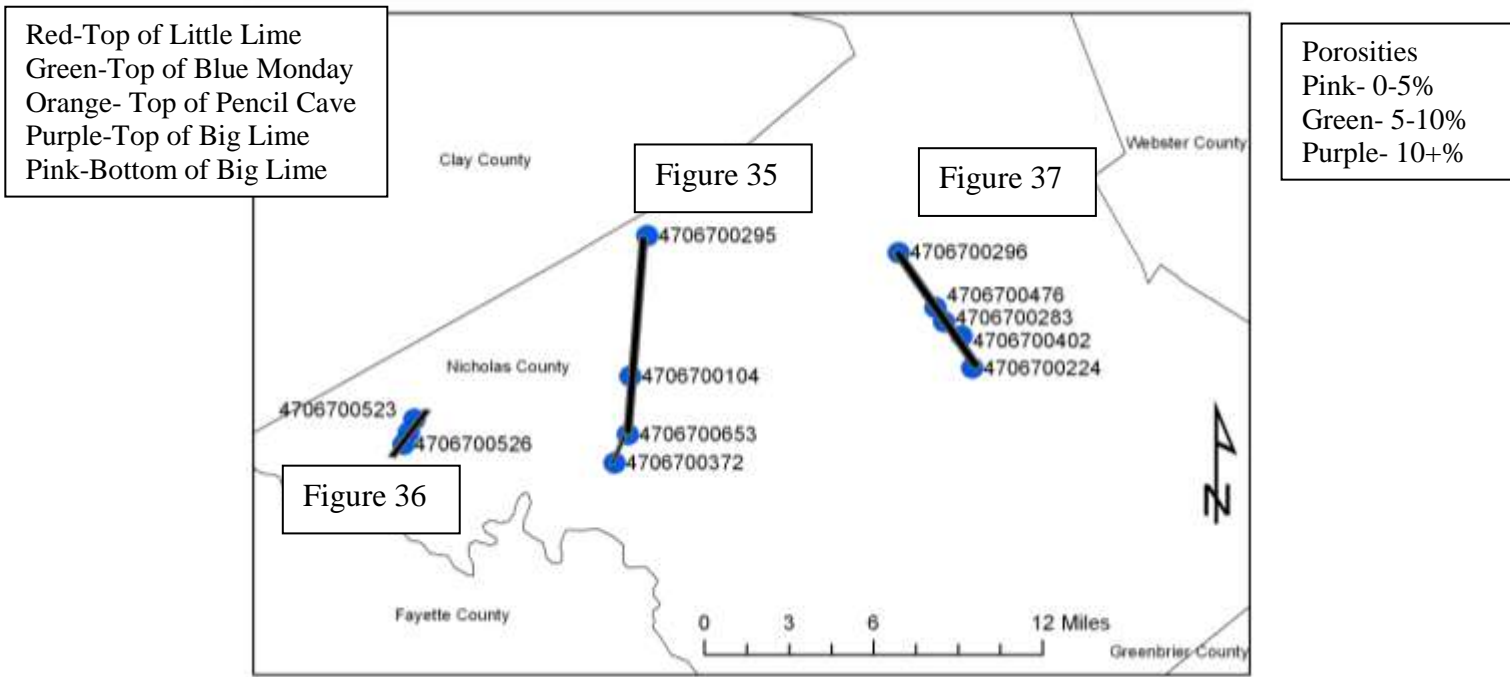


Figure 38: Location Map for Figures 35, 36 and 37

Well 104N has no available porosity data. Well 653N has between zero and 5% well log porosity in the upper lens of sand; no well log porosity is apparent in the lower lens of sand.

Well 372N shows a consistent well log porosity of 10%.

Figure 36 is a western Nicholas County cross-section in which all the wells are producing wells. The well logs show a consistent well log porosity of up to 5%. The northernmost well, 451N, has a thick bed of Blue Monday sandstone and shows the most consistent well log porosity in this cross-section. The central well, 523N, shows the well log porosity located near the top of the sandstone body, where it is showing shaly intervals on the gamma ray log. This location stays stratigraphically consistent with the last well, 526N, which has good well log porosity.

Figure 37 is an eastern Nicholas County cross-section. The northernmost well, 296N, shows well log porosity from 5-10% at the base of the unit. Well 476N has a log porosity of 12% at the base, 8% in the center, and 6% at the top. Well 283N shows a similar trend, without the minimum pink trend. The base is a thick sandstone body with 15% well log porosity, the top sandstone body is 9%. This shows stratigraphic similarity to well 476N. Well 402N is the last well in this cross-section with available porosity data. It shows a consistent 5% well log porosity across the sand body with a small spike up to 8% in the center of the body.

Figure 40 shows an east-west trending cross-section in southern Braxton County. The first well to the west, 2105B, does not have any porosity data. Well 1135B, however shows a strong consistent well log porosity of 11%. The final well in this cross-section, 1409B, shows a consistent well log porosity of about 5%.

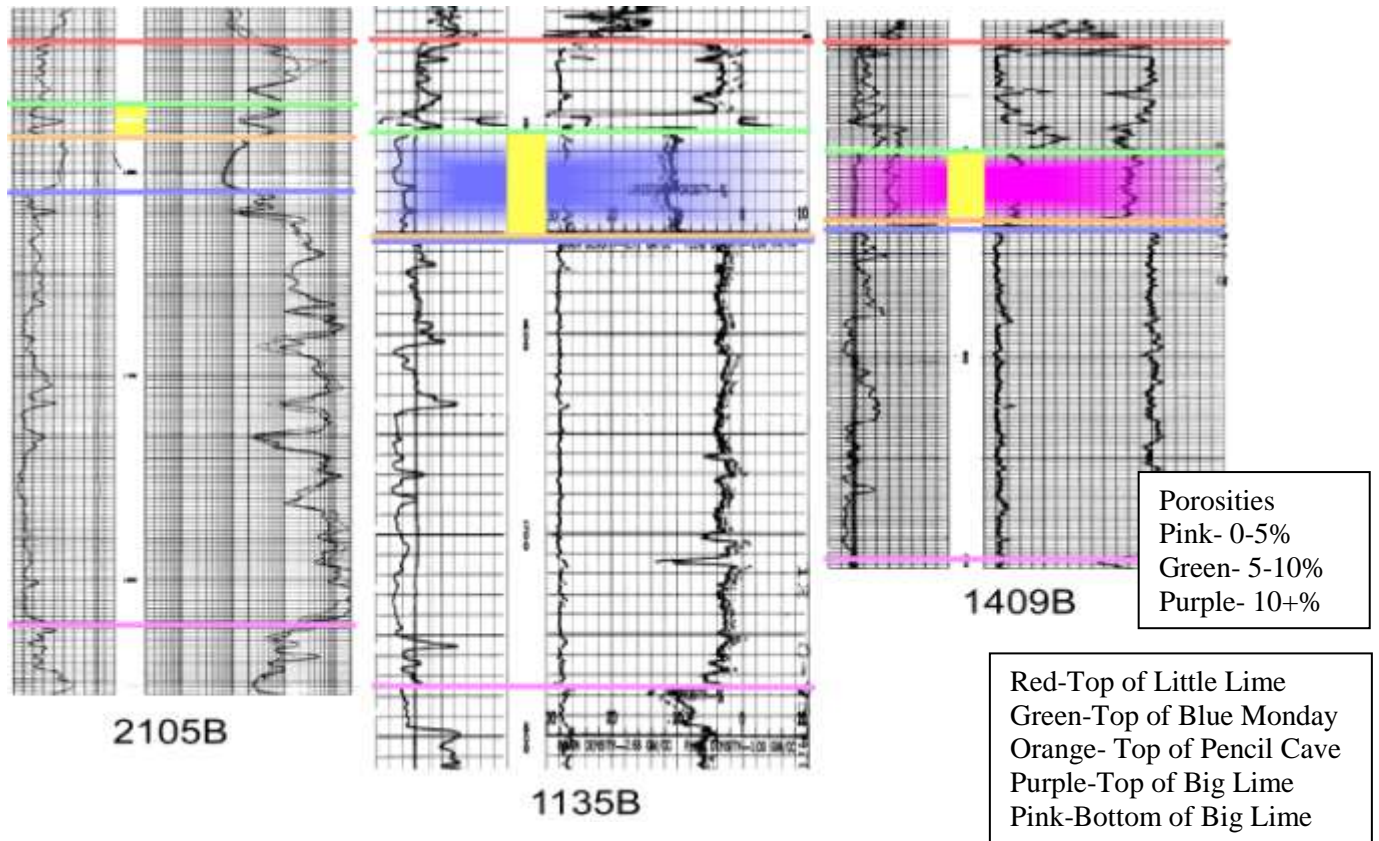


Figure 39: Southern Braxton County porosity cross-section. Location of cross-section shown in Figure 42.

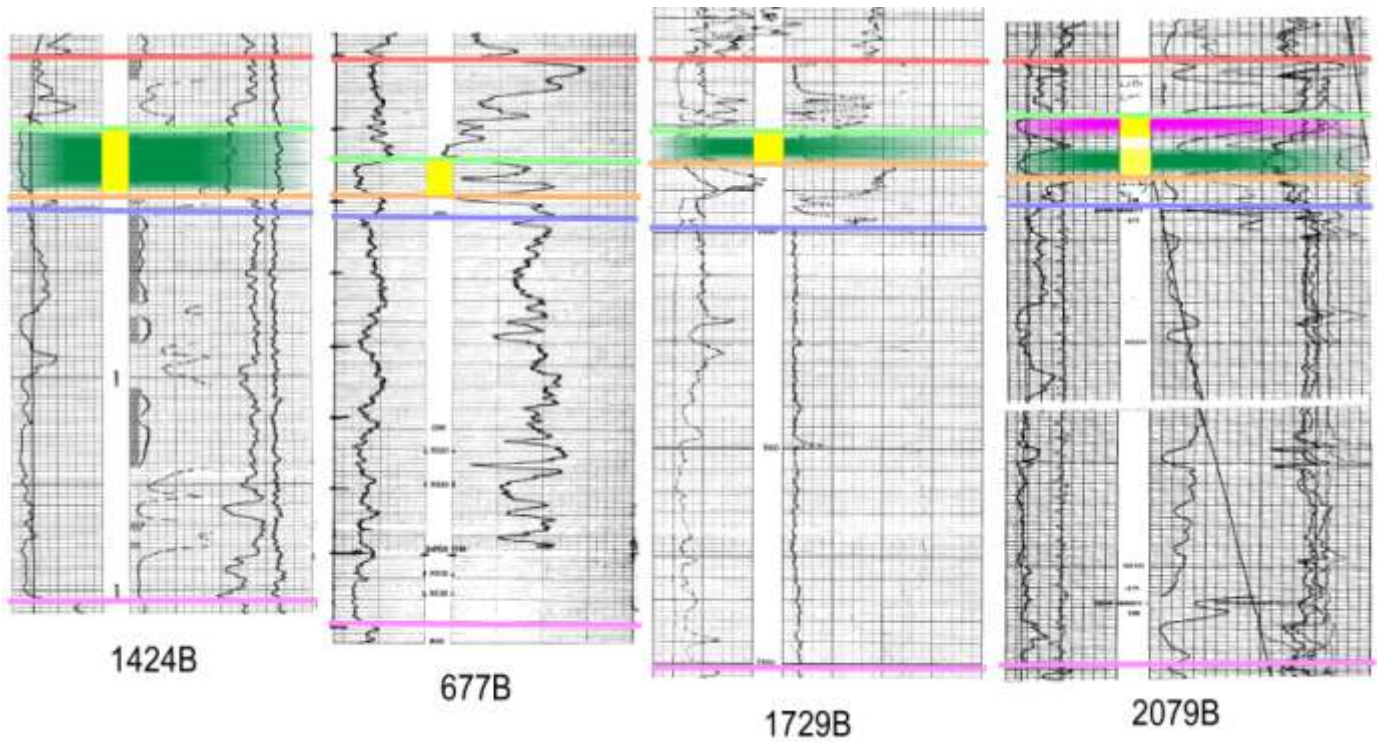


Figure 40: Central Braxton County porosity cross-section. Location of cross-section shown in Figure 42.

Figure 37 shows an east-west trending cross-section in central Braxton County. In well 1424B on the western end of the cross-section, the sandstone is relatively thick and has a consistent log porosity of 8%. Well 677B has no porosity data associated with it. Well 1729B shows a thin Blue Monday sandstone body with a well log porosity of 9%. The final well in this line shows two interval of the Blue Monday sandstone. The lower sandstone interval in this well has a well log porosity of 9% while the upper unit above a shale lens has a log porosity of 3%.

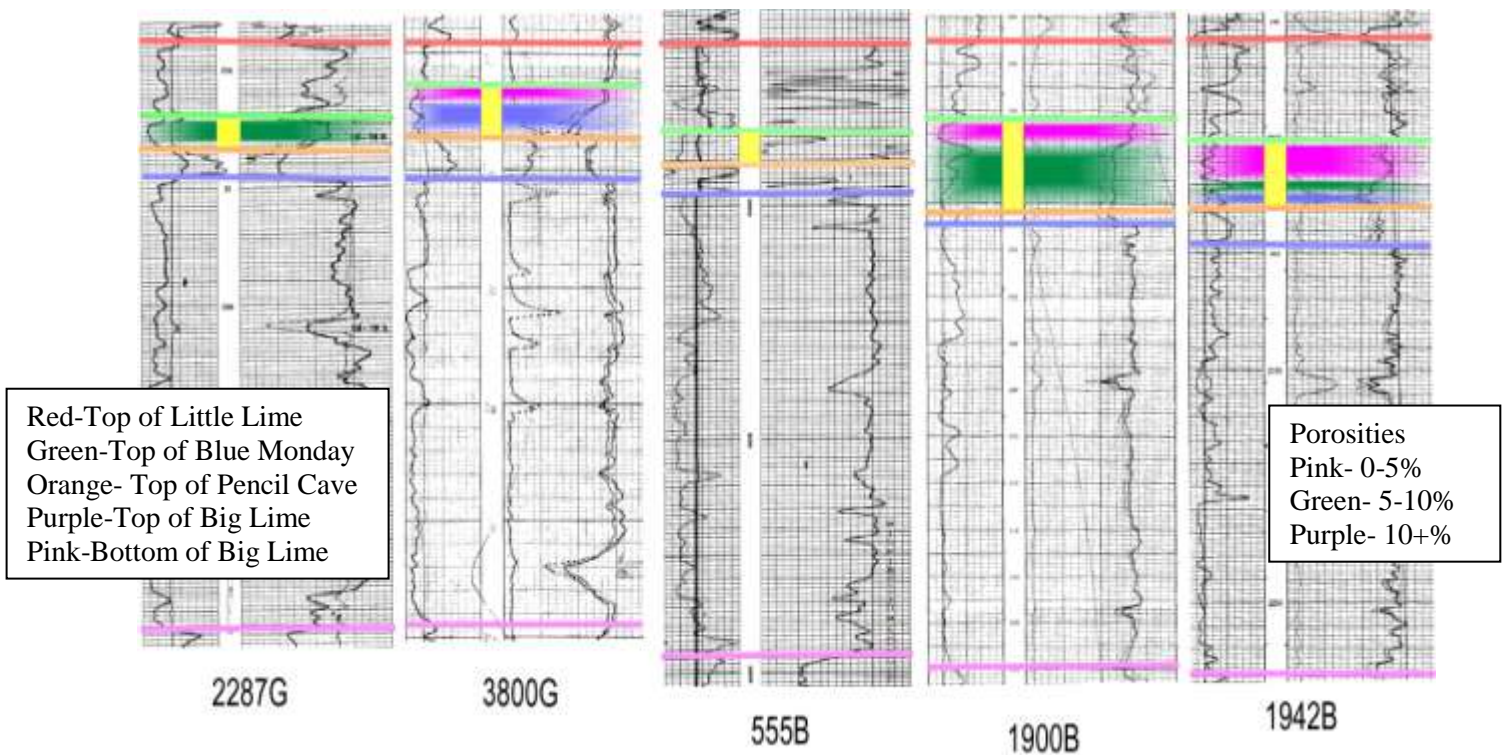


Figure 41: Northern Braxton County porosity cross-section. Location of cross-section shown in Figure 42.

Figure 38 shows the final east-west trending cross-section in northern Braxton and Gilmer counties. The westernmost well, 2287G, shows a thin Blue Monday sandstone with a well log porosity of 9%. Next is well 3800G which has two intervals of the Blue Monday sandstone, with two different log porosities. The log porosity of the lower sandstone body is

12% while that of the upper sandstone body is 4%. Well 555B has no porosity data available. Well 1900B has a thicker lower sandstone body with well log porosity of 9% while the upper sandstone body has a porosity of 2%. Well 1924B is the last in this section. It has a thick Blue Monday sandstone interval that has three different well log porosities: 12% at the base, 8% in the center and 5% at the top of the unit.

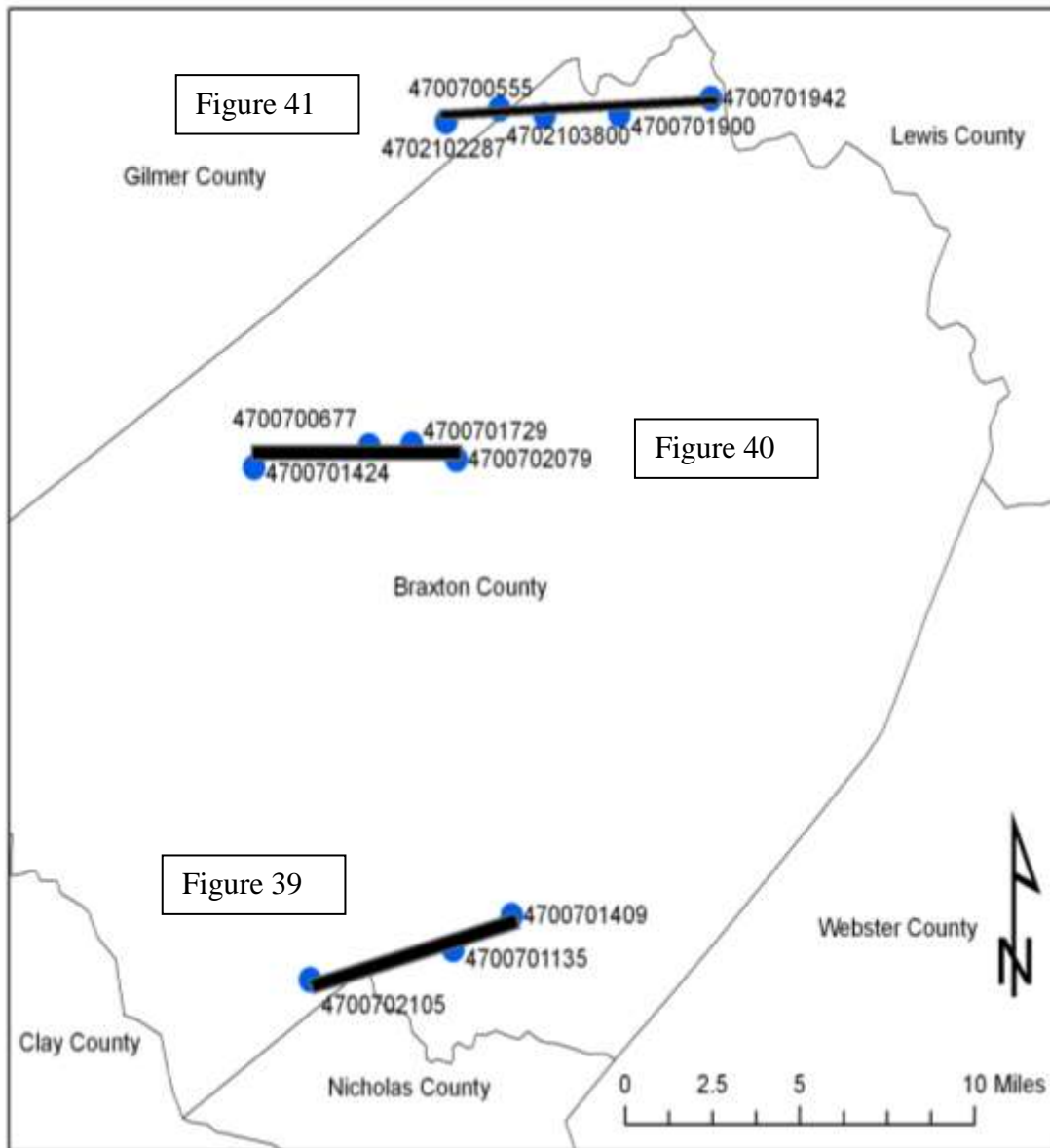


Figure 42: Location Map for Figures 39, 40 and 41.

3 DISCUSSION

STRATIGRAPHY

The isopach maps show the different thicknesses of the units associated with this study. The clastic units between the under- and overlying limestones gradually thicken towards the southeast (Fig. 8). From the thickness pattern, there is no obvious structural control on deposition of this clastic interval.

The Blue Monday sandstone is thickest (Fig. 9) in narrow north-south linear trends in central Braxton and eastern Clay counties. A similar trend is recognized in eastern Webster County. These trends are interpreted to represent fluvial channels. Away from these channels the map shows a thinning of the Blue Monday sandstone indicating lesser channels or floodplains. An east-west trend of thick Blue Monday is seen in Nicholas and Webster counties. This trend truncates the north-south linear trends to the north and is thicker and wider than the interpreted fluvial trends. There are no apparent equivalent sandstone bodies trending south of Nicholas County.

The Little Lime (Reynolds Limestone) (Fig. 10) shows areas of thickening above areas where the Blue Monday sandstone is thin suggesting some control on the deposition of the Little Lime by the location of the Blue Monday channels. The underlying Big Lime and Pencil Cave shale have similar trends on the isopach maps (Figs. 11 and 13) showing a thickening to the southeast. The Big Lime was deposited by numerous transgressive-regressive cycles in an overall transgressing shallow sea setting (Al-Tawi, et al., 2003). The Pencil Cave was deposited as part of the final transgression of the Big Lime with deeper water clastic deposits overstepping to the north. In some areas there is no Pencil Cave in the column due to the scouring by the

overlying Blue Monday channels into the softer shale (Fig. 12) as the sea regressed; this lack of strata shows in areas of Blue Monday thickness where the channels were located.

The cross-sections in this study (Figs. 15-20) are purposefully placed over the areas of interpreted Blue Monday sandstone channels. The cross-sections show a thick channel sandstone incised into the underlying Pencil Cave shale. These channels are not considered to be paleovalley fills but rather multi-story sheet sands. Sections away from that main channel of sandstone show how the sandstone thins and becomes more likely interbedded with shales. This may have happened during a time of flooding pulses to the flood plain. The width-thickness ratio is greater than 15 which would also suggest this is a sheet sand rather than a paleovalley fill with isolated sand ribbons dispersed within fine grained floodplain facies (Miall, 1996).

During this time of deposition, this area would have been in the Appalachian foreland basin. The basin was developed as a result of the convergence of Gondwanaland with Laurasia in the Appalachian orogeny (Fig. 3). The foreland basin began to develop in the Late Mississippian and at the time of deposition of the Blue Monday sandstone it would still be considered to be an underfilled foreland (Jordan, 1995). The Blue Monday sandstone was deposited as part of an axial or longitudinal drainage system flowing from the north to south within the foreland. The Blue Monday sandstone is not found west of the study area due to the cross-strike basement faults reactivating and controlling depositional areas (Fig. 22).

The lithology is typical of material deposited in a fluvial system. The sand is well sorted, white to light gray, very fine to fine-grained quartz and has calcite cementation apparent in the well cuttings. As seen in Figure 25, equivalent sediments in the outcrop belt show that these are sand dominated units with a paucity of gravel. The distribution of the facies and the

predominance of sand suggests this might have formed in a braided sheetflood fluvial system but definitive characteristics are lacking in the study area.

The log signatures show a trend of cylinder and bell-shaped deposition throughout the areas identified as the channels and immediate flood plains in the Blue Monday sandstone isopach map (Fig. 9). The pattern is consistent with multi-story, multi-lateral channel formation. The data do not allow for finer resolution of channels. The funnel type of deposition occurs around the margin of the study area, indicating an increase in energy up section. The funnel pattern is commonly associated with coastal coarsening upward sand deposits. Perhaps the distribution of this pattern suggests a boundary between shallow sea and fluvial waters. Log signatures do not provide conclusive evidence for any specific environment.

DEPOSITIONAL ENVIRONMENT

The Late Mississippian is known for being a time of high-frequency sea level cycles (Fig. 43) with the overall Late Mississippian sea level at a relative lowstand (Haq and Schutter, 2008). The sea transgressed from the south inundating the central Appalachian foreland basin depositing the cyclically deposited Big Lime. The Greenbrier Limestone was deposited after a widespread subaerial exposure of the central Appalachian foreland in an epeiric sea (De Witt and McGrew, 1979; Donaldson and Shumaker, 1981; Carney and Smosna, 1989; Yang, 1998). Al-Tawil et al. (2003) studied the Greenbrier Group in depth and concluded it was deposited in 12 cyclic sequences, including the Blue Monday sandstone at the top in sequence 11-12. They labeled the Blue Monday sandstone and surrounding shales as a lowstand-transgressive sequence, but admitted to not really studying it specifically. This sequence is just what they would predict to

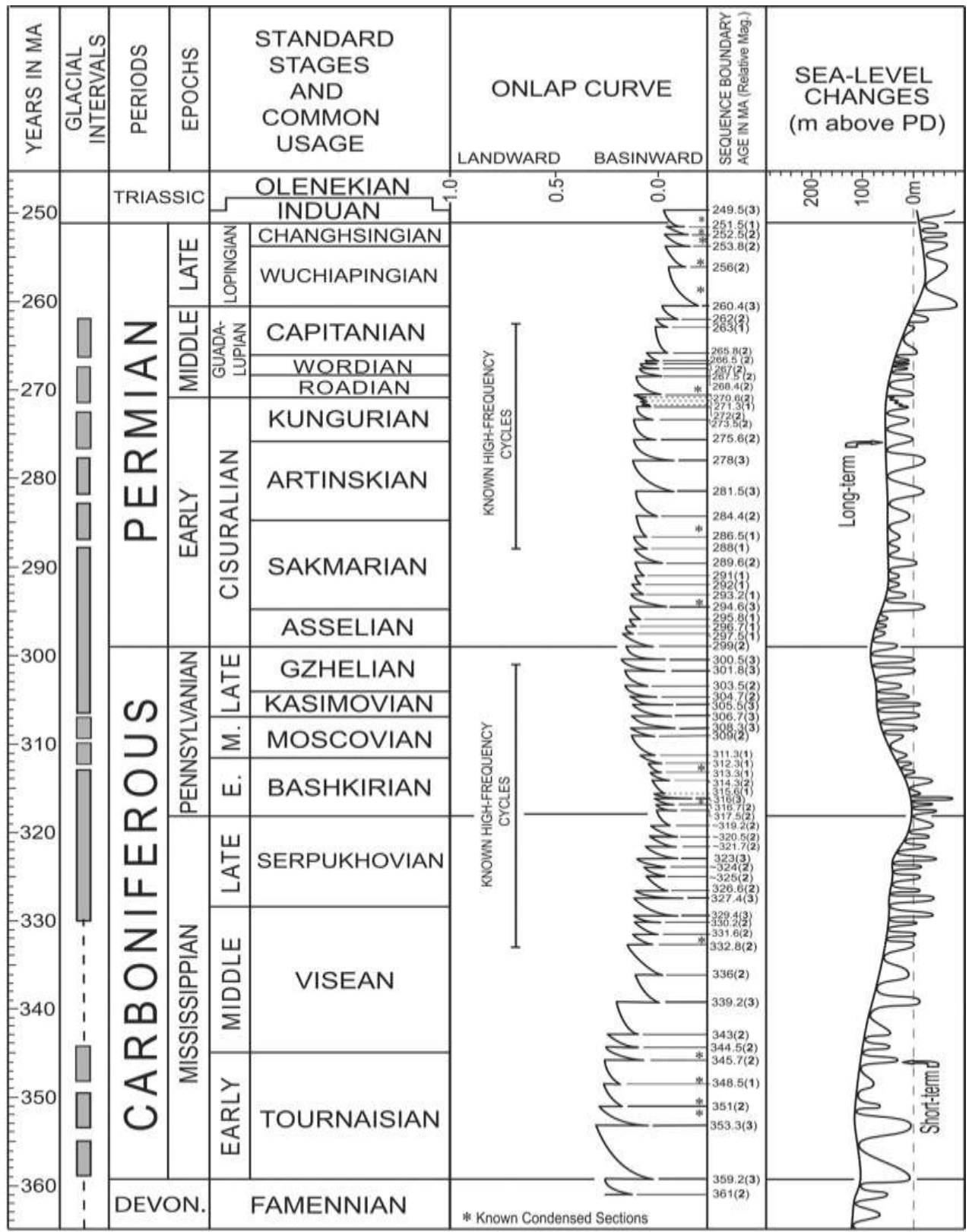


Figure 43: Sea level change chart for the Carboniferous and Permian (Haq and Schutter, 2008).

come next. The progradation of the fluvial-deltaic Mauch Chunk Group followed the deposition of the Greenbrier carbonate wedge (De Witt and McGrew, 1979; Donaldson and Shumaker, 1981; Yang, 1998). The transition from marine dominated deposition in the Greenbrier Limestone to the non-marine dominated Mauch Chunk Group is not abrupt but involves the interdigitation of marine and non-marine sediments that comprise the study interval.

The Pencil Cave shale, the basal unit of this transition, was deposited during the sea's maximum transgression (Fig 3). The red and green colors to the north are representative of continental deposition, whereas the grey to black colors found in the south is indicative of a deeper water marine depositional setting (Neal, 1997). The Blue Monday sandstone was then deposited as a sheet sand in laterally anastomosing fluvial channels and terminating in a delta/barrier system to the south as the sea level cycle shifted from transgressive to regressive. The overlying Bickett Shale was deposited in an estuarine environment as the sea once again quickly transgressed into the basin with the Little Lime beginning the subsequent sea level cycle.

A modern analogue is the Kosi River (a tributary of the Ganges River) which runs adjacent to the Himalayan Mountains. The river covers a large areal extent and has evidence of channels shifting laterally east to west over a distance of 75 miles in the past 250 years (Reineck and Singh, 1973). In a single year the channel has been documented to shift over 18 miles laterally (Reineck and Singh, 1973). Most deposits have high lateral continuity and are less than 100 feet thick. Multiple fining upward sequences are common, as is scour, both of which were exemplified in the Blue Monday sandstone. They both also formed adjacent to areas of large uplift, which may increase the amount of sediment being transported due to steeper slopes and erosion.

There are several possible depositional models for the Blue Monday sandstone. The first is shown in Figure 44. This model shows the channels (blue lines with arrows giving direction) flowing from the north and east into the depo-center in Nicholas County. The major trunk stream could flow from east to west across Nicholas County with secondary drainage derived from the smaller tributaries. Another possibility shown in Figure 45 would have the north-south trending channels feed into a delta/barrier system located in Nicholas County (shown by black dots), connecting it to the Bluefield Sea (Figure 3). It is not possible with the data available to provide a more refined depositional model.

PETROLEUM GEOLOGY

The Blue Monday sandstone is a productive unit in the Upper Mississippian of West Virginia. There are 13 gas fields across Braxton, Clay and Nicholas counties with reported production from the Blue Monday sandstone. Production is primarily natural gas although a few wells in Braxton and Clay counties also produce oil. Production data are reported from these wells but most data include pays above and below the Blue Monday sandstone and these commingled data do not provide specific production data for the Blue Monday sandstone. A few wells produce exclusively from the Blue Monday sandstone and those data are reported here. The decline curves (Figs. 29, 30, 31) show initial strong production of 3300-900 MCF (thousand cubic feet per month), and taper to less than 100 MCF/month over time. The decline curves show hyperbolic to exponential decreases in production but because of the limited data it is impossible to predict ultimate recoverable volumes.

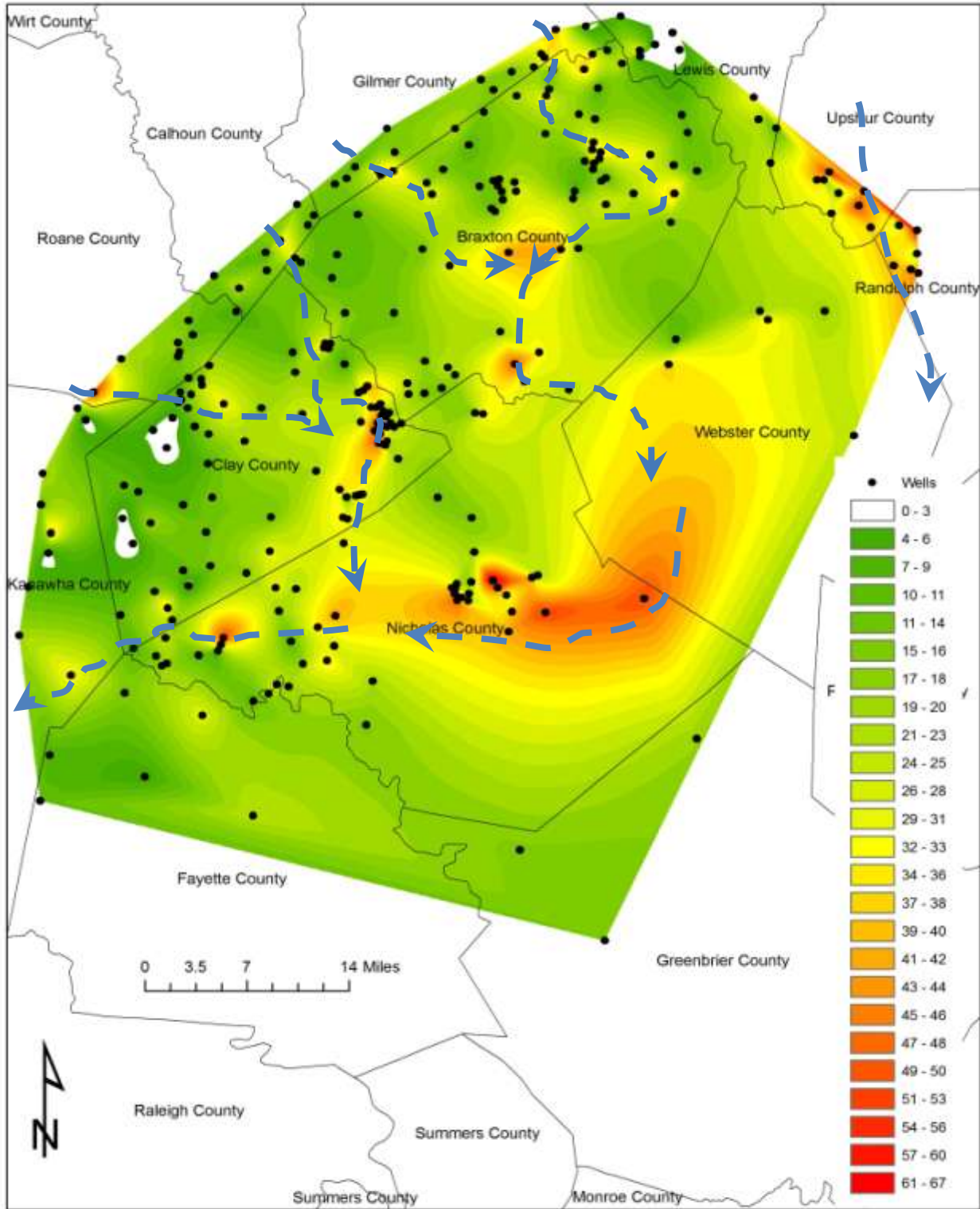


Figure 44: First possible depositional model shown overlying Blue Monday isopach map. The water courses (blue lines) move from the north and east to a delta in Nicholas County, then move towards the sea to the southwest.

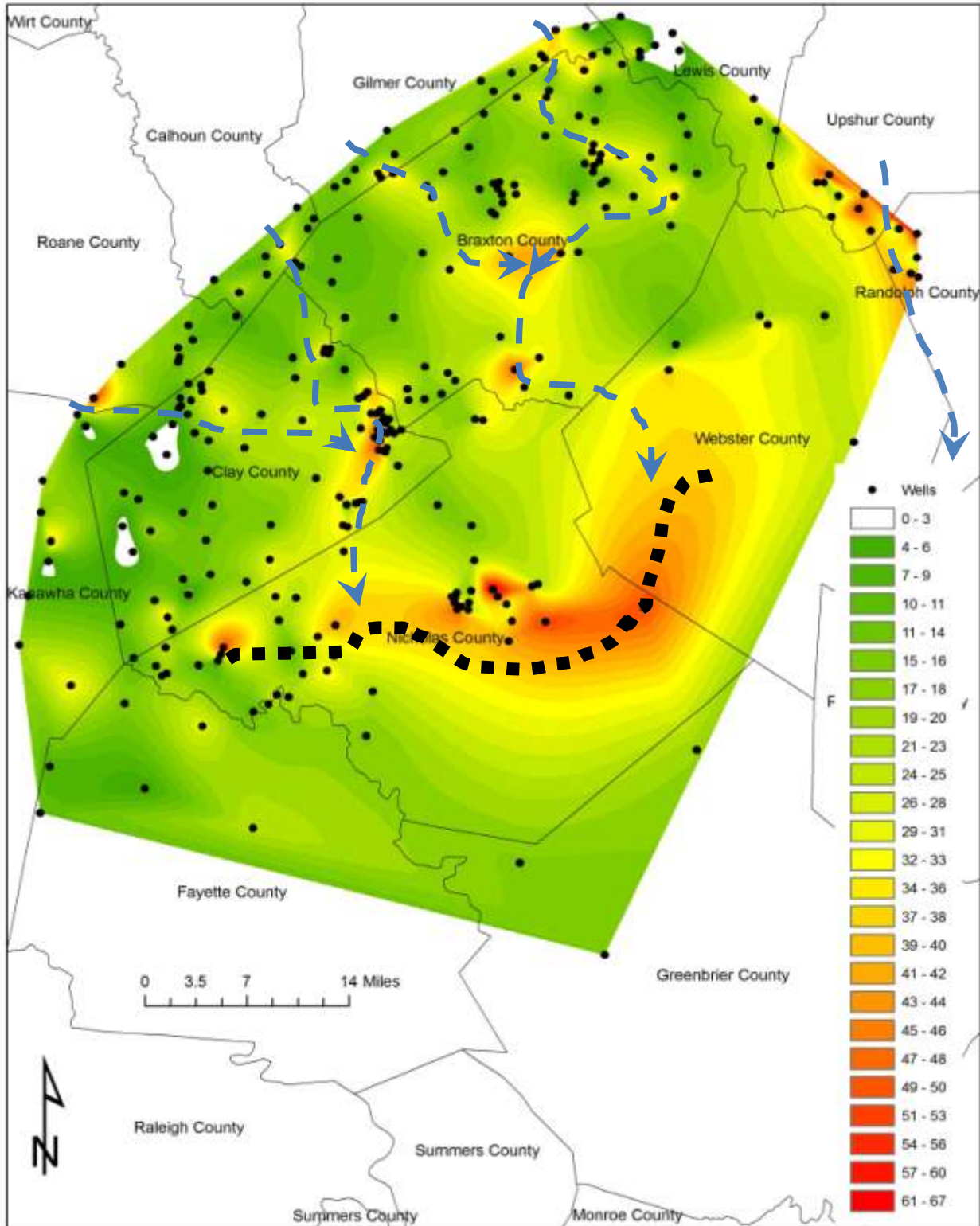


Figure 45: A second depositional model for the Blue Monday sandstone shows the water courses (blue lines) coming from the north and east to a delta/barrier system (black dots) in Nicholas County, which is the buffer zone between land and the sea to the southwest.

Well log porosity varies from zero to 20% over the study area. Areas with high log porosity are often in the stacked/incised channels described above, but sometimes can be located in the thinner channel/floodplain sands of the Blue Monday sandstone. Porosity in the thick Blue Monday sandstone in Nicholas County is not as high as would be expected. Well logs exemplify the fact that the sand has lenses of more and less porous material and porosity can change going up-section. Porosity is generally higher in the center to bottom of the Blue Monday sandstone.

Laterally extensive reservoir bodies like the Blue Monday sandstone usually require some type of structural deformation to provide a trapping mechanism (Miall, 1996). The structure contour map on the top of the Big Lime (Fig.21) shows little in the way of high amplitude folds that might provide a trap for hydrocarbons. Low amplitude folds appear to be beyond the resolution of the data. Therefore, the trapping mechanism must be stratigraphic.

Sheet-like porous reservoirs commonly display a degree of homogeneity. The Blue Monday reservoir shows a considerable amount of internal heterogeneity. Flow units are inferred to be discrete rather than far-reaching due to the numerous shale partings separating thinner sand bodies as seen in the cross sections or due to post-depositional cementation by carbonates. Calcite cemented sands were observed in the samples examined for this study. The unit would perhaps benefit from acidizing and fracturing in the future to remove calcification and open pores to gas movement.

4 CONCLUSIONS

1. The Blue Monday sandstone is a primarily gas producing unit found in several central West Virginia gas fields. Stratigraphically, with the underlying Lillydale Shale (Pencil Cave), it occupies a position between the Greenbrier Limestone (Big Lime) below and the Reynolds Limestone Member of the Bluefield Formation (Little Lime) above.
2. The progradation of the fluvial-deltaic Mauch Chunk Group followed the deposition of the Greenbrier carbonates. The Pencil Cave shale, the basal unit of this transition, was deposited during the sea's maximum transgression. The Blue Monday sandstone was then deposited as a sheet sand in laterally anastomosing fluvial channels and terminating in a delta/barrier system to the south as the sea level cycle shifted from transgressive to regressive. The overlying Bickett Shale was deposited in an estuarine environment as the sea once again quickly transgressed into the basin to deposit the Little Lime.
3. The Blue Monday sandstone has and continues to be a hydrocarbon reservoir in central West Virginia. The well log porosity varies from zero to 20%, with the higher numbers in the center to bottom of the stratum. Due to post-depositional cementation flow units are not uniform and therefore completion methods of acidization and fracturing are typically required to open pore space. The gas decline curves show initial strong production of 3300-900 MCF (thousand cubic feet per month), and decrease to less than 100 MCF/month over time. The decline curves show hyperbolic to exponential decreases in production but because of the limited data it is impossible to predict ultimate recoverable volumes.

5 REFERENCES CITED

- Al-Tawil, A., T. C. Wynn, and J. F. Read, 2003, Sequence response of a distal-to-proximal foreland ramp during Mississippian glacio-eustasy, Appalachian Basin, eastern U.S.A, *in* W. M. Ahr, P. M. Harris, W. A. Morgan, and I. D. Somerville, eds., *Permo-Carboniferous carbonate platforms and reefs: SEPM Special Publication 78*, p. 9–32.
- Asquith, G.B., and Gibson, C.R., 1982, *Basic Well Log Analysis for Geologists*: Tulsa, OK, The American Association of Petroleum Geologists, 216 p.
- Barlow, C.A., 1996, Play Mmc, The Mississippian Mauch Chunk Play: *in*: Roen, J.B., and Walker, B.J., eds., *The Atlas of Major Appalachian Gas Plays: WVGES, Volume V-24*, p. 31-36.
- Beavers, M.K., 1998, *The Geology of Ramsey Gas Field, Fayette and Nicholas Counties, West Virginia: Unpublished MS Thesis: East Carolina University*, 169 p.
- Blakey, R. C., 2011, <http://cpgeosystems.com/index.html>.
- Cardwell, D.H., Erwin, R.B., and Woodward, H.P., 1968, *Geologic map of West Virginia: Map 1, scale 1:250,000, 1 sheet(s)*.
- Carney, C., and Smosna, R.A., 1989, Carbonate deposition in a shallow marine gulf, the Mississippian Greenbrier Limestone of the Central Appalachian Basin: *Southeastern Geology*, v. 30, p. 25-48.
- Carpenter, T.W., 1976, *Stratigraphy and sedimentation of middle Mississippian rocks of Gilmer and Braxton counties, West Virginia: Unpublished MS Thesis: West Virginia University*, 205 p.
- Cole III, S.L., 2005, *Paleoenvironmental Reconstruction of the Upper Mississippian Reynolds Limestone in the Central Appalachian Basin of West Virginia: Unpublished MS Thesis: West Virginia University*, 144 p.
- Corbitt, L.B., 1986, *The Petrology and Stratigraphy of the Reynolds Limestone Member of the Bluefield Formation (Mississippian) in Southeastern West Virginia: Unpublished MS Thesis: East Carolina University*, 106 p.
- Cox, B.B., 1946, Transformation of organic material into petroleum under geological conditions ("The Geological Fence"): *Bulletin of the American Association of Petroleum Geologists*, v. 30, p. 645-659.
- De Witt, W., Jr., and McGrew, L.W., 1979, Appalachian basin region in Craig, L.C., and Conner, C.W., coordinator, *Paleotectonic investigations of the Mississippian System in the United States: USGS Professional Paper 1010-C, p. C13-C48*.

- Donaldson, A.C., and Shumaker, R.C., 1981, Late Paleozoic Molasse of Central Appalachians: Geological Association of Canada, Special Paper 23, p. 25.
- Flowers, R.R., 1956, A subsurface study of the Greenbrier Limestone in West Virginia: West Virginia Geological Survey Report of Investigations, Report 15, 17 p.
- Haq, B.U., and Schutter, S.R., 2008, A Chronology of Paleozoic Sea-Level Change: *Science*, v. 322, p. 64-68, doi: 10.1126/science.1161648.
- Hennen, R.V., 1917, Braxton and Clay County Reports: West Virginia Geological Survey, 883 p.
- Hoque, M.U., 1968, Sedimentologic and paleocurrent study of Mauch Chunk Sandstones (Mississippian), South-Central and Western Pennsylvania: *American Association of Petroleum Geologists Bulletin*, v. 52, p. 246-263.
- Humphreville, R.G., 1981, Stratigraphy and Paleocology of the Upper Mississippian Bluefield Formation: Unpublished MS Thesis: West Virginia University, 366 p.
- Jordan, T. E. 1995. Retroarc foreland basins. In *Tectonics of Sedimentary Basins*, ed. C. Busby and R. V. Ingersall: Cambridge, MA: Blackwell Scientific, p. 330-362.
- Kirkland, M.J., 1985, Petrology and Diagenesis of Sandstones of the Bluefield Formation (Upper Mississippian) Southeast West Virginia: Unpublished MS Thesis: East Carolina University, 120 p.
- Miall, A.D., 1996, *The Geology of Fluvial Deposits: Sedimentary Facies, Basin Analysis, and Petroleum Geology*: New York, Springer, 582 p.
- Neal, D.W., 1997, Hydrocarbon resources in upper Mississippian sandstone reservoirs, Central Appalachian Foreland Basin, West Virginia: XIII International Congress on the Carboniferous and Permian, p. 361-365.
- Reger, D.B., 1920, Webster County Reports: West Virginia Geological Survey, 682 p.
- Reger, D.B., 1921, Nicholas County Reports: West Virginia Geological Survey, 847 p.
- Reger, D.B., and Price, P.H., 1926, Mercer, Monroe, and Summers Counties Report: WV, West Virginia Geological Survey, 963 p.
- Reineck, H.E., and Singh, I.B., 1973, *Depositional Sedimentary Environments*: New York, Springer-Verlag, 439 p.
- Schlumberger Limited, 1972, *Log Interpretation: Volume I-Principles*, p. 113.
- Serra, O., 1989, *Sedimentary Environments from Wireline Logs*: Schlumberger, France, 243 p.

Society for Sedimentary Geology, 2009, SEPM Sequence Stratigraphy Web: v. 2011.

Trask, P.D., 1937, Inferences about the origin of oil as indicated by the composition of the organic constituents of sediments: USGS Professional Paper 186-H, p. 147-157.

WVDEP, 2010, West Virginia Department of Environmental Protection, Office of Oil and Gas: v. 2010. <http://gis.wvdep.org/oog/>

WVGES, 2011, West Virginia Geological and Economic Survey: v. 20006, 2008, 2009, 2010. <http://www.wvgs.wvnet.edu/oginfo/pipeline/pipeline2.asp>

Wynn, T.C., 2003, State-wide Sequence Framework of Mixed Carbonate-Siliciclastic Ramp Reservoirs: Mississippian Big Lime, West Virginia, USA: Unpublished MS Thesis: Virginia Polytechnic Institute, 112 p.

Yang, C., 1998, Basin analysis of the carboniferous strata in central and southern West Virginia using sequence-stratigraphic principles: Unpublished MS Thesis : West Virginia University, 350 p.

APPENDIX I: WELL CUTTINGS DESCRIPTION

Braxton County- Well #4700700573

1797-1808 feet

80%- LS- gray, mottled with white (mud?), subangular to rounded

20%- SS- white, very fine-grained, sub-rounded, well-rounded grains

1808-1811 feet

70%- LS- gray, rounded grains, sub-rounded pieces

20%- SS- clean, white, well-rounded grains, sub angular to rounded pieces, calcite cement

10%- SH- gray, rounded, micaceous

1811-1821 feet

75%- SS- white, clean, angular to rounded shape, grains are well-rounded

25%- SH- gray, sub-angular to angular, some oxidation which has left orange splotches on sample

1821-1830 feet

60%- SS- white, clean, angular to rounded shape, grains are well-rounded

40%- SH- gray, sub-angular to angular, some oxidation which has left orange splotches on sample

1830-1836 feet

90%- LS- sub-angular to rounded

5%- SS- white (caving?)

5%- SH- well-rounded

Braxton County- Well #4700700590

1735-1745 feet

50%- SS- white, clean, well-rounded grains, sub-rounded shape

25%- LS- gray, rounded to sub-angular, gray

25%- SH- layered, rounded

1745-1752 feet

75%- SS- white, clean, rounded to sub-angular, stains with oxidation, fine-grained

25%- LS/SH- very fine, rounded grains

1752-1763 feet

95%- SH- gray, angular to rounded, very fine grains

5%- SS- white, clean, rounded to sub-angular, stains with oxidation, fine-grained

1763-1776 feet

70%- SH-

25%- LS-

5%- SS- oxidation present

1776-1783 feet

70%- SH- some oxidation present

25%- LS-

5%- SS-

Clay County- Well #4701500835

1743-1750 feet

60%- LS-sub-angular to rounded grains, gray

35%- SH- gray, rounded grains

5%- SS- white, clean, rounded

1750-1760- Gap in samples.

1760-1765 feet

100%- LS- gray to white, angular to rounded, some oxidation

1765-1773- Gap in samples.

1773-1777 feet

80%- LS-

10%- SH-

10%- SS-

1777-1789- Gap in samples.

1789-1792 feet

50%- SS- white, clean, rounded, some oxidation

50%- LS- sub-angular to rounded grains

1792-1797 feet

80%- SS- individual grains, ~25% oxidized

20%- LS/SH- rounded

1797-1803 feet
100%- SH- angular to sub-rounded

1803-1810 feet
70%- SH- rounded grains
25%- LS- angular grains
5%- SS- sub-angular grains.

Clay County- Well #4701500779

1783-1790 feet
95%- LS-angular to sub-rounded, gray
5%- CG- small, red rock and calcite

1790-1803- Gap in samples.

1803-1808 feet
85%- LS- angular to rounded grains, gray
10%- SH- gray, no reaction to HCL, rounded grains
5%- SS- quartz grains

1808-1819- Gap in samples.

1819-1827 feet
50%- LS- gray, sub-angular grains
25%- SS- angular to rounded grains, quartz grains as large as sand concretions
25%- SH- angular grains, micaceous, no reaction to HCL

1827-1836- Gap in samples.

1836-1844 feet
80%- SS- clean, white, sand grains are rounded, stores are sub-angular to sub-rounded
20%- LS- angular to sub-rounded grains (caving?)

1844-1857- Gap in samples.

1857-1865 feet
90%- SS- clean, white, rounded grains
10%- SH/LS- sub-angular, gray

1865-1871- Gap in samples.

1871-1880 feet
50%- SS- clean, quartz

50%- LS- calcite reaction strong

1880-1888- Gap in samples.

1888-1891 feet

All sand sized particles, moderate calcite to react to HCL, abundant quartz leftover, some shale pieces rounded, looks like beach sand

1891-1900- Gap in samples.

1900-1907 feet

All sand sized particles, more calcite than above to react to HCL, less quartz leftover, some shale pieces rounded, looks like beach sand

APPENDIX II: CROSS-SECTIONS

This section is composed of the cross-sections that were created using RockWorks15 from the data gathered from Appendix IV. It shows the thicknesses as they change over the study area.

Each cross-section has a vertical exaggeration of 20x.

Explanation:

Blue= Little Lime

Yellow= Pencil Cave shale

Orange= Blue Monday sandstone

Green= Big Lime

Depths and distances (both axes) are given in feet.

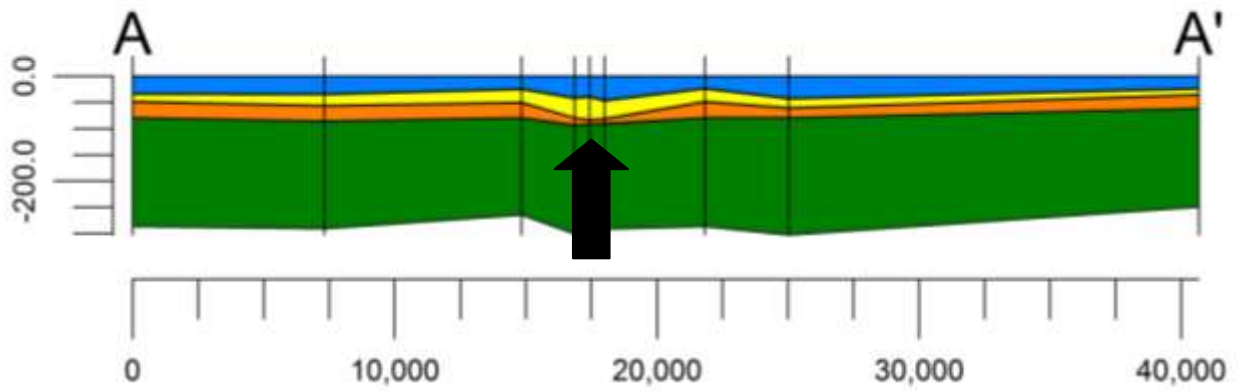


Figure 46: Cross-section A-A' showing a scour channel into the Pencil Cave shale, indicated by arrow. Location shown in Figure 46.

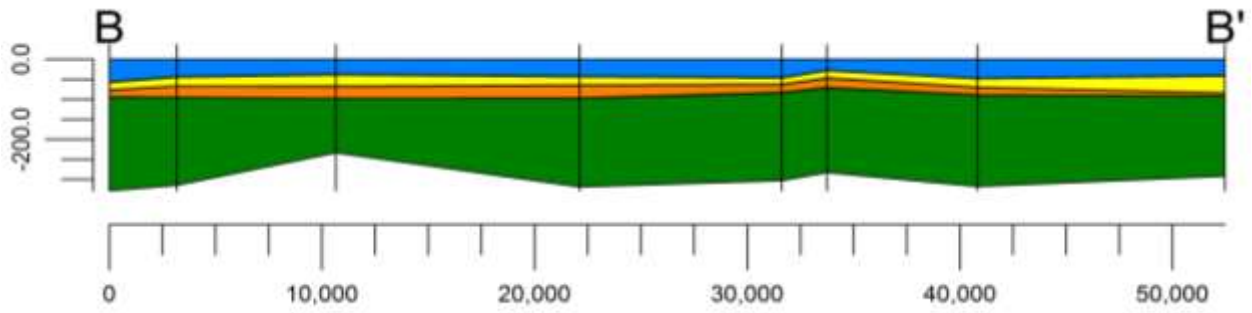


Figure 47: Cross-section B-B' showing the regional trends of the strata. Location shown in Figure 46.

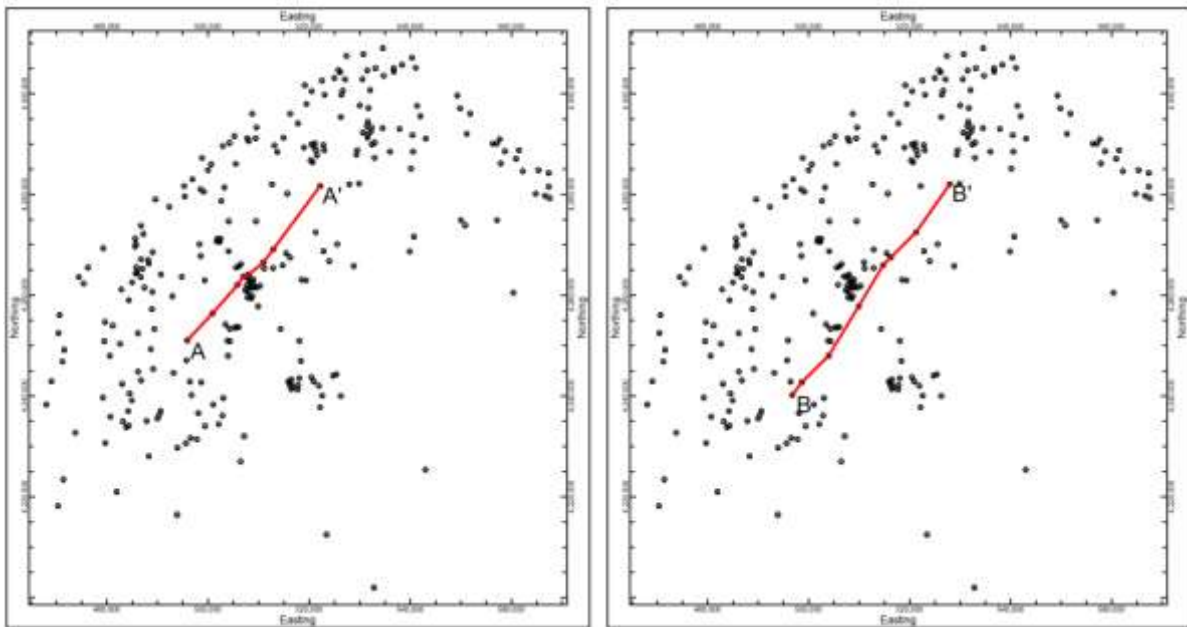


Figure 48: Location maps for cross-sections A, Figure 44, and B, Figure 45.

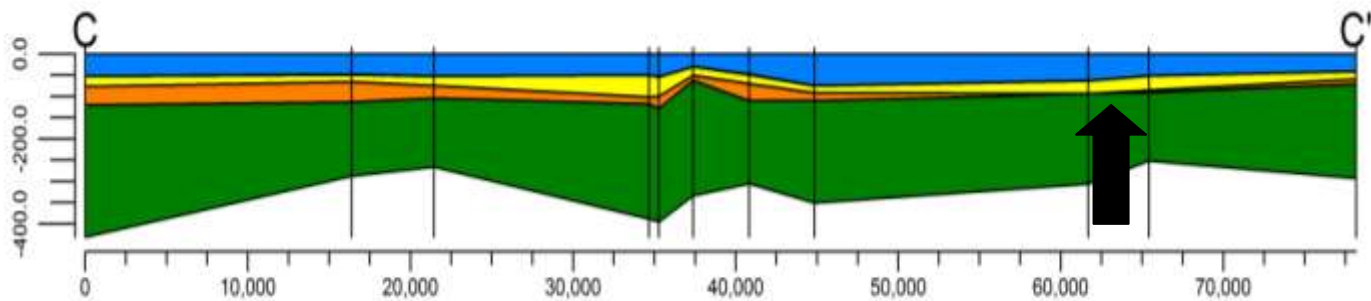


Figure 49: Cross-Section C-C' showing scour in the study area, indicated by arrow, as well as the regional trends of the strata. Location shown in Figure 49.

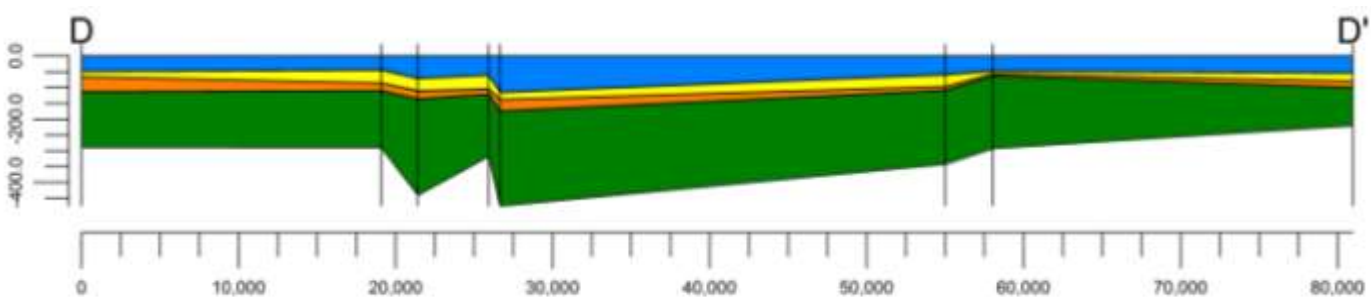


Figure 50: Cross-section D-D' showing regional trends. Location shown in Figure 49.

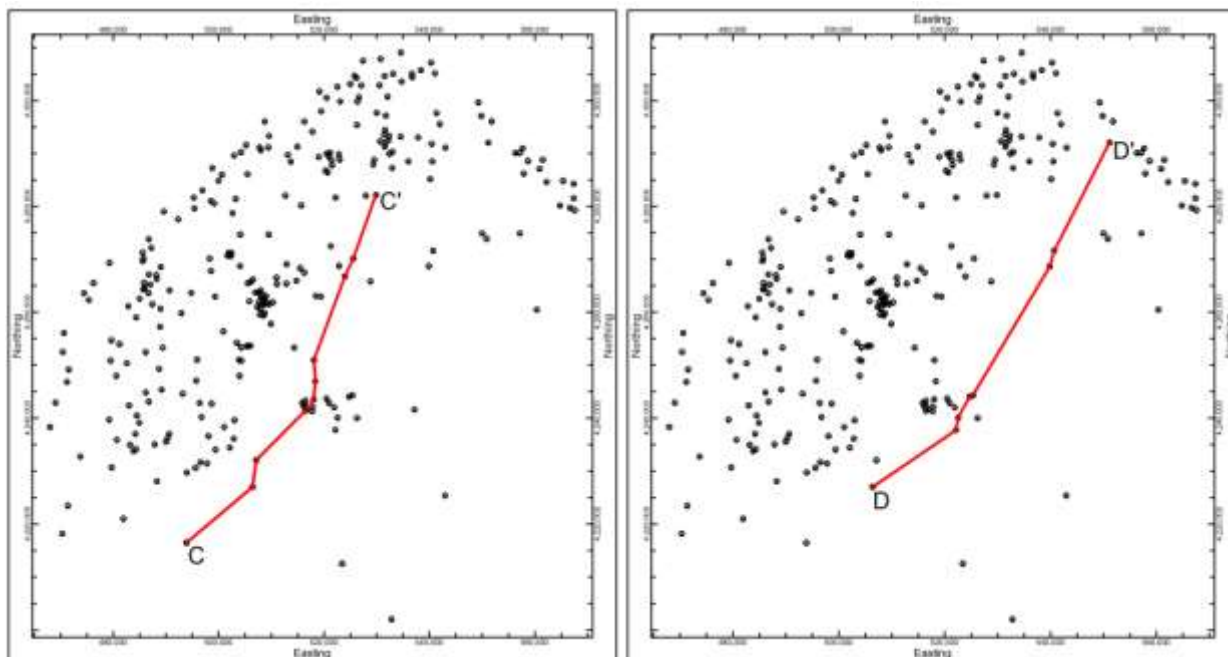


Figure 51: F: Location maps of cross-sections C, Figure 47, and D, Figure 48.

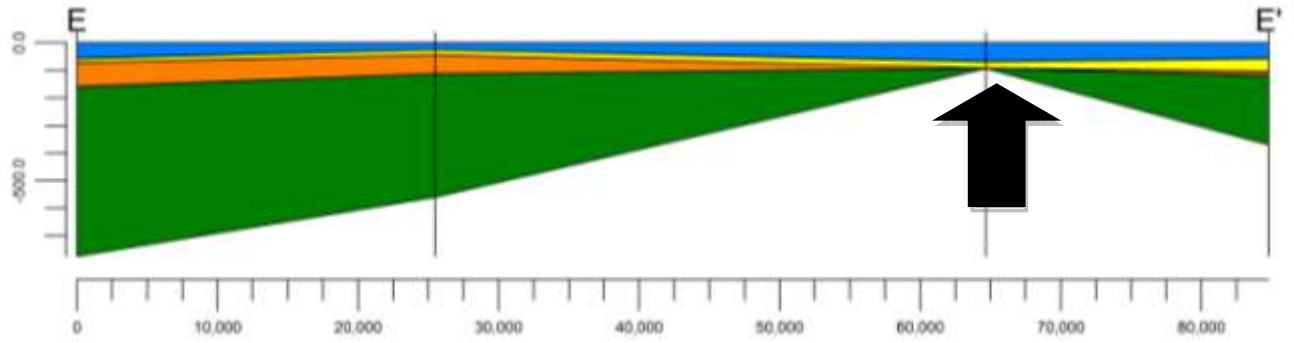


Figure 52: Cross-Section E-E' showing a floodplain of Pencil Cave, moving into a channel of BMS, indicated by arrow. Location shown in Figure 52.

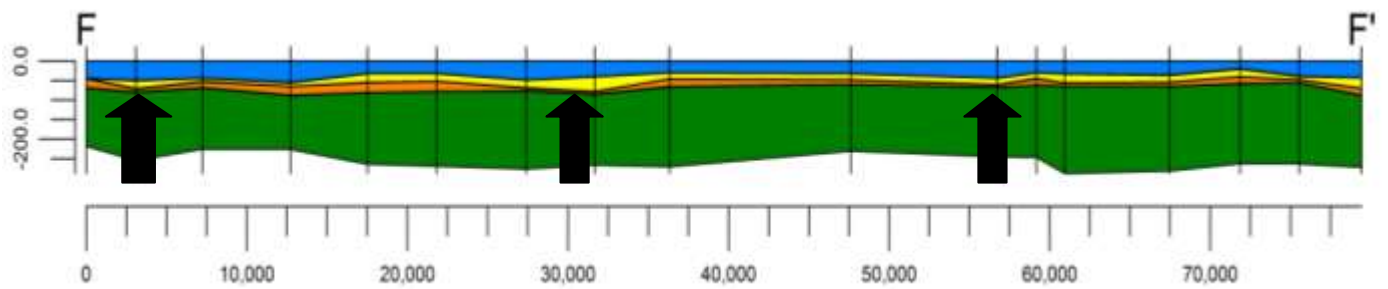


Figure 53: Cross-section F-F' shows channels, indicated by arrows, and floodplains between. Location shown in Figure 52.

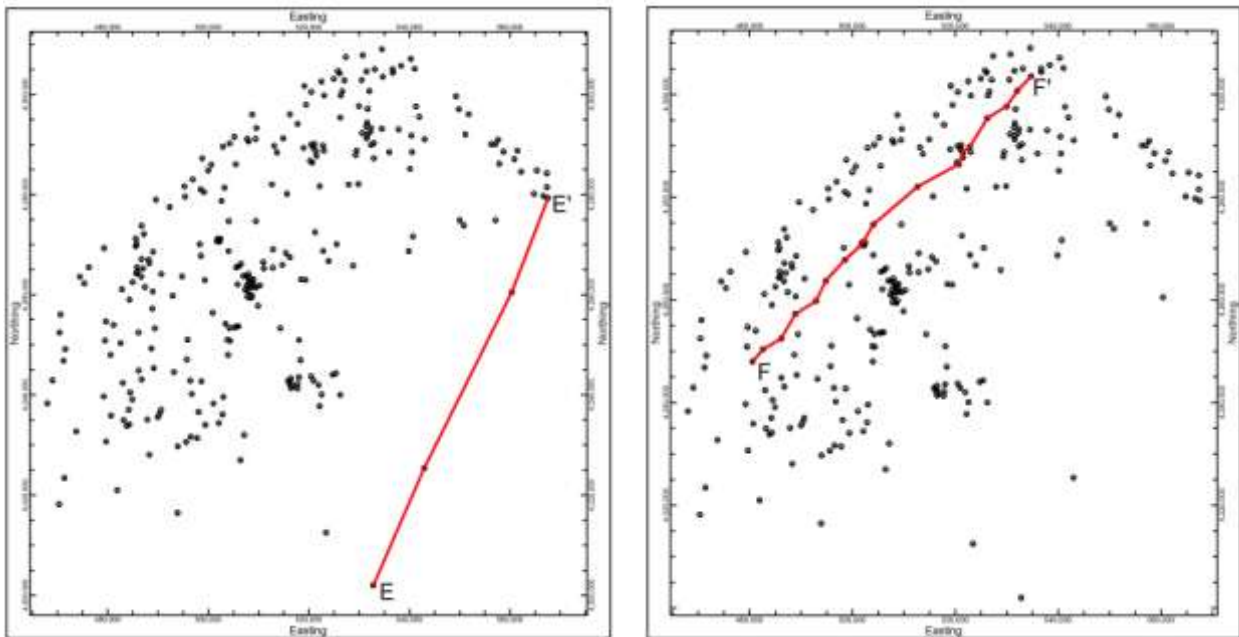


Figure 54: Locations maps of cross-sections E, Figure 50, and F, Figure 51.

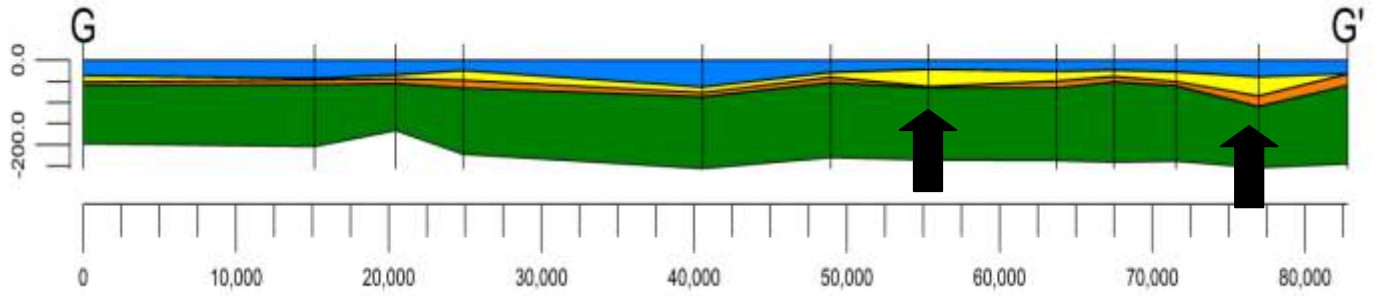


Figure 55: Cross-section G-G' showing BMS channels, indicated by arrows. Location shown in Figure 55.

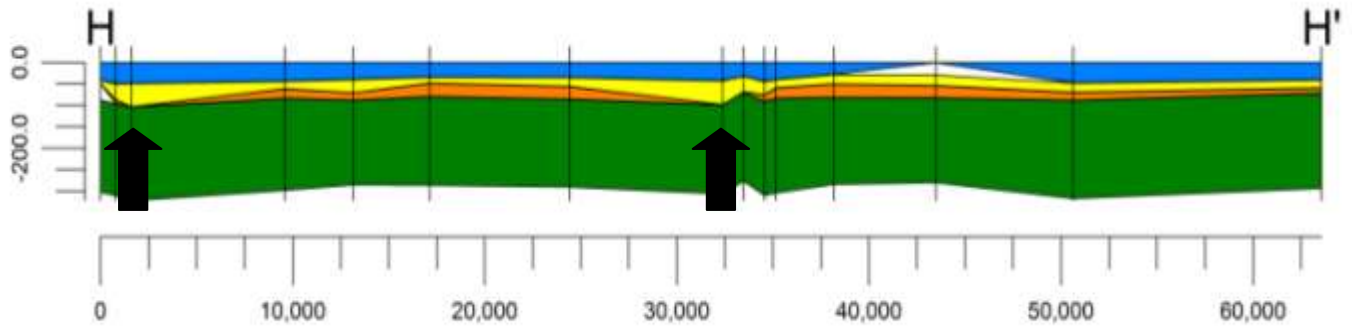


Figure 56: Cross-section H-H' showing multiple channels indicated by arrows, with flood plain in between. Location shown in Figure 55.

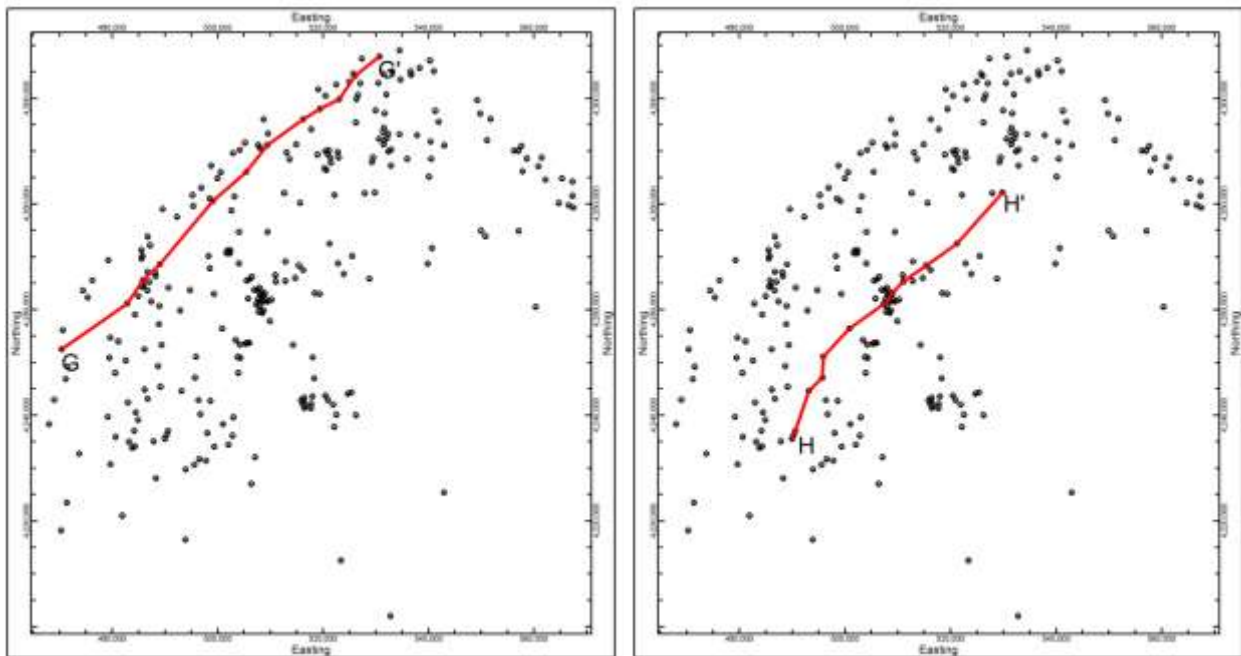


Figure 57: Location maps of cross-sections G, Figure 53, and H, Figure 54.

APPENDIX III: WELL LOG CROSS-SECTIONS

This appendix is composed of stratigraphic data for the wells used in the cross-sections constructed for this study. It is broken down into two sections: Producing Wells and Non-Producing Wells. The Producing Wells section is of cross-sections I've composed whereas the Non-Producing Section has the well data in order as opposed to lines because these data points were used in construction of the maps but not the cross-sections.

Explanation:

Red line= Top of Reynolds Limestone

Green line= Top of Webster Springs Sandstone

Yellow line= Top of Lillydale Shale

Purple Line=Top of Greenbrier Limestone

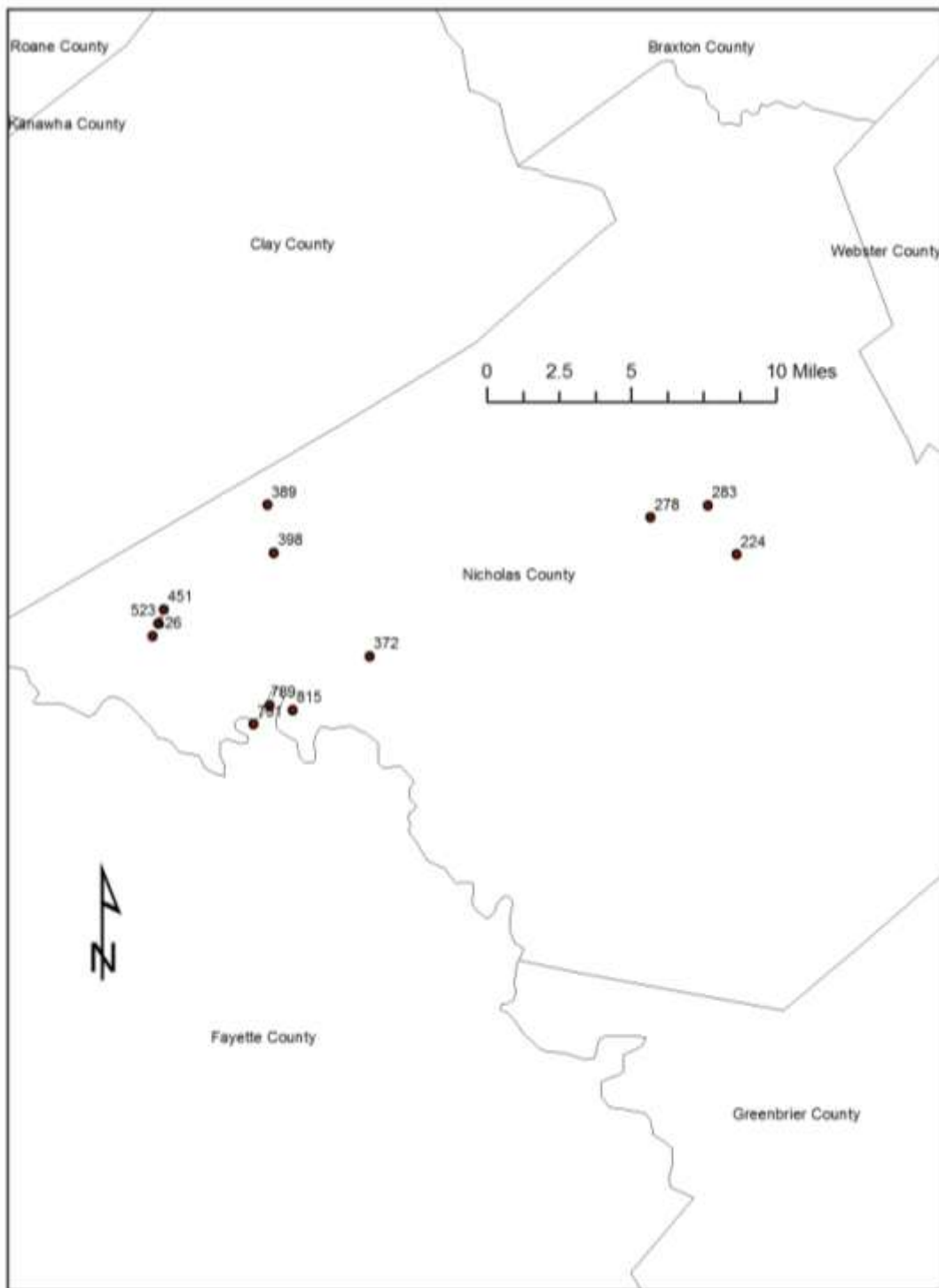
Pink Line=Base of Greenbrier Limestone

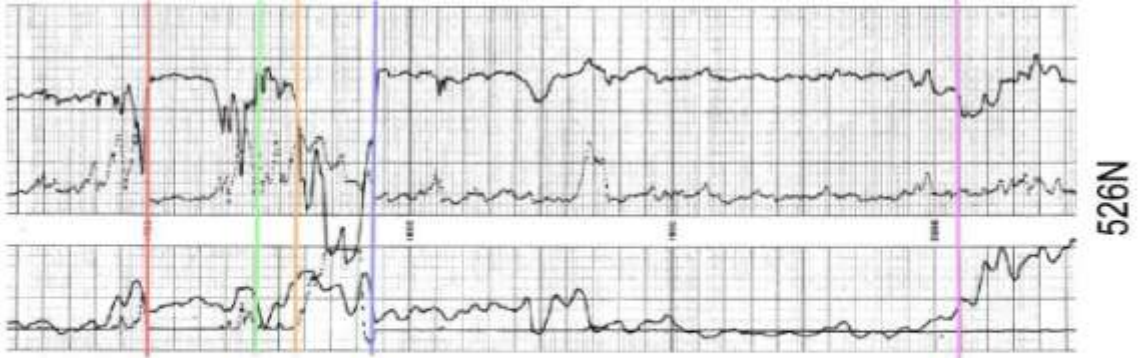
Translation of letter codes used to identify wells along with permit number:

B = Braxton, C = Clay, F = Fayette, G = Gilmer, Gr = Greenbrier, K = Kanawha, L = Lewis, N = Nicholas, Ra = Randolph, Ro = Roane, U = Upshur, W = Webster

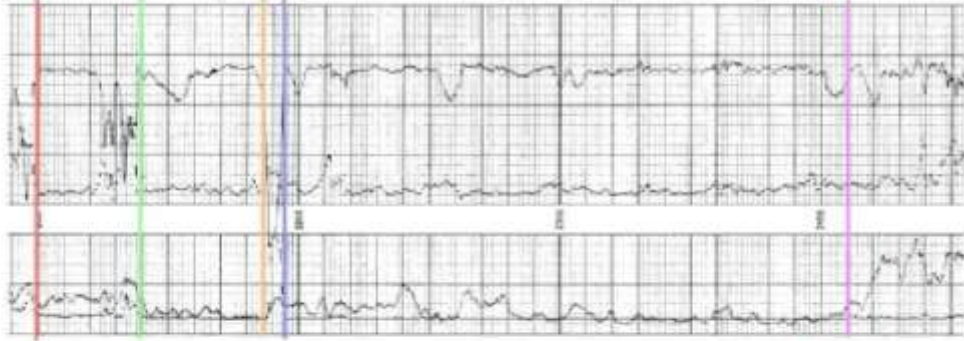
Also, a location map is included to show the locations of wells used in the study by county.

Producing Wells





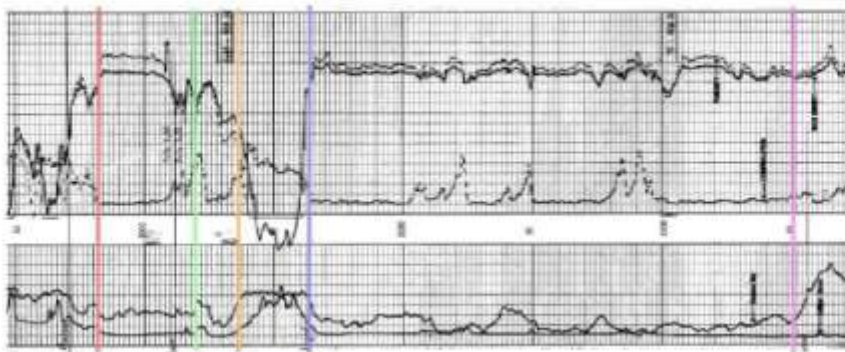
526N



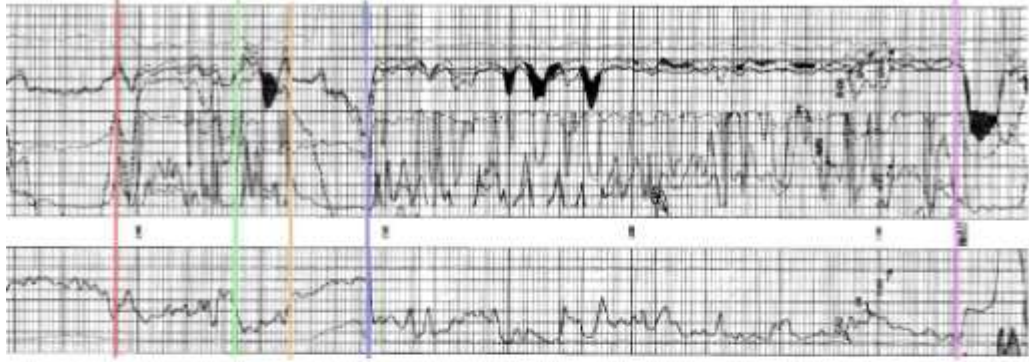
523N



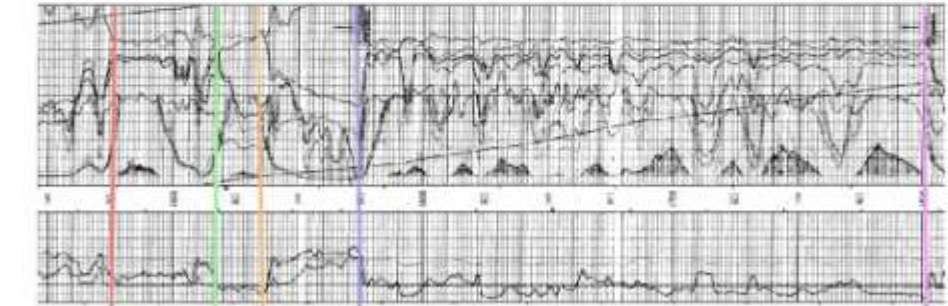
451N



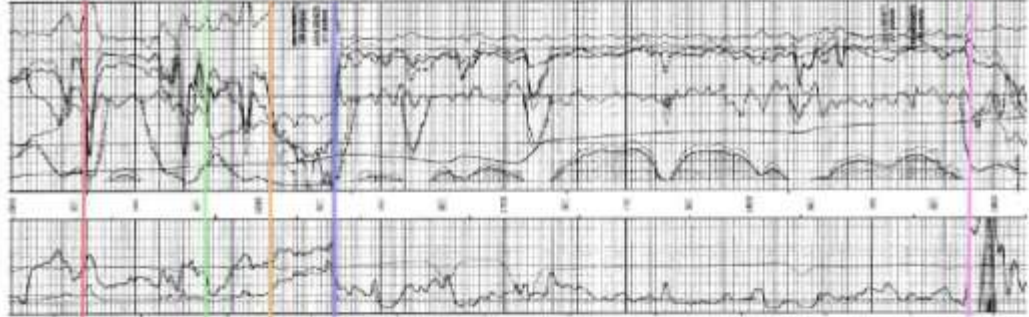
1315C



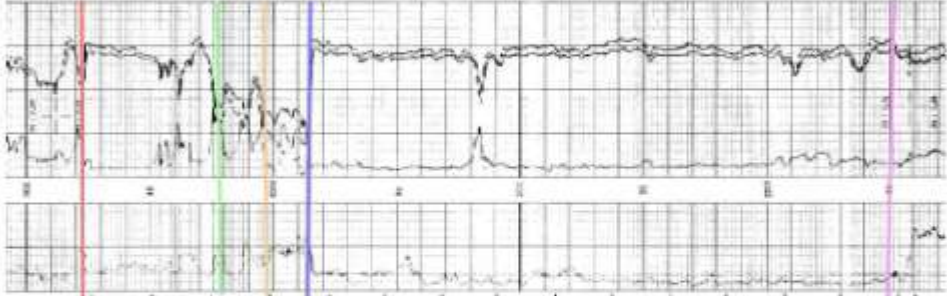
791N



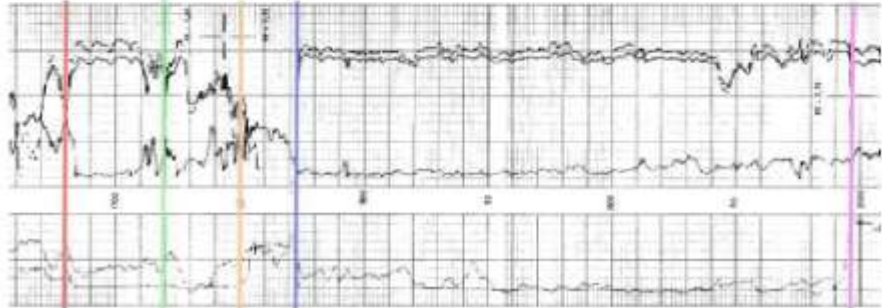
815N



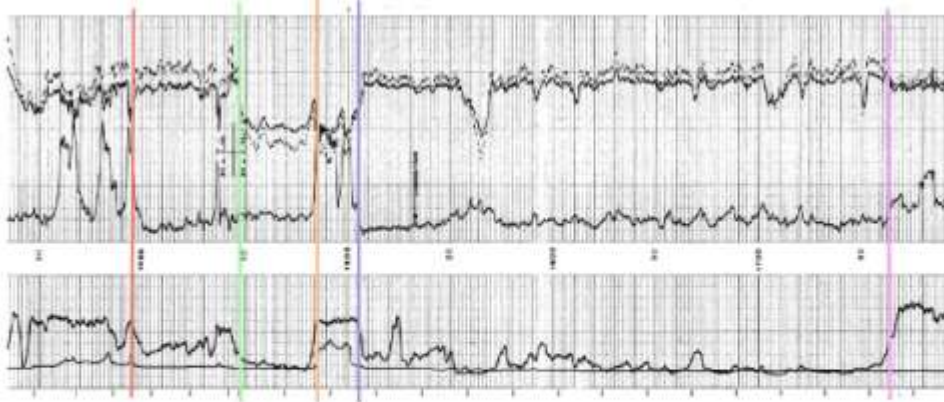
789N



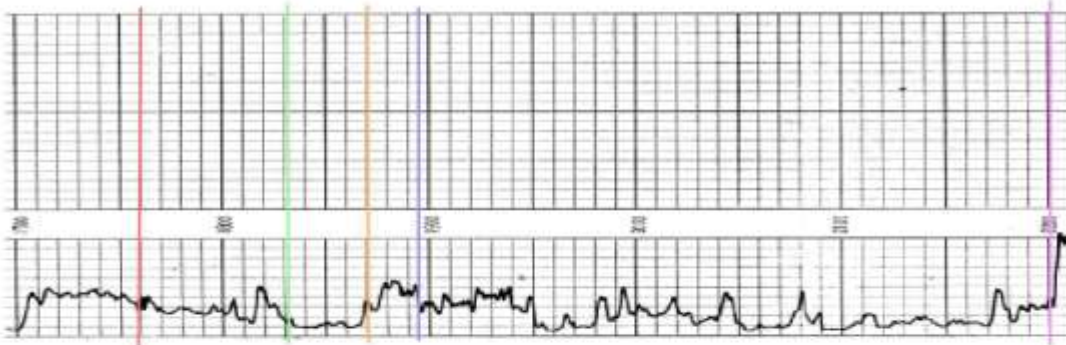
398N



389N



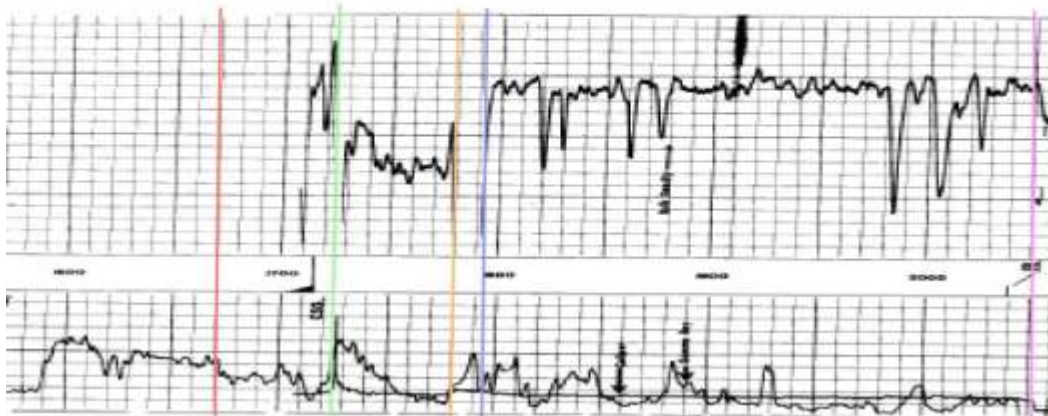
372N



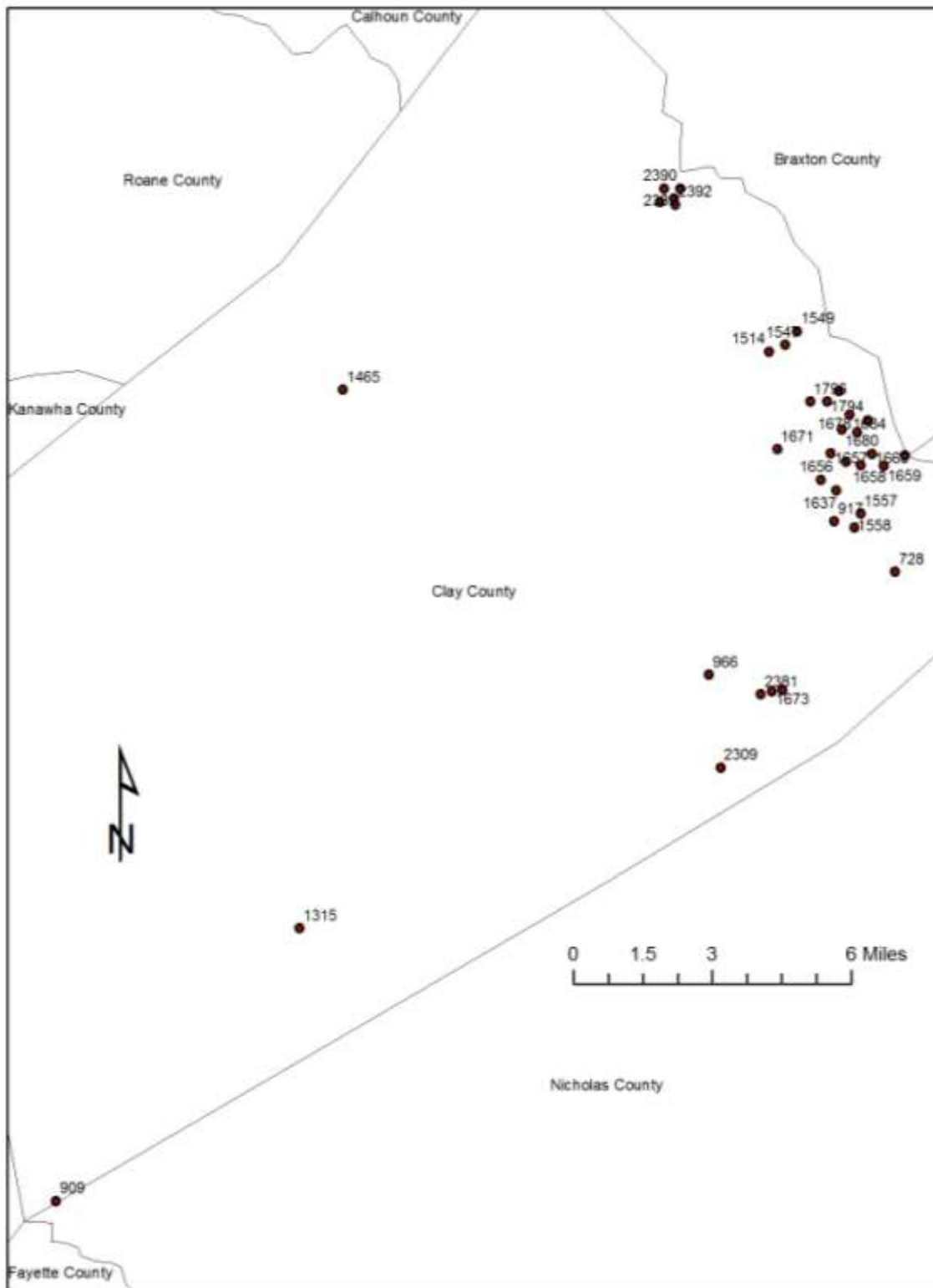
224N

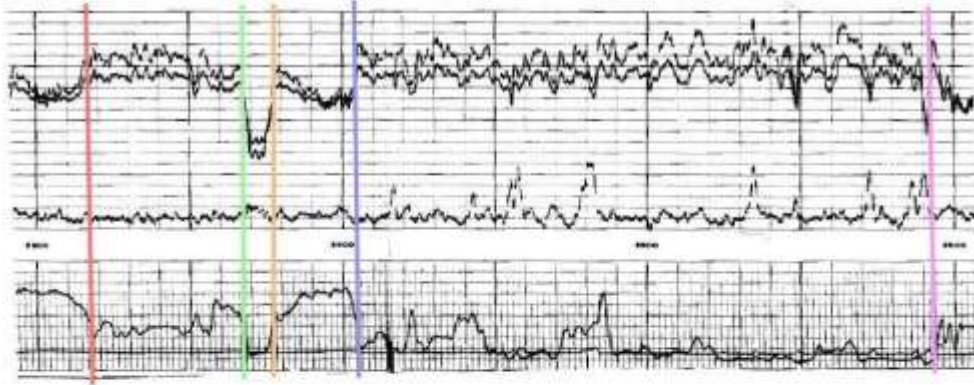


278N

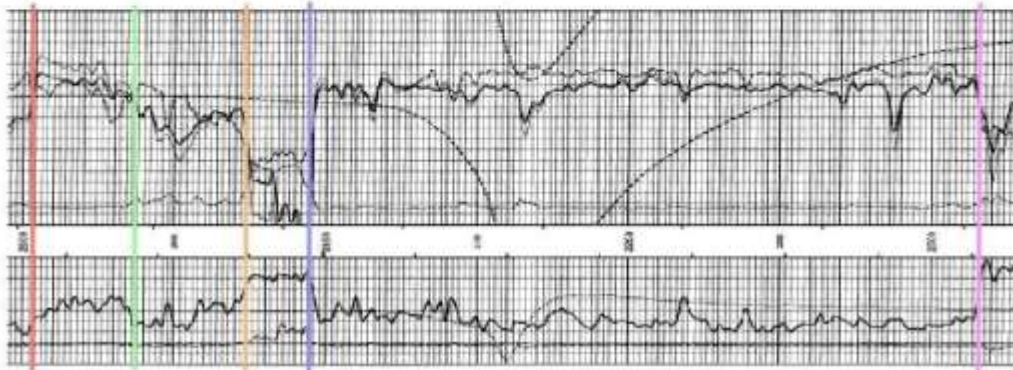


283N

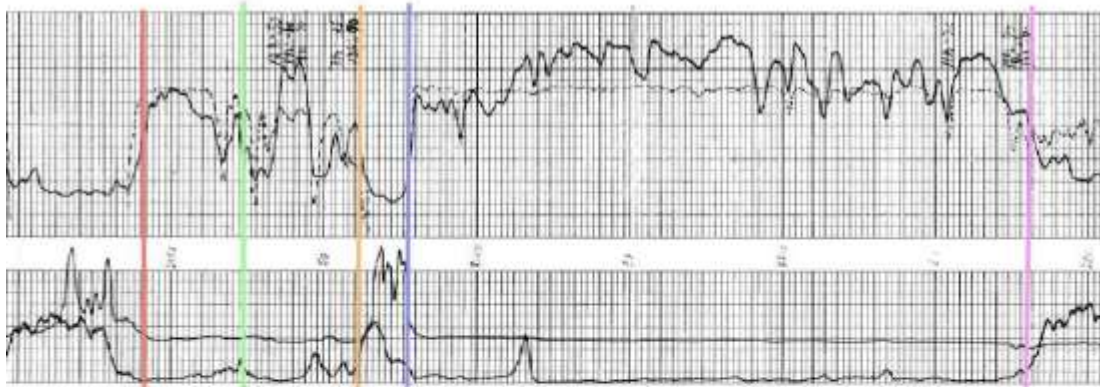




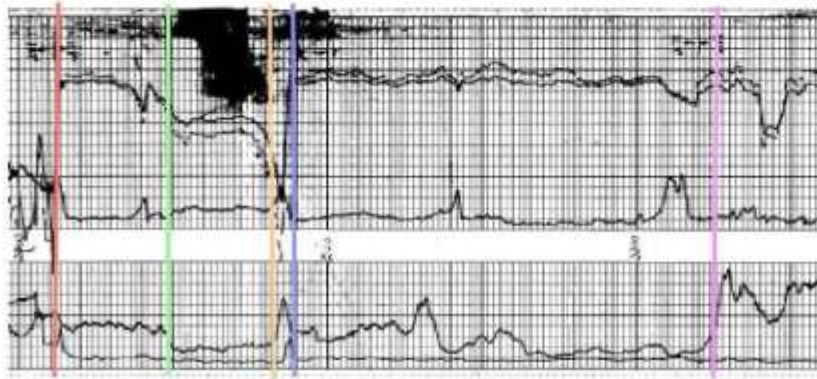
909C



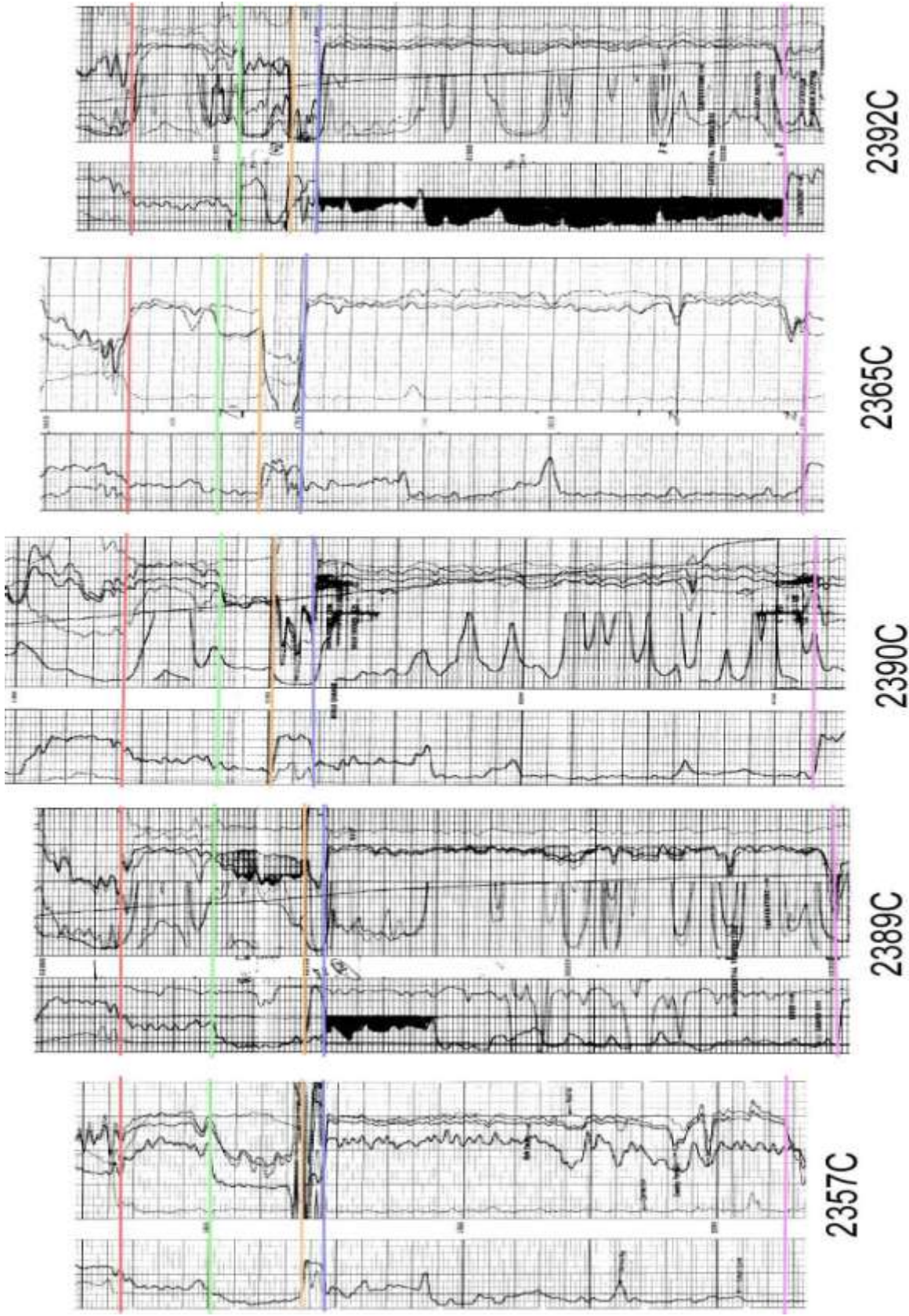
2309C

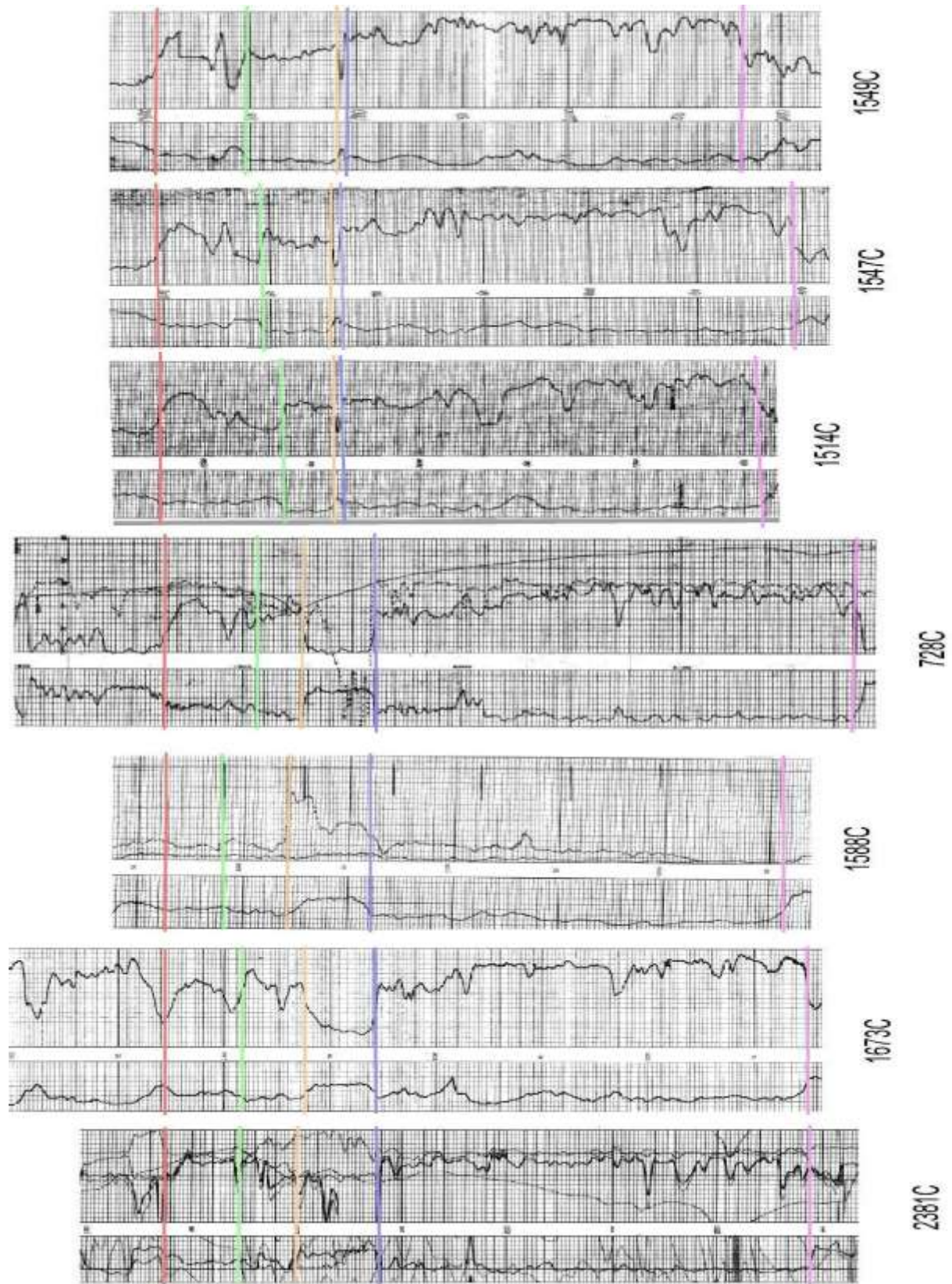


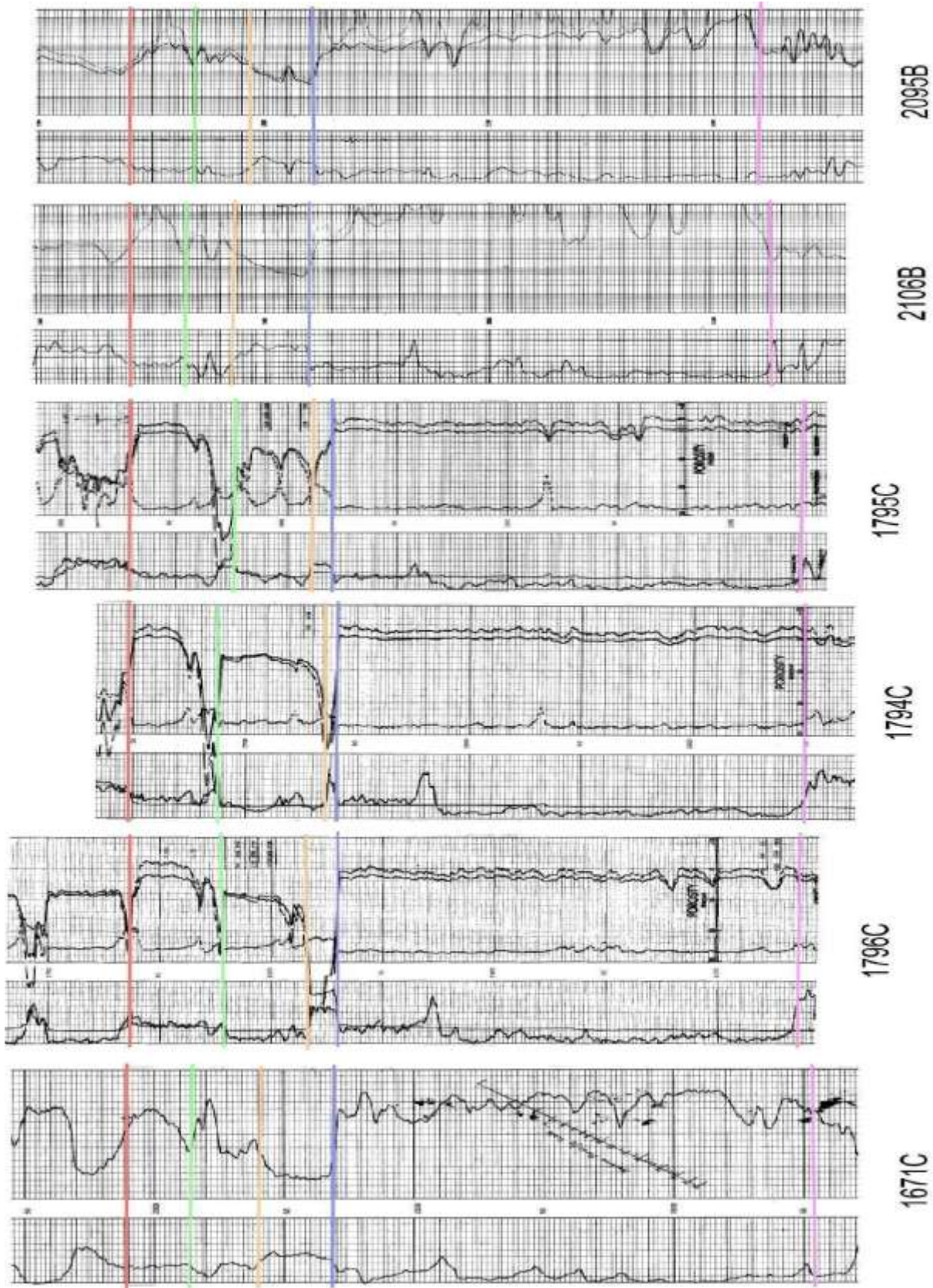
966C

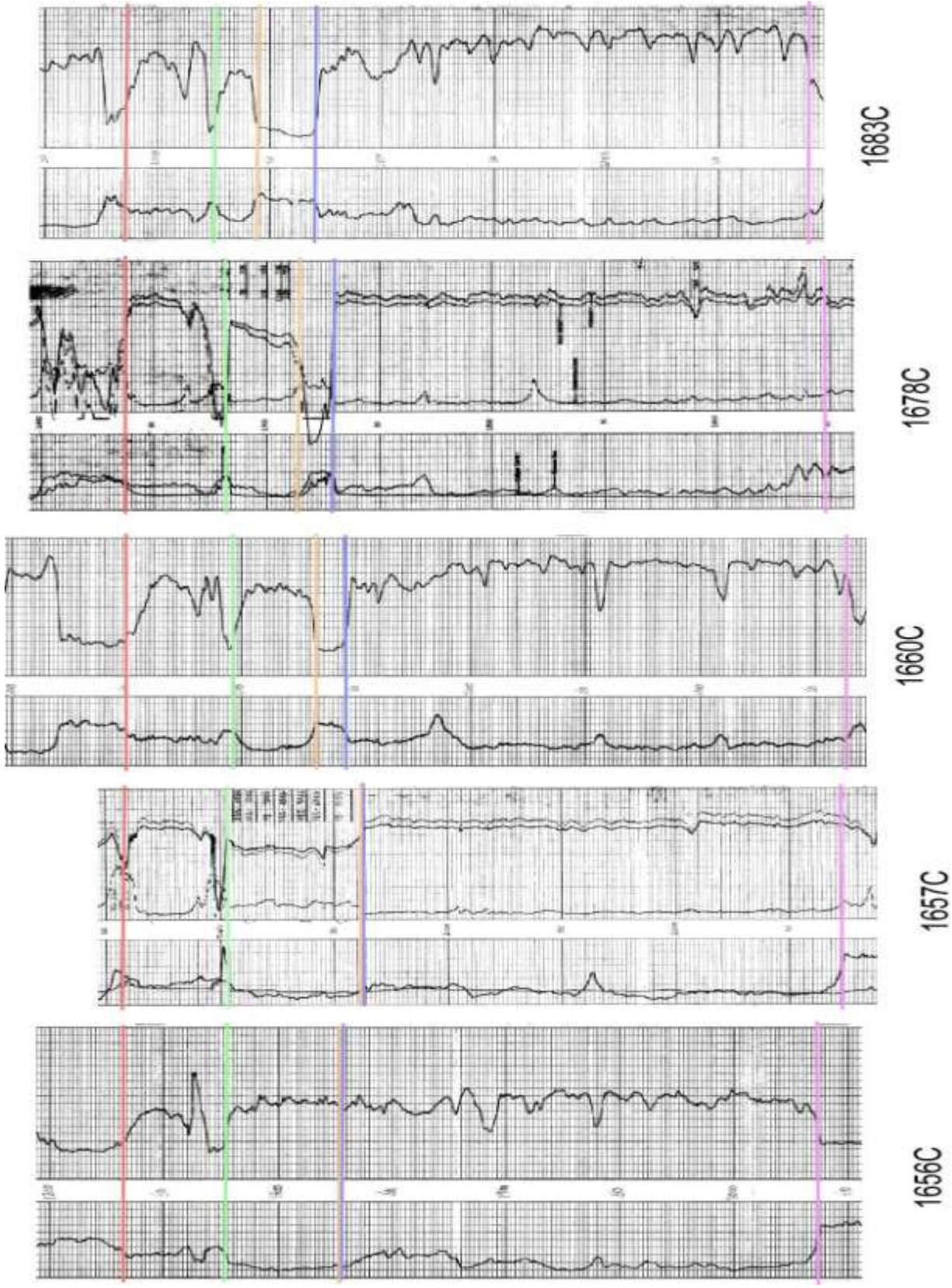


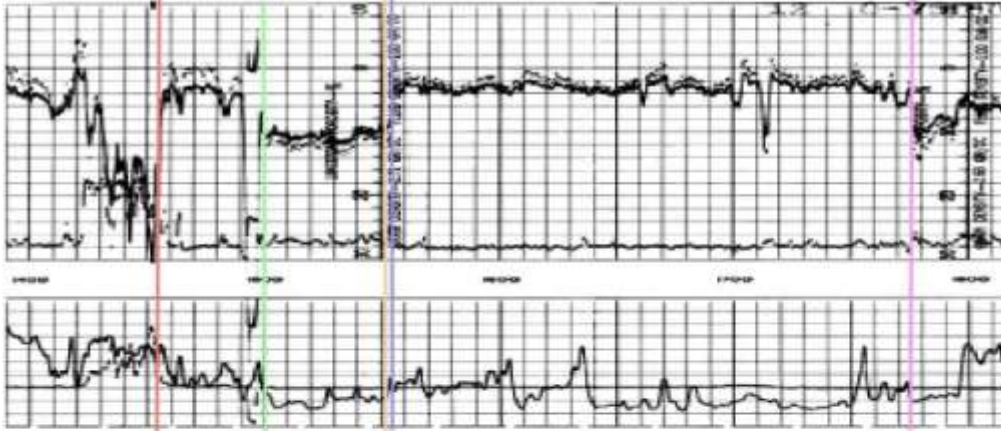
1465C



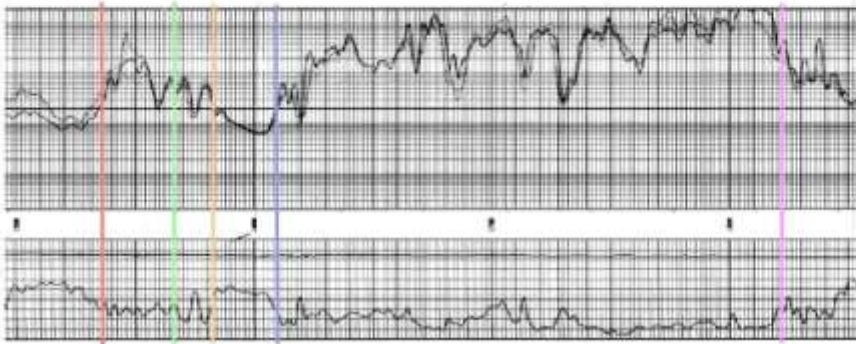




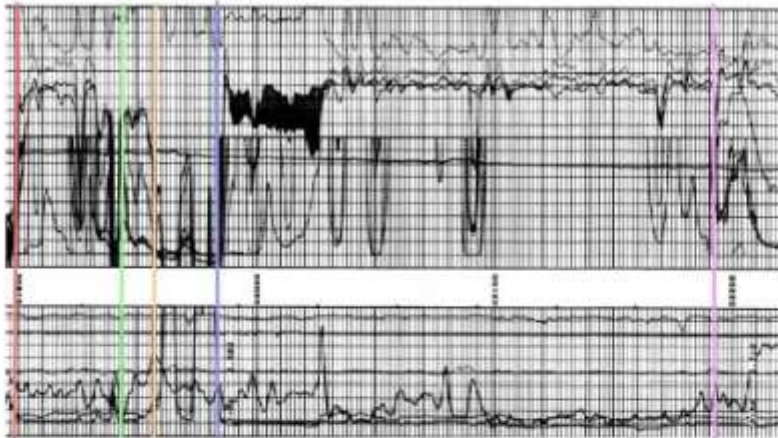




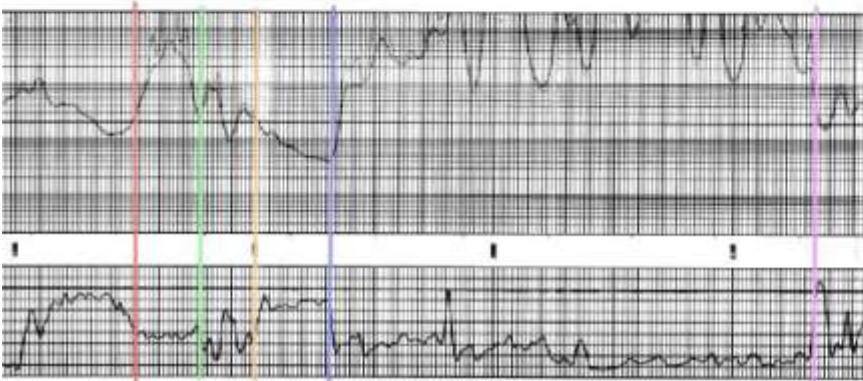
1135B



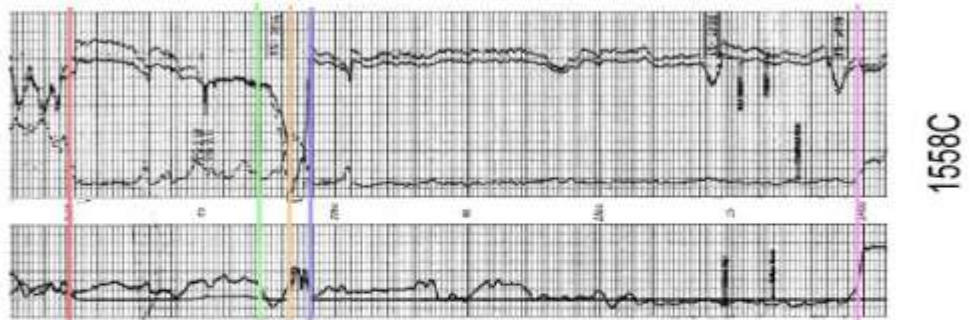
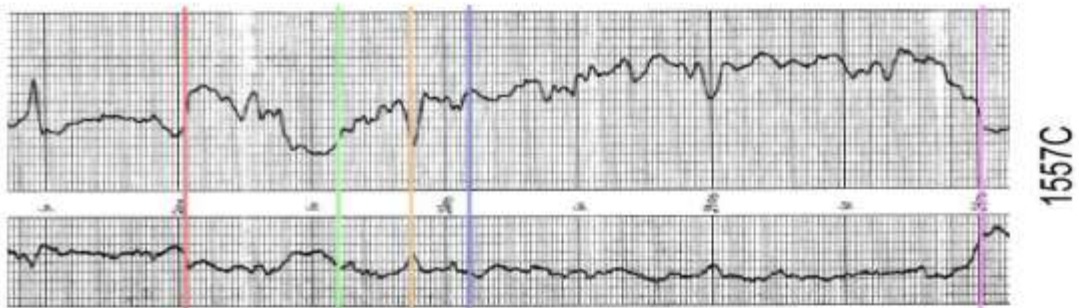
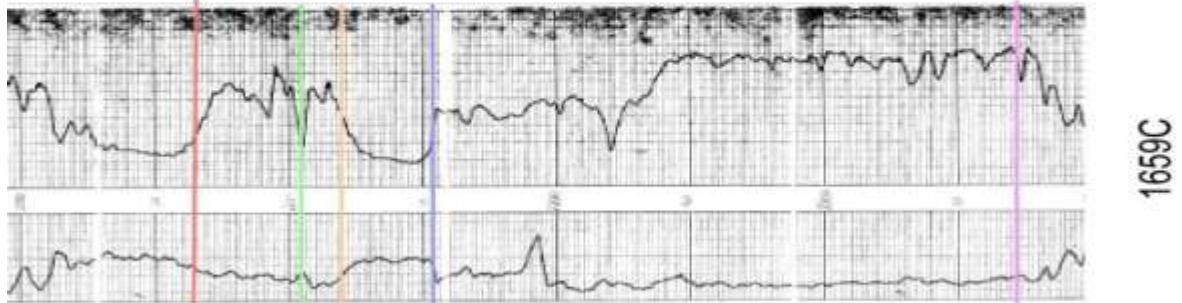
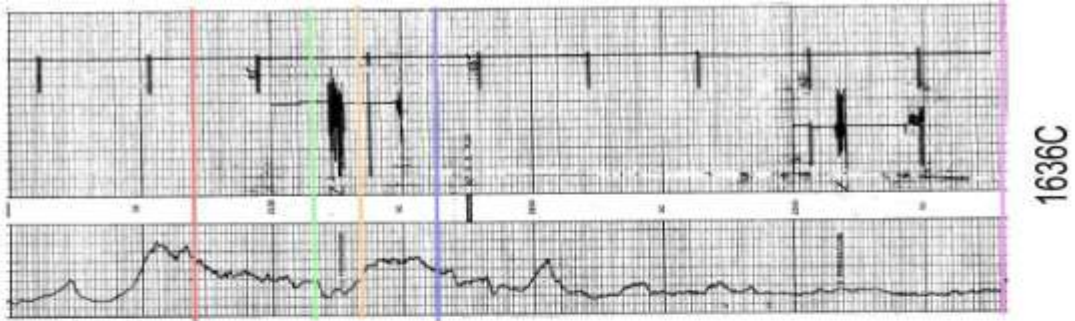
2105B

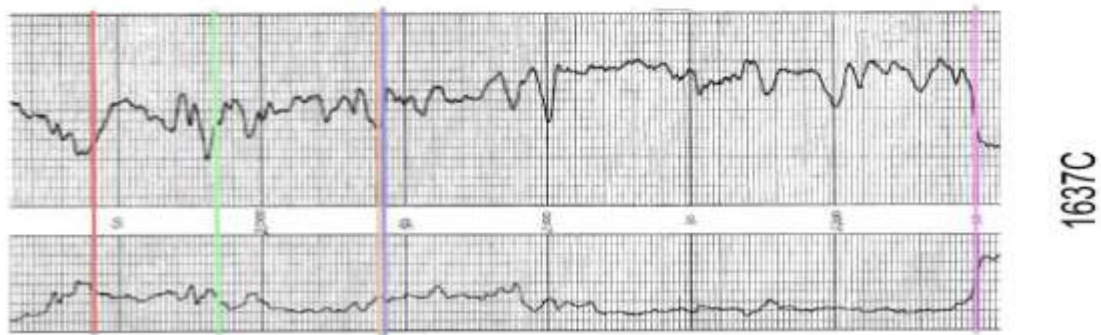
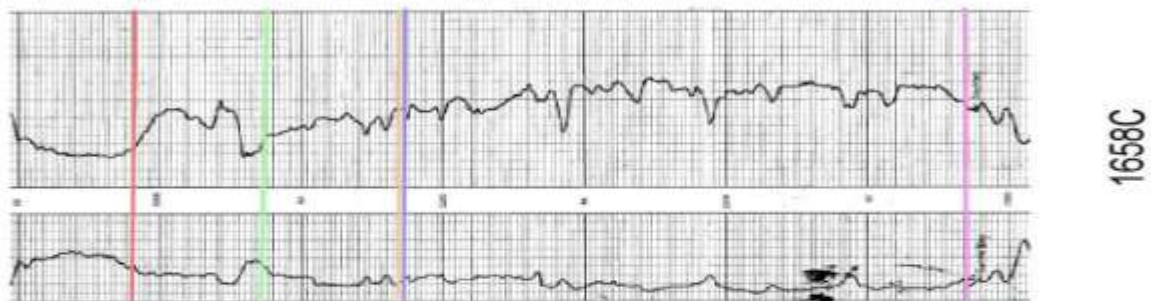
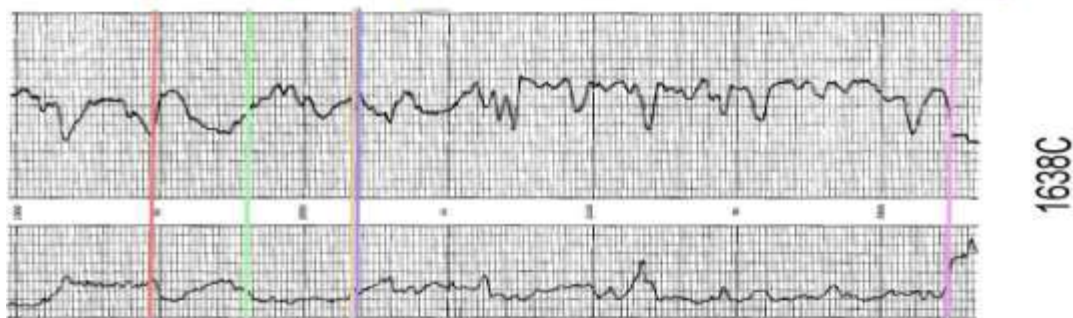
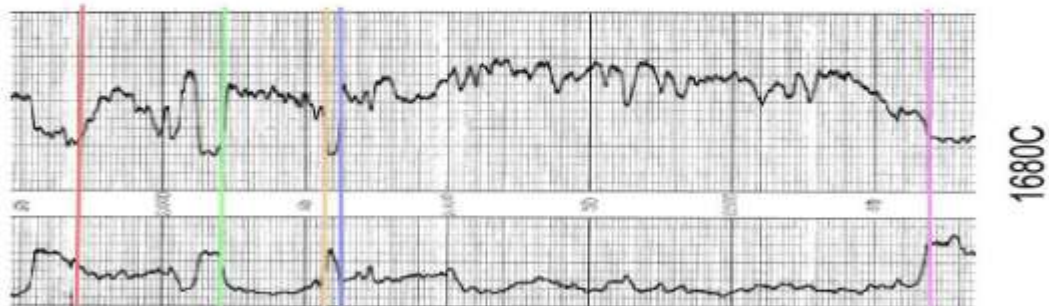
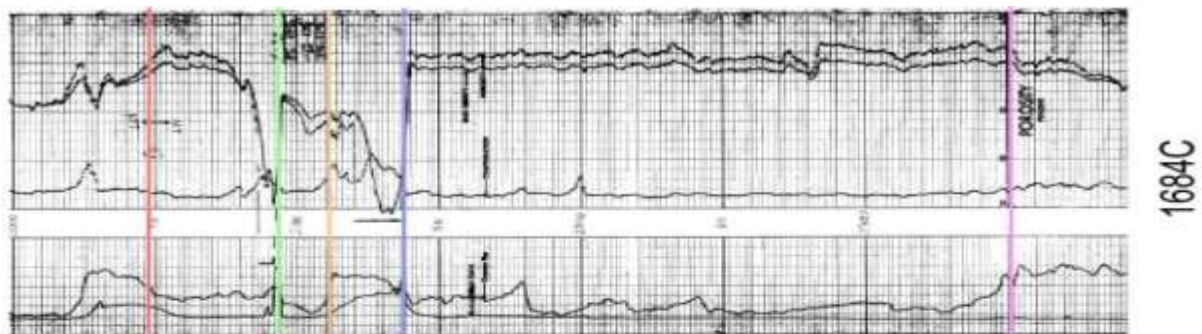


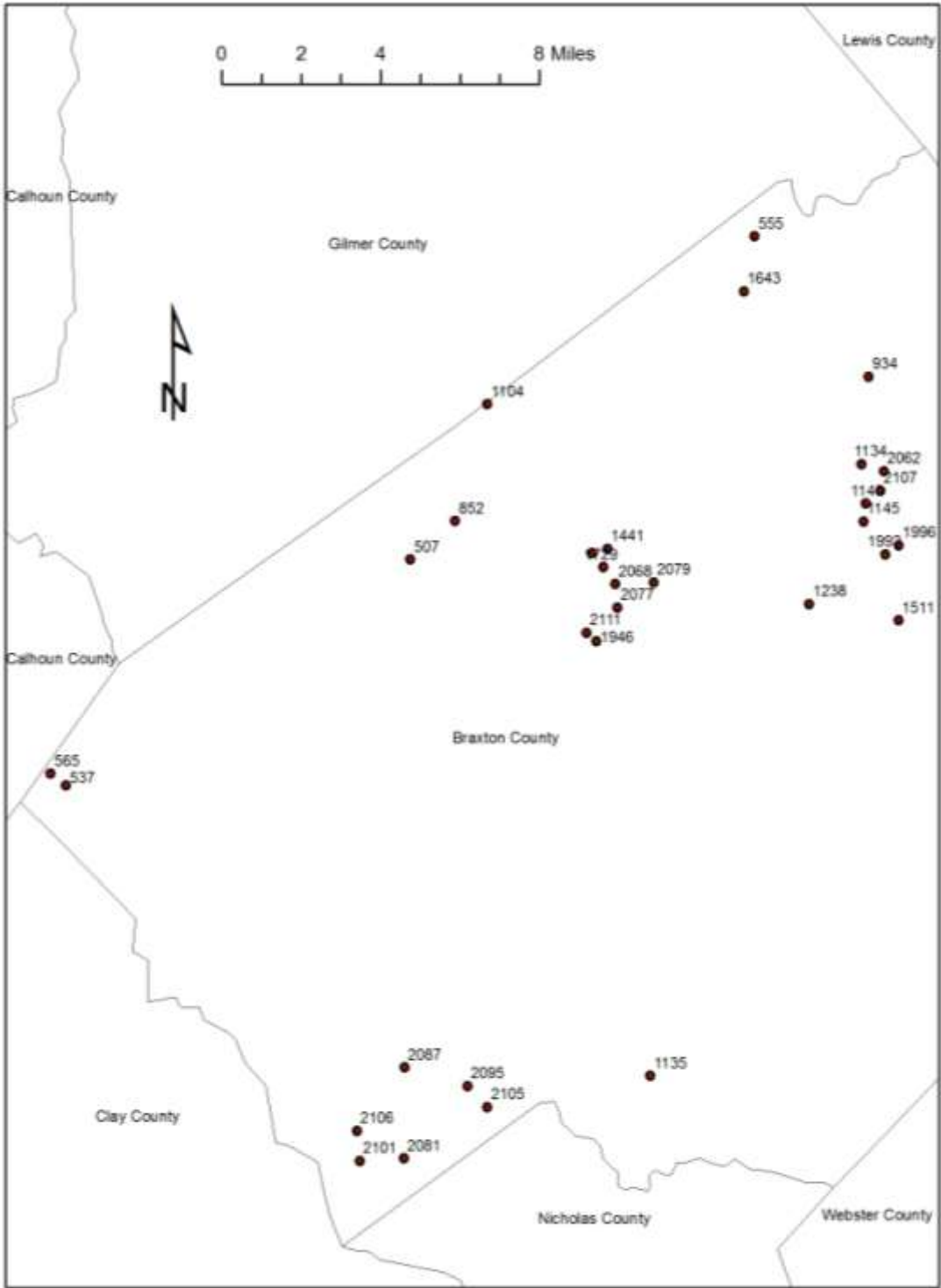
2081B

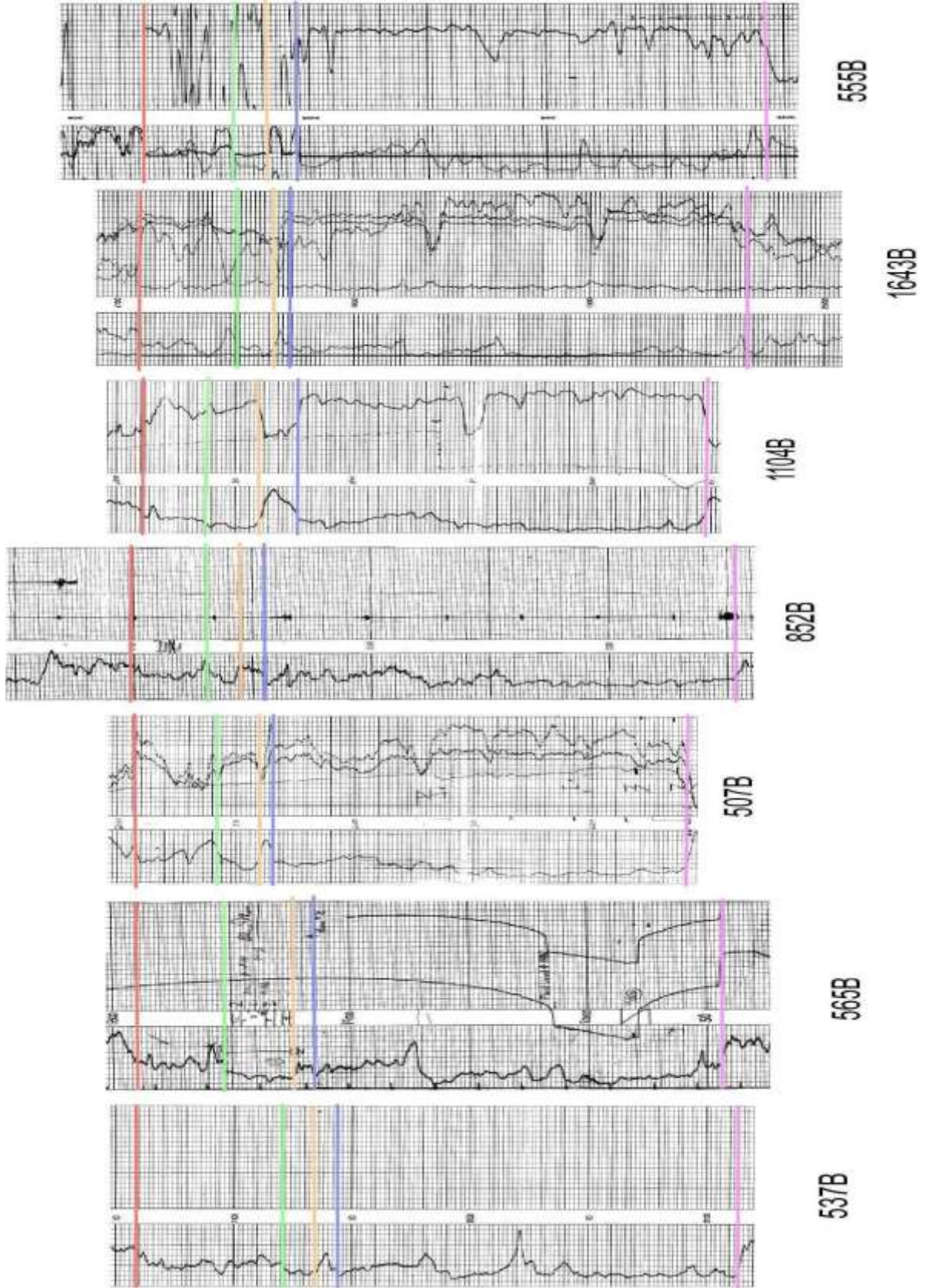


2101B



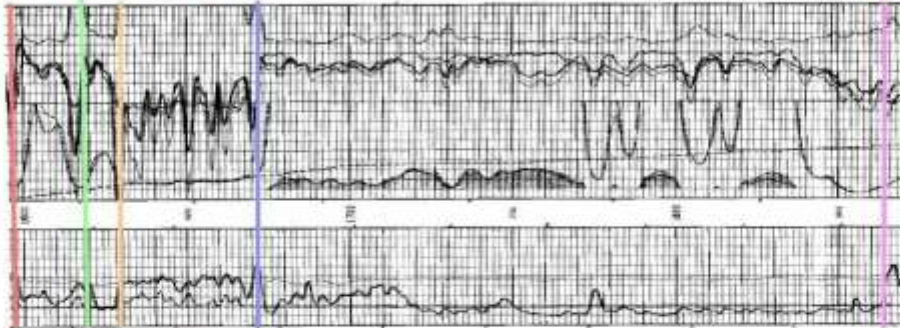








1145B



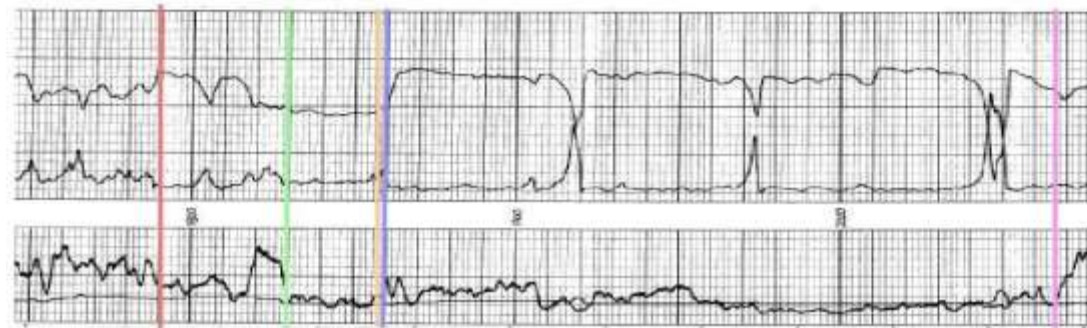
1996B



1992B



1238B



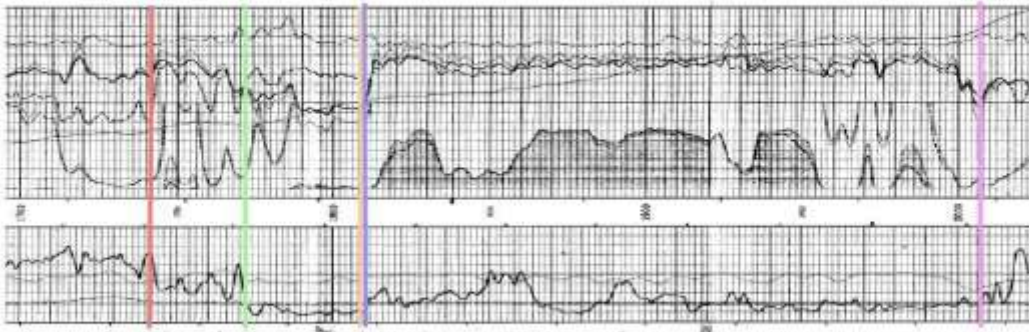
1511B



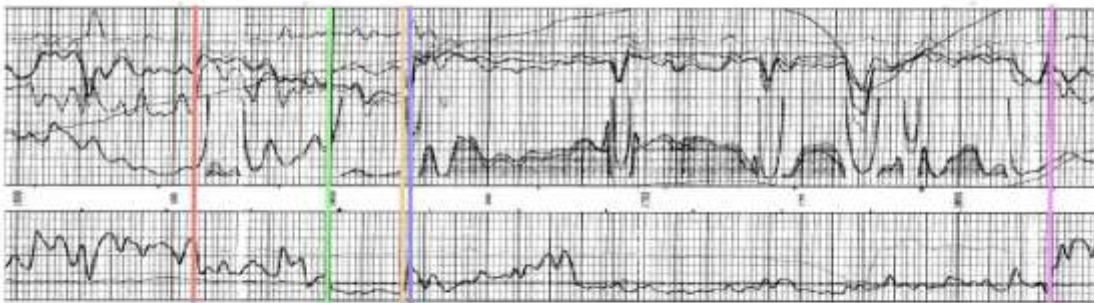
934B



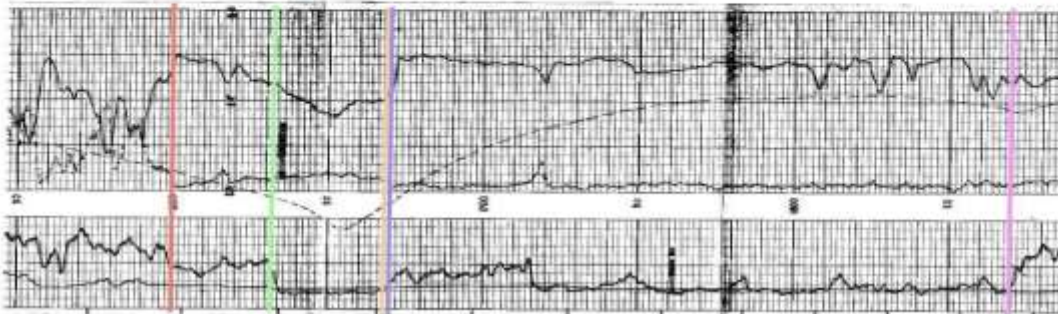
1134B



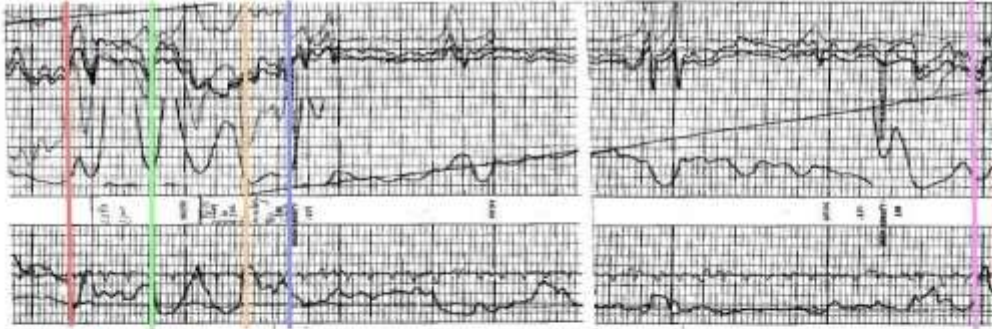
2062B



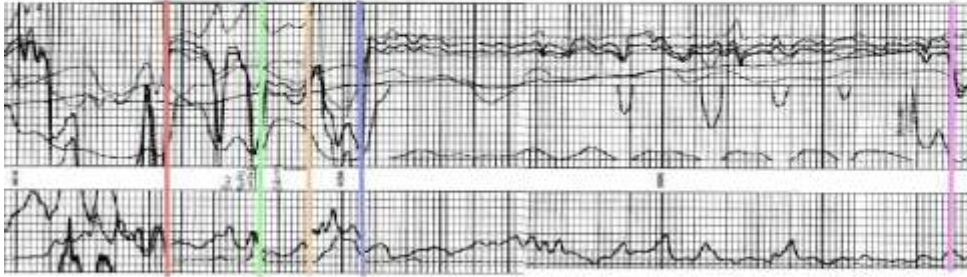
2107B



1140B



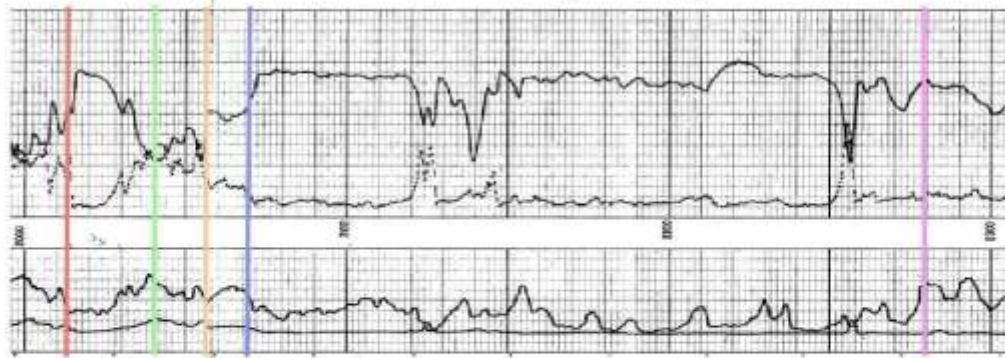
2079B



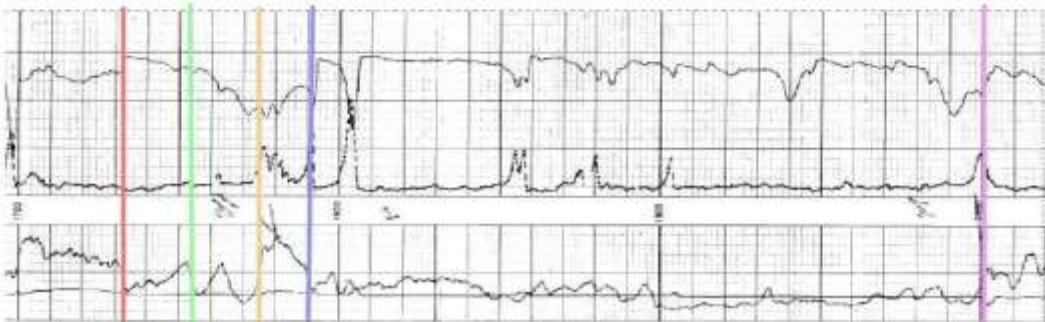
2068B



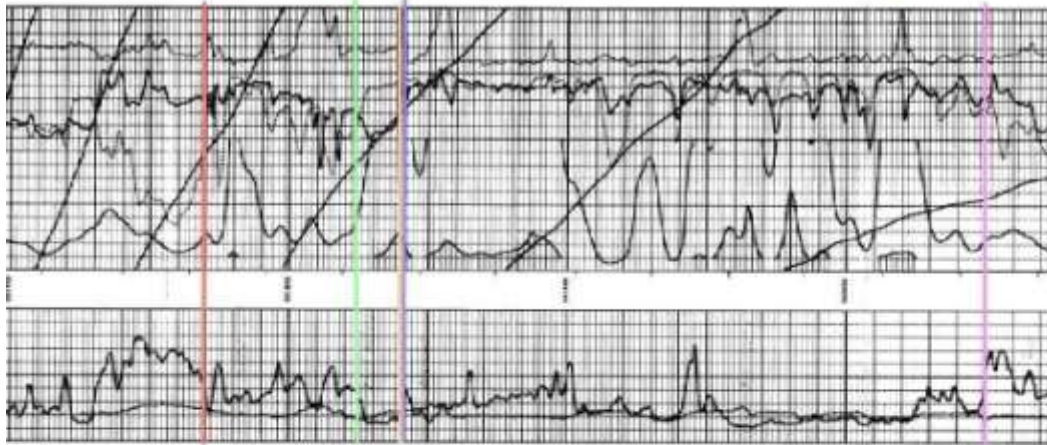
1729B



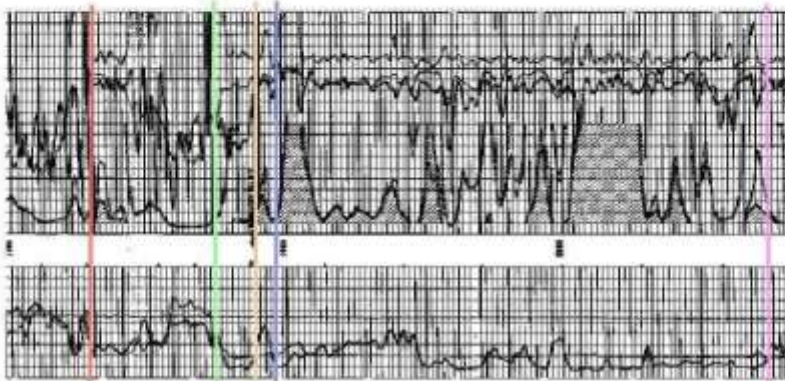
1728B



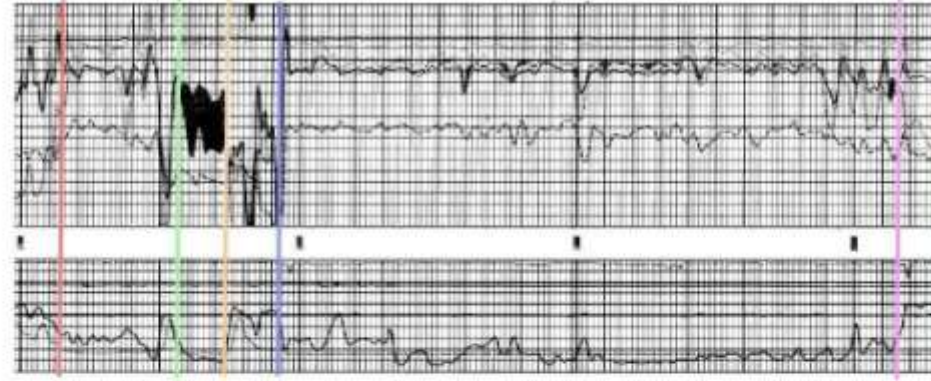
1441B



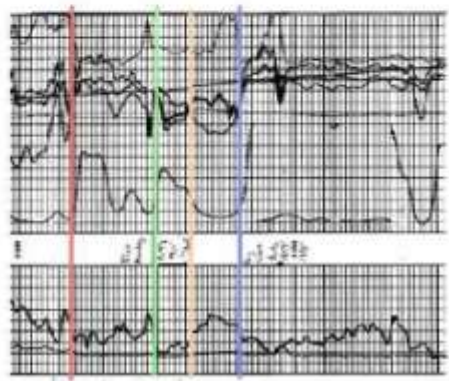
2111B



1946B

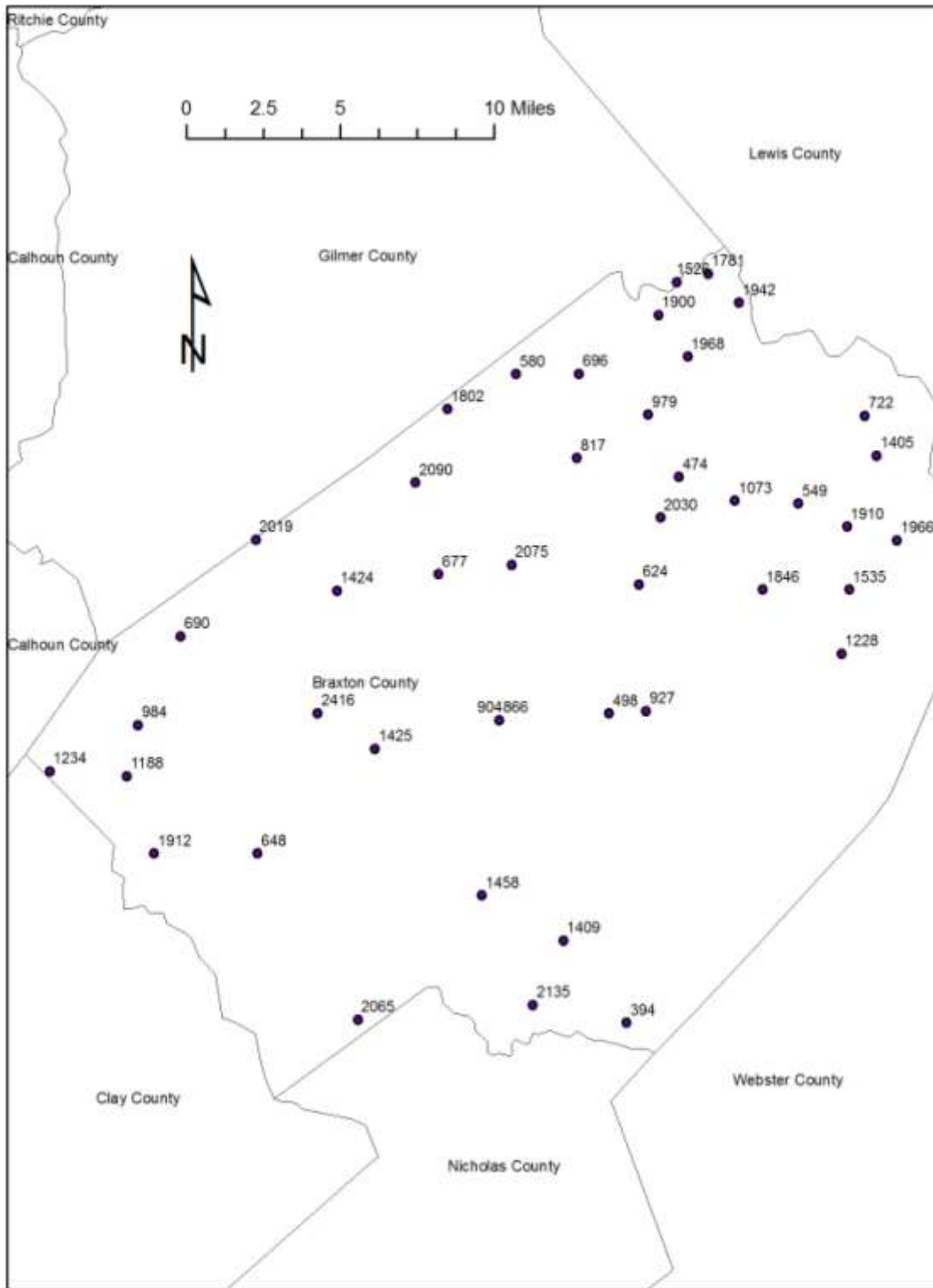


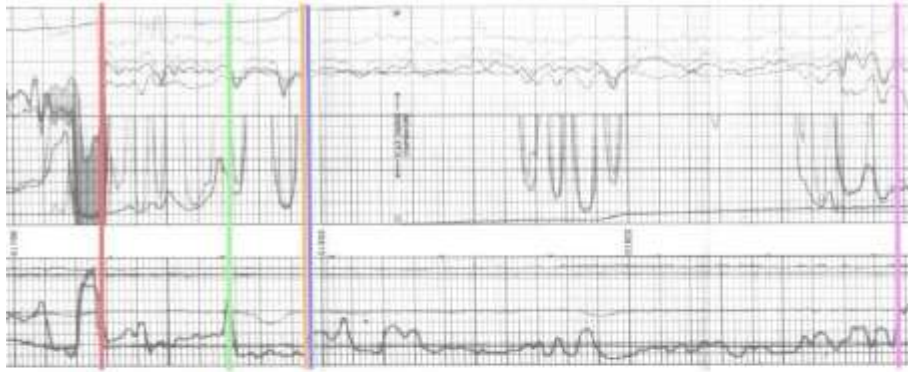
2087B



2077B

Non-Producing Wells

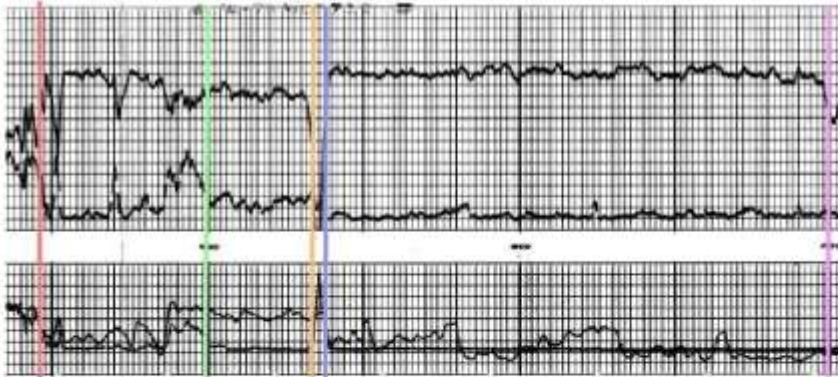




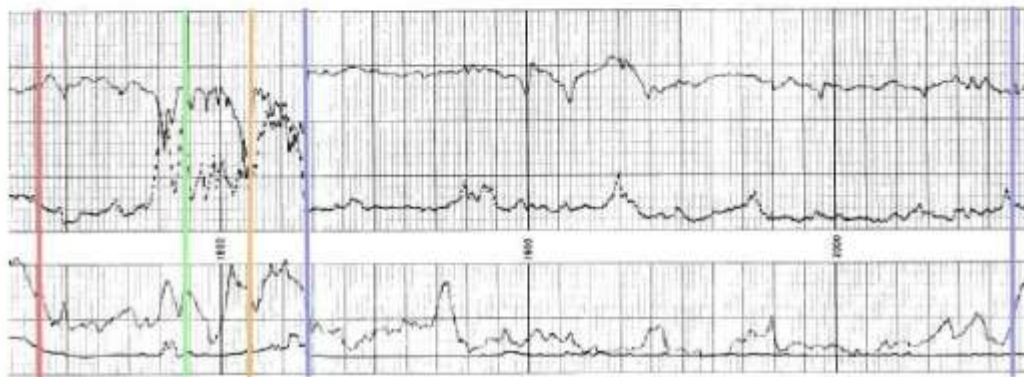
394B



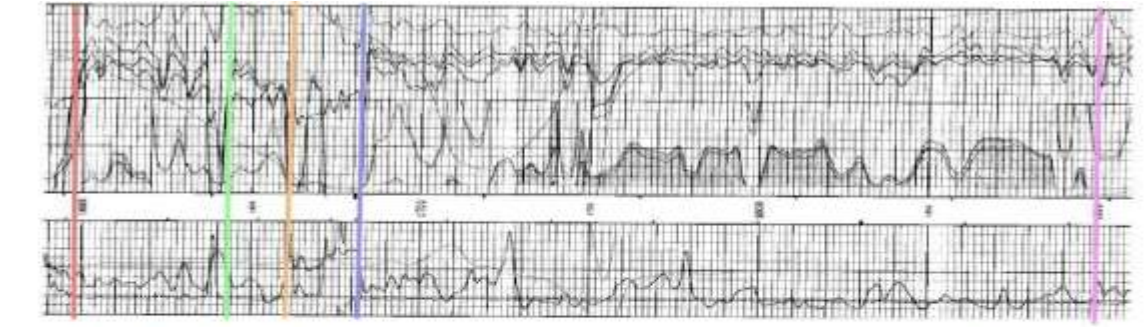
2135B



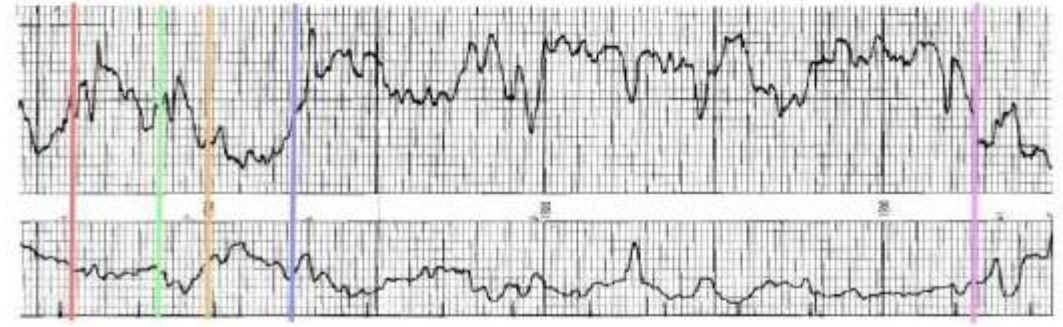
1409B



1458B



2065B



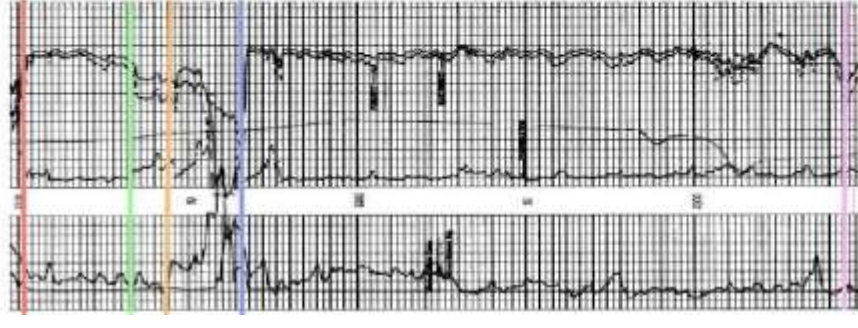
648B



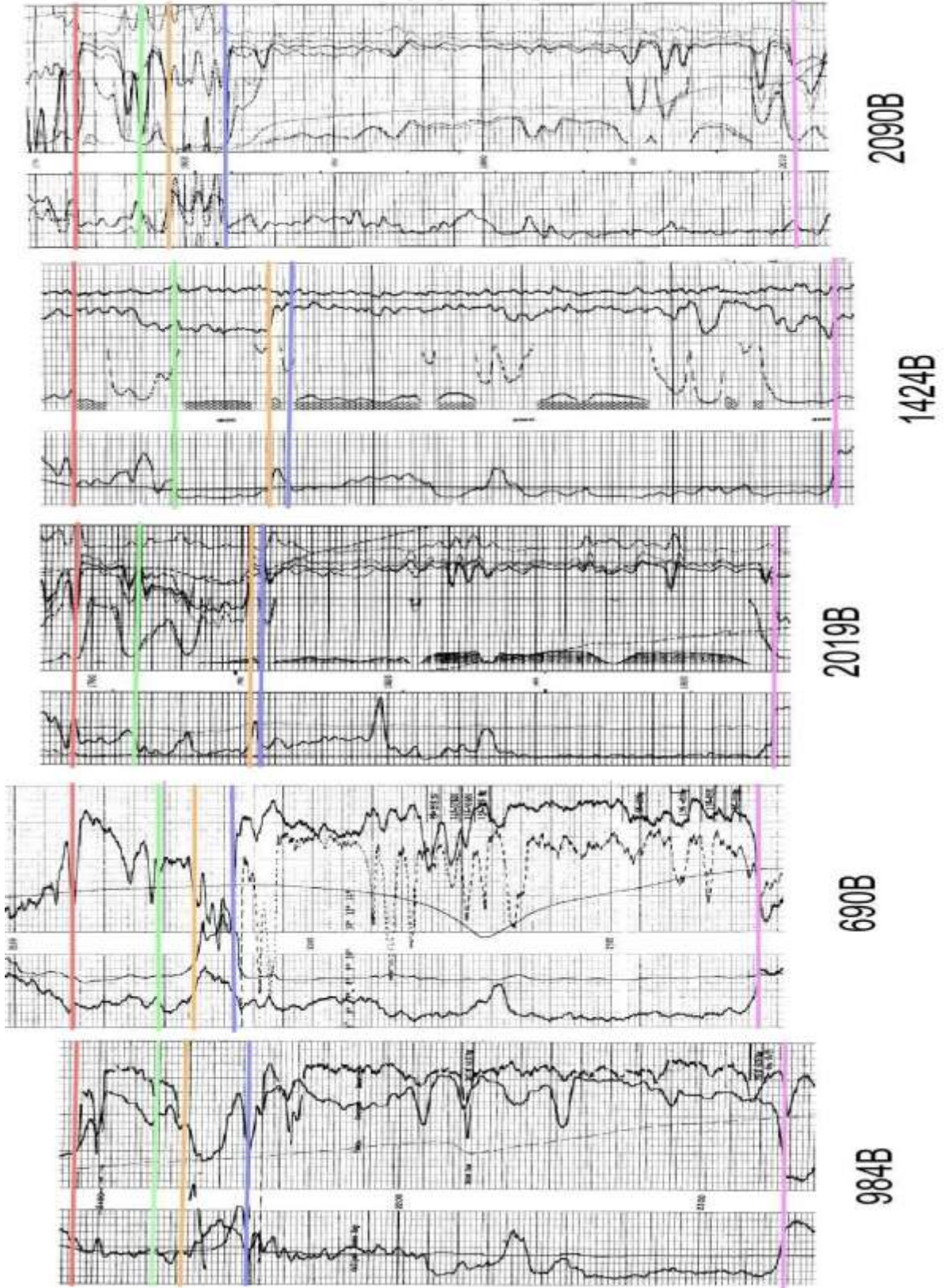
1912B

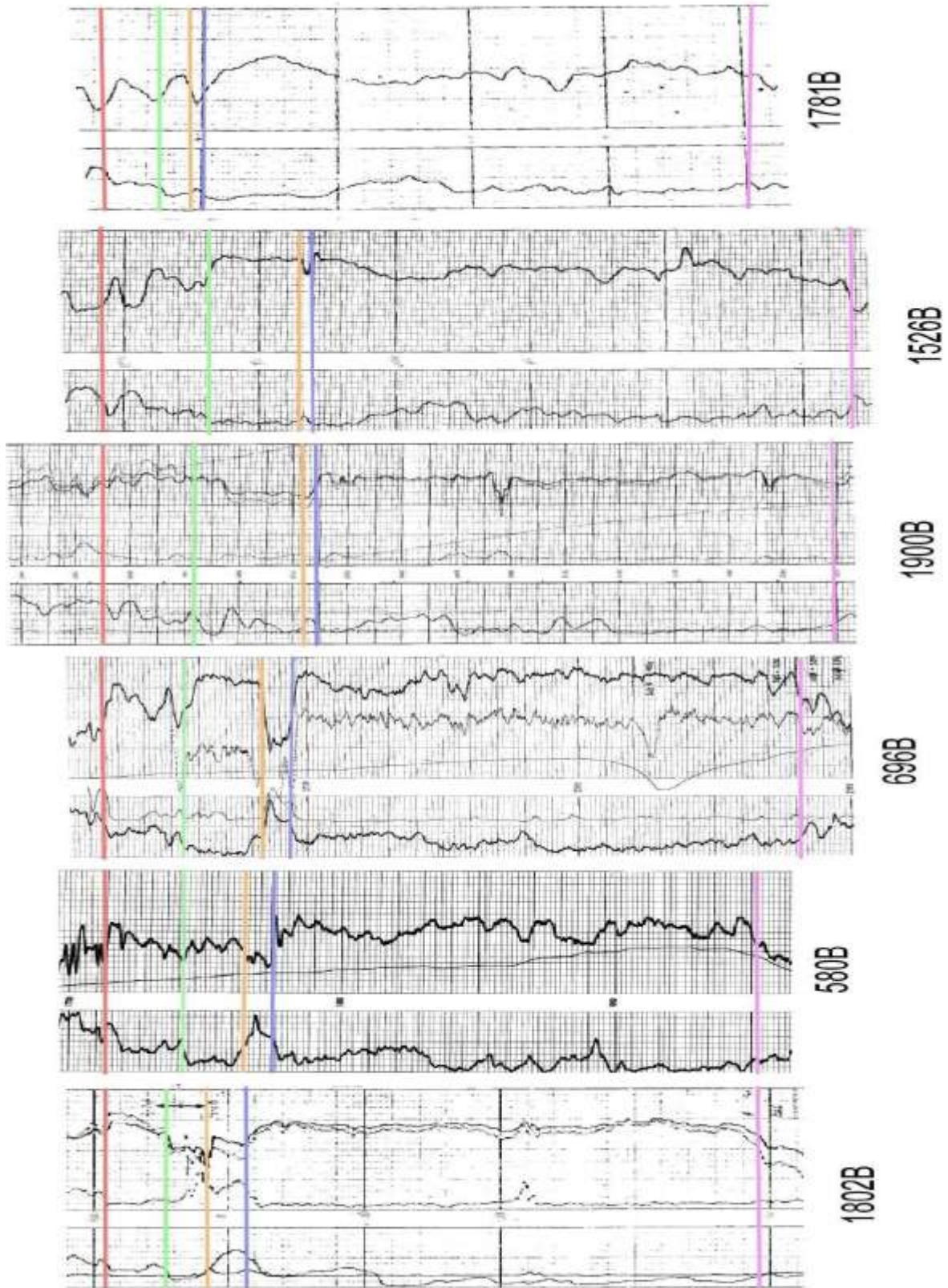


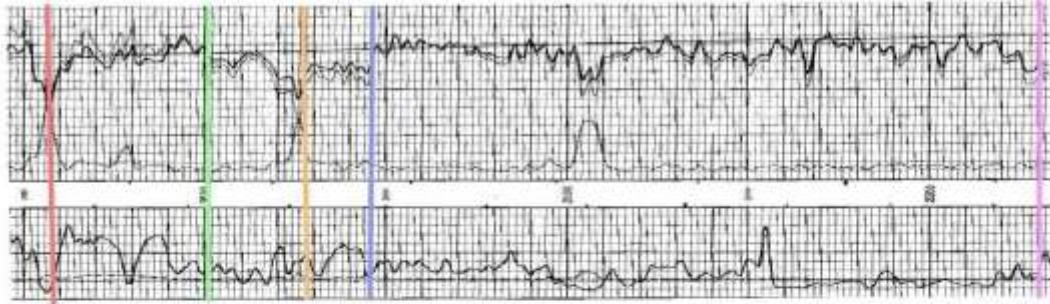
1188B



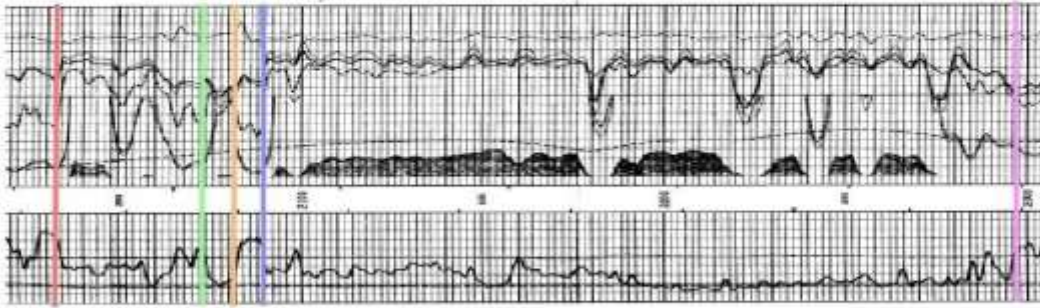
1234B



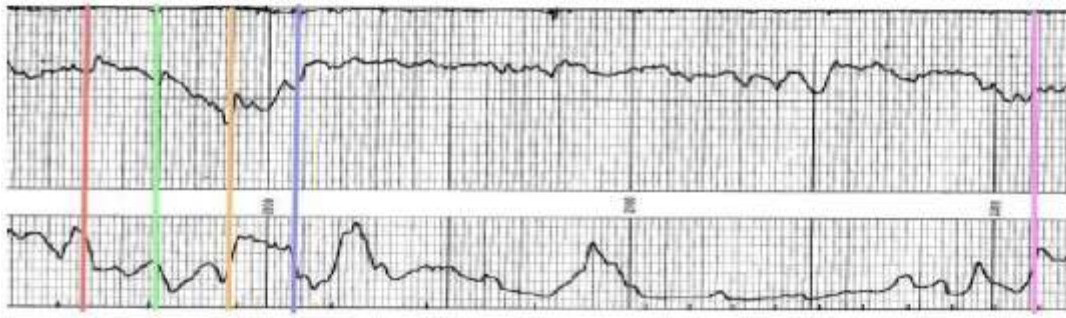




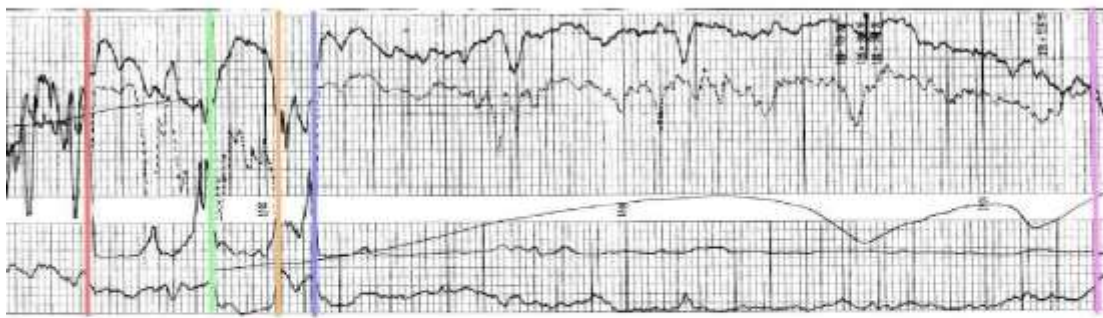
1942B



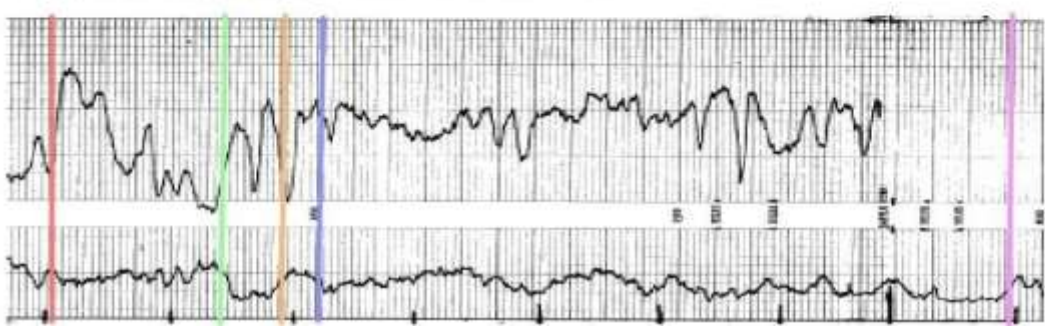
1968B



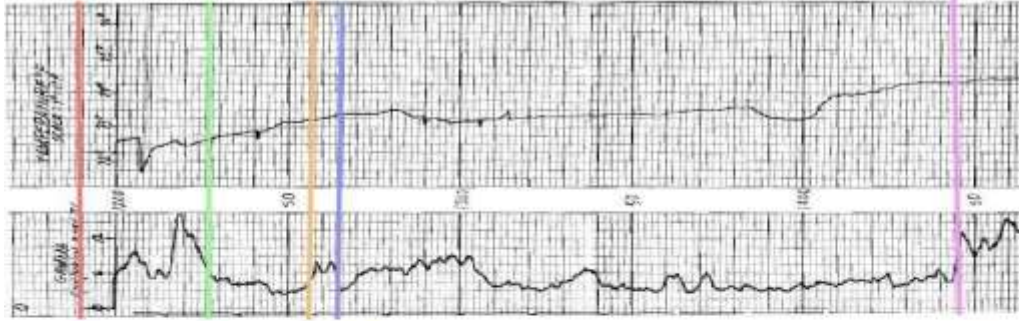
979B



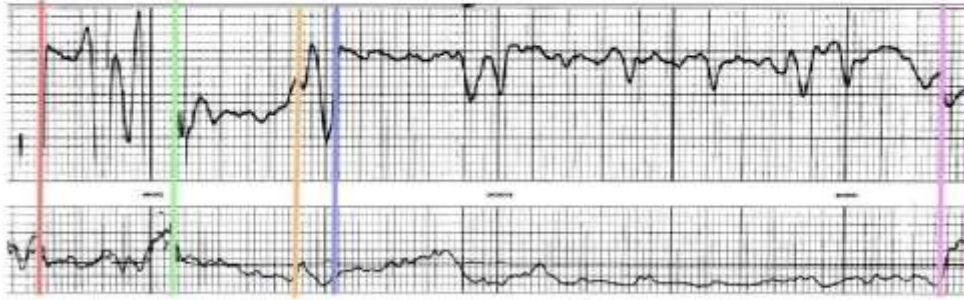
817B



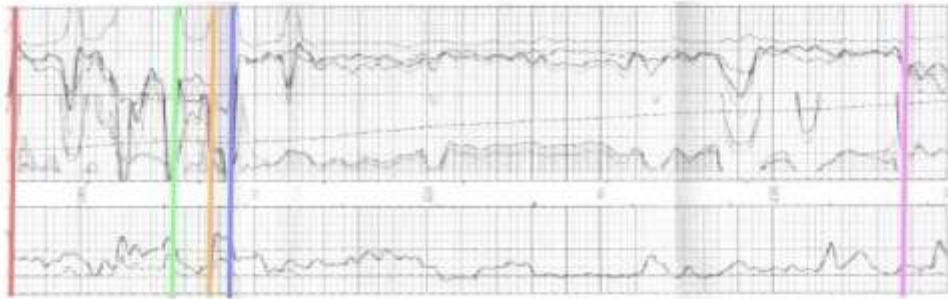
677B



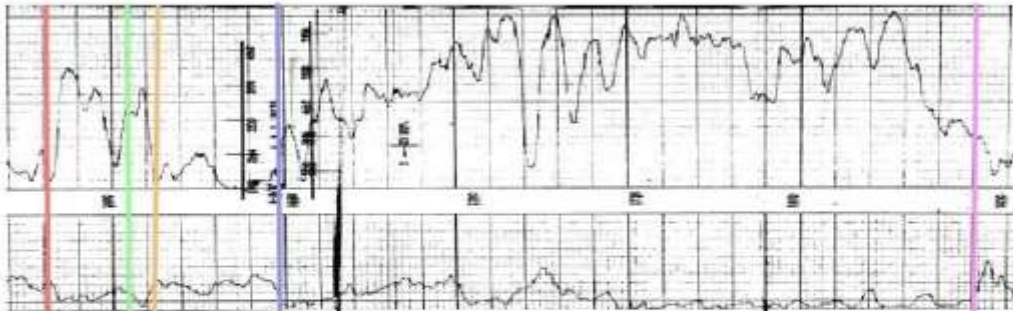
549B



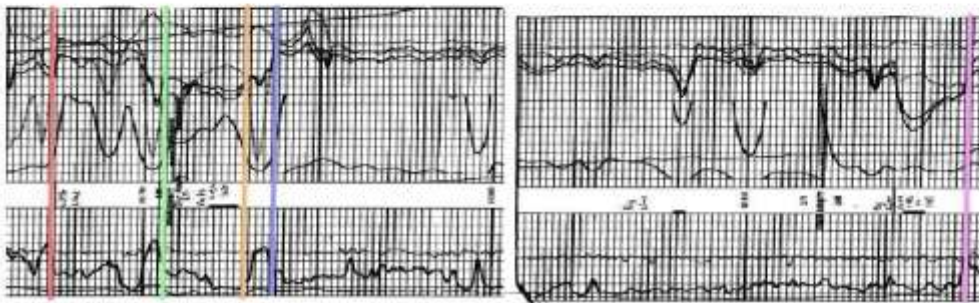
1073B



2030B



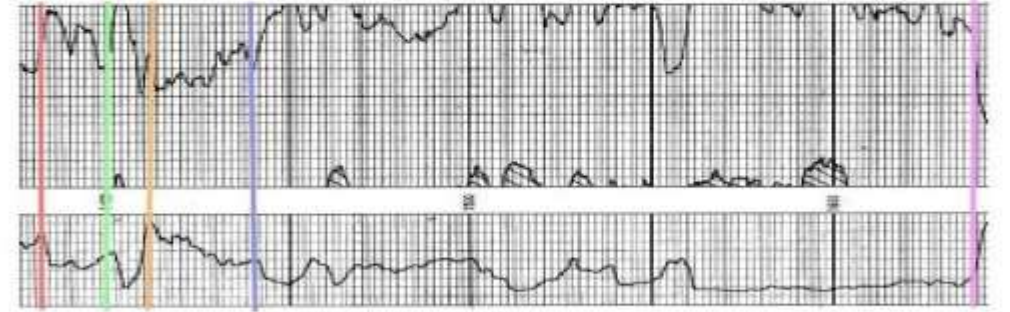
624B



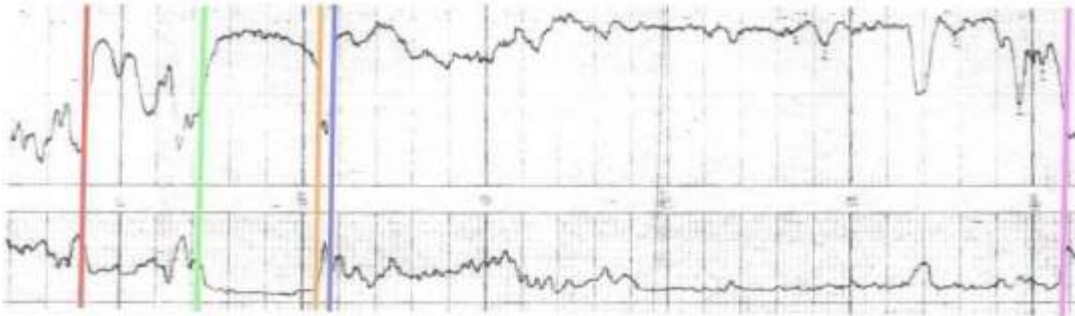
2075B



1405B



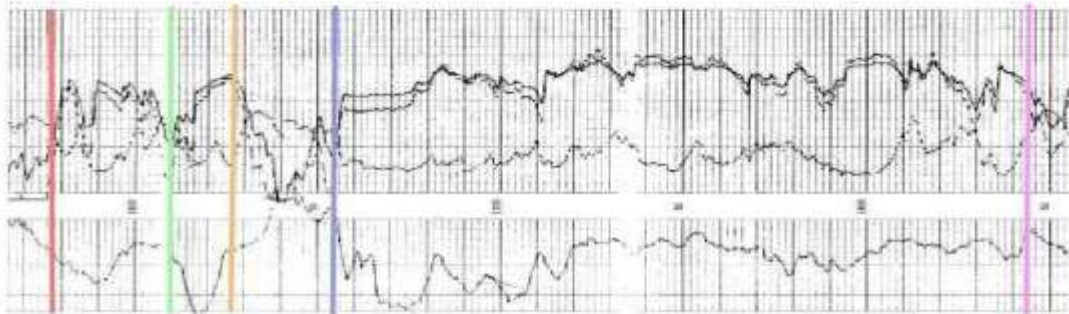
722B



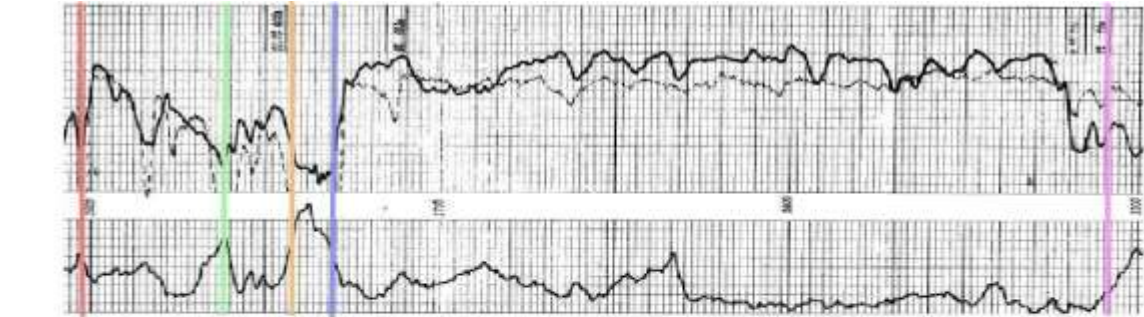
474B



1966B



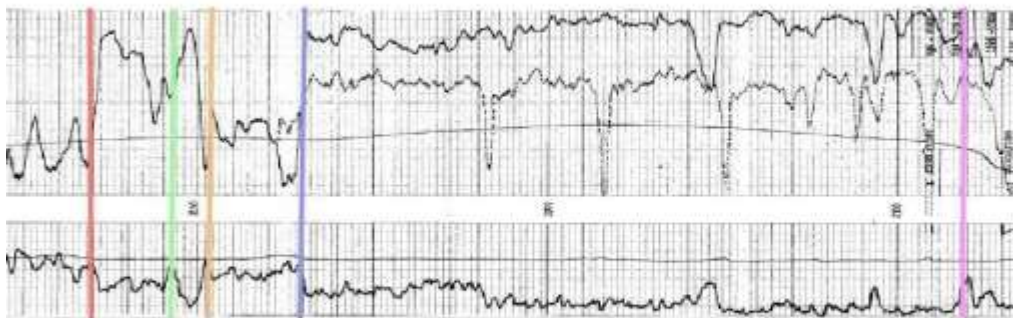
1910B



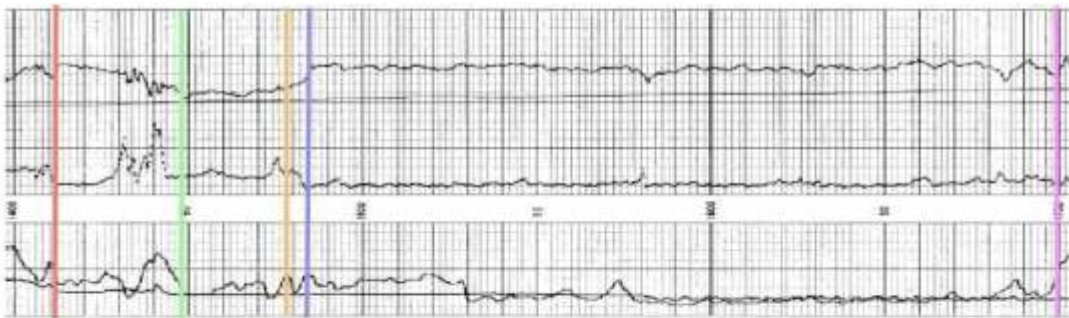
927B



498B



866B



1425B



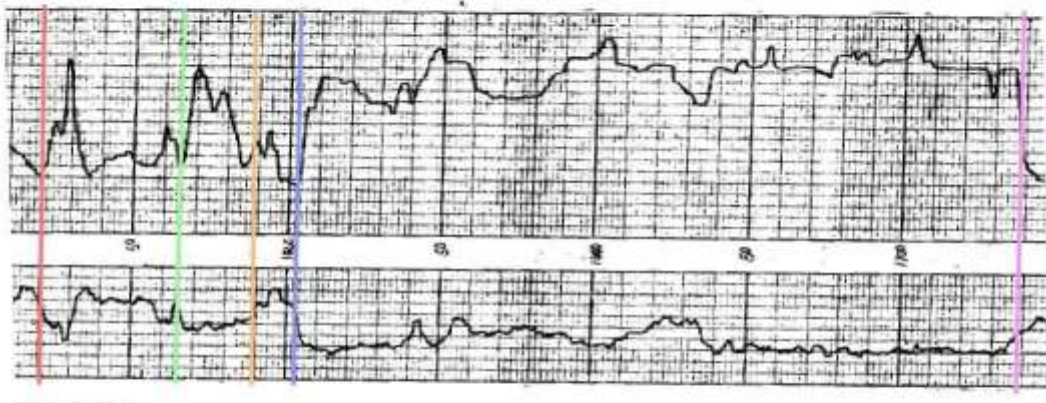
2416B



1228B



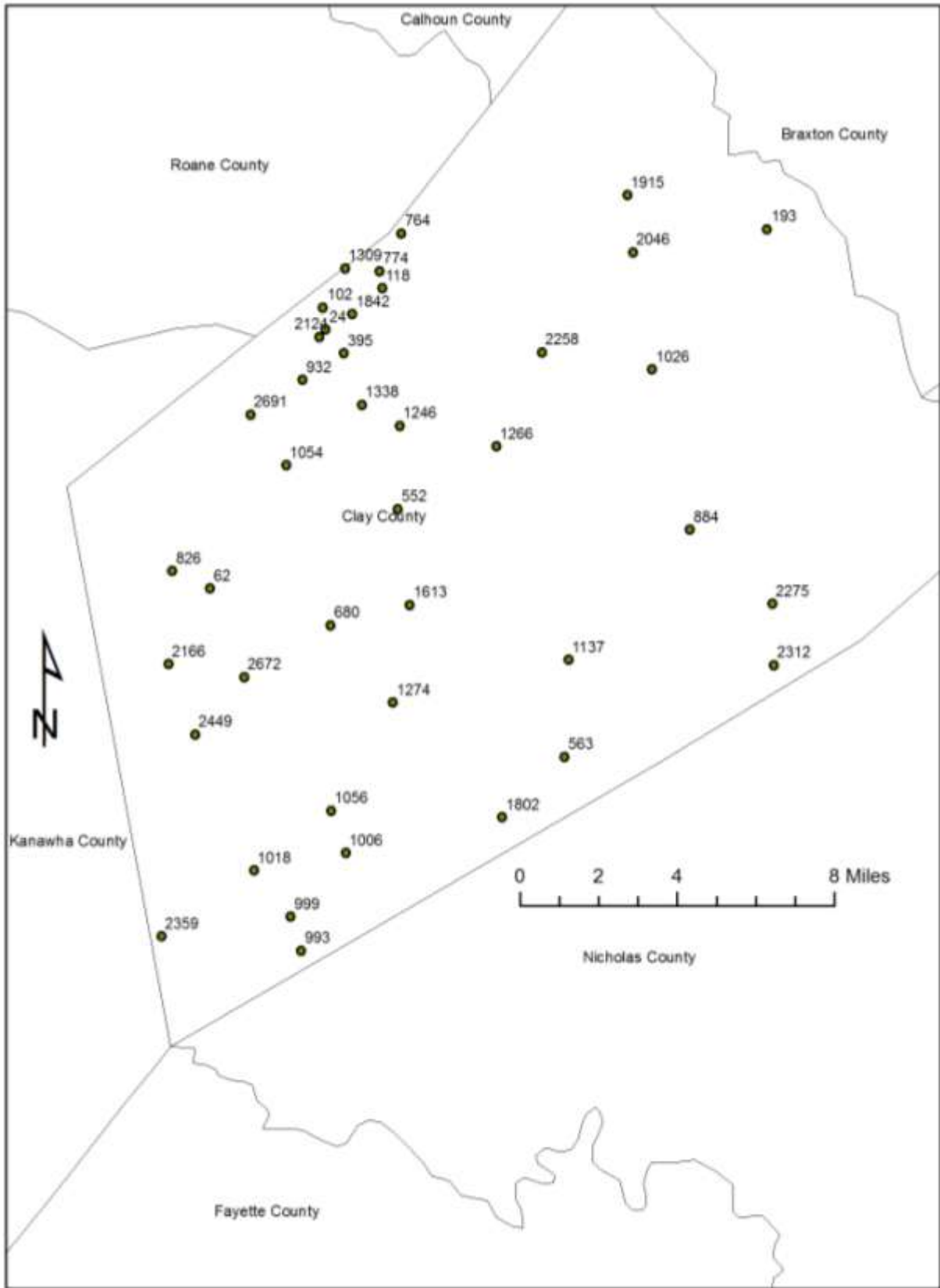
1535B

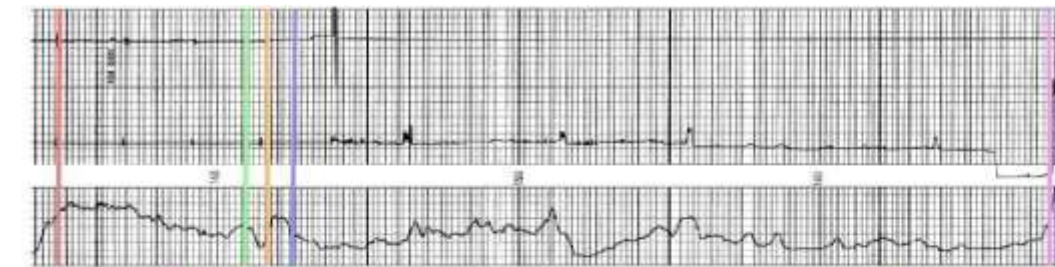


1846B

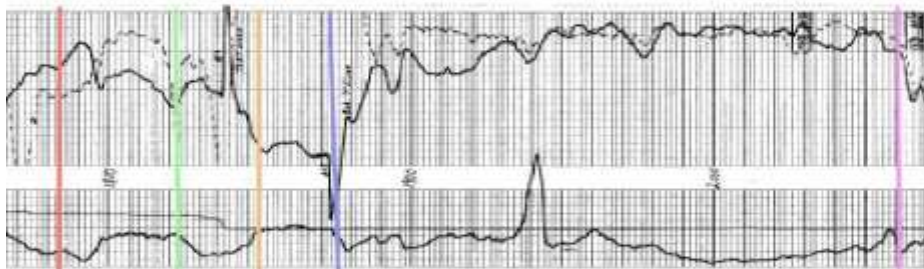


904B





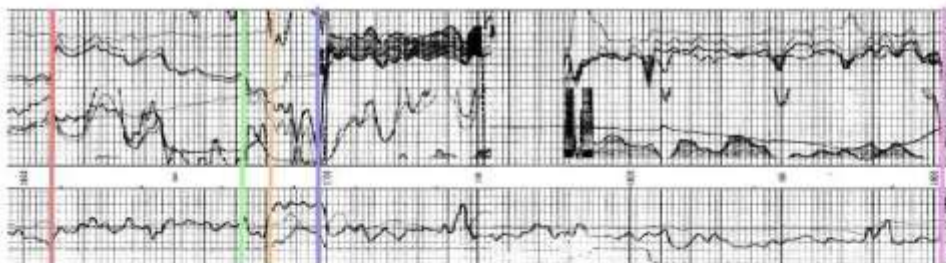
193C



1026C



884C



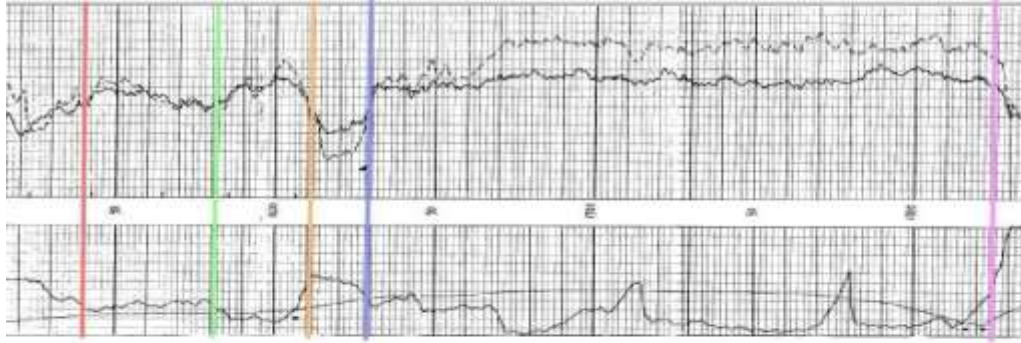
2275C



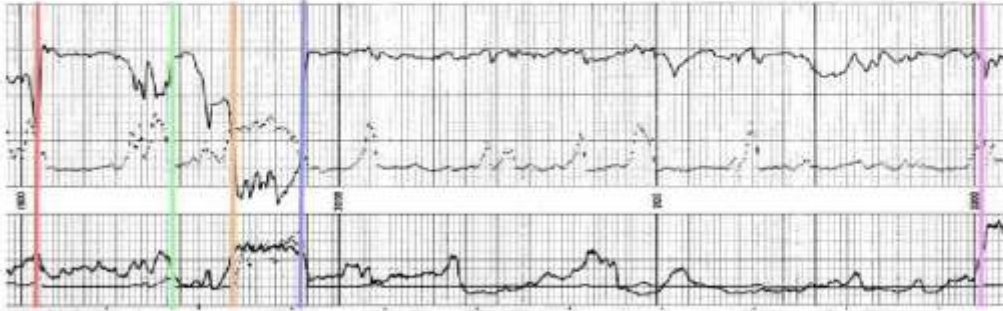
2312C



1137C



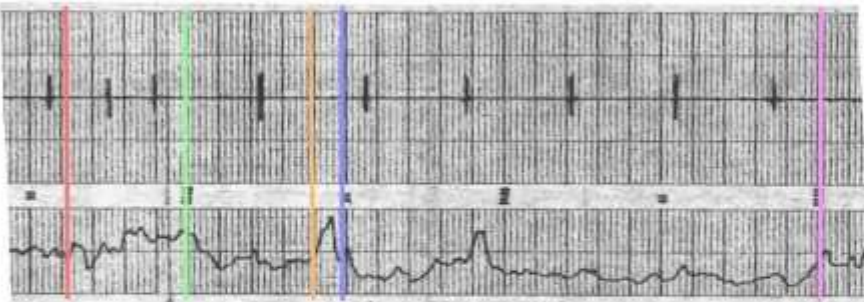
563C



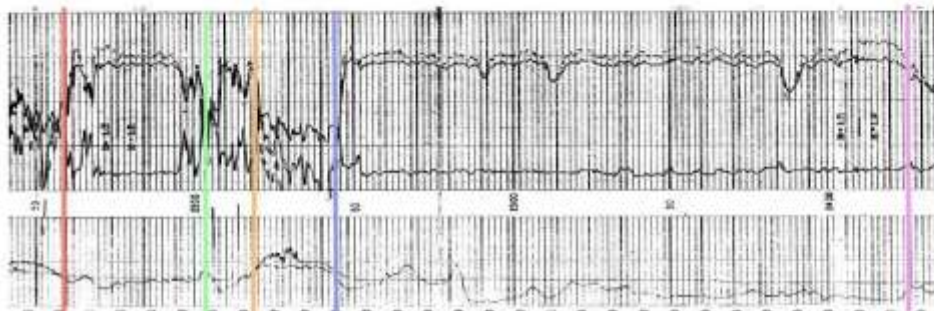
1802C



1006C



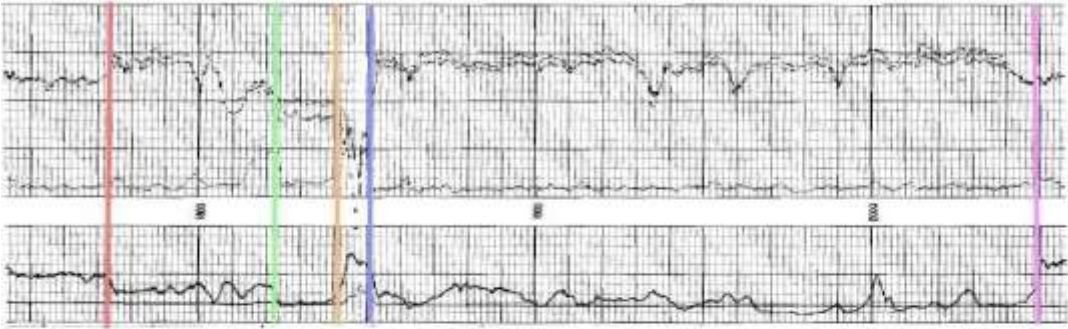
999C



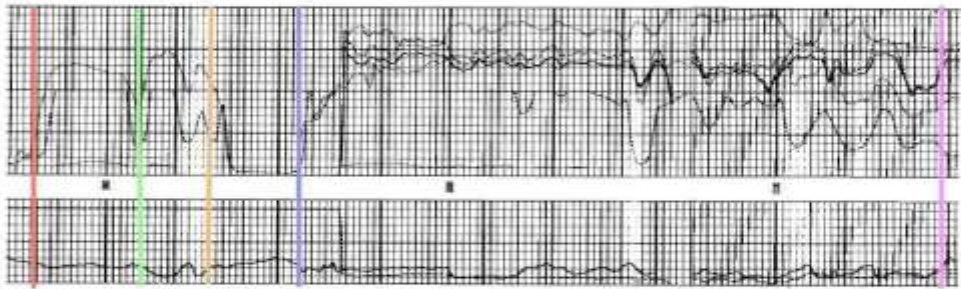
993C



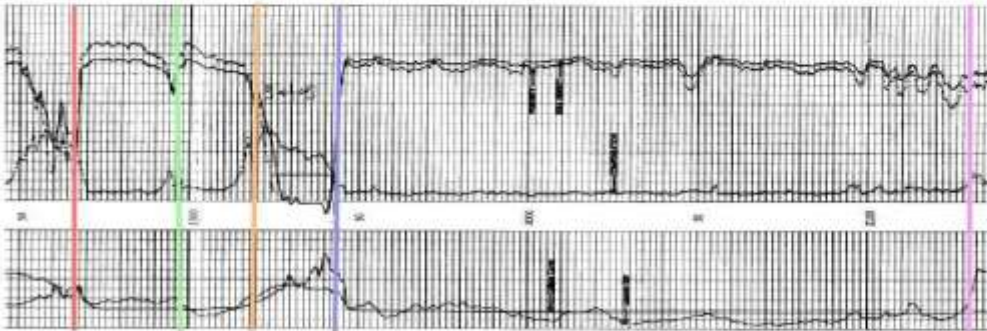
1915C



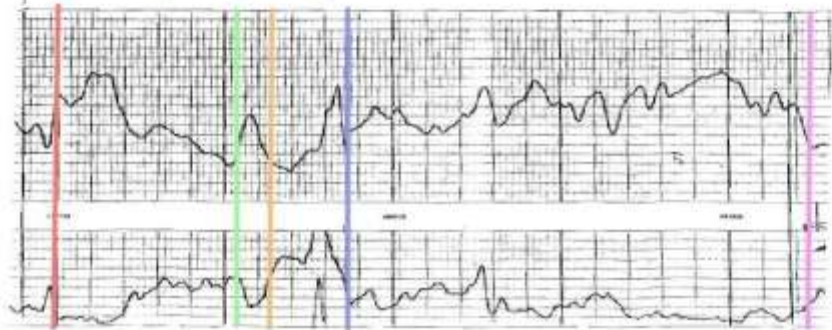
2046C



2258C



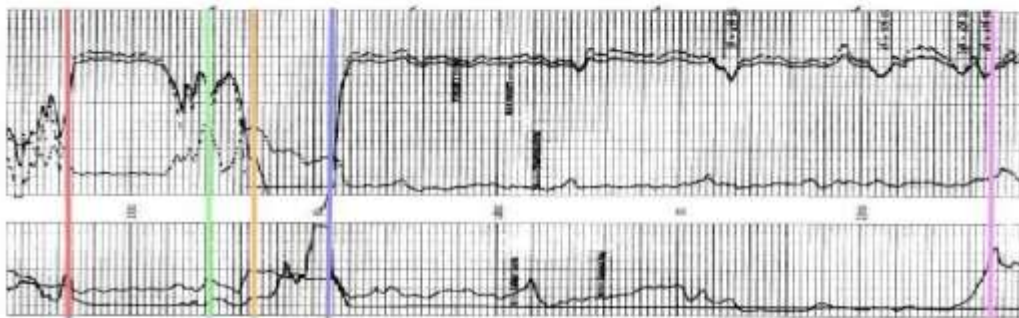
1266C



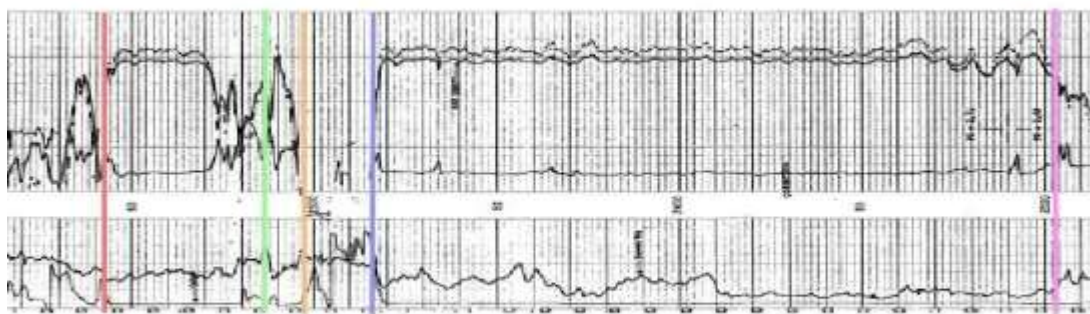
552C



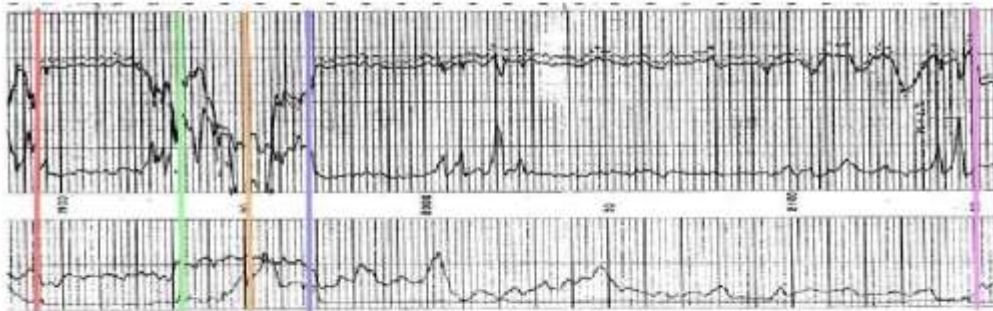
1613C



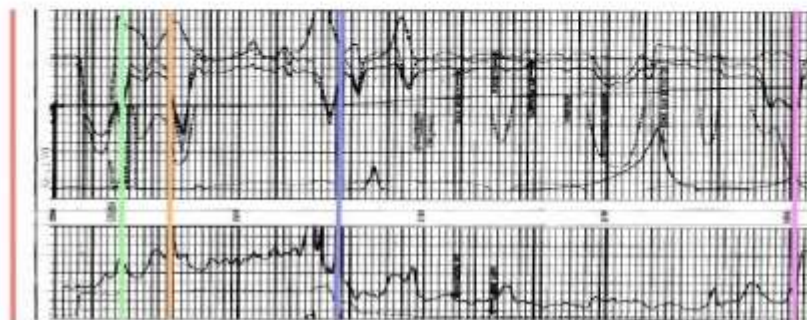
1274C



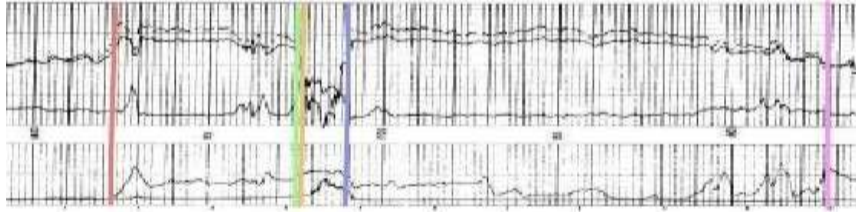
1056C



1018C



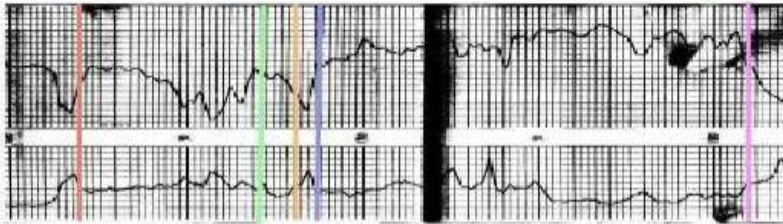
2359C



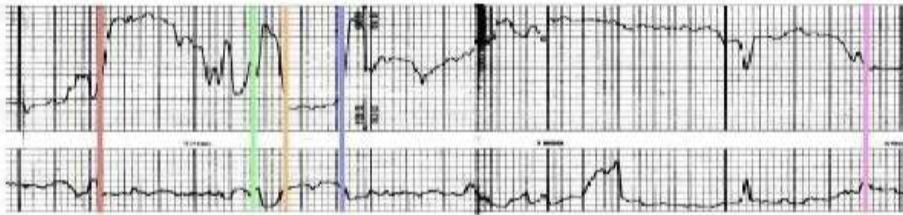
1054C



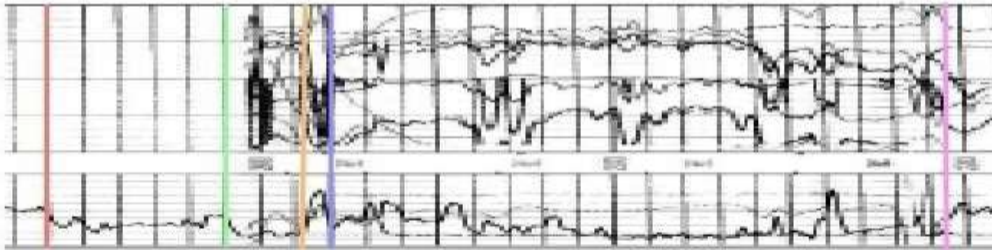
826C



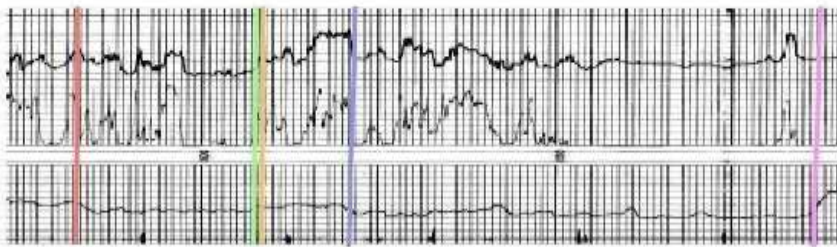
62C



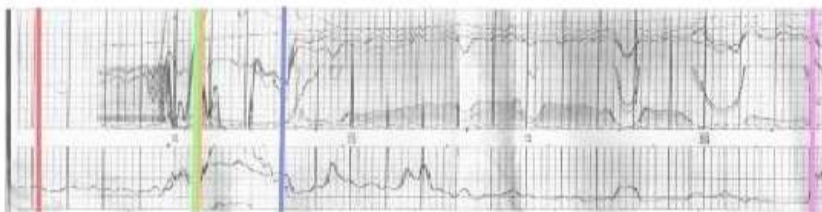
680C



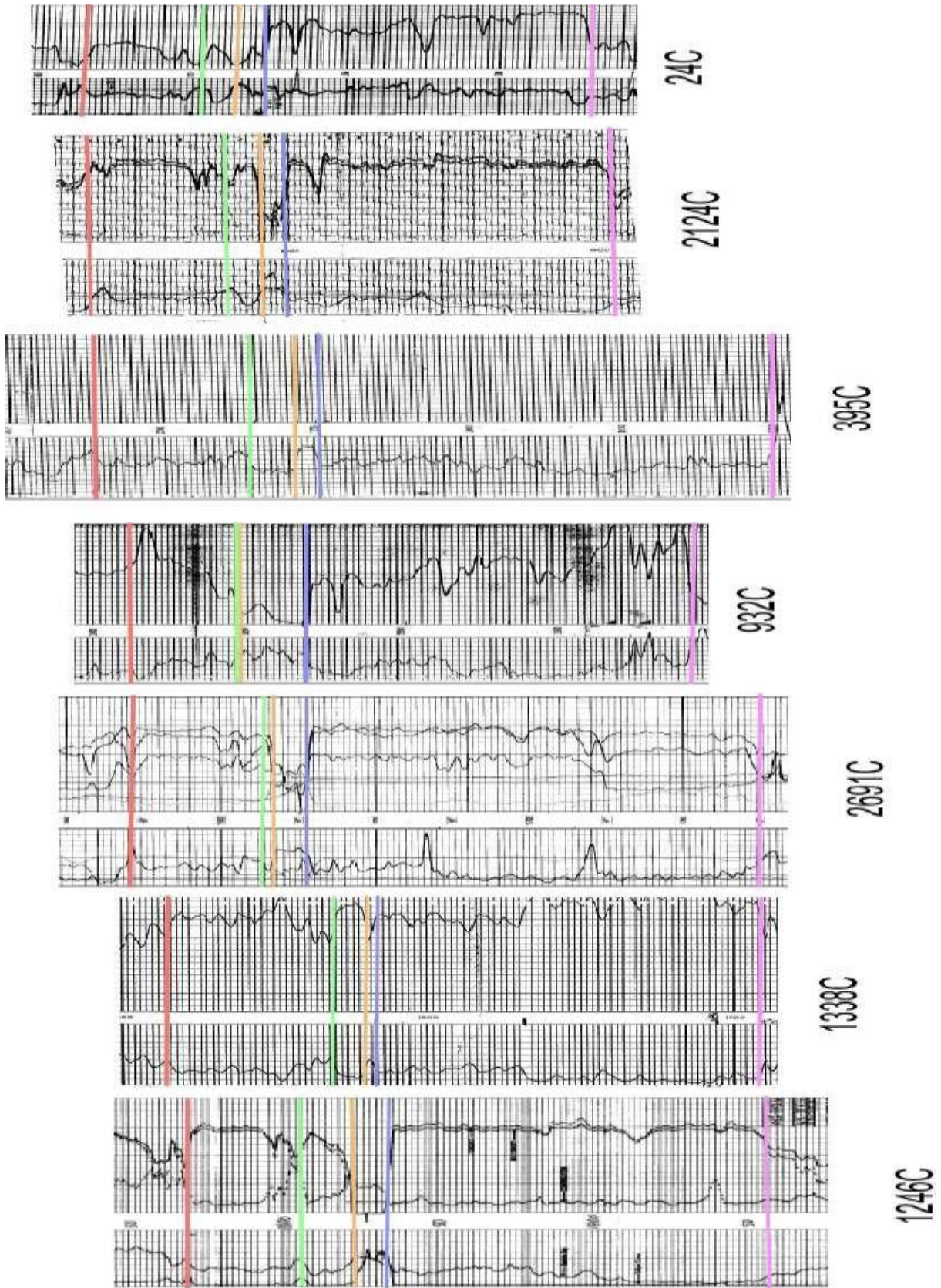
2672C



2166C



2449C

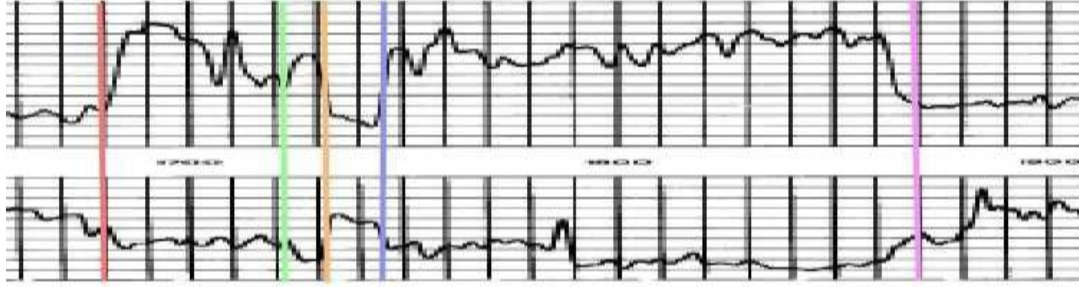




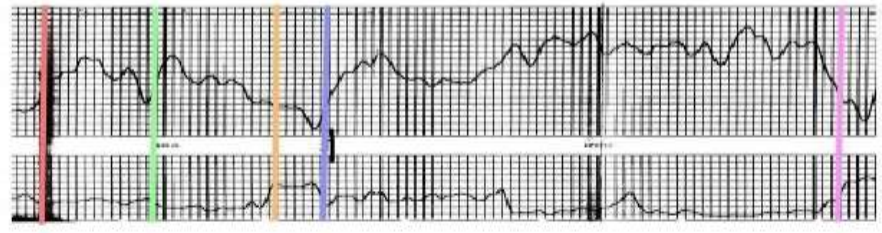
764C



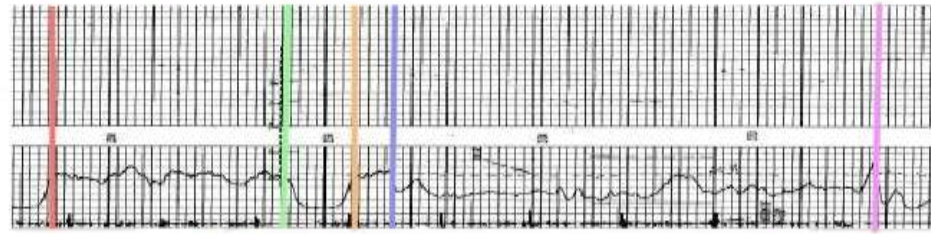
1309C



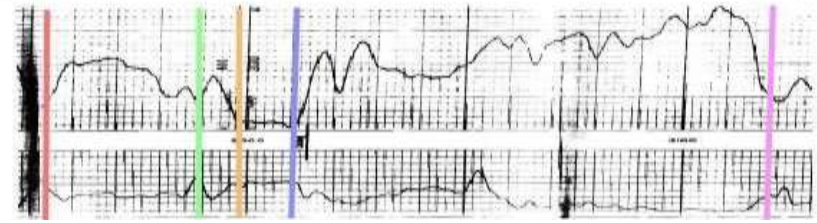
774C



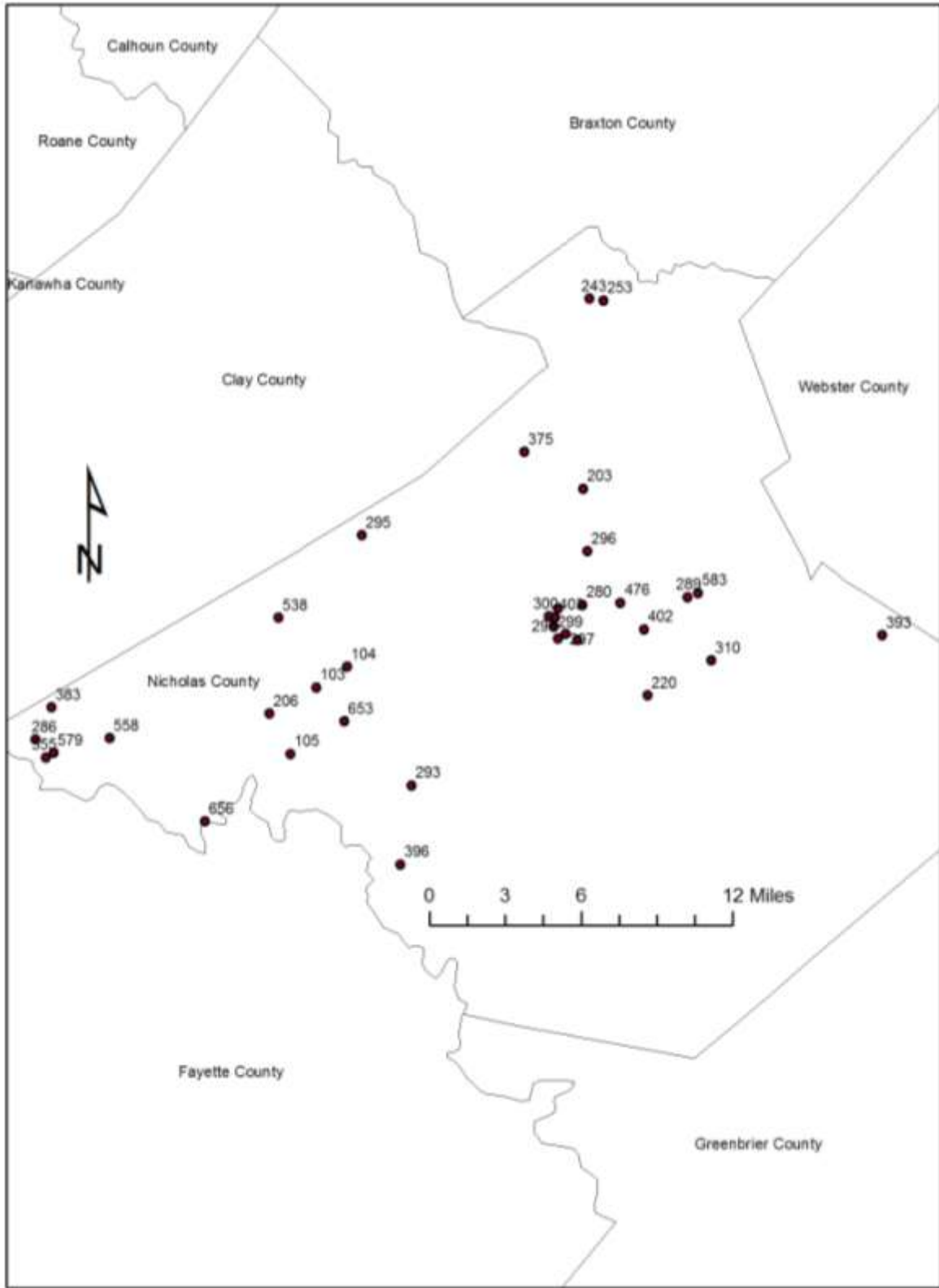
118C



1842C

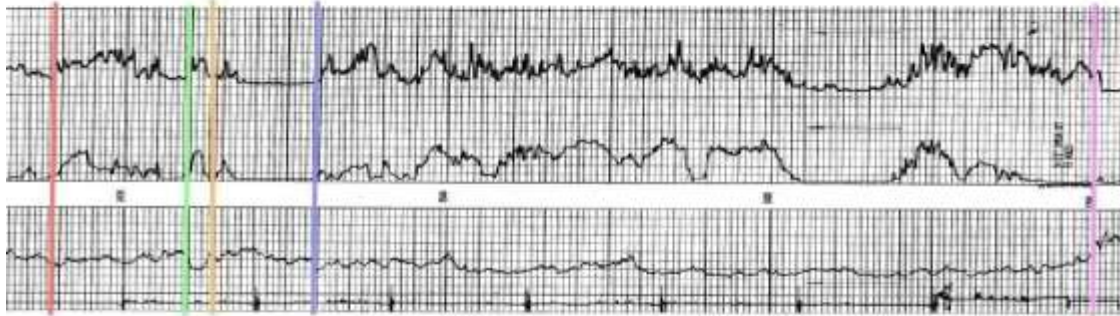


102C





538N



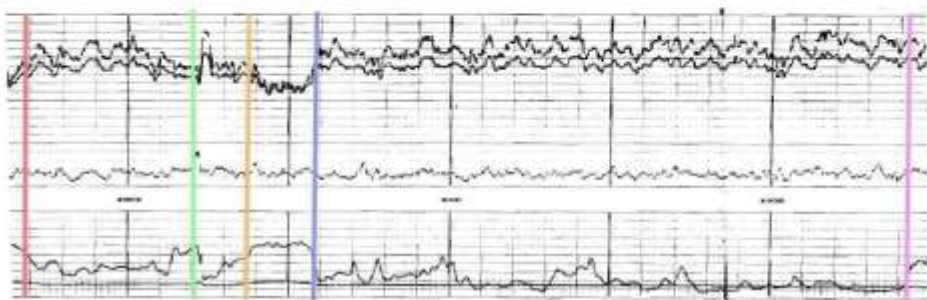
558N



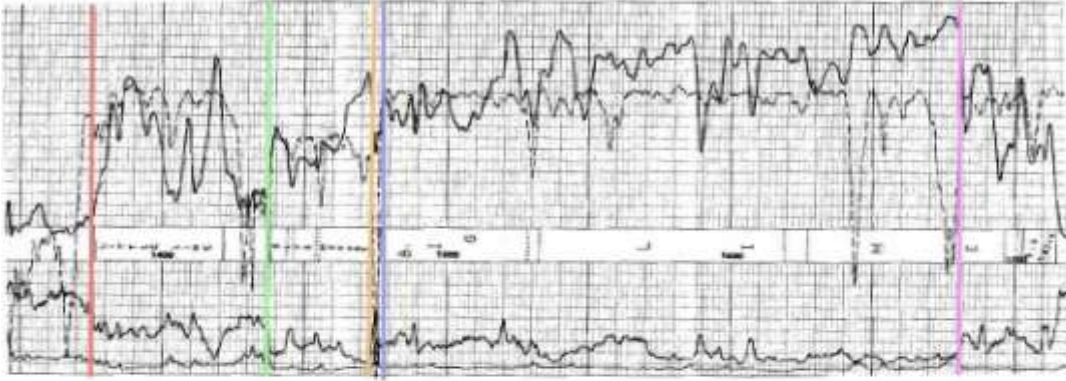
579N



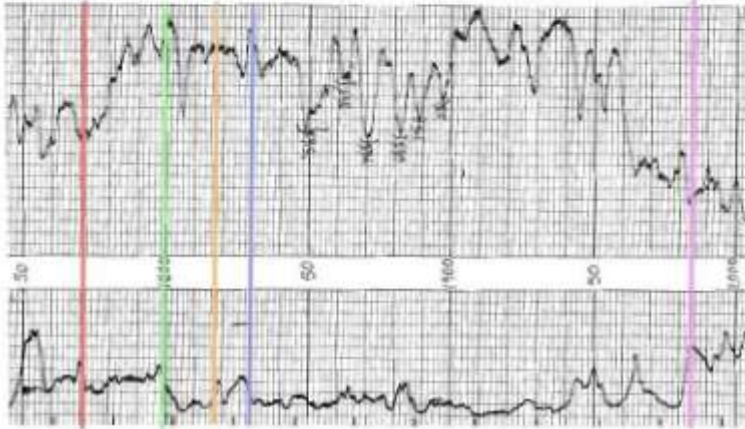
355N



286N



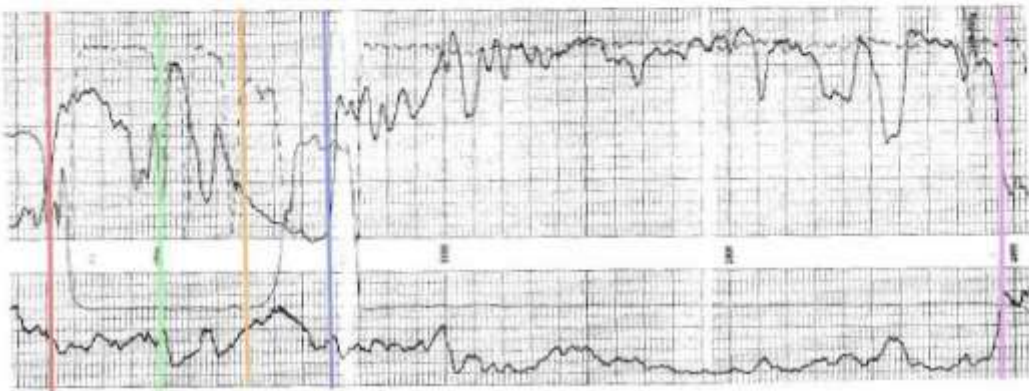
253N



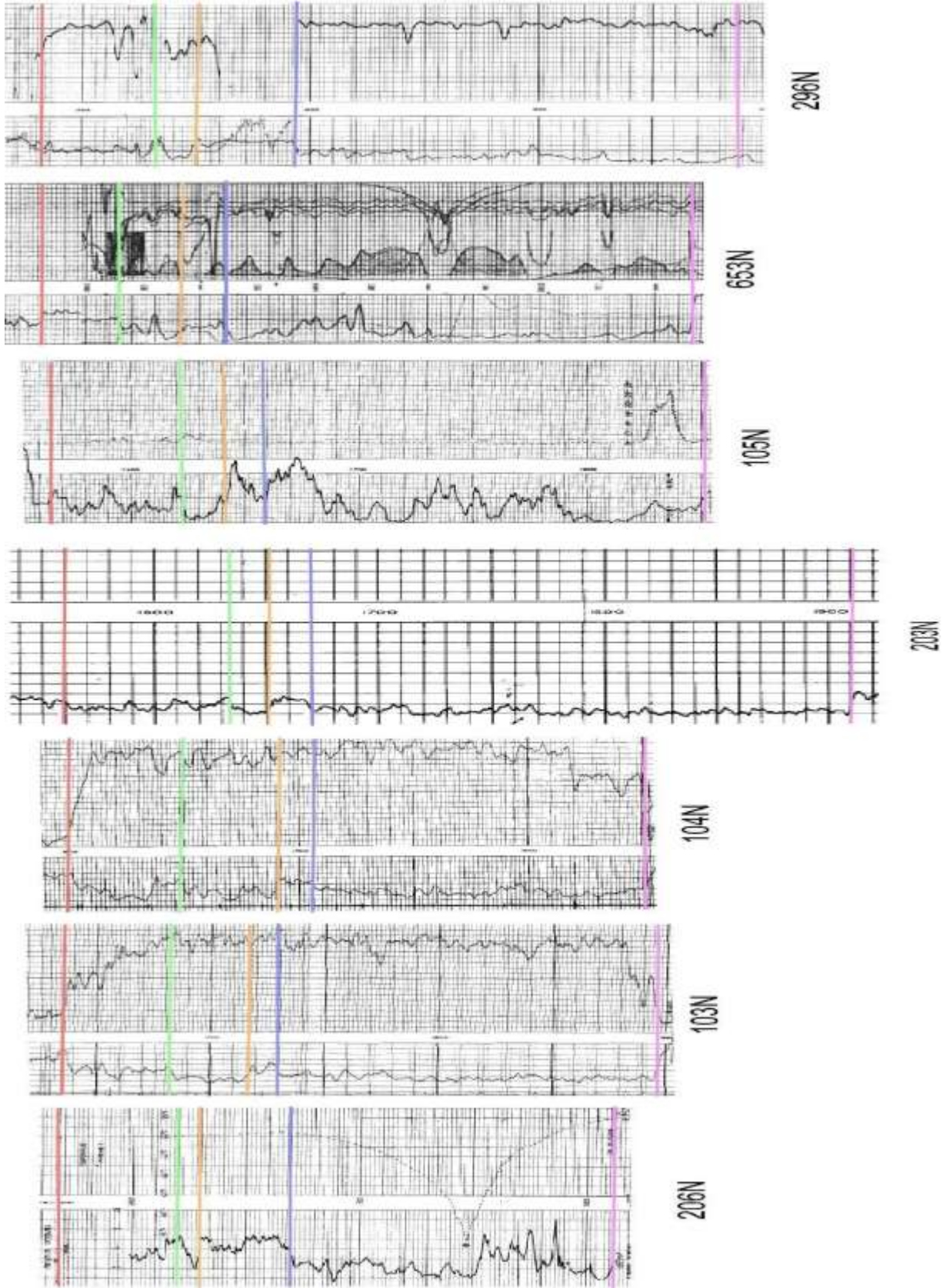
243N

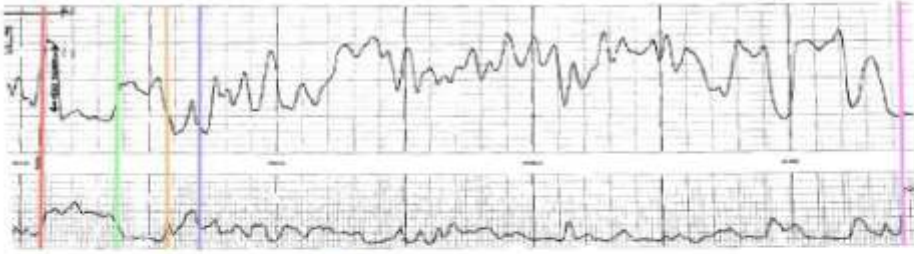


375N

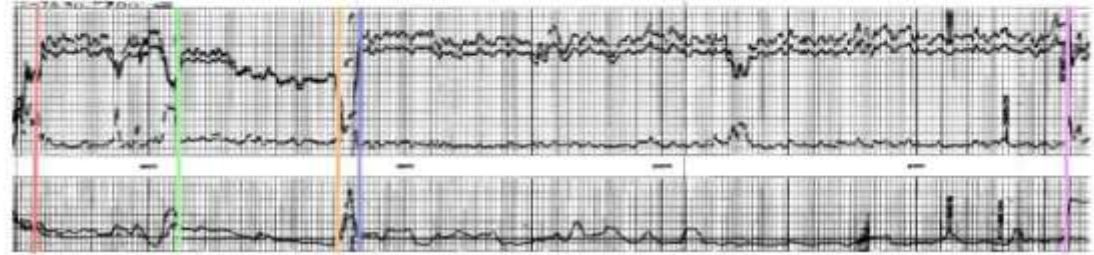


295N

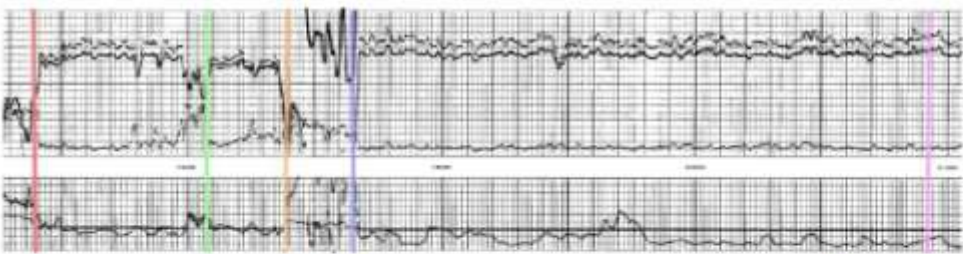




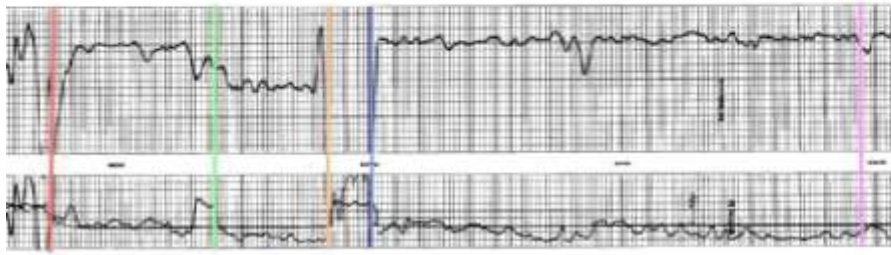
280N



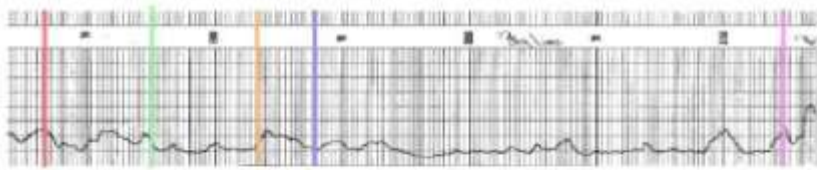
476N



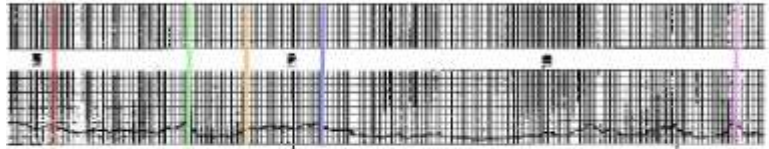
402N



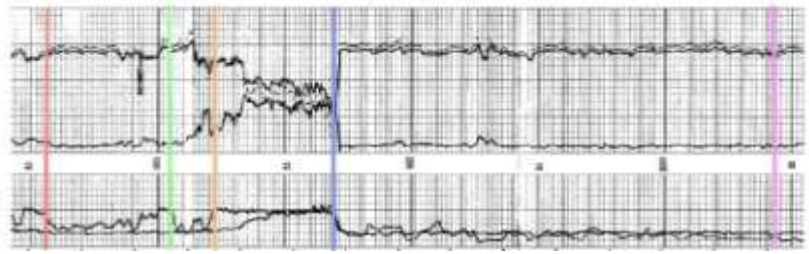
289N



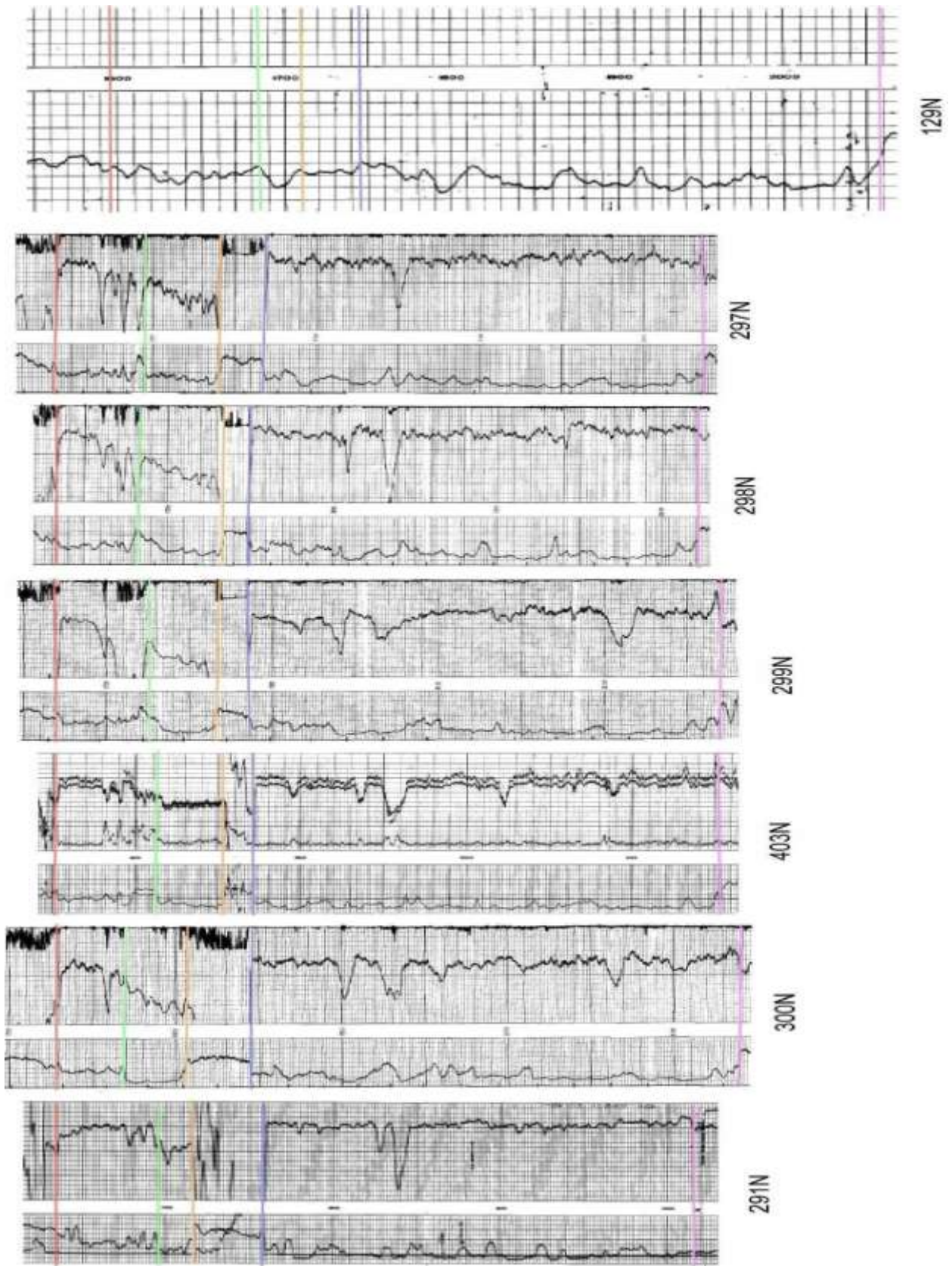
220N

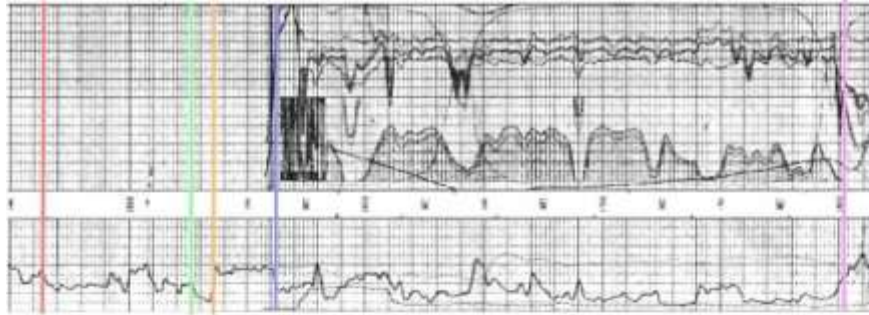


293N

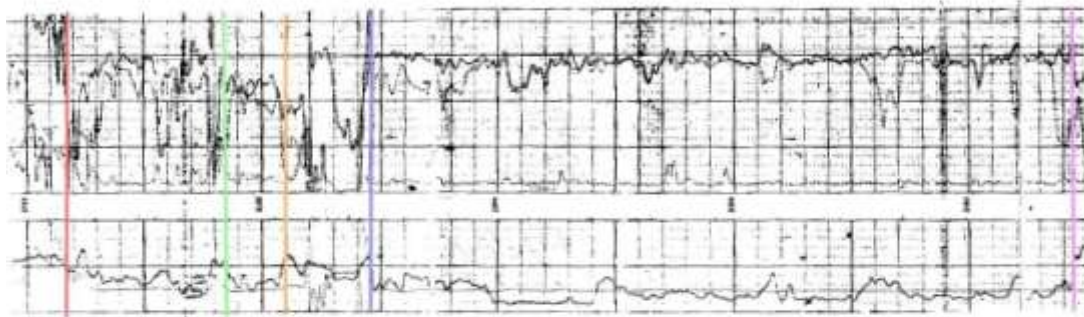


396N





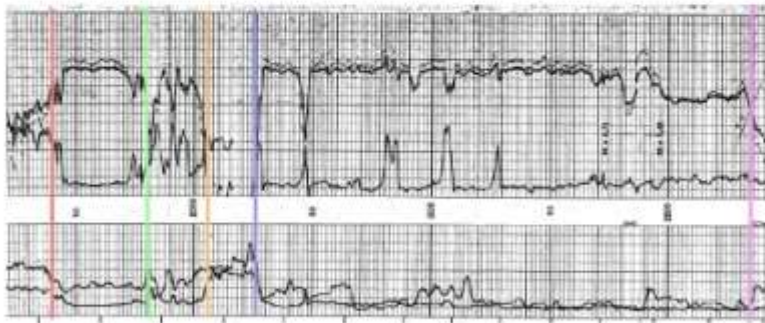
656N



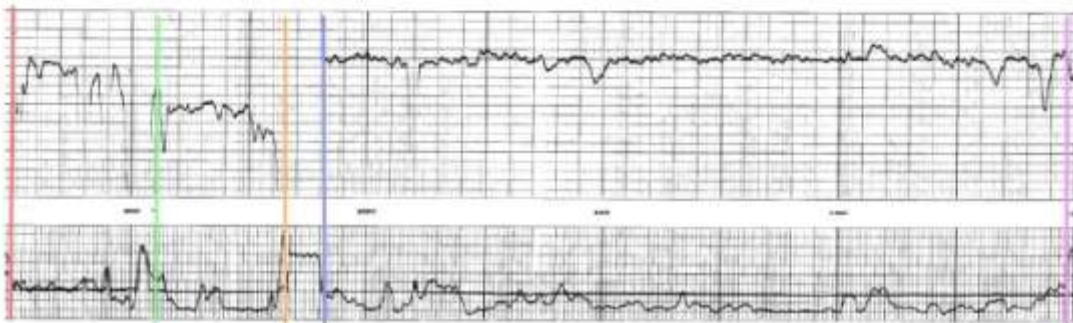
583N



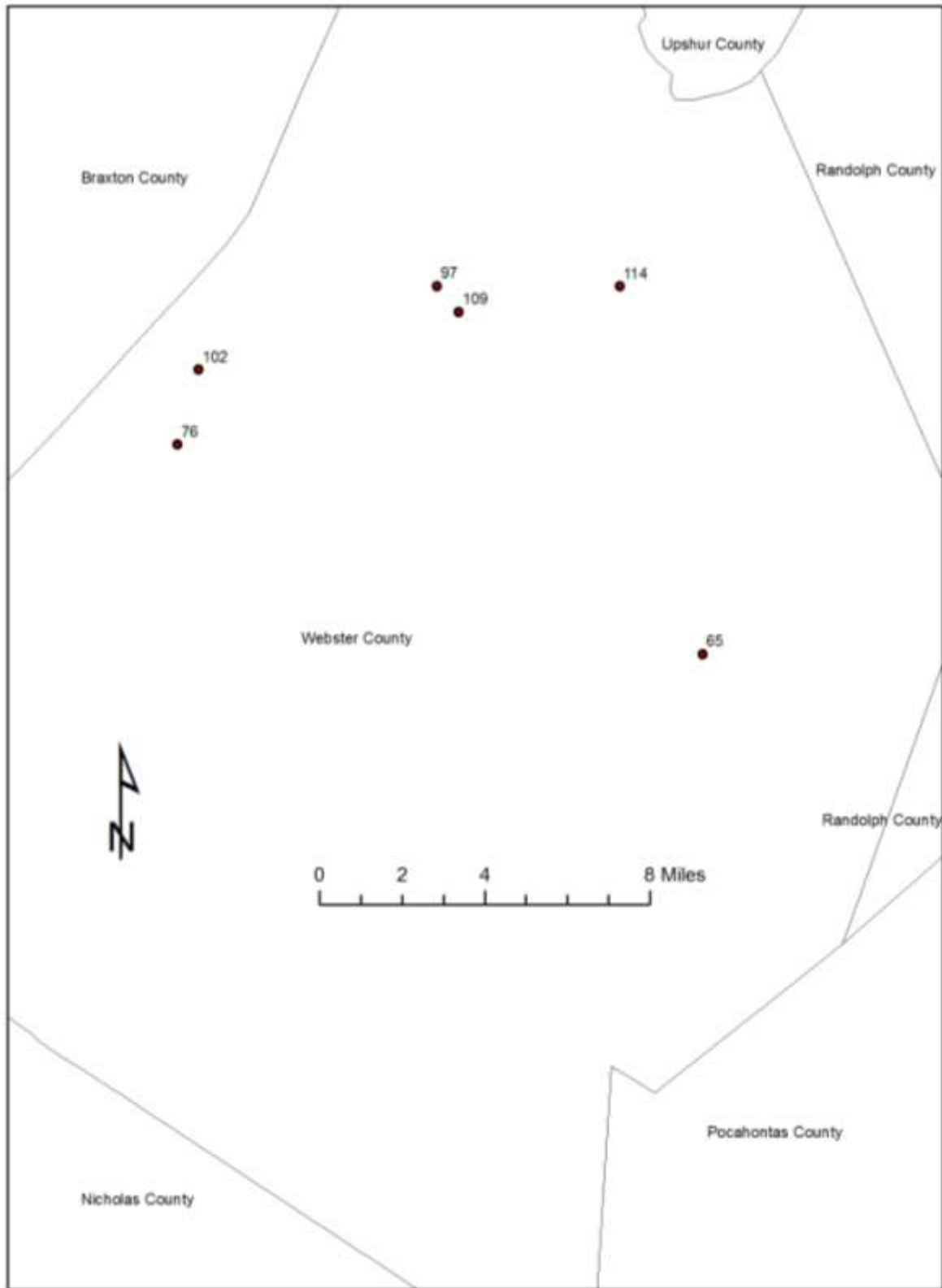
393N

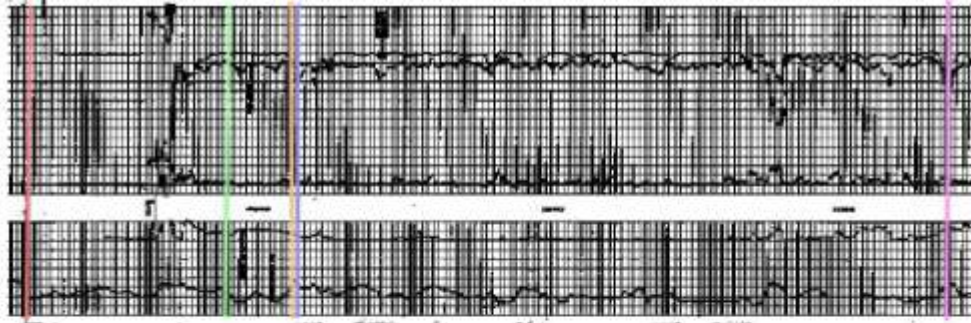


383N

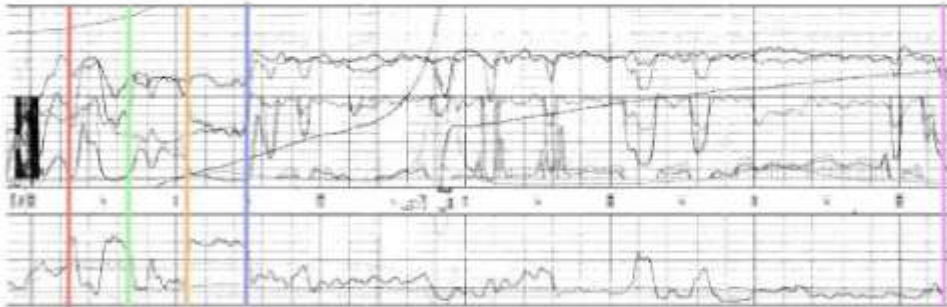


310N

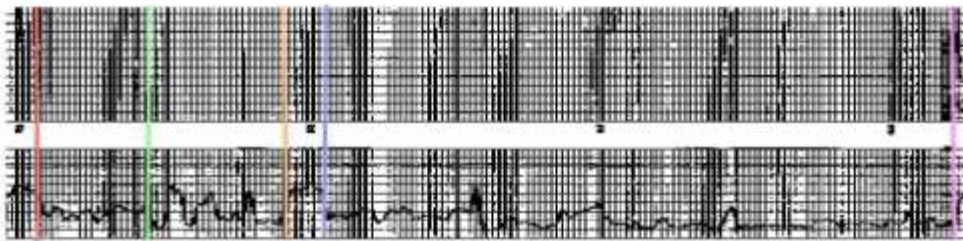




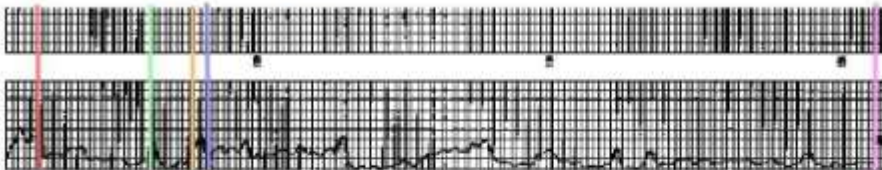
65W



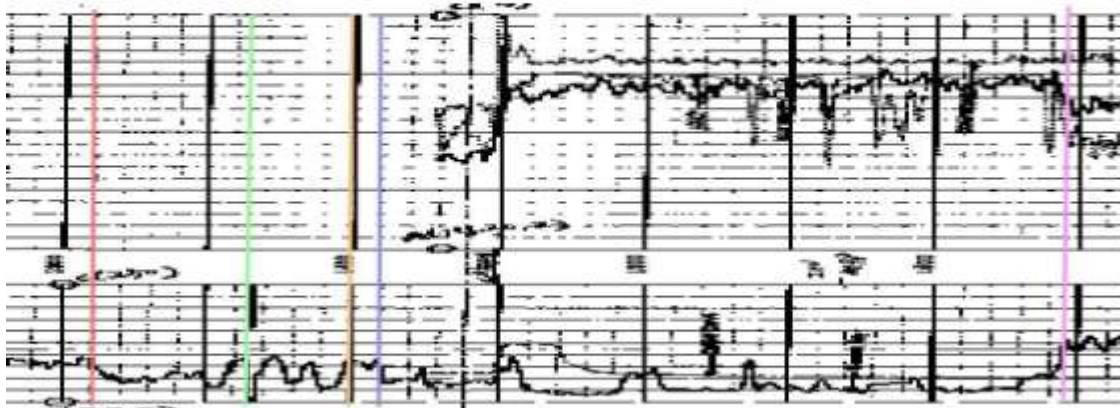
114W



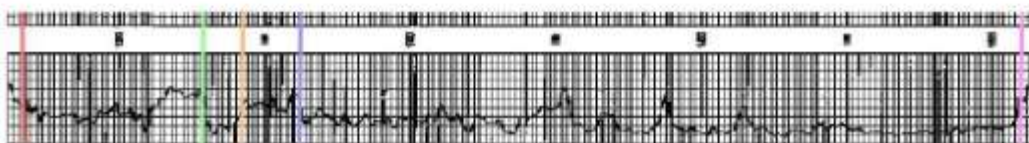
109W



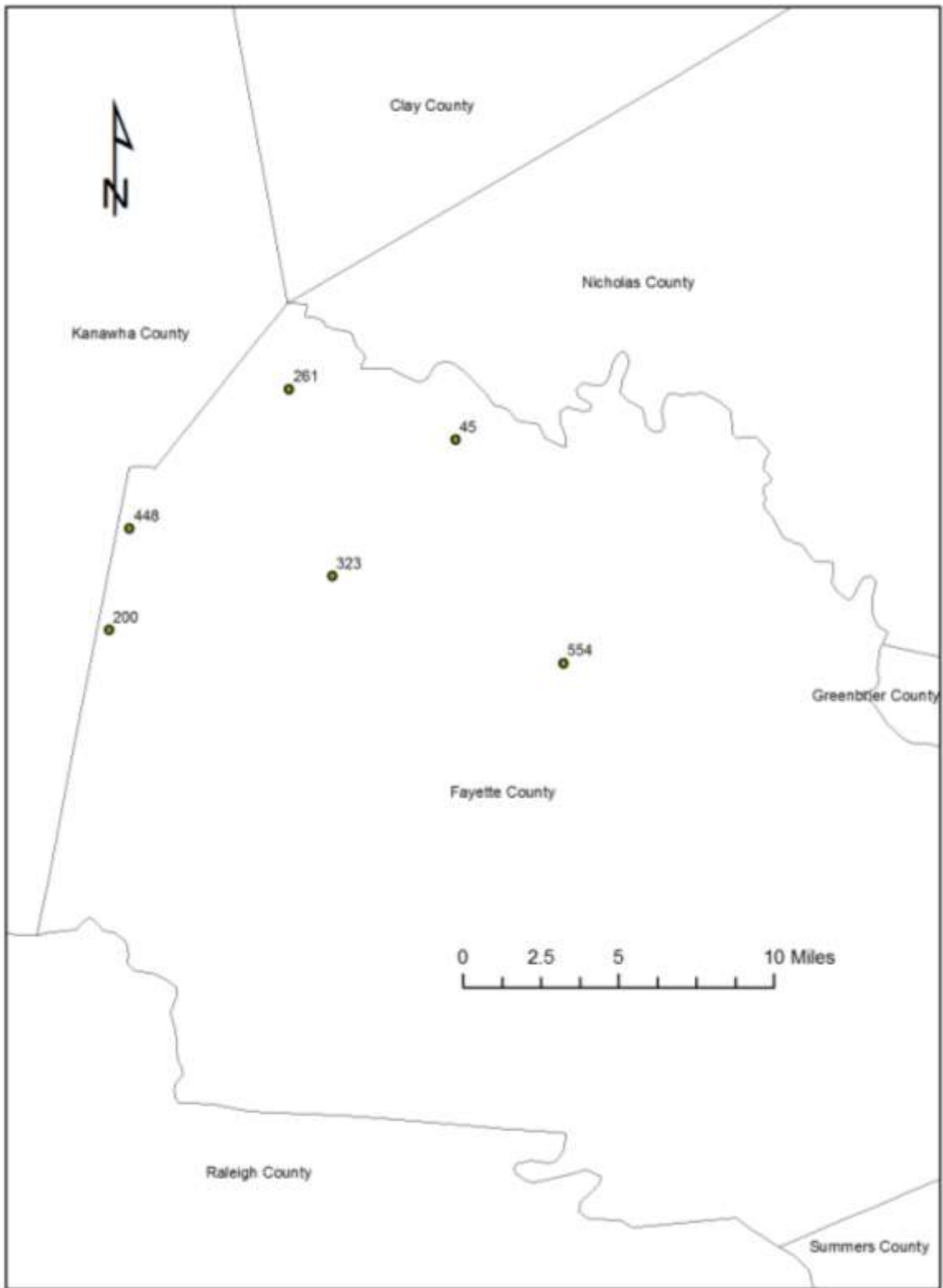
102W

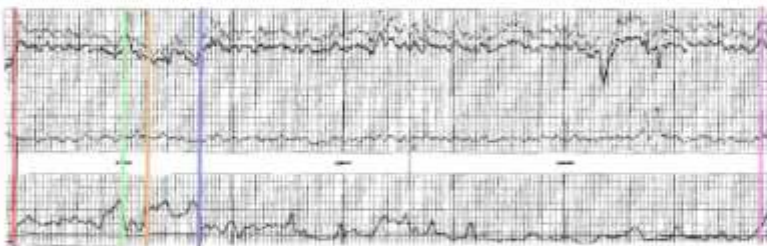
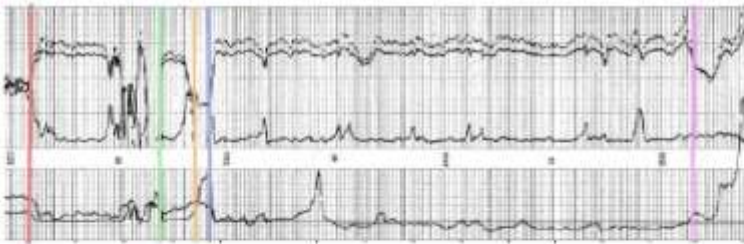
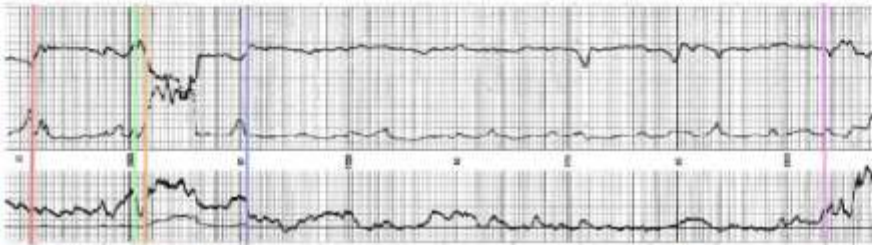
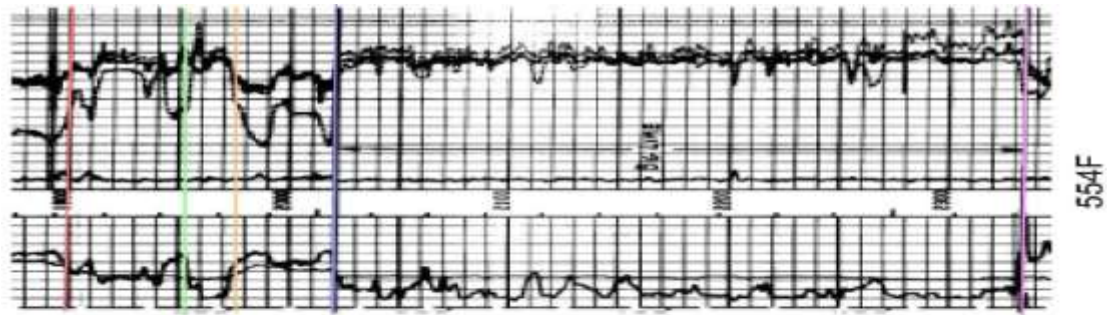


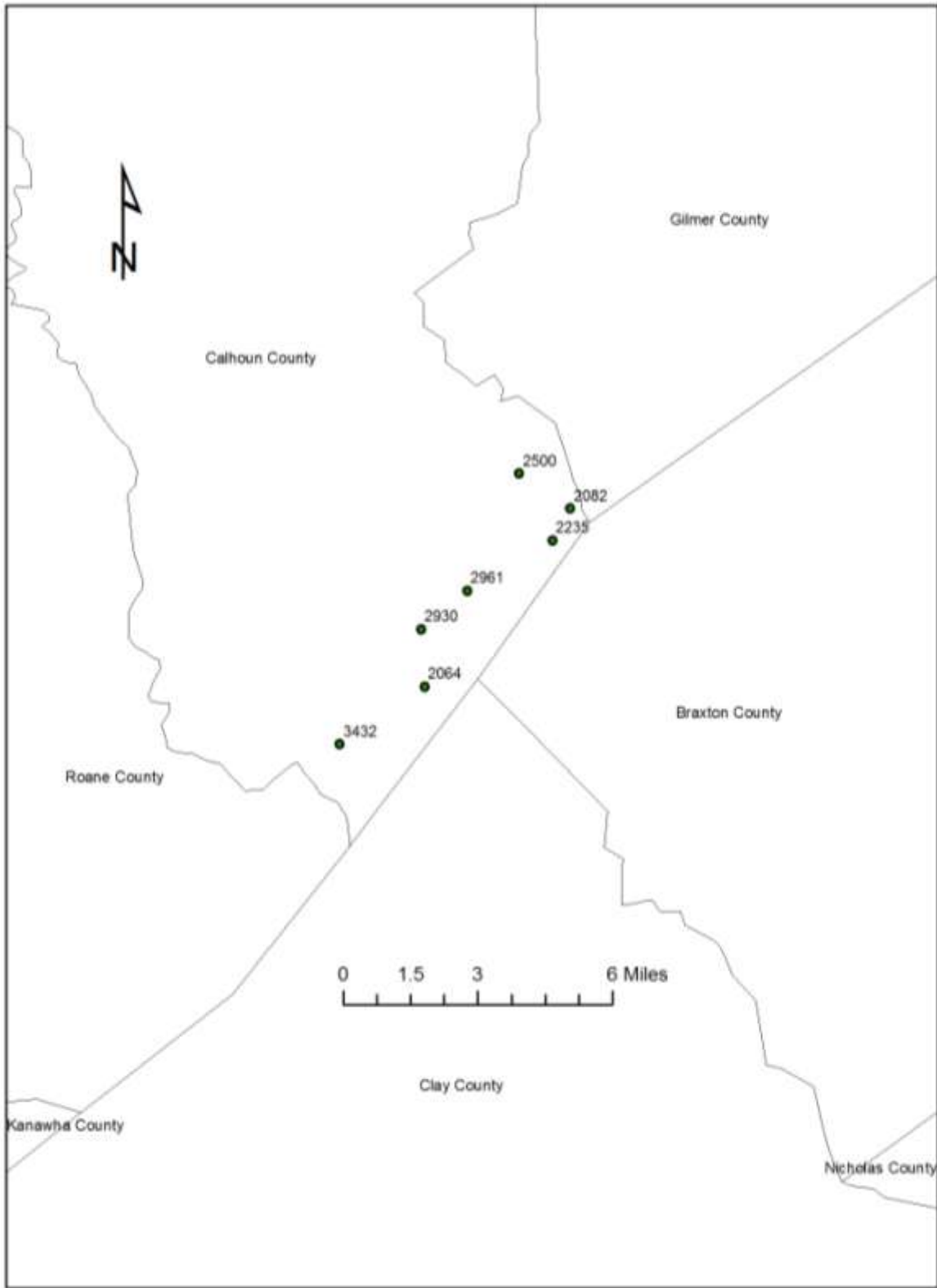
76W

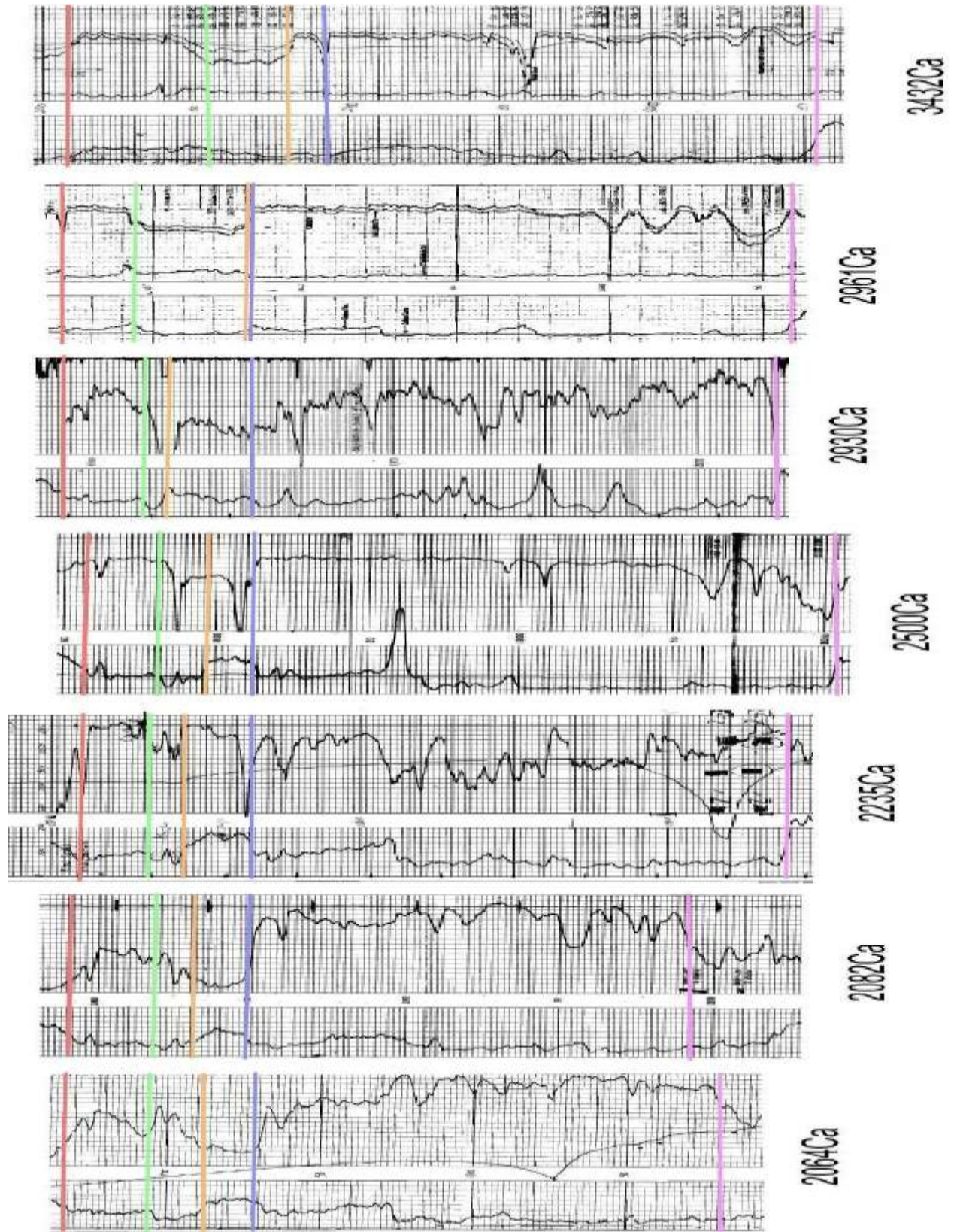


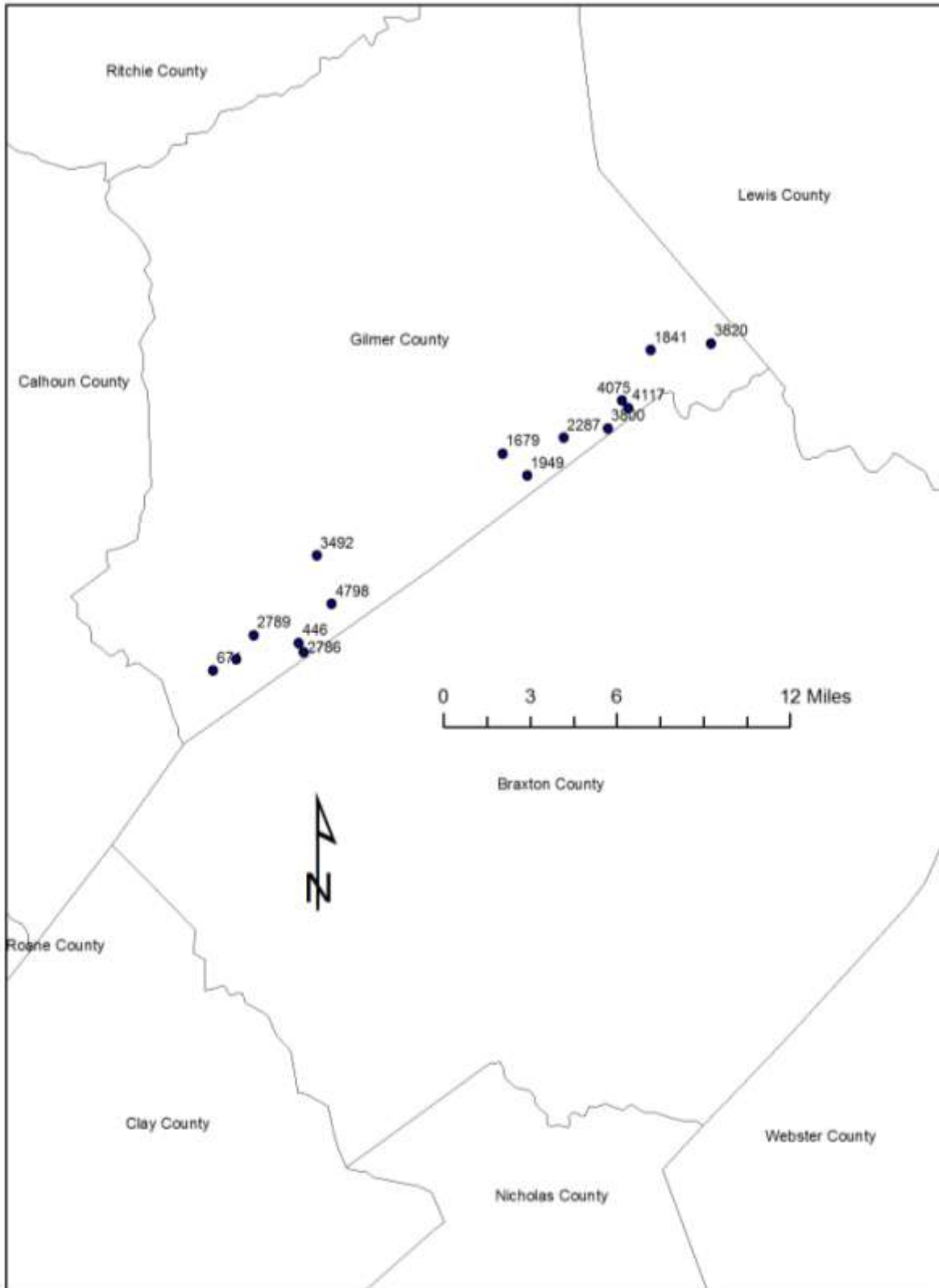
97W

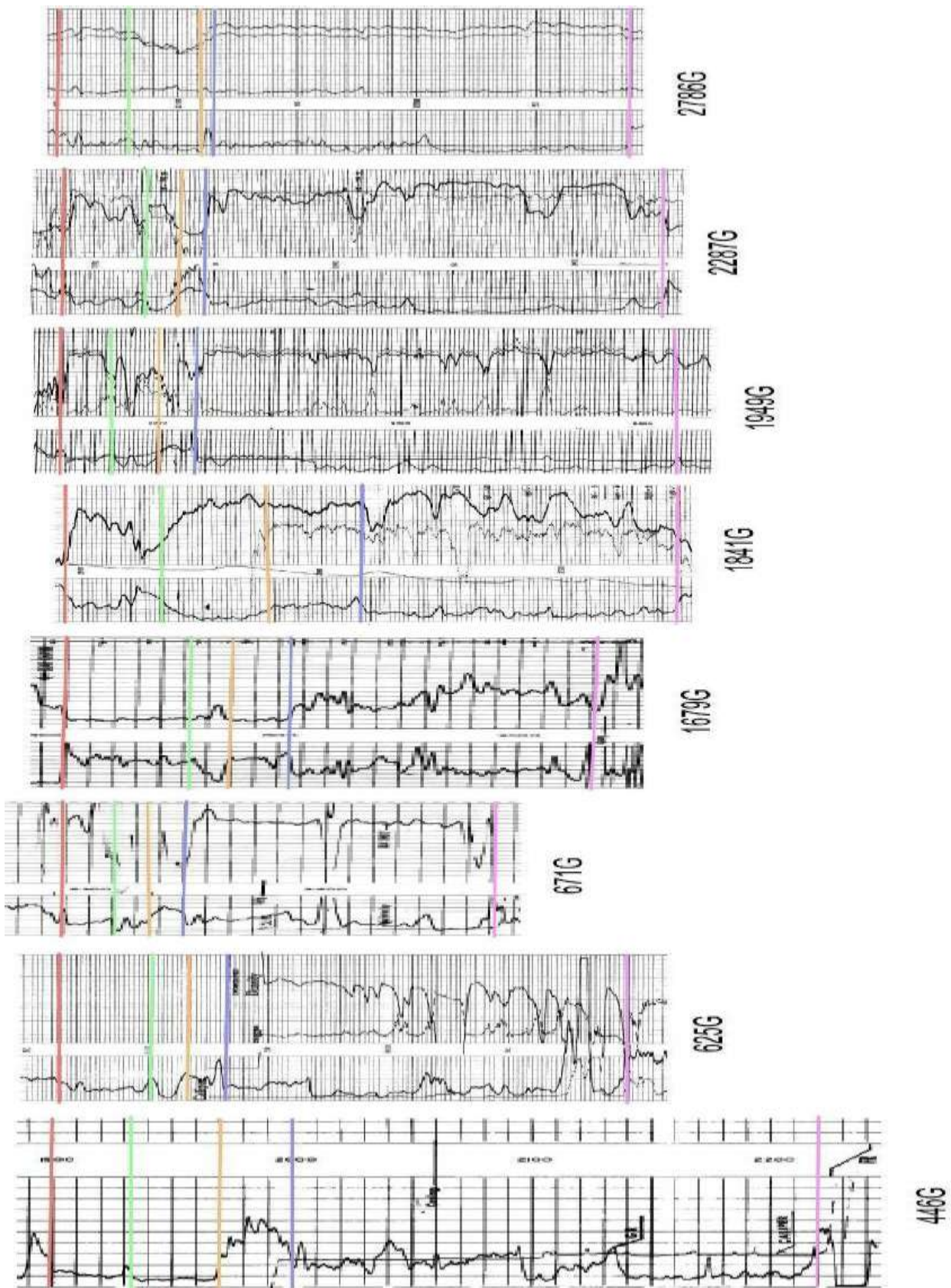


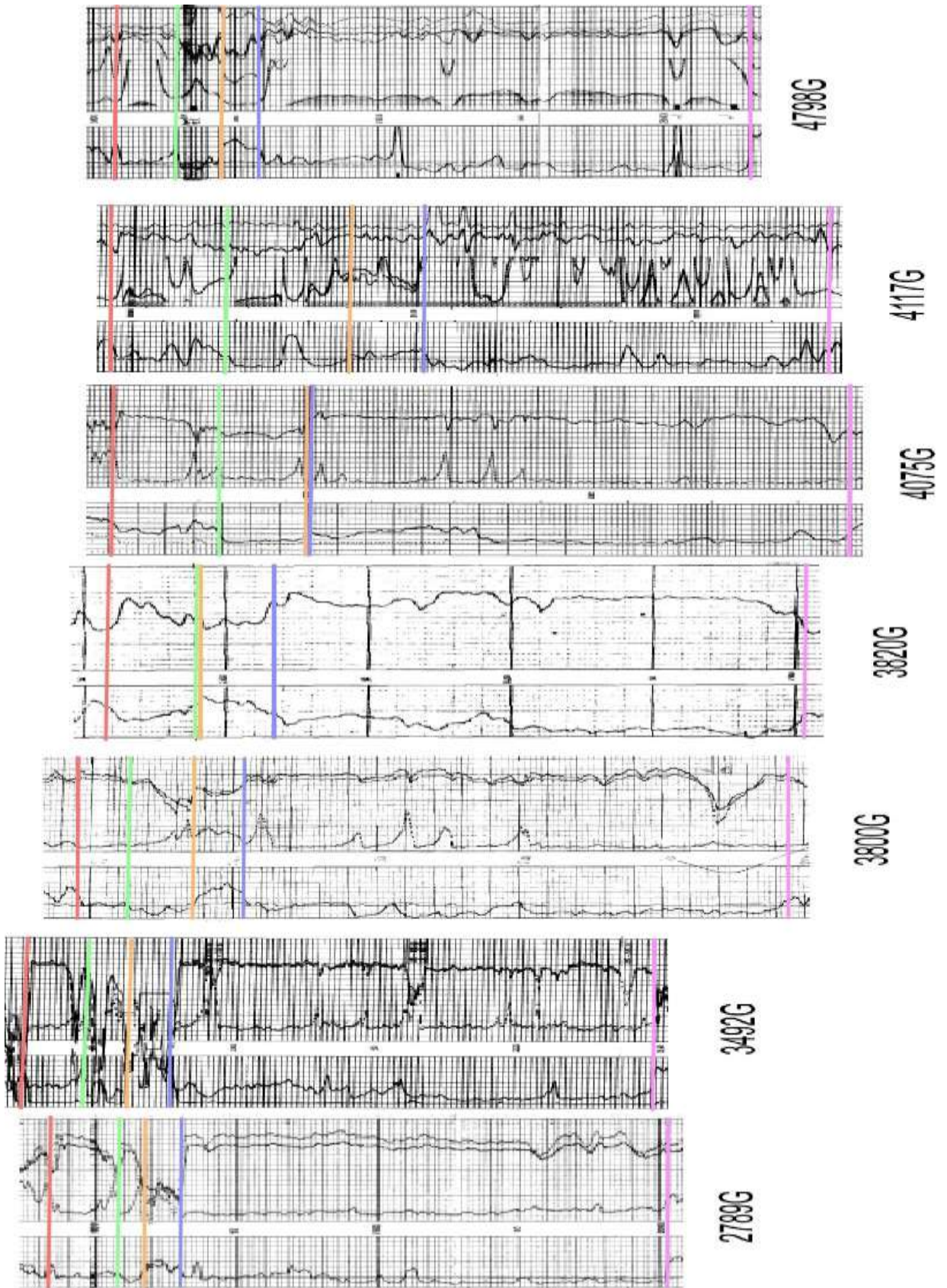


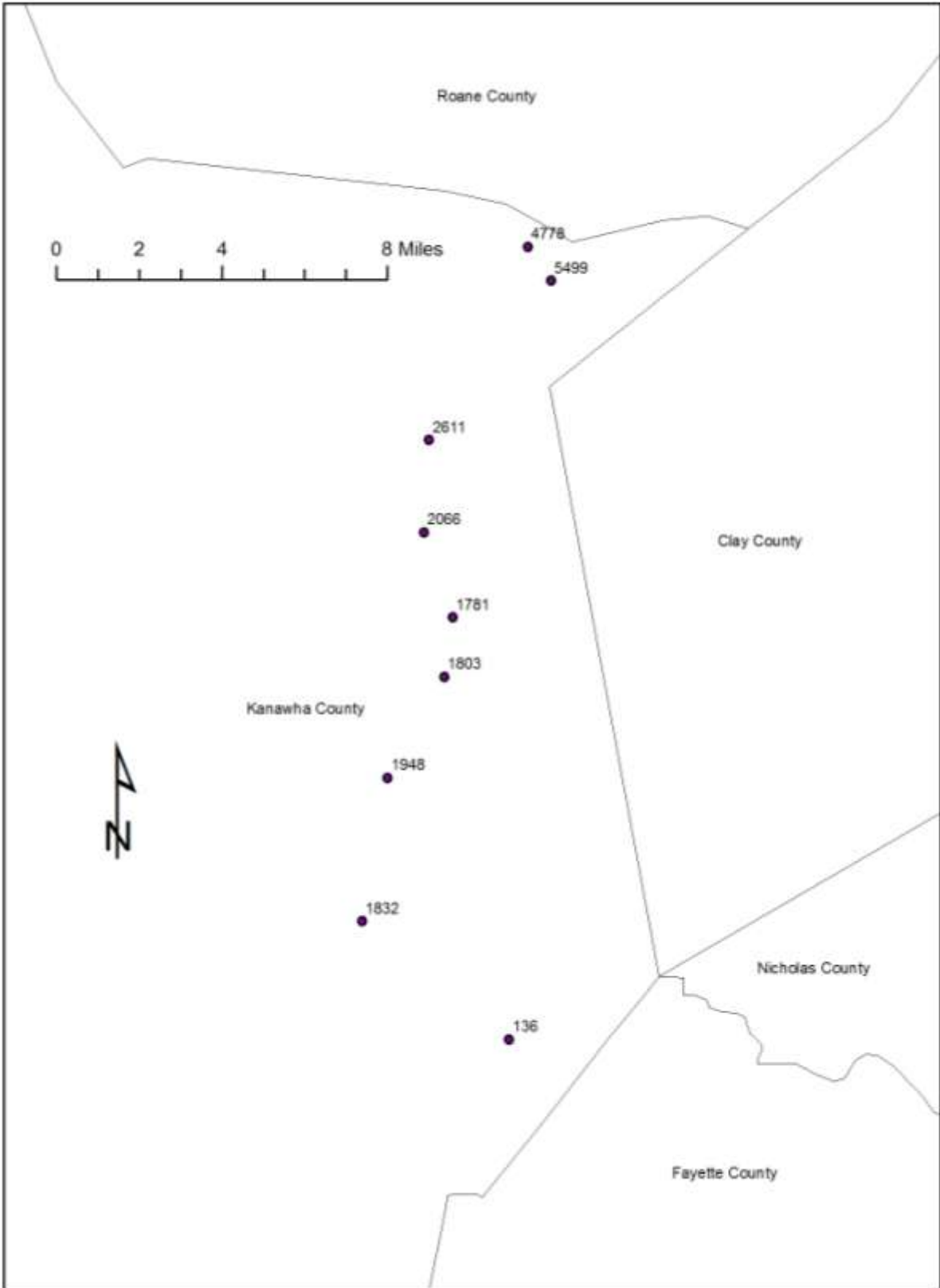


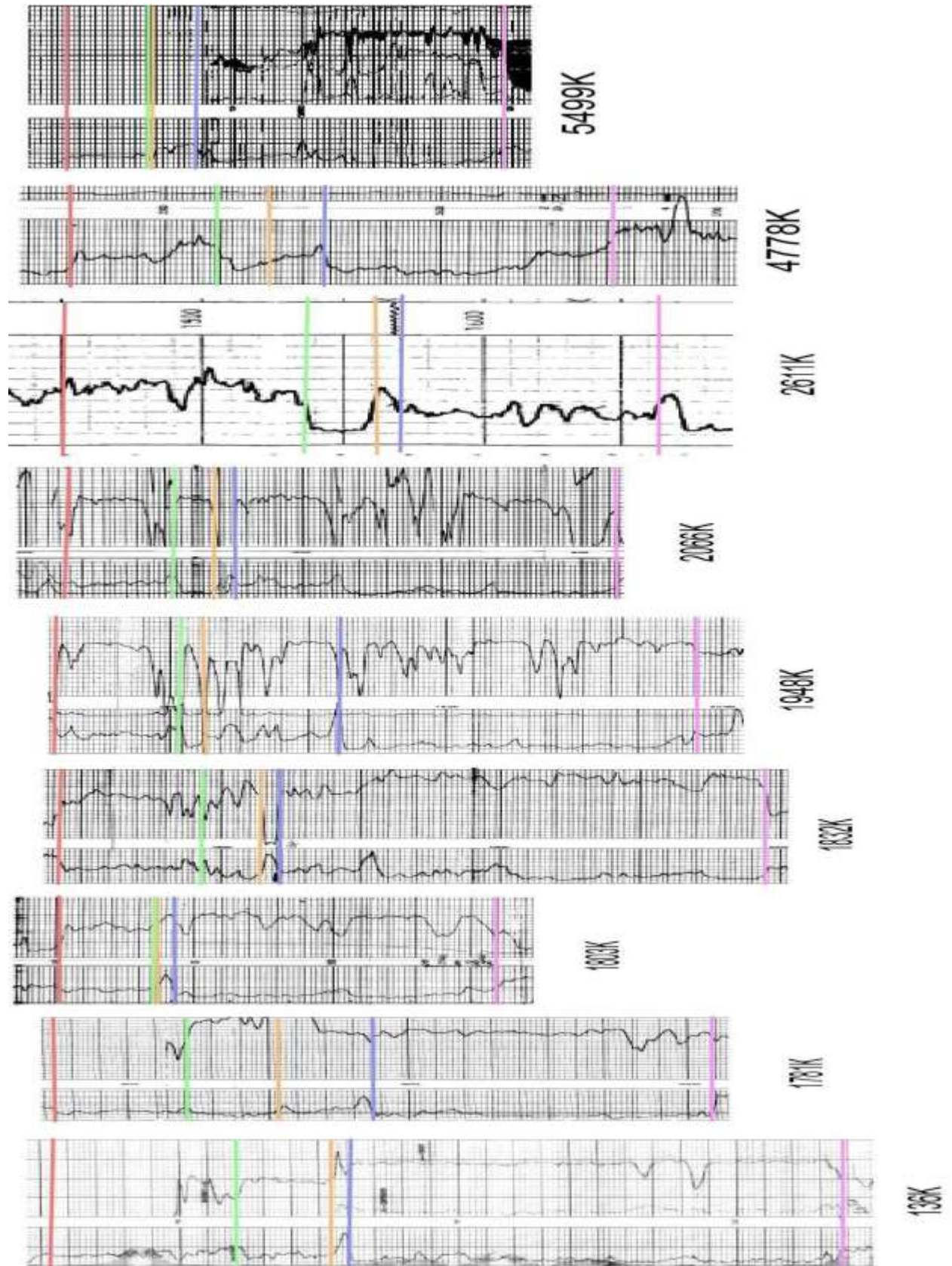


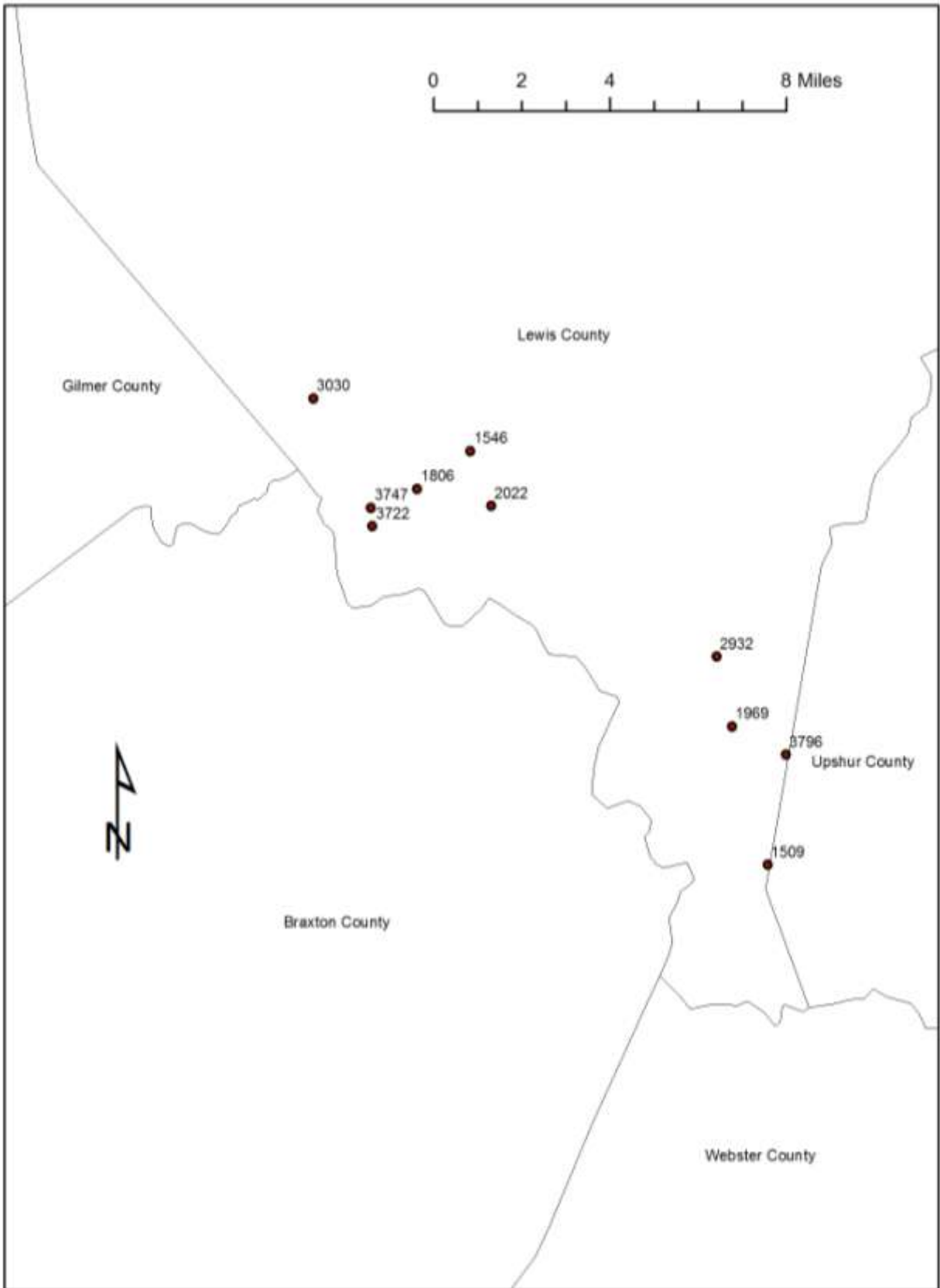


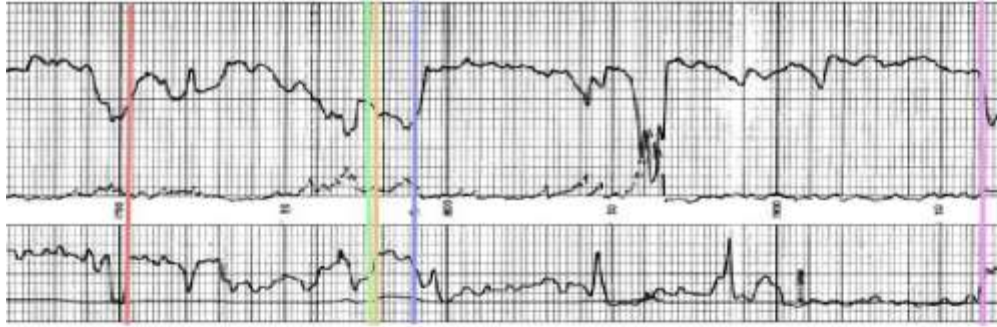












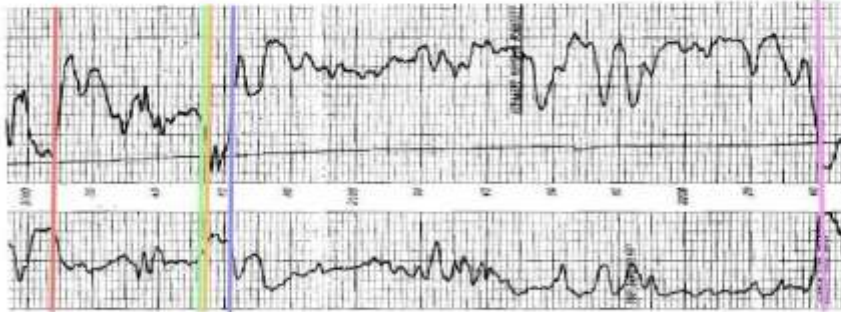
2022L



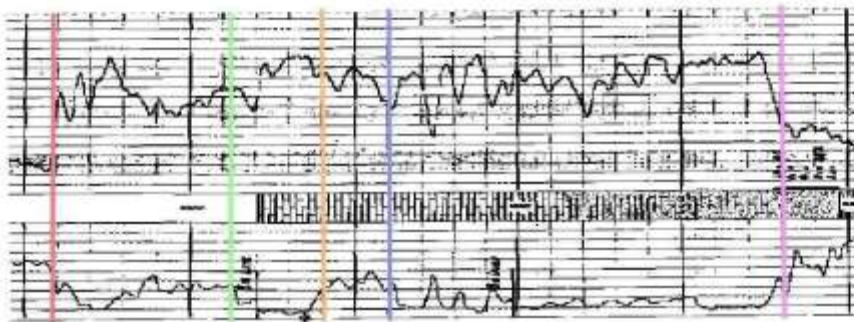
1969L



1806L



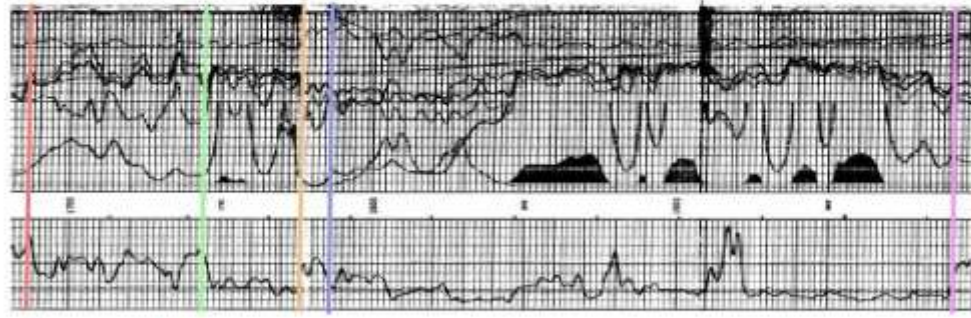
1546L



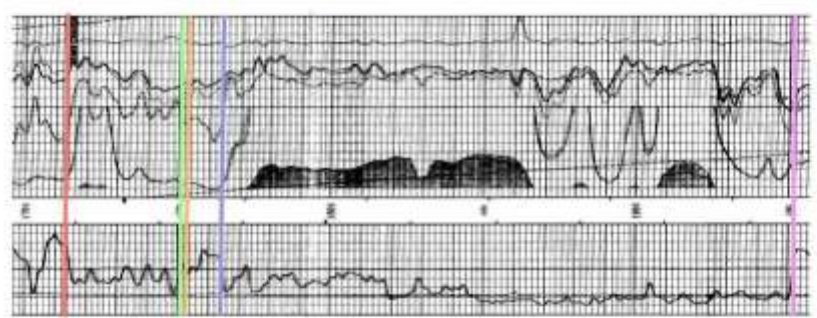
1509L



3796L



3747L



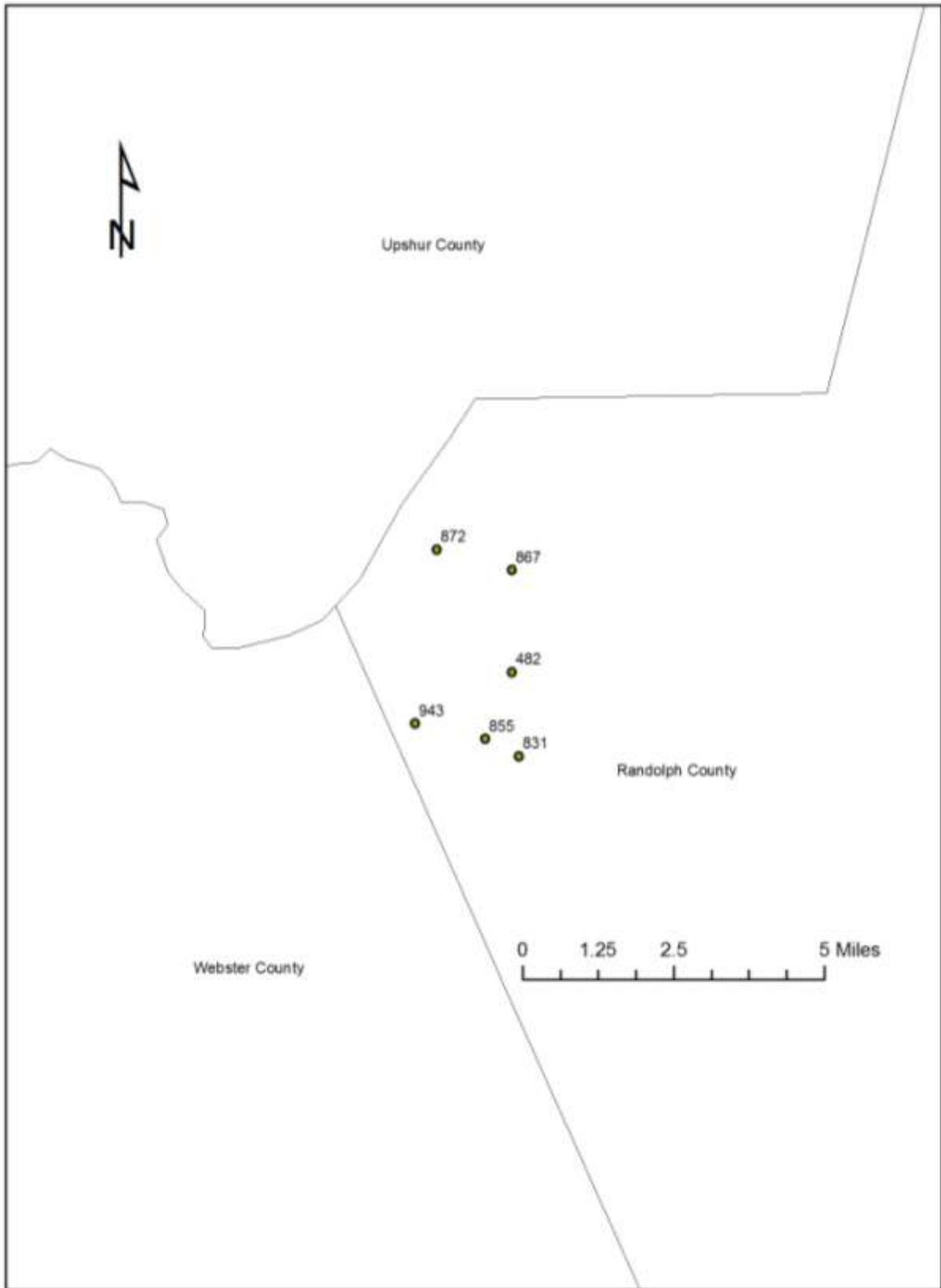
3722L

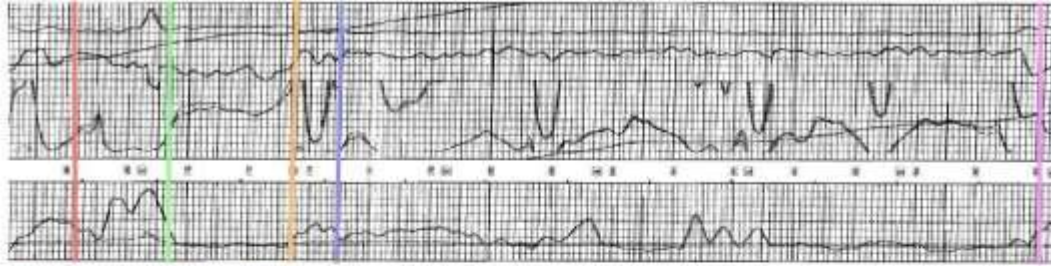


3030L



2932L

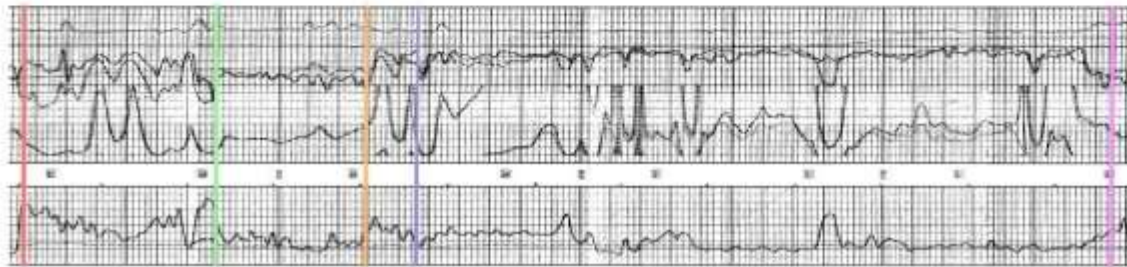




943Ra



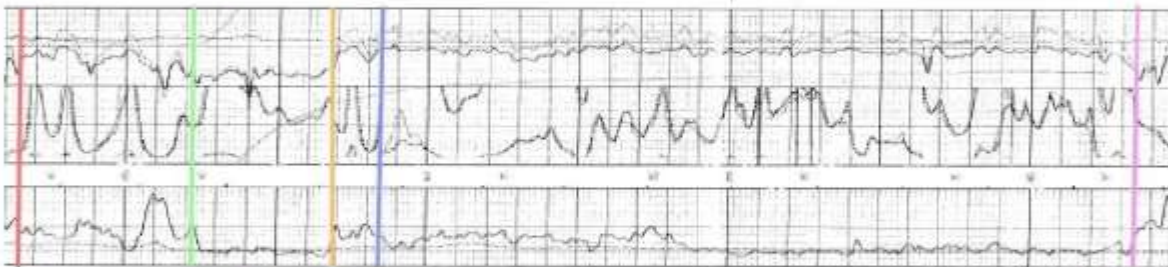
872Ra



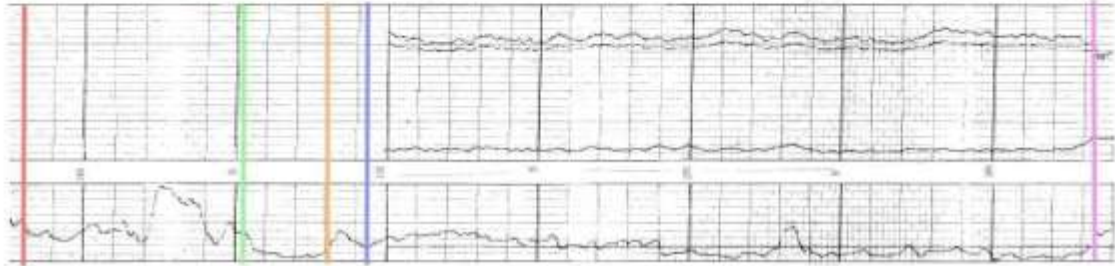
867Ra



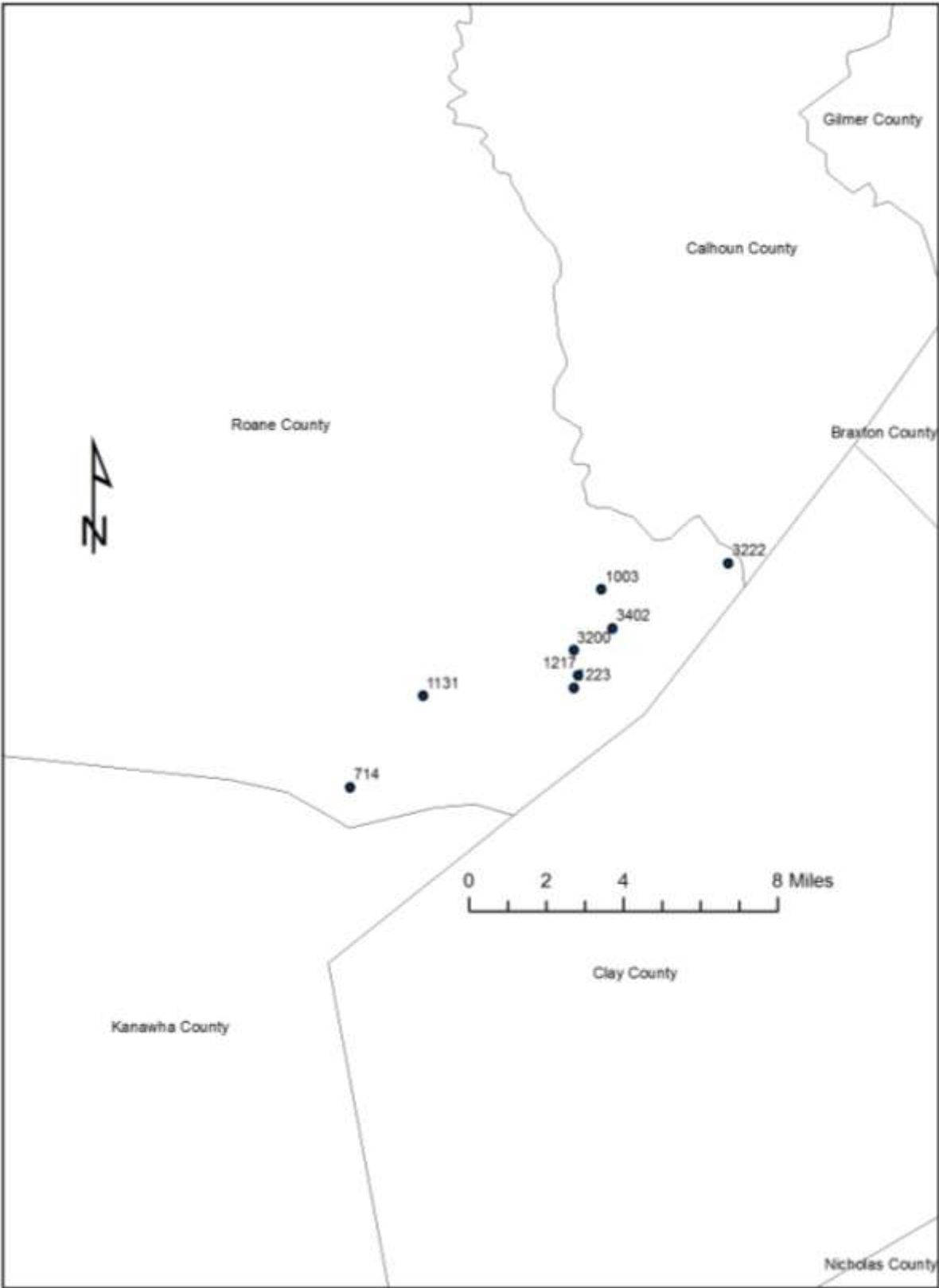
855Ra

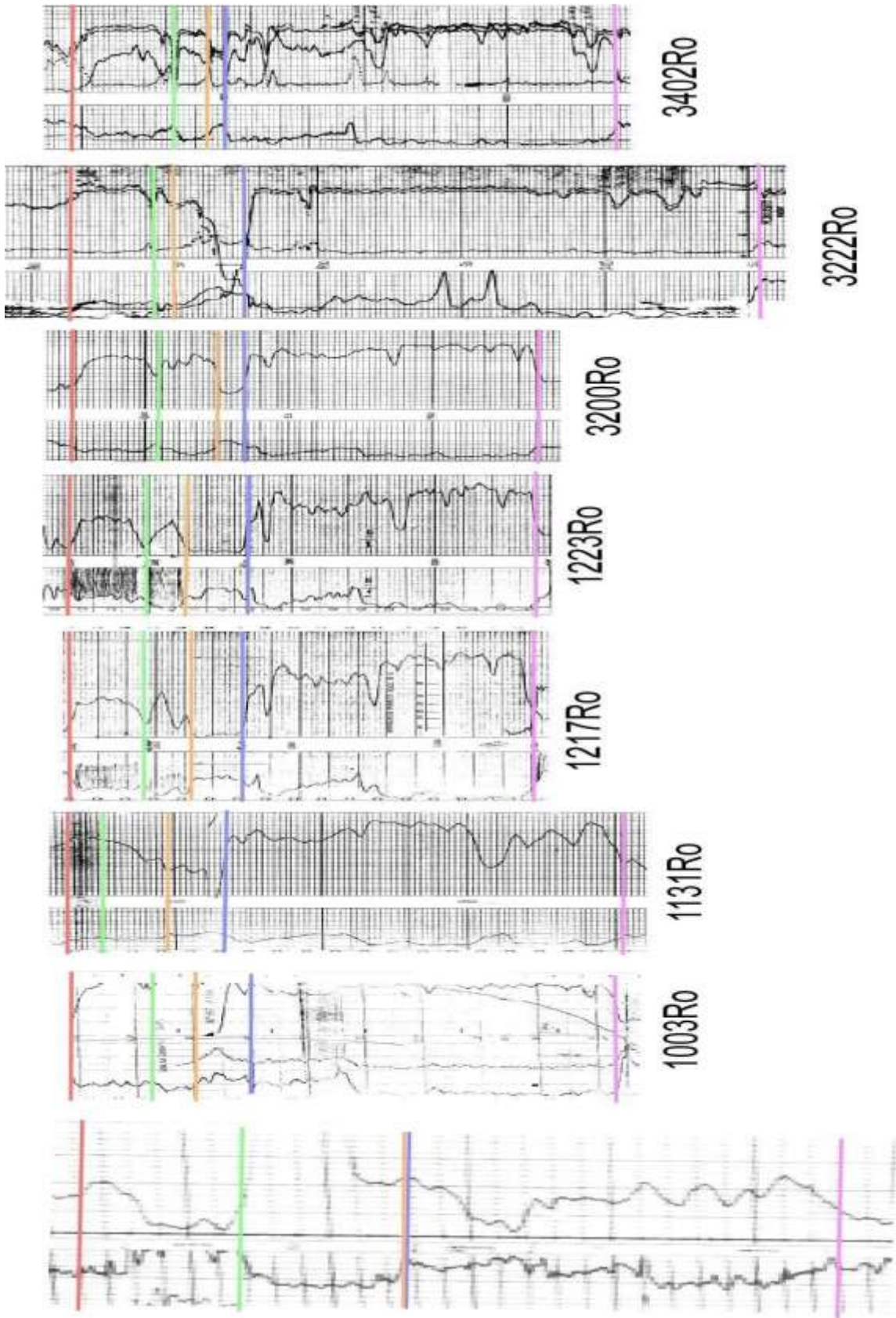


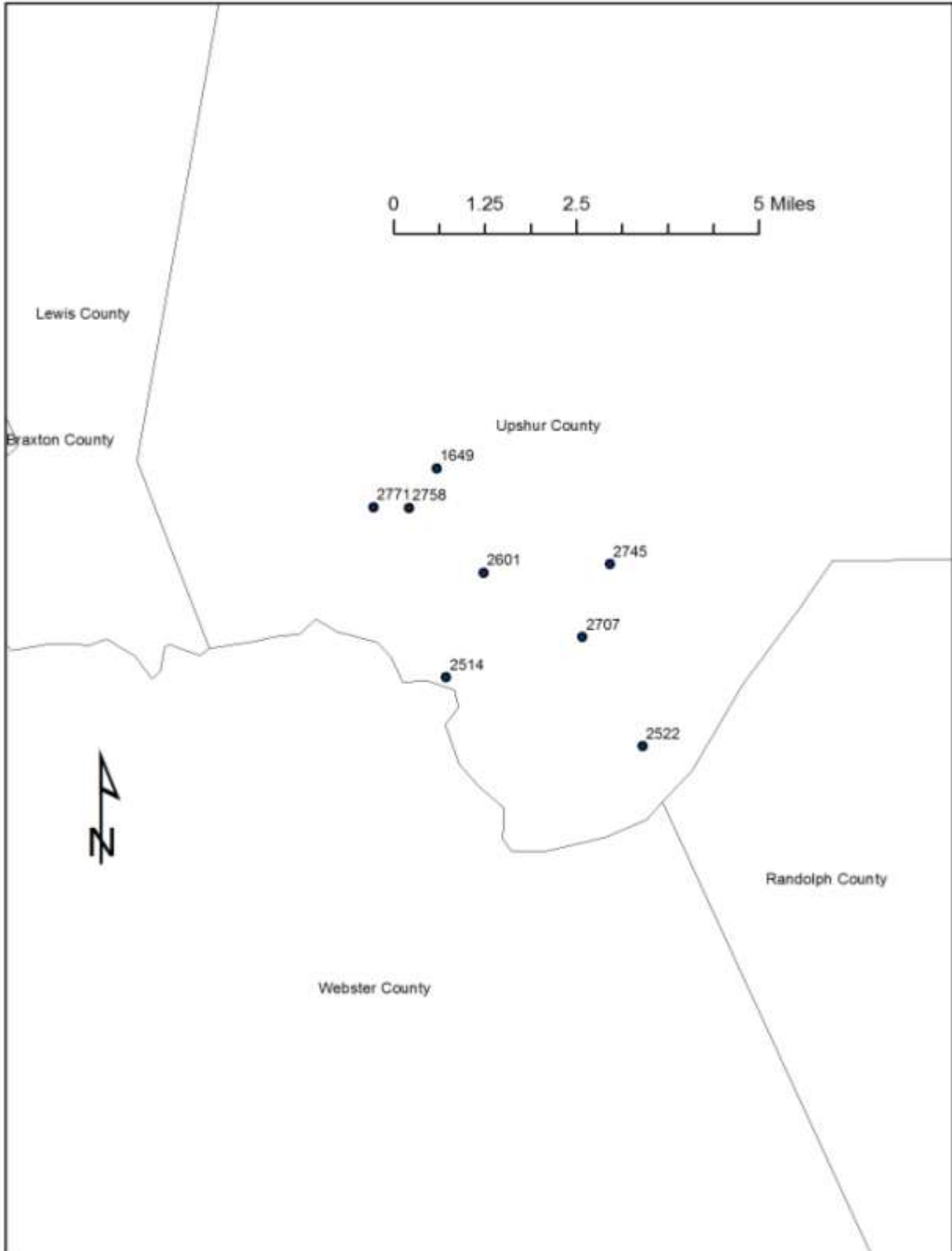
831Ra

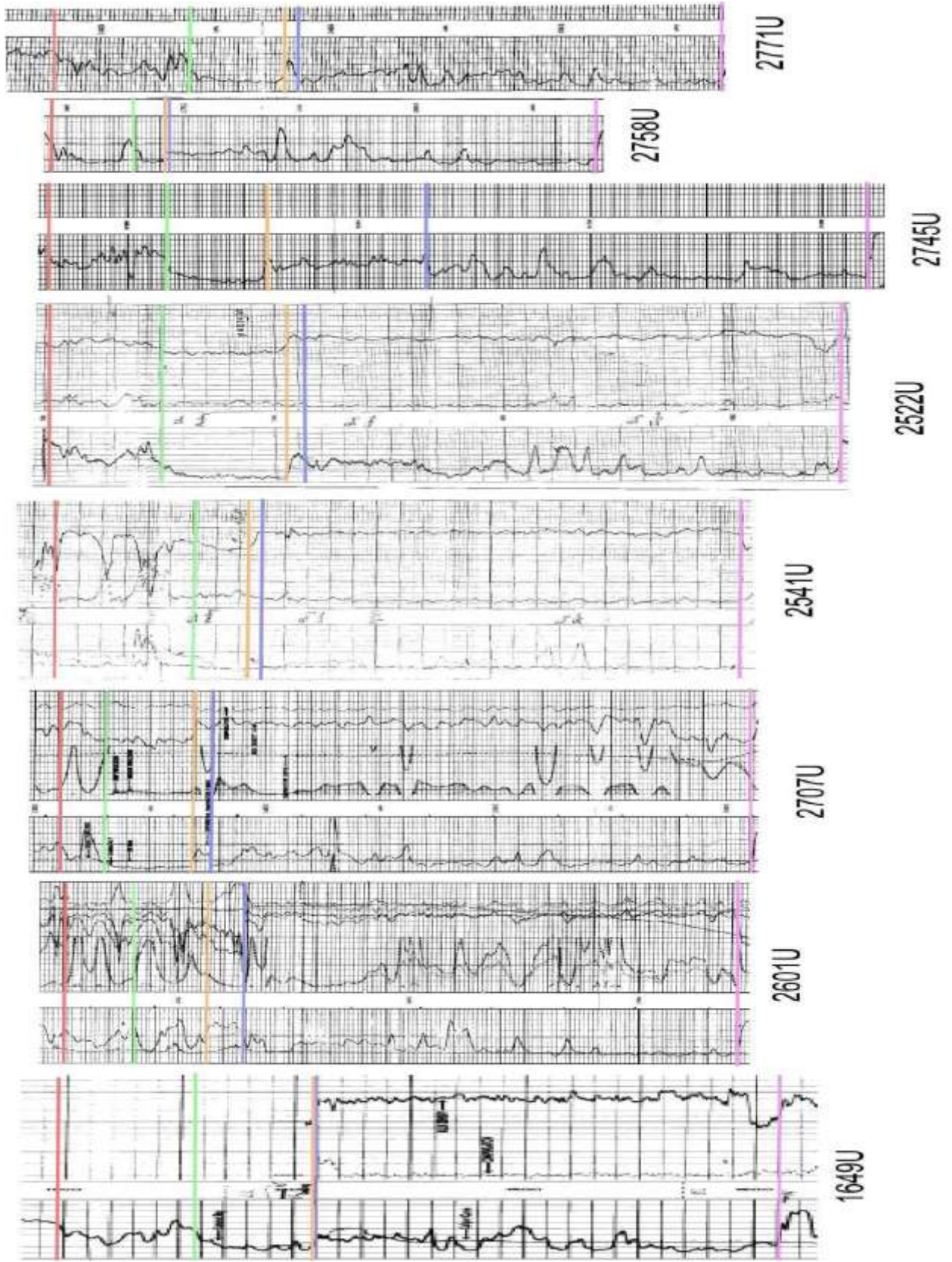


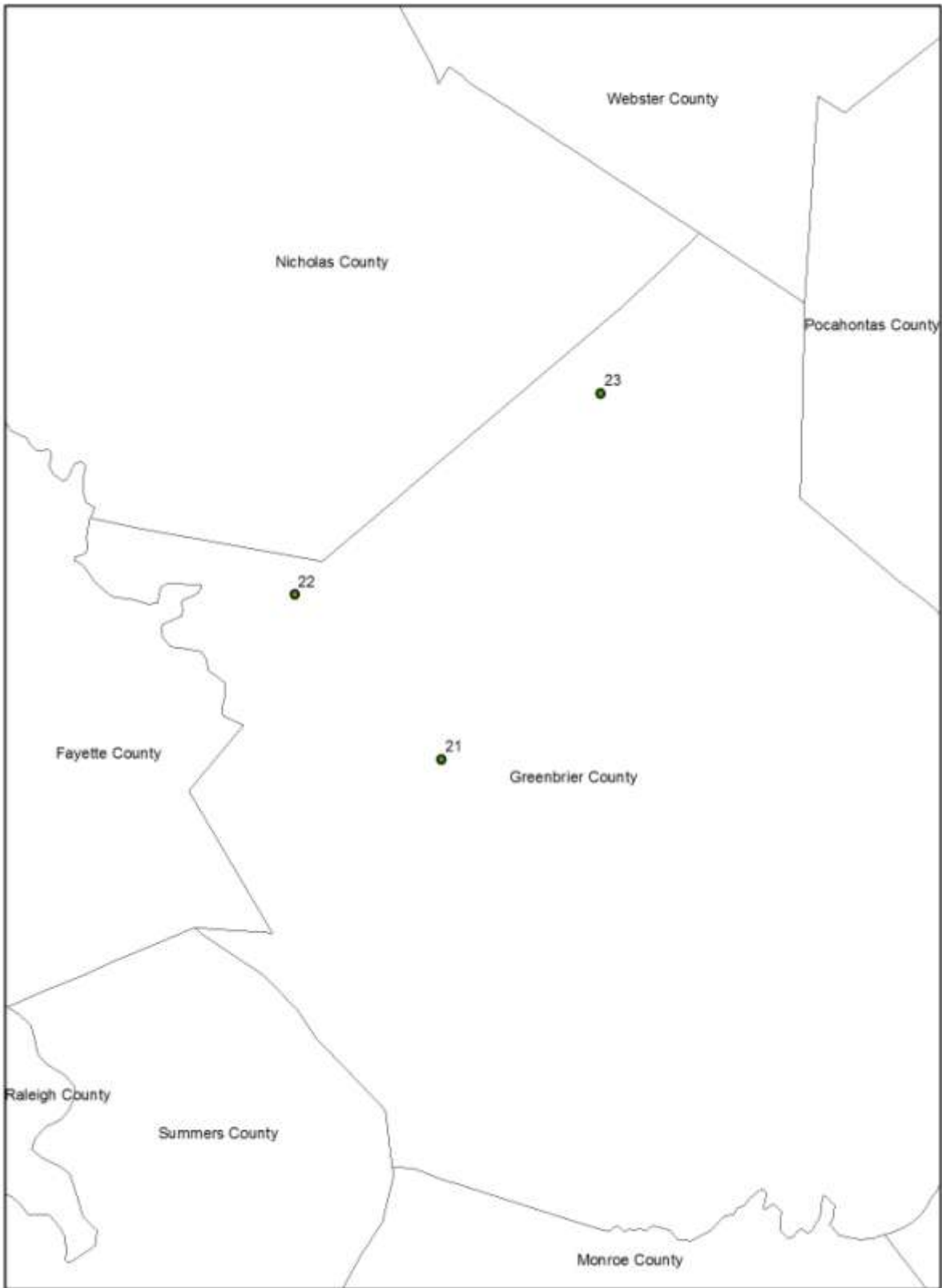
482Ra

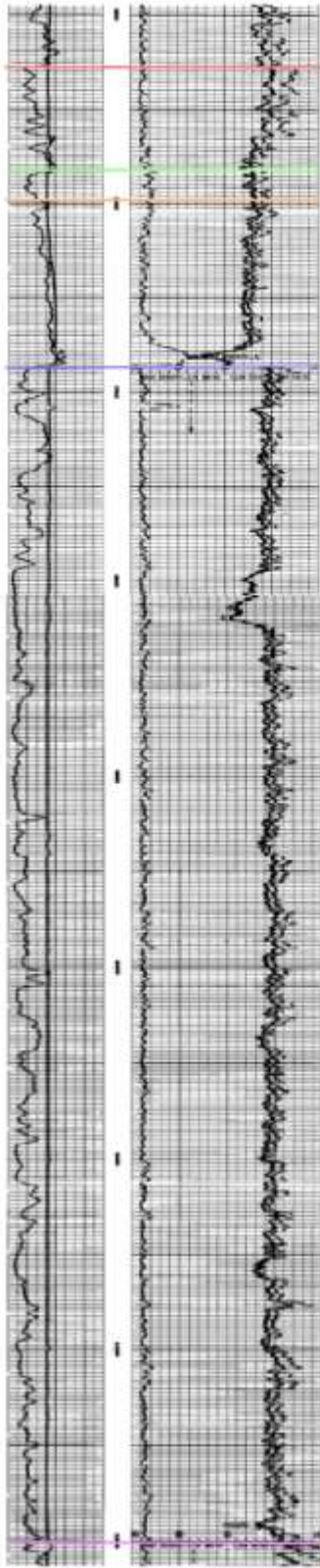




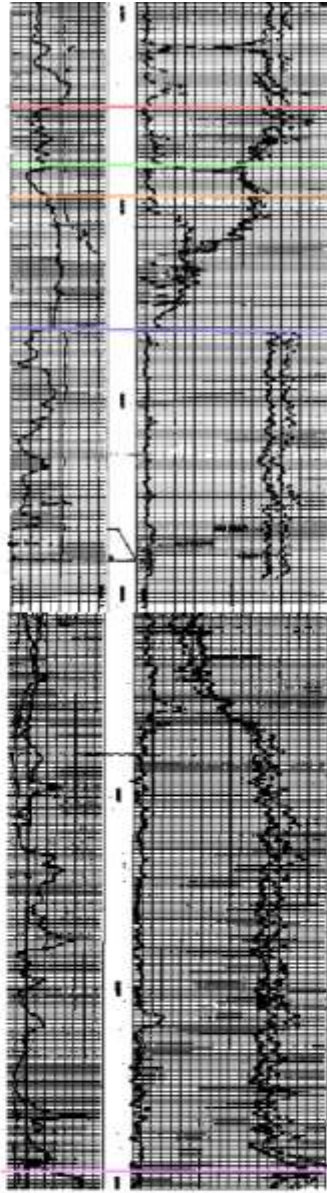




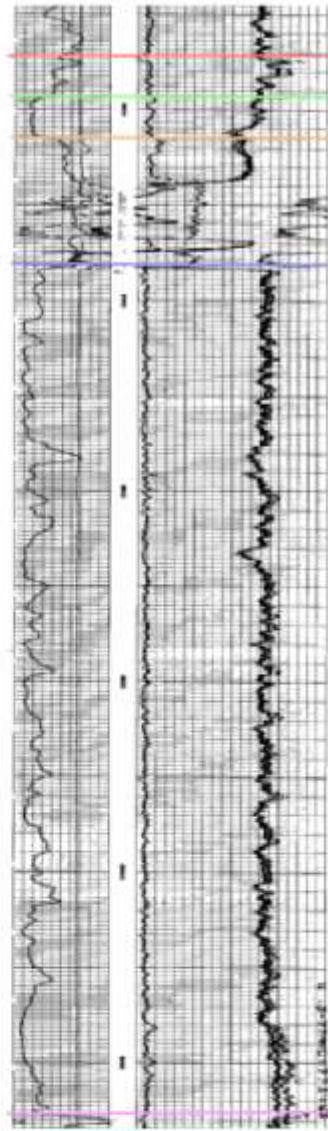




21Gr



22Gr



23Gr

APPENDIX IV: DATA COMPILATION

Datum: NAD83

Source: WVGES, 2010.

Bolded log type were the logs chosen out of available logs.

PRODUCING WELLS

API	CNTYNM	PRMT	Lat	Long	UTME	UTMN
4701500728	Clay	728	38.470355	-80.886583	509894	4257803.3
4701500909	Clay	909	38.272705	-81.221157	480654.6	4235889.7
4701500917	Clay	917	38.486283	-80.910724	507786.3	4259568.4
4701500966	Clay	966	38.438134	-80.96081	503420.3	4254222.7
4701501315	Clay	1315	38.358469	-81.124249	489144.3	4245389.8
4701501465	Clay	1465	38.527543	-81.107133	490661.5	4264148.2
4701501514	Clay	1514	38.539564	-80.936901	505499.3	4265478.4
4701501547	Clay	1547	38.541678	-80.93025	506078.7	4265713.5
4701501549	Clay	1549	38.545955	-80.925492	506493	4266188.4
4701501557	Clay	1557	38.488694	-80.900246	508700	4259836.8
4701501558	Clay	1558	38.484406	-80.902631	508492.4	4259360.8
4701501588	Clay	1588	38.433263	-80.931429	505984.9	4253683.8
4701501636	Clay	1636	38.507003	-80.882504	510244.7	4261870.2
4701501637	Clay	1637	38.495936	-80.90985	507861.5	4260639.5
4701501638	Clay	1638	38.504913	-80.905896	508205.4	4261635.9
4701501656	Clay	1656	38.499357	-80.916096	507316.5	4261018.6
4701501657	Clay	1657	38.507559	-80.912054	507668.1	4261929
4701501658	Clay	1658	38.503863	-80.900224	508700	4261519.9
4701501659	Clay	1659	38.503643	-80.890782	509523.3	4261496.5
4701501660	Clay	1660	38.507412	-80.895688	509095.1	4261914.2
4701501671	Clay	1671	38.508865	-80.933476	505800.2	4262072.4
4701501673	Clay	1673	38.43279	-80.935652	505616.3	4253631
4701501678	Clay	1678	38.514157	-80.901636	508575.7	4262662
4701501680	Clay	1680	38.515206	-80.907719	508045.2	4262777.9
4701501683	Clay	1683	38.518021	-80.897378	508946.4	4263091.1
4701501684	Clay	1684	38.519816	-80.9047	508307.9	4263289.6
4701501794	Clay	1794	38.523911	-80.913587	507532.7	4263743.2
4701501795	Clay	1795	38.527203	-80.908675	507960.6	4264108.9
4701501796	Clay	1796	38.523815	-80.919991	506947.5	4263732.1
4701502309	Clay	2309	38.408974	-80.956127	503830.5	4250987.4
4701502357	Clay	2357	38.586538	-80.980499	501698.5	4270689
4701502365	Clay	2365	38.587699	-80.974957	502181.1	4270818
4701502381	Clay	2381	38.431918	-80.940085	505229.5	4253534
4701502389	Clay	2389	38.590892	-80.978652	501859.2	4271172.2
4701502390	Clay	2390	38.590892	-80.972371	502406.2	4271172.4
4701502392	Clay	2392	38.585812	-80.974403	502229.4	4270608.7

Elevation	Total Depth	Log Types	LL Top	LL Base	LL Thickness	BMS Top
1481	2200	dngc/DNGT/gn	1864	1906	42	1907
1525	3160	gdc	2318	2367	49	2368
1568	2609	DG/DGC/I/NG	2034	2076	42	2077
1402	2325	GCDN	1990	2023	33	2024
1192	2362	GBOP/ GCD /GN	1984	2020	36	2021
1310	2300	GCD	2010	2048	38	2049
879	1795	gn	1478	1534	56	1535
987	1950	gn /gpo	1598	1646	48	1647
1175	2145	gn/gpo	1806	1846	40	1847
1628	2440	gn	2102	2160	58	2161
1640	2444	gdc /gn/gpo	2100	2170	70	2171
1536	2315	gbo /I	1960	1989	29	1990
1521	2431	gpo/ I	2080	2107	27	2108
1415	2316	gn /gpbo/i	1942	1981	39	1982
1368	2290	gdc/ gn /i	1948	1979	31	1980
1334	2088	gn	1732	1774	42	1775
1386	2345	gdc /gn/gpo	1958	2003	45	2004
1485	2350	gbo/gdc/ gn /gpo	1990	2038	48	2039
1584	2442	gn	2074	2104	30	2105
1532	2413	gn /gpo	2050	2097	47	2098
1331	2305	gn /i	1990	2014	24	2015
1511	2314	gn	1972	2007	35	2008
1043	1980	gdc /gn	1638	1682	44	1683
1387	2325	gn	1970	2020	50	2021
1400	2310	gn	1986	2025	39	2026
1441	2410	gdc /gn/gpo	2048	2093	45	2094
1219	2000	gdc /gn/gpo	1648	1687	39	1688
1368	2359	gdc /gn/gpo/i	2029	2064	35	2076
926	2075	gdc /gn/gpo/i	1736	1777	41	1778
1530	2424	TGDN	2004	2034	30	2035
1025	2125	gdnce /gio/o/t	1760	1799	39	1800
889	1995	gdnce /gi/gpo/gt/_a	1633	1667	34	1668
1480	2398	dn	1938	1970	32	1971
1237	2370	dnitgco	2030	2064	34	2065
1237	2180	dtingc	1842	1879	37	1880
1036	2025	itdnlgco	1767	1819	52	1820

BMS Base	BMS Thickness	PC Top	PC Base	PC Thickness	BL Top	BL Base	BL Thickness	Cross-Section Line #
1928	21	1929	1960	31	1961	2182	221	11
2377	9	2378	2402	24	2403	2594	191	8,5
2129	52	2130	2144	14	2145	2336	191	13
2061	37	2062	2077	15	2078	2280	202	8, 6
2036	15	2037	2065	28	2066	2266	200	1, 8
2082	33	2083	2088	5	2089	2230	141	6, 15
1560	25	1561	1563	2	1564	1760	196	9
1678	31	1679	1684	5	1685	1896	211	9
1890	43	1891	1895	4	1896	2080	184	9
2188	27	2189	2209	20	2210	2400	190	13
2183	12	2184	2191	7	2192	2398	206	13
2021	31	2022	2060	38	2061	2257	196	11
2134	26	2135	2162	27	2163	2380	217	13
2036	54	0	0	0	2037	2250	213	14
2016	36	0	0	0	2017	2224	207	14
1830	55	0	0	0	1831	2038	207	12
2060	56	0	0	0	2061	2272	211	12
2080	41	0	0	0	2081	2288	207	14
2121	16	2122	2154	32	2155	2372	217	13
2132	34	2133	2147	14	2148	2364	216	12
2040	25	2041	2069	28	2070	2254	184	10
2038	30	2039	2070	31	2071	2276	205	11
1713	30	1714	1729	15	1730	1948	218	12
2057	36	2058	2063	5	2064	2268	204	14
2045	19	2046	2069	23	2070	2290	220	12
2110	16	2111	2138	27	2139	2351	212	14
1731	43	1732	1739	7	1740	1950	210	10
2110	34	2111	2119	8	2120	2320	200	10
1815	37	1816	1829	13	1830	2036	206	10
2071	36	2072	2096	24	2097	2318	221	6
1837	37	1838	1844	6	1845	2026	181	7
1683	15	1684	1701	17	1702	1900	198	7
2000	29	2001	2037	36	2038	2246	208	11
2100	35	2101	2106	5	2107	2302	195	7
1902	22	1903	1916	13	1917	2116	199	7
1832	12	1833	1840	7	1841	2026	185	7

Well Log Porosity (%)	Type of Curve	Completion method	Producing Strata	Available Production Data
-	B	Acid and Frac	BMS	
17	C	Frac	BMS, Keener, Big Injun	*
-	B	Frac	BMS	
20	E	Frac	BMS, Big Injun	
16	E	Acid and Frac	BMS, Big Lime, Big Injun	
14	C	Acid and Frac	BMS, Big Lime	
-	C	Acid and Frac	BMS, Big Lime, Big Injun	
-	C	Acid and Frac	BMS	
-	C	Acid and Frac	BMS	*
6	E	Acid and Frac	BMS, Big Injun	
-	E	Acid and Frac	BMS, Big Lime, Big Injun	*
-	E	Acid and Frac	BMS, Big Injun	
-	C	Acid and Frac	BMS, Big Injun	*
-	C	Acid and Frac	BMS, Big Lime, Big Injun	*
-	C	Acid and Frac	BMS	
14	C	Acid and Frac	BMS	*
-	C	Acid and Frac	BMS	
-	E	Acid and Frac	BMS	
-	C	Acid and Frac	BMS	*
-	E	Acid and Frac	BMS, Big Injun	
-	C	Acid and Frac	BMS	*
13	B	Acid and Frac	BMS, Big Injun	*
-	C	Acid and Frac	BMS, Big Injun	*
-	C	Acid and Frac	BMS	*
15	B	Acid and Frac	BMS	*
10	C	Acid and Frac	BMS	*
16	C	Acid and Frac	BMS	
20	C	Acid and Frac	BMS, Big Injun	*
18	F	Acid and Frac	BMS, Big Lime, Big Injun	
18	C	Shot Plus	BMS, Big Lime	*
12	C	Frac	BMS, Big Lime	
20	E	Acid and Frac	BMS, Big Injun	
14	C	Frac	Maxton, BMS, Big Lime	*
7	C	Frac	BMS, Big Lime	*
10	E	Frac	Maxton, BMS	

API	CNTYNM	PRMT	Lat	Long	UTME	UTMN	Elevation
4700700507	Braxton	507	38.757849	-80.849274	513096.3	4289708.8	1175
4700700537	Braxton	537	38.675371	-81.010012	499129.1	4280545.9	1067
4700700555	Braxton	555	38.875737	-80.688206	527046.7	4302825.7	1165
4700700565	Braxton	565	38.679644	-81.01748	498479.5	4281020.2	1230
4700700852	Braxton	852	38.771868	-80.828422	514905.2	4291267.5	1297
4700700934	Braxton	934	38.824317	-80.634903	531693.3	4297136.9	1110
4700701104	Braxton	1104	38.81461	-80.813207	516217.3	4296013	986
4700701134	Braxton	1134	38.792238	-80.638418	531402.3	4293576	904
4700701135	Braxton	1135	38.56873	-80.737929	522830.9	4268745.4	1080
4700701140	Braxton	1140	38.777859	-80.636655	531561.7	4291981	1037
4700701145	Braxton	1145	38.771293	-80.63751	531490.3	4291252.1	940
4700701238	Braxton	1238	38.741203	-80.663007	529287.6	4287904.7	946
4700701441	Braxton	1441	38.761603	-80.757155	521099.3	4290142.5	930
4700701511	Braxton	1511	38.735095	-80.621409	532905.6	4287241.1	1269
4700701643	Braxton	1643	38.855651	-80.693218	526619.4	4300595.3	964
4700701728	Braxton	1728	38.760063	-80.764689	520445.2	4289969.9	1211
4700701729	Braxton	1729	38.754889	-80.75925	520919.3	4289397	1131
4700701946	Braxton	1946	38.727939	-80.762397	520653.5	4286405.8	1068
4700701992	Braxton	1992	38.759301	-80.62741	532373.2	4289924.9	1017
4700701996	Braxton	1996	38.762494	-80.621146	532915.9	4290281.5	1027
4700702062	Braxton	2062	38.78978	-80.627966	532311.1	4293306.9	1195
4700702068	Braxton	2068	38.748694	-80.753701	521403.3	4288710.8	1350
4700702077	Braxton	2077	38.740131	-80.752776	521486.3	4287760.9	1075
4700702079	Braxton	2079	38.749274	-80.735718	522965.8	4288779.6	1370
4700702081	Braxton	2081	38.538764	-80.852728	512835.2	4265398.1	1372
4700702087	Braxton	2087	38.572012	-80.852359	512861.5	4269087.4	1109
4700702095	Braxton	2095	38.565191	-80.823068	515414.6	4268335	1374
4700702101	Braxton	2101	38.537893	-80.873231	511048.5	4265298.8	1266
4700702105	Braxton	2105	38.557499	-80.813832	516220.9	4267483	1027
4700702106	Braxton	2106	38.548935	-80.874524	510934.1	4266523.9	1238
4700702107	Braxton	2107	38.782523	-80.629634	532169.5	4292501	902
4700702111	Braxton	2111	38.730987	-80.767208	520234.5	4286742.9	1021
API	CNTYNM	PRMT	Lat	Long	UTME	UTMN	Elevation
4706700224	Nicholas	224	38.329307	-80.742306	522529.7	4240093.8	2165
4706700278	Nicholas	278	38.335452	-80.796996	517743.7	4242166.4	1986
4706700283	Nicholas	283	38.25406	-80.760552	520927.3	4242855.8	1979
4706700372	Nicholas	372	38.335812	-80.976303	502073.3	4234426.9	1387
4706700389	Nicholas	389	38.311708	-81.041417	496380.2	4242869.5	1205
4706700398	Nicholas	398	38.283105	-81.037552	496717	4240194.8	1467
4706700451	Nicholas	451	38.276137	-81.107538	490594.6	4237026	1032
4706700523	Nicholas	523	38.269793	-81.110945	490295.7	4236253.2	1499
4706700526	Nicholas	526	38.234906	-81.114542	489980.3	4235549.7	1110
4706700789	Nicholas	789	38.225326	-81.039876	496510.1	4231673.3	1283
4706700791	Nicholas	791	38.232583	-81.050487	495580.8	4230610.9	1237
4706700815	Nicholas	815	38.232583	-81.025175	497796.6	4231415.2	1259

Total Depth	Log Types	LL Top	LL Base	LL Thickness	BMS Top	BMS Base
2266	a/tgn	2008	2042	34	2043	2062
2142	d/g/i	1858	1921	63	1922	1934
2260	a/gcd/go/t	1930	1966	36	1967	1982
2077	do/tg	1811	1845	34	1846	1876
2390	gp/o	2099	2128	29	2129	2144
2118	gcd/i	1770	1800	30	1801	1817
2211	gdc/gnt	1811	1837	26	1838	1860
2730	bgpo/dgc/gcd/i/t1/tz	1543	1574	31	1575	1609
1893	a/dgc/iz	1454	1499	45	1500	1551
2403	gctd/i	1600	1632	32	1633	1668
2400	dgct/i	1543	1597	54	1598	1612
4701	gdc_a/gpo1/gpo2/izl/po	1566	1614	48	1615	1634
5272	dgct	1732	1754	22	1755	1774
4700	dgc/gdct/gn/i	1790	1830	40	1831	1858
2020	gcdn	1710	1750	40	1751	1765
5610	gdte	2012	2040	28	2041	2056
5556	gdte	1920	1952	32	1953	1967
5454	dingc	1829	1872	43	1873	1889
3300	dinigtc	1580	1630	50	1631	1650
3300	gdnitco	1598	1619	21	1620	1630
4050	gdintco	1742	1772	30	1773	1808
2554	gdintc1/gdintc2	2145	2174	29	2175	2189
2799	gdintc	1818	1849	31	1850	1861
2582	gcidn	2162	2187	25	2188	2220
Unknown	dnilgco	1898	1941	43	1942	1957
Unknown	dntgco	1714	1756	42	1757	1774
2508	iglo	1940	1968	28	1969	1994
2450	igo	1850	1877	27	1878	1900
2103	iglo	1538	1565	27	1566	1584
2445	gi	1840	1863	23	1864	1888
3937	gdintco	1557	1600	43	1601	1625
2809	gdintc	1770	1823	53	1824	1836
Total Depth	Log Types	LL Top	LL Base	LL Thickness	BMS Top	BMS Base
2240	gr/i/grd/hsqp/i	1760	1830	70	1831	1870
2171	d/i/fd/i/dgr	1700	1767	67	1768	1788
2060	/-d.gr/-dl,sp/-l/- n,gr/dil/fd/n	1671	1725	54	1726	1780
1865	d/i	1396	1448	52	1449	1486
2168	d/i	1680	1719	39	1720	1750
2351	d/i	1922	1978	56	1979	1998
2010	cf/i	1600	1648	48	1649	1703
2600	bcgf/cd/i/rt	2100	2149	49	2150	2186
2250	bcgr/cd/gr/i	1700	1741	41	1742	1749
2051	cdendi	1529	1579	50	1580	1605
1921	sdgenthri	1390	1437	47	1438	1460
2000	sdendi	1472	1517	45	1518	1538

BMS Thickness	PC Top	PC Base	PC Thickness	BL Top	BL Base	BL Thickness	Cross-Section Line #
19	2063	2068	5	2069	2240	171	15
12	1935	1944	9	1945	2114	169	15
15	1983	1994	11	1995	2192	197	15
30	1877	1884	7	1885	2059	174	15
15	2145	2155	10	2156	2354	198	15
16	1818	1832	14	1833	2025	192	16
22	1861	1876	15	1877	2048	171	15
34	0	0	0	1610	1804	194	16
51	0	0	0	1552	1772	220	12
35	0	0	0	1669	1870	201	16
14	0	0	0	1613	1804	191	16
19	0	0	0	1635	1833	198	16
19	1775	1790	15	1791	2000	209	17
27	0	0	0	1859	2066	207	16
14	1766	1773	7	1774	1966	192	15, 19
15	2057	2069	12	2070	2279	209	17
14	1968	1998	30	1999	2202	203	17
16	1890	1896	6	1897	2074	177	17
19	0	0	0	1651	1834	183	16
10	1631	1672	41	1673	1864	191	16
35	0	0	0	1809	2007	198	16
14	2190	2206	16	2207	2391	184	17
11	1862	1879	17	1880	-	-	17
32	2221	2235	14	2236	2450	214	17
15	1958	1985	27	1986	2192	206	12
17	1775	1793	18	1794	2016	222	17
25	1995	2022	27	2023	2220	197	10
22	1901	1931	30	1932	2134	202	12
18	1585	1608	23	1609	1820	211	12
24	1889	1919	30	1920	2126	206	10
24	0	0	0	1626	1830	204	16
12	0	0	0	1837	2050	213	17
BMS Thickness	PC Top	PC Base	PC Thickness	BL Top	BL Base	BL Thickness	Cross-Section Line #
39	1871	1895	24	1896	2200	304	3, 4
20	1789	1822	33	1823	2100	277	4
54	1781	1795	14	1796	2050	254	4
37	1487	1505	18	1506	1764	258	3
30	1751	1772	21	1773	1994	221	2
19	1999	2015	16	2016	2250	234	2
54	0	0	0	1704	1922	218	1
36	2187	2195	8	2196	2410	214	1
7	1750	1787	37	1788	2002	214	1
25	1606	1631	25	1632	1890	258	2
22	1461	1493	32	1494	1734	240	2
20	1539	1574	35	1575	1801	226	2

Well Log Porosity (%)	Type of Curve	Completion method	Producing Strata	Available Production Data
-	E	Frac	BMS	
-	E	Frac	Salt Sands, BMS, Big Injun	*
-	C	Frac	Mauch Chunk, BMS, Big Injun, Squaw, Big Injun	
-	B	Frac	Salt Sands, BMS, Big Lime, Big Injun	*
-	E	Frac	Mauch Chunk, BMS, Big Injun	
-	E	Frac	BMS	
-	C	Acid and Frac	BMS, Big Injun, Squaw	*
-	C	Frac	BMS, Big Injun, Gordon	
13	C	Frac	BMS, Big Injun, Squaw	
-	C	Frac	BMS, Fifth	
-	C	Frac	BMS, Big Injun, Fifth	*
12	B	Acid and Frac	BMS, Benson	
-	E	Frac	BMS, Big Injun, Fifth, Benson	
-	C	Acid and Frac	BMS	
6	B	Frac	BMS, Keener, Big Injun, Squaw	
-	B	Frac	BMS, Benson	*
-	E	Frac	BMS, Benson	
6	C	Frac	Maxton, BMS	*
13	B	Acid and Frac	BMS, Big Injun, Gordon	
6	E	Acid and Frac	BMS, Big Injun, Gordon	
16	C	Frac	BMS, Balltown	
10	F	Frac	Maxton, BMS, Big Injun	*
8	F	Frac	Salt Sands, Maxton, BMS, Fifth	*
14	E	Acid and Frac	Maxton, BMS, Squaw	*
9	F	Unknown	BMS, Big Lime, Weir	
17	C	Unknown	BMS, Big Lime, Weir	
-	C	Frac	BMS, Weir	
-	E	Frac	BMS, Big Lime	
-	E	Frac	BMS, Big Lime, Weir	
-	E	Frac	BMS, Big Lime	
14	C	Acid and Frac	BMS, Gordon, Balltown	
6	C	Frac	Maxton, BMS, Fifth	*
Well Log Porosity (%)	Type of Curve	Completion method	Producing Strata	Available Production Data
-	C	Acid and Frac	BMS, Big Lime	
-	C	Nat/Open H	BMS	
-	B	Acid and Frac	BMS, Big Lime	
13	C	Acid and Frac	BMS, Big Lime	
13	E	Acid and Frac	BMS	
16	F	Acid and Frac	BMS, Big Lime	
5	C	Acid and Frac	BMS, Big Lime, Big Injun	
-	C	Acid and Frac	Maxton, BMS, Big Injun	
-	F	Acid and Frac	BMS, Big Injun	
11	F	Acid and Frac	BMS, Big Lime	
9	F	Acid and Frac	BMS, Weir	
20	C	Acid and Frac	BMS, Big Lime	

NON-PRODUCING WELLS

API	CNTYNM	PRMT	UTME	UTMN	Elevation	Total Depth	LL Top	LL Base
4701500024	Clay	24	485899.2	4264619.5	986	1880	1664	1702
4701500062	Clay	62	481155.6	4253983.4	950	1899	1630	1670
4701500102	Clay	102	485804	4265520.8	1286	2294	1954	1988
4701500118	Clay	118	488236.2	4266308.1	823	1861	1572	1597
4701500193	Clay	193	504017.7	4268734.4	774	1735	1348	1408
4701500395	Clay	395	486654.3	4263635.9	975	1900	1676	1727
4701500552	Clay	552	488858.8	4257244.5	1176	1964	1700	1754
4701500563	Clay	563	495713.1	4247078.3	993	2203	1540	1579
4701500680	Clay	680	486114.3	4252469.4	991	1922	1674	1717
4701500764	Clay	764	489012	4268561.6	843	1884	1626	1650
4701500774	Clay	774	488124.6	4267016.892	923	1981	1680	1721
4701500826	Clay	826	479606.4	4254698.4	958	1797	1580	1618
4701500884	Clay	884	500857.1	4256394	1173	2100	1758	1792
4701500932	Clay	932	484968.3	4262543.7	1176	2028	1812	1849
4701500993	Clay	993	484899.4	4239121.9	1278	2532	2159	2203
4701500999	Clay	999	484454.2	4240507.5	1362	2620	2262	2299
4701501006	Clay	1006	486730.4	4243115.9	1142	2280	1920	1971
4701501018	Clay	1018	482970.9	4242402.7	1080	2265	1894	1932
4701501026	Clay	1026	499302	4262970.8	1105	2091	1784	1822
4701501054	Clay	1054	484301.8	4259035.5	944	1930	1622	1675
4701501056	Clay	1056	486141.1	4244861.3	1442	2635	2242	2285
4701501137	Clay	1137	495874	4251053.7	1377	2380	2036	2069
4701501246	Clay	1246	488954.1	4260656.4	1201	2197	1770	1805
4701501266	Clay	1266	492908.3	4259815.8	1152	2249	1866	1897
4701501274	Clay	1274	488675.7	4249294.9	1028	2256	1683	1720
4701501309	Clay	1309	486708.3	4267131.8	1062	2083	1753	1799
4701501338	Clay	1338	487393.1	4261528.1	907	1775	1514	1569
4701501613	Clay	1613	489361.4	4253308.7	1268	2348	2016	2051
4701501802	Clay	1802	493155.6	4244589.2	1303	2338	1904	1947
4701501842	Clay	1842	487011.2	4265245.7	1361	2281	1987	2039
4701501915	Clay	1915	498280	4270123.7	875	6413	1527	1555
4701502046	Clay	2046	498524.1	4267794.6	1064	2173	1773	1821
4701502124	Clay	2124	485657.2	4264314	1029	2060	1750	1779
4701502166	Clay	2166	479460.1	4250878.1	1236	2330	1866	1914
4701502258	Clay	2258	494773.3	4263676.4	1279	2240	1879	1910
4701502275	Clay	2275	504231.3	4253351.2	1081	1960	1610	1672
4701502312	Clay	2312	504297.9	4250836.3	1550	2362	1540	1579
4701502359	Clay	2359	479176.3	4239700.2	1173	4983	2043	2078
4701502449	Clay	2449	480562.8	4247993.6	1330	5314	2012	2056
4701502672	Clay	2672	482564.9	4250354.8	1328	4907	1940	1989
4701502691	Clay	2691	482825.6	4261129.7	983	5000	1571	1613

LL Thickness	BMS Top	BMS Base	BMS Thickness	PC Top	PC Base	PC Thickness	BL Top	BL Base	BL Thickness	Type of Curve
38	1703	1714	11	1715	1724	9	1725	1830	105	E
40	1671	1680	9	1681	1687	6	1688	1810	122	E
34	1989	1997	8	1998	2009	11	2010	2120	110	E
25	1598	1625	27	1626	1636	10	1637	1758	121	C
60	1409	1415	6	1416	1425	9	1426	1677	251	E
51	1728	1743	15	1744	1751	7	1752	1900	148	C
54	1755	1764	9	1765	1787	22	1788	1926	138	E
39	1580	1610	30	1611	1628	17	1629	1825	196	E
43	1718	1726	8	1727	1742	15	1743	1899	156	E
24	1651	1673	22	1674	1691	17	1692	1848	156	C
41	1722	1731	9	1732	1744	12	1745	1869	124	E
38	1619	1630	11	1631	1640	9	1641	1766	125	E
34	1793	1814	21	1815	1843	28	1844	2048	204	C
37	0	0	0	1850	1871	21	1872	1993	121	-
44	2204	2218	14	2219	2243	24	2244	2426	182	E
37	2300	2339	39	2340	2349	9	2350	2500	150	E
51	0	0	0	1972	1999	27	2000	2192	192	-
38	1933	1950	17	1949	1968	19	1969	2150	181	C
38	1823	1850	27	1851	1876	25	1877	2061	184	E
53	0	0	0	1676	1690	14	1691	1828	137	-
43	2286	2297	11	2298	2315	17	2316	2503	187	F
33	2070	2084	14	2085	2115	30	2116	2322	206	E
35	1806	1823	17	1824	1834	10	1835	1958	123	E
31	1898	1920	22	1921	1946	25	1947	2130	183	E
37	1721	1734	13	1735	1751	16	1752	1936	184	E
46	1800	1815	15	1816	1853	37	1854	1952	98	E
55	1570	1580	10	1581	1584	3	1585	1708	123	B
35	2052	2066	14	2067	2090	23	2091	2250	159	E
43	1948	1965	17	1966	1987	21	1988	2202	214	E
52	2040	2056	16	2057	2065	8	2066	2178	112	C
28	1556	1565	9	1566	1595	29	1596	1768	172	E
48	1822	1841	19	1842	1849	7	1850	2049	199	C
29	1780	1791	11	1792	1799	7	1800	1906	106	E
48	0	0	0	1915	1943	28	1944	2075	131	-
31	1911	1930	19	1931	1956	25	1957	2148	191	E
62	1673	1682	9	1683	1698	15	1699	1902	203	E
39	1580	1609	29	1610	1628	18	1629	1825	196	E
35	2079	2090	11	2091	2126	35	2127	2251	124	E
44	0	0	0	2057	2080	23	2081	2230	149	-
49	1990	2010	20	2011	2019	8	2020	2194	174	C
42	1614	1617	3	1618	1628	10	1629	1775	146	E

API	CNTYNM	PRMT	UTME	UTMN	Elevation	Total Depth	LL Top
4706700103	Nicholas	103	501018.3	4238302.8	1374	1920	1636
4706700104	Nicholas	104	502985.2	4239612.5	1401	1859	1600
4706700105	Nicholas	105	499380.6	4234058.5	1328	2160	1565
4706700129	Nicholas	129	517694.7	4241337.2	1923	7208	1596
4706700203	Nicholas	203	518046.3	4250966.7	1879	7272	1560
4706700206	Nicholas	206	498050.5	4236624.2	1270	1803	1568
4706700220	Nicholas	220	522136.1	4237781	2032	3197	1833
4706700243	Nicholas	243	518440.6	4263093	1331	2485	1770
4706700253	Nicholas	253	519341.1	4262973.5	1082	1775	1376
4706700280	Nicholas	280	518004.9	4243551.6	2034	2200	1808
4706700286	Nicholas	286	483159	4234965.9	1256	2809	1968
4706700289	Nicholas	289	524702.8	4244049.8	2157	2341	1879
4706700291	Nicholas	291	516420.3	4243307.4	1914	2088	1628
4706700293	Nicholas	293	507101.2	4232040.3	1584	7642	1607
4706700295	Nicholas	295	503930.9	4247996.9	1343	2279	1762
4706700296	Nicholas	296	518324.9	4246977.9	1904	2421	1684
4706700297	Nicholas	297	516943.2	4241728.2	2003	2134	1640
4706700298	Nicholas	298	516430.4	4241386.9	2007	2109	1633
4706700299	Nicholas	299	516154	4242176.8	2051	2251	1768
4706700300	Nicholas	300	515840.5	4242827.7	2006	2205	1728
4706700310	Nicholas	310	526213.5	4240013.3	2257	2593	1850
4706700355	Nicholas	355	483801.4	4233820.3	1354	2455	2053
4706700375	Nicholas	375	514296.6	4253317	1424	2500	1711
4706700383	Nicholas	383	484175.7	4237028.1	1154	2356	1940
4706700393	Nicholas	393	537119.5	4241610.2	2751	2711	1934
4706700396	Nicholas	396	506393	4227009.6	1829	2323	1756
4706700402	Nicholas	402	521913.1	4242000.9	2045	2320	1740
4706700403	Nicholas	403	516269.2	4242763.3	2020	2382	1754
4706700476	Nicholas	476	520433.2	4243704	2045	2200	1758
4706700538	Nicholas	538	498631.2	4242731.4	1129	2000	1586
4706700558	Nicholas	558	487856.6	4235059.4	1667	2812	2378
4706700579	Nicholas	579	484296.6	4234111.6	1705	2831	2429
4706700583	Nicholas	583	525364.6	4244328.2	2320	2652	1970
4706700653	Nicholas	653	502823.2	4236129.3	1695	6713	1770
4706700656	Nicholas	656	493921.6	4229737.5	1426	6388	1464
API	CNTYNM	PRMT	UTME	UTMN	Elevation	Total Depth	LL Top
4710100065	Webster	65	560342.6	4260486.3	2334	7474	720
4710100076	Webster	76	539849.3	4268687.6	1650	5676	1302
4710100097	Webster	97	549976.4	4274897.1	1594	6850	1162
4710100102	Webster	102	540663.2	4271625.4	1215	6740	918
4710100109	Webster	109	550810.5	4273872.4	1028	3770	708
4710100114	Webster	114	557118.9	4274880.8	1396	4322	1615

LL Base	LL Thickness	BMS Top	BMS Base	BMS Thickness	PC Top	PC Base	PC Thickness	BL Top	BL Base	BL Thickness	Type of Curve
1682	46	1683	1718	35	1719	1730	11	1731	1896	165	C
1647	47	1648	1690	42	1691	1706	15	1707	1851	144	C
1621	56	1622	1641	19	1642	1658	16	1659	1851	192	F
1684	88	1685	1709	24	1710	1745	35	1746	2058	312	E
1634	74	1635	1651	16	1652	1670	18	1671	1911	240	B
1619	51	1620	1629	9	1630	1669	39	1670	1812	142	B
1876	43	1877	1918	41	1919	1942	23	1943	2123	180	C
1800	30	1801	1818	17	1819	1830	11	1831	1984	153	C
1437	61	1438	1473	35	1474	1480	6	1481	1680	199	C
1838	30	1839	1858	19	1859	1870	11	1871	2142	271	C
2021	53	2022	2037	15	2038	2057	19	2058	2242	184	F
1939	60	1940	1983	43	1984	1999	15	2000	2196	196	C
1693	65	1694	1713	19	1714	1757	43	1758	2016	258	C
1659	52	1660	1681	21	1682	1711	29	1712	1873	161	C
1799	37	1800	1829	29	1830	1859	29	1860	1995	135	E
1732	48	1733	1754	21	1755	1794	39	1795	1990	195	E
1694	54	1695	1739	44	1740	1768	28	1769	2036	267	C
1682	49	1683	1734	51	1735	1750	15	1751	2022	271	B
1826	58	1827	1867	40	1868	1886	18	1887	2170	283	C
1768	40	1769	1806	37	1807	1844	37	1845	2141	296	C
1909	59	1910	1963	53	1964	1979	15	1980	2297	317	C
2094	41	2095	2113	18	2114	2136	22	2137	2325	188	C
1757	46	1758	1772	14	1773	1805	32	1806	2060	254	E
1979	39	1980	2006	26	2007	2026	19	2027	2234	207	E
1987	53	1988	2039	51	2040	2057	17	2058	2241	183	E
1804	48	1805	1821	16	1822	1869	47	1870	2044	174	E
1810	70	1811	1839	28	1840	1868	28	1869	2092	223	C
1816	62	1817	1852	35	1853	1869	16	1870	2150	280	C
1806	48	1807	1874	67	1875	1882	7	1883	2158	275	B
1629	43	1630	1652	22	1653	1680	27	1681	1900	219	C
2419	41	2420	2430	10	2431	2459	28	2460	2700	240	E
2465	36	2466	2485	19	2486	2509	23	2510	2702	192	C
2084	114	2085	2107	22	2108	2144	36	2145	2444	299	C
1816	46	1817	1842	25	1843	1862	19	1863	2067	204	E
1525	61	1526	1535	9	1536	1551	15	1552	1802	250	E
LL Base	LL Thickness	BMS Top	BMS Base	BMS Thickness	PC Top	PC Base	PC Thickness	BL Top	BL Base	BL Thickness	Type of Curve
787	67	788	812	24	0	0	0	813	1036	223	C
1360	58	1361	1398	37	1399	1410	11	1411	1644	233	E
1209	47	1210	1230	20	1231	1261	30	1262	1510	248	E
964	46	965	974	9	975	981	6	982	1210	228	E
754	46	755	789	34	790	803	13	804	1022	218	E
1634	19	1635	1654	19	1655	1674	19	1675	1918	243	E

API	CNTYNM	PRMT	UTME	UTMN	Elevation	Total Depth	LL Top	LL Base
4701900045	Fayette	45	488269.3	4228067.6	958	2326	1413	1512
4701900200	Fayette	200	470312.3	4218192.2	1864	3206	2651	2700
4701900261	Fayette	261	479651.7	4230705.3	1484	2656	2208	2268
4701900323	Fayette	323	481898.6	4220989.8	1358	2604	1856	1901
4701900448	Fayette	448	471376.8	4223456.8	819	2892	1675	1725
4701900554	Fayette	554	493867.6	4216463.9	1765	2545	1900	1952
API	CNTYNM	PRMT	UTME	UTMN	Elevation	Total Depth	LL Top	LL Base
4701302064	Calhoun	2064	495365.9	4279606.3	905	1921	1666	1695
4701302082	Calhoun	2082	500594.6	4285985.4	1016	2016	1791	1819
4701302235	Calhoun	2235	499959.9	4284836.5	925	1970	1710	1733
4701302500	Calhoun	2500	498763.6	4287238.1	943	2050	1757	1781
4701302930	Calhoun	2930	495232.6	4281662.3	1140	2060	1798	1816
4701302961	Calhoun	2961	496892.6	4283031.6	1030	2035	1720	1743
4701303432	Calhoun	3432	492322.5	4277531.6	1341	2305	2008	2053
API	CNTYNM	PRMT	UTME	UTMN	Elevation	Total Depth	LL Top	LL Base
4702100446	Gilmer	446	507706.4	4291135.3	1183	2290	1900	1932
4702100625	Gilmer	625	504219.6	4290231.2	771	2043	1763	1800
4702100671	Gilmer	671	502914.2	4289591.6	1215	2593	2287	2310
4702101679	Gilmer	1679	519093	4301691.1	1193	2305	1809	1861
4702101841	Gilmer	1841	527341.7	4307468.4	1015	2387	2093	2133
4702101949	Gilmer	1949	520462.2	4300472.1	1175	2548	2159	2182
4702102287	Gilmer	2287	522496.7	4302580	941	2170	1786	1821
4702102786	Gilmer	2786	507986.5	4290612.2	1213	2390	2050	2079
4702102789	Gilmer	2789	505178	4291566	947	2040	1783	1807
4702103492	Gilmer	3492	508715.3	4295998.3	815	2626	1925	1948
4702103800	Gilmer	3800	524951.4	4303104.9	1025	5100	1946	1962
4702103820	Gilmer	3820	530690.1	4307845.3	1381	5772	2258	2290
4702104075	Gilmer	4075	525742.6	4304650	1246	5613	2132	2168
4702104117	Gilmer	4117	526093.2	4304251.1	1141	5511	1992	2031
4702104798	Gilmer	4798	509551.5	4293304	979	2876	1808	1828
API	CNTYNM	PRMT	UTME	UTMN	Elevation	Total Depth	LL Top	LL Base
4703900136	Kanawha	136	473718.9	4232722.7	1042	2308	1854	1920
4703901781	Kanawha	1781	471533.4	4249163	1214	2234	1774	1811
4703901803	Kanawha	1803	471196	4246856.4	1263	2325	1801	1836
4703901832	Kanawha	1832	467994.6	4237326.2	1137	2230	1742	1792
4703901948	Kanawha	1948	468998.7	4242923.6	1193	2225	1738	1803
4703902066	Kanawha	2066	470398.5	4252484.2	787	1812	1416	1452
4703902611	Kanawha	2611	470612.6	4256087.7	962	5036	1450	1537
4703904778	Kanawha	4778	474443.6	4263618.7	850	1959	1466	1519
4703905499	Kanawha	5499	475352.6	4262296.2	1074	4915	1631	1669

LL Thickness	BMS Top	BMS Base	BMS Thickness	PC Top	PC Base	PC Thickness	BL Top	BL Base	BL Thickness	Type of Curve
99	1513	1542	29	1543	1549	6	1550	1772	222	B
49	2701	2712	11	2713	2735	22	2736	2989	253	E
60	2269	2284	15	2285	2291	6	2292	2512	220	F
45	1902	1906	4	1907	1953	46	1954	2218	264	E
50	1726	1733	7	1734	1758	24	1759	1984	225	B
52	1953	1976	23	1977	2020	43	2021	2332	311	B
LL Thickness	BMS Top	BMS Base	BMS Thickness	PC Top	PC Base	PC Thickness	BL Top	BL Base	BL Thickness	Type of Curve
29	1696	1711	15	1712	1728	16	1729	1880	151	F
28	1820	1832	12	1833	1849	16	1850	1992	142	E
23	1734	1744	10	1745	1765	20	1766	1938	172	B
24	1782	1798	16	1799	1812	13	1813	2004	191	F
18	1817	1825	8	1826	1853	27	1854	2026	172	E
23	1744	1779	35	0	0	0	1780	1959	179	C
45	2054	2079	25	2080	2093	13	2094	2252	158	B
LL Thickness	BMS Top	BMS Base	BMS Thickness	PC Top	PC Base	PC Thickness	BL Top	BL Base	BL Thickness	Type of Curve
32	1933	1970	37	1971	2000	29	2001	2219	218	C
37	1801	1817	16	1818	1831	13	1832	2000	168	E
23	2311	2324	13	2325	2339	14	2340	2470	130	F
52	1862	1879	17	1880	1904	24	1905	2032	127	B
40	2134	2173	39	2174	2216	42	2217	2349	132	E
23	2183	2199	16	2200	2215	15	2216	2414	198	E
35	1822	1836	14	1837	1846	9	1847	2038	191	E
29	2080	2109	29	2110	2115	5	2116	2290	174	E
24	1808	1817	9	1818	1829	11	1830	2002	172	E
23	1947	1961	14	1962	1977	15	1978	2147	169	E
16	1963	1985	22	1986	2003	17	2004	2194	190	E
32	0	0	0	2291	2317	26	2318	2503	185	-
36	2169	2199	30	0	0	0	2200	2390	190	C
39	2032	2076	44	2077	2101	24	2102	2246	144	E
20	1829	1844	15	1845	1857	12	1858	2030	172	E
LL Thickness	BMS Top	BMS Base	BMS Thickness	PC Top	PC Base	PC Thickness	BL Top	BL Base	BL Thickness	Type of Curve
66	1921	1954	33	1955	1960	5	1961	2138	177	C
37	1812	1854	42	1855	1888	33	1889	2009	120	C
35	0	0	0	1837	1843	6	1844	2059	215	-
50	1793	1813	20	1814	1820	6	1821	1995	174	B
65	1804	1813	9	1814	1861	47	1862	1992	130	B
36	1453	1467	14	1468	1475	7	1476	1613	137	C
87	1538	1561	23	1562	1570	8	1571	1663	92	C
53	1520	1538	18	1539	1567	28	1568	1662	94	F
38	0	0	0	1670	1685	15	1686	1797	111	-

API	CNTYNM	PRMT	UTME	UTMN	Elevation	Total Depth	LL Top
4704101509	Lewis	1509	551121	4292031.2	1070	7838	860
4704101546	Lewis	1546	540268.7	4307114.5	1247	2672	2008
4704101806	Lewis	1806	538327.7	4305735.7	1240	2249	1896
4704101969	Lewis	1969	549811.8	4297084.1	1452	4240	1411
4704102022	Lewis	2022	541027.6	4305120.2	996	4600	1702
4704102932	Lewis	2932	549255.3	4299625.3	1195	4510	1315
4704103030	Lewis	3030	534523.9	4309035.5	924	4781	1755
4704103722	Lewis	3722	536693	4304373.9	1062	3792	1714
4704103747	Lewis	3747	536641.4	4305049.5	1112	3633	1686
4704103796	Lewis	3796	551785.5	4296047.7	1657	4392	1490
API	CNTYNM	PRMT	UTME	UTMN	Elevation	Total Depth	LL Top
4708300482	Randolph	482	567331.8	4281527.7	2760	5583	1480
4708300831	Randolph	831	567513.1	4279280.1	2820	4150	1465
4708300855	Randolph	855	566623.9	4279739.3	2790	4109	1466
4708300867	Randolph	867	567325.2	4284256.4	2642	4251	1416
4708300872	Randolph	872	565324.7	4284807.8	2670	4405	1566
4708300943	Randolph	943	564749.5	4280147	2925	4478	1643
API	CNTYNM	PRMT	UTME	UTMN	Elevation	Total Depth	LL Top
4708700714	Roane	714	476229.7	4265512	666	7158	1160
4708701003	Roane	1003	486719.4	4273784.3	767	1637	1378
4708701131	Roane	1131	479259.3	4269337.7	868	1925	1564
4708701217	Roane	1217	485731.9	4270177.2	794	1670	1420
4708701223	Roane	1223	485570.1	4269662.1	832	1703	1422
4708703200	Roane	3200	485556.9	4271241.7	1137	2085	1775
4708703222	Roane	3222	492019.1	4274876	992	2130	1814
4708703402	Roane	3402	487183.1	4272156.9	890	1980	1646
API	CNTYNM	PRMT	UTME	UTMN	Elevation	Total Depth	LL Top
4709701649	Upshur	1649	557645.5	4290965.5	1834	4525	1298
4708702514	Upshur	2514	557856.1	4286167.4	1845	4162	1451
4708702522	Upshur	2522	562185.1	4284586.1	2655	4530	1311
4709702601	Upshur	2601	558677	4288570.2	1970	4201	1260
4709702707	Upshur	2707	560861.2	4287089.9	2125	4219	1602
4708702745	Upshur	2745	561459.8	4288768.3	2320	4250	1566
4708702758	Upshur	2758	557040.5	4290059.8	2125	4369	1644
4708702771	Upshur	2771	556251.8	4290070.3	1805	4046	1280
API	CNTYNM	PRMT	UTME	UTMN	Elevation	Total Depth	LL Top
4702500021	Greenbrier	21	532786.5	4201999.2	2875	3392	1527
4702500022	Greenbrier	22	523398.3	4212516.4	3462	10128	2750
4702500023	Greenbrier	23	542942	4225387.5	3343	4286	1570

LL	LL	BMS	BMS	BMS	PC	PC	PC	BL	BL	BL	Type of
Base	Thickness	Top	Base	Thickness	Top	Base	Thickness	Top	Base	Thickness	Curve
913	53	914	939	25	940	959	19	960	1080	120	B
2053	45	0	0	0	2054	2062	8	2063	2242	179	-
1943	47	0	0	0	1944	1949	5	1950	2125	175	-
1431	20	1432	1455	23	1456	1480	24	1481	1692	211	E
1777	75	0	0	0	1778	1789	11	1790	1963	173	-
1367	52	1368	1400	32	0	0	0	1401	1598	197	C
1801	46	1802	1810	8	1811	1829	18	1830	2022	192	E
1752	38	0	0	0	1753	1763	10	1764	1952	188	-
1743	57	1744	1775	31	1776	1785	9	1786	1990	204	C
1510	20	1511	1521	10	1522	1549	27	1550	1753	203	E
LL	LL	BMS	BMS	BMS	PC	PC	PC	BL	BL	BL	Type of
Base	Thickness	Top	Base	Thickness	Top	Base	Thickness	Top	Base	Thickness	Curve
1551	71	1552	1579	27	1580	1593	13	1594	1834	240	C
1521	56	1522	1567	45	1568	1583	15	1584	1834	250	C
1530	64	1531	1569	38	0	0	0	1570	1826	256	C
1466	50	1467	1530	63	1531	1546	15	1547	1775	228	C
1615	49	1616	1645	29	1646	1651	5	1652	1911	259	B
1673	30	1674	1714	40	1715	1730	15	1731	1980	249	C
LL	LL	BMS	BMS	BMS	PC	PC	PC	BL	BL	BL	Type of
Base	Thickness	Top	Base	Thickness	Top	Base	Thickness	Top	Base	Thickness	Curve
1218	58	1219	1275	56	0	0	0	1276	1430	154	C
1407	29	1408	1422	14	1423	1440	17	1441	1566	125	F
1574	10	1575	1597	22	1598	1617	19	1618	1752	134	C
1447	27	1448	1461	13	1462	1479	17	1480	1580	100	E
1449	27	1450	1463	13	1464	1485	21	1486	1585	99	E
1804	29	1805	1824	19	1825	1834	9	1835	1937	102	C
1843	29	1844	1850	6	1851	1874	23	1875	2054	179	E
1682	36	1683	1693	10	1694	1699	5	1700	1838	138	E
LL	LL	BMS	BMS	BMS	PC	PC	PC	BL	BL	BL	Type of
Base	Thickness	Top	Base	Thickness	Top	Base	Thickness	Top	Base	Thickness	Curve
1355	57	1356	1409	53	0	0	0	1410	1610	200	C
1480	29	1481	1512	31	1513	1529	16	1530	1743	213	E
1330	19	1331	1368	37	1369	1376	7	1377	1611	234	C
1319	59	1320	1343	23	1344	1349	5	1350	1560	210	B
1650	48	1651	1704	53	1705	1712	7	1713	1946	233	C
1616	50	1617	1659	42	1660	1728	68	1729	1919	190	C
1678	34	1679	1692	13	0	0	0	1693	1878	185	B
1338	58	1339	1379	40	1380	1384	4	1385	1670	285	C
LL	LL	BMS	BMS	BMS	PC	PC	PC	BL	BL	BL	Type of
Base	Thickness	Top	Base	Thickness	Top	Base	Thickness	Top	Base	Thickness	Curve
1583	56	1584	1598	14	1599	1686	87	1687	2300	613	E
2779	29	2780	2796	16	2797	2863	66	2864	3297	433	F
1594	24	1595	1614	19	1615	1682	67	1683	2129	446	C